

Ruthenium promotion of platinum for the electrocatalytic oxidation of methanol

Citation for published version (APA):

Frelink, T. (1995). *Ruthenium promotion of platinum for the electrocatalytic oxidation of methanol*. [Phd Thesis 1 (Research TU/e / Graduation TU/e), Chemical Engineering and Chemistry]. Technische Universiteit Eindhoven. <https://doi.org/10.6100/IR445489>

DOI:

[10.6100/IR445489](https://doi.org/10.6100/IR445489)

Document status and date:

Published: 01/01/1995

Document Version:

Publisher's PDF, also known as Version of Record (includes final page, issue and volume numbers)

Please check the document version of this publication:

- A submitted manuscript is the version of the article upon submission and before peer-review. There can be important differences between the submitted version and the official published version of record. People interested in the research are advised to contact the author for the final version of the publication, or visit the DOI to the publisher's website.
- The final author version and the galley proof are versions of the publication after peer review.
- The final published version features the final layout of the paper including the volume, issue and page numbers.

[Link to publication](#)

General rights

Copyright and moral rights for the publications made accessible in the public portal are retained by the authors and/or other copyright owners and it is a condition of accessing publications that users recognise and abide by the legal requirements associated with these rights.

- Users may download and print one copy of any publication from the public portal for the purpose of private study or research.
- You may not further distribute the material or use it for any profit-making activity or commercial gain
- You may freely distribute the URL identifying the publication in the public portal.

If the publication is distributed under the terms of Article 25fa of the Dutch Copyright Act, indicated by the "Taverne" license above, please follow below link for the End User Agreement:

www.tue.nl/taverne

Take down policy

If you believe that this document breaches copyright please contact us at:

openaccess@tue.nl

providing details and we will investigate your claim.

Ruthenium Promotion of Platinum for
the Electrocatalytic Oxidation
of Methanol

Timoer Frelink

RUTHENIUM PROMOTION OF PLATINUM FOR
THE ELECTROCATALYTIC OXIDATION
OF METHANOL

PROEFSCHRIFT

ter verkrijging van de graad van doctor aan de
Technische Universiteit Eindhoven, op gezag van
de Rector Magnificus, prof.dr. J.H. van Lint,
voor een commissie aangewezen door het College
van Dekanen in het openbaar te verdedigen op
dinsdag 3 oktober 1995 om 16.00 uur

door

Timoer Frelink

geboren te Amsterdam

Dit proefschrift is goedgekeurd door de promotoren:

prof.dr. J.A.R. van Veen

en

prof.dr. V. Ponec

Co-promotor: dr. W.H.M. Visscher

The research in this thesis has been carried out in the Laboratory for Inorganic Chemistry and Catalysis at the Eindhoven University of Technology with financial support of the Dutch Organisation of Scientific Research (NWO/SON).



CIP-DATA KONINKLIJKE BIBLIOTHEEK, DEN HAAG

Frelink, Timoer

Ruthenium promotion of platinum for the electrocatalytic oxidation of methanol / Timoer Frelink. -[S.l. : s.n.].

-Ill., graf., tab.

Thesis Technische Universiteit Eindhoven. -With ref.-

With summary in Dutch.

ISBN 90-386-0436-x

Subject Headings: electrocatalysis / platinum / methanol

"Io pensavo ad un'altra morale, piu terrena e concreta, e credo che ogni chimico militante la potrà confermare: che occorre diffidare del quasi-uguale, del praticamente identico, del pressapoco, dell'oppure, di tutti i surrogati e di tutti i rappezzi."

Primo Levi "Il sistema periodico"

"Behind the tireless efforts of the investigator there lurks a stronger, more mysterious drive: it is existence and reality that one wishes to comprehend."

Albert Einstein (1934).

Contents

1	Introduction	1
2	Catalytic aspects of the Electrochemical Oxidation of Methanol over Platinum: A Review	7
3	Experimental Methods	31
4	A DEMS study on the nature of the adsorbate in the electrooxidation of methanol over Platinised Platinum.	43
5	On the particle size effect of carbon supported Pt catalysts for the electrooxidation of methanol.	65
6	The adsorbate in methanol and CO electrooxidation over carbon supported Pt. A DEMS study	81
7	Ellipsometry and DEMS study of the electrooxidation of methanol at Pt and Ru- and Sn- promoted Pt.	93
8	The role of surface oxides in the electrooxidation of methanol, formic acid and CO on Pt, Ru and codeposited PtRu.	107
9	On the role of Ru and Sn as promoters of methanol electrooxidation over Pt	119
10	Measurement of the Ru surface content of electrocodeposited PtRu electrodes with the Electrochemical Quartz Crystal Microbalance: Implications for Methanol and CO electrooxidation.	131
11	The effect of Sn on Pt/C catalysts for the methanol electrooxidation.	145
12	Metal Oxide supported catalysts for the electrooxidation of methanol	155
	Summary	165
	Samenvatting	169
	Dankwoord	173
	List of Publications	175
	Curriculum Vitae	176

CHAPTER 1

Introduction

Fuel cells are electrochemical devices that directly convert chemical energy into electrical energy. They are not Carnot limited machines, in the sense that they operate directly on available chemical free energy and not on heat. The theoretical efficiency of the conversion of chemical energy into electrical energy (defined as $\Delta G/\Delta H$) is very high (80-120%).

The best known example is the hydrogen-oxygen fuel cell, in which hydrogen is oxidized to protons and oxygen is reduced to water (Fig. 1 and eq. 1).



The overall reaction is then:



which is essentially the combustion of hydrogen to water, but now the energy is directly

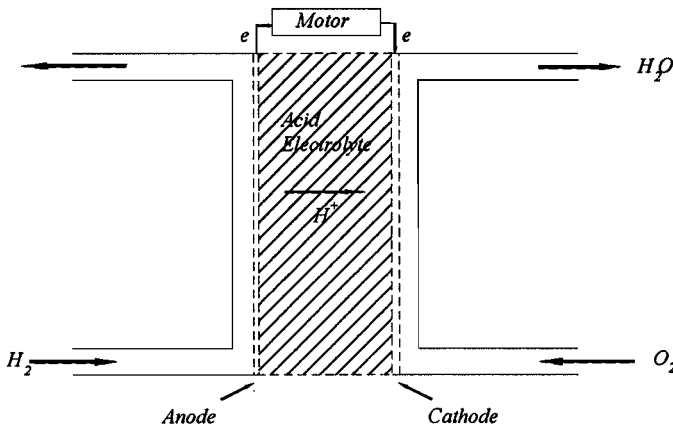


Figure 1 Example of a hydrogen-oxygen fuel cell.

converted into electrical energy and not into heat. If it were possible to carry out the combustion in a controlled, reversible manner, then the (perfect Carnot) heat engine would

have the same efficiency as a perfect isothermal fuel cell, using the same fuel.[1]

The reactions occur at spatially separated electrodes, upon closing the circuit a net current will flow from the hydrogen to the oxygen side. This then, gives the possibility to use such a hydrogen-oxygen system as an alternative source of electrical power.

Oxygen, which is directly available from air, is used as an oxidant in most fuel cells. As a fuel either hydrogen, hydrocarbons, alcohols, or pure carbon have been proposed. Since the only products from the electrochemical burning of these fuels will be CO_2 and H_2O , the emission of noxious gases, such as NO_x would be greatly reduced with the use of fuel cells. This makes them very attractive, also from an environmental point of view. One of the systems with great potential for application in vehicle traction is the Direct Methanol Fuel Cell, where methanol is oxidised to CO_2 and $\frac{1}{2} \text{O}$. A few major problems however have to be solved before the DMFC can be used as an alternative source of power. Besides the problems concerning the cell and electrode design, there are the problems of catalysing the anode and cathode reactions. For the anode, the results sofar show that the activity for the electrooxidation of methanol is too low, and that the catalyst material deactivates rapidly, therefore the research described in this thesis is concerned with the electrochemical oxidation of methanol in an aqueous-acidic environment, in the context of the development of a Direct Methanol Fuel Cell (DMFC). The experiments described, are thus so-called half-cell experiments, where a potential is applied to the electrode where methanol is to be oxidised. This research belongs to the area of the electrocatalysis, i.e. the borderline between electrochemistry and catalysis.

In this chapter the context of this research and the scope of the thesis are given.

A short history

Sir William Grove(1811-1896) must be regarded as the inventor of the fuel cell. He described in 1839[2] an experiment in which electricity was generated by supplying hydrogen and oxygen to two separate electrodes in sulphuric acid. Soon thereafter, in 1845[3], he reported that "volatile bodies such as camphor, essential oils, ether and alcohol associated with oxygen give continuous currents".

Most research has been directed towards the development of $\text{H}_2\text{-O}_2$ fuel cells. For applications in electric vehicles the Direct Methanol Fuel Cell (DMFC) is, however, the theoretically ideal solution: methanol is relatively cheap and is easy to transport. Investigation of this cell started in the early 1960's. At first attention was directed towards a system with an alkaline electrolyte and some practical cells were built (e.g. by Allis and Chalmers Manufacturing Company in 1961 [4]). A disadvantage of these alkaline systems is however that upon CO_2 production carbonates are formed, which disturb the fuel cell performance. Therefore research was soon directed towards the development of an acidic DMFC, although Parsons and VanderNoot[5] advocate that more research should be directed towards the removal of carbonate from the solution.

Acidic Methanol Fuel Cells.

In an acidic electrolyte, the two half cell reactions given in eq. (3) occur. The theoretical voltage difference between the electrode potentials of the two reactions is 1.2 V, which corresponds to $\Delta G = -702.5$ kJ/mol [1].



The total reaction of the cell is given in eq. (4)



Although acidic electrolytes do not suffer from carbonate formation, they present another problem. The oxidation of methanol to CO_2 is considerably slower in acid than in alkaline electrolyte which leads to very small effective cell voltages upon operation. Furthermore whereas in an alkaline electrolyte metals like Ni are also active for the methanol oxidation, in an acid electrolyte the choice of the catalyst is confined to Pt. Because of the difficulty to overcome the carbonate formation problem however, most research has been directed towards the development of an acidic DMFC. Probably the first operating direct methanol fuel cell was built by Shell Research in 1965[6], which gave only 0.25 V at 30 mA/cm², i.e less than one fourth of the theoretical value. More recent research[7] on a laboratory scale fuel cell gave 0.5 V at 300 mA/cm², at a temperature of 90°C. One of the causes of this drop in cell performance is the difficult oxidation of methanol on Pt electrodes. Because of this poor performance research has been directed towards the development of better methanol oxidation catalysts. In spite of extensive research in the last 30 years, which is extensively discussed in chapter 2 of this thesis, still no acceptable Pt based catalyst has been developed.

Scope of this thesis.

The work described in this thesis is aimed towards a better understanding of the methanol electrooxidation mechanism over Pt and especially the influence of promotor metals, like Ru and Sn, on the behavior of Pt. To achieve this a variety of in-situ electrochemical techniques were employed, which are described in chapter 3.

It is known that the oxidation of methanol, proceeds via the formation and successive oxidation of an adsorbed intermediate. To get a better insight in the reaction and the problems concerned with the catalysis of the reaction it is necessary to know via which type of adsorbed intermediate the reaction proceeds. One of the in-situ techniques that is very useful in studying the adsorbed intermediate is Differential Electrochemical Mass Spectroscopy (DEMS).

Chapter 1

Results obtained with this technique on methanol adsorbates, formed under different experimental conditions on platinised platinum, are described in Chapter 4.

In a real fuel cell Pt will often be dispersed on a conducting carbon support in order to minimise the amount of platinum. The surface area of the platinum can then further be increased by decreasing the size of the Pt particles on the carbon support. Furthermore a difference in preparation method of the catalyst may very well cause a different Pt-support interaction. The effect of finely divided platinum on carbon and especially the effect of the particle size and the Pt-carbon interaction on the activity for the methanol electrooxidation is described in Chapter 5. Both factors were varied by changing the preparation method of the catalyst. It is shown that both factors do influence the activity for the methanol oxidation. In order to reveal the structure of the adsorbed intermediate on carbon supported Pt, DEMS is again employed in Chapter 6, where the effect of the Pt particle size on the type of reaction intermediate is studied.

The chapters so far have been concerned with obtaining a better understanding of the methanol oxidation over supported and unsupported Pt. Since the activity for Pt itself is too low, it is necessary to improve the catalyst, by for example adding a promotor metal, in this case ruthenium. This is the subject of the chapters 7-11.

The chapters 7 to 10 deal with the effect of the promotor metal Ru on the methanol electrooxidation. The main goal of these chapters is to reveal by which mechanism Ru actually acts; although it is well established that it does promote the methanol electrooxidation over Pt, it is still not clear how. Chapter 7 describes the results on Ru (and Sn) deposited on smooth Pt. With another in-situ technique, ellipsometry the species which are present on the surface during methanol oxidation were investigated. Thereby it was possible to obtain some more insight in the mechanism by which Ru actually acts.

In the chapters 8,9 and 10 the discussion is mainly concerned with a slightly more advanced model system; electrochemically co-deposited PtRu. Chapter 8 describes some ellipsometry results on the action of PtRu surface oxides on the oxidation of small organic molecules as CO and HCOOH. This also proved to be helpful to reveal the "promoting-mechanism" of Ru.

Chapter 9 describes both DEMS and ellipsometry results on the electrochemical oxidation of methanol on supported as well as rough unsupported PtRu systems. Some results described in this chapter suggest another mechanism for the effect of Ru than the results in chapters 7 and 8.

In studying the behavior of a catalyst its exact composition must be known. However, for codeposited PtRu systems this composition cannot be straightforwardly analysed. In order to establish the surface coverage with Ru in the catalysts used, we developed an electrochemical method using the Electrochemical Quartz Crystal Microbalance technique. This method is described in Chapter 10 for codeposited systems. The implications of the results, on the CH₃OH and CO oxidation are discussed. Furthermore, to further substantiate the results in

Chapter 9, some in-situ IR results on adsorbed CO on PtRu are described.

Sn is also known to be a good promotor for the electrooxidation of methanol. In Chapter 11 the results on supported Pt catalysts with the promotor metal Sn are discussed, where the focus is on the effect of the catalyst preparation method.

Although in the previous chapters it has been shown that there is an increase in the activity for the oxidation of methanol in the presence of both Sn and Ru, the performance of the promoted systems is still too poor for practical applications. Therefore some research was also directed towards the development of alternative catalysts. The results of this are described in the last Chapter (12). Pt/WO₃ and PtAu/C are shown to be the most active.

References

- 1.A.J. Appleby, F.R. Foulkes, *Fuel Cell Handbook*, van Nostrand Reinhold New York 1989. Chapter 2.
- 2.W.R. Grove *Phil. Mag.* **14**, 127 (1839).
- 3.W.R. Grove *Proc. R. Soc. London* **5**, 557 (1845).
- 4.P.G. Grimes, B. Fidler, J. Adams *Proc. Ann. Power Sources Conf.* **15**, 29 (1961).
- 5.R. Parsons, T. VanderNoot *J. Electroanal. Chem.* **257**, 9 (1988).
- 6.M.R. Andrew, R.W. Glazebrook in *An Introduction to fuel cells* Ed. K.R. Williams Elsevier Amsterdam 1966. p.111–147.
- 7.S. Surampudi, S.R. Narayanan, E. Vamos, H. Frank, G. Halpert, A. LaConti, J. Kosek, G.K. Surya Prakash, G.A. Olah *J. Pow. Sourc.* **47**, 377 (1994).

Chapter 1

Catalytic Aspects of the Electrochemical Oxidation of Methanol on Platinum: a Review.

Introduction

Through the years a number of review articles on the methanol electrooxidation has appeared[1],[2],[3],[4]. The focus in this review will be on the catalytic aspects of the methanol electrooxidation, relevant for the work described in this thesis. This implies that subjects such as the nature of the platinum substrate (polycrystalline as well as roughened surface and supported small Pt particles), the type of reaction intermediates, the role of the adsorbed oxygen species, the origin of the decrease in activity and the effect of promotor and support on the reaction mechanism, will be discussed. For each of these subjects we will try to show what is (in our view) the current state of the research, which topics still need some work to be done and in which direction future research might have to be directed.

A more extensive review will be published elsewhere[5].

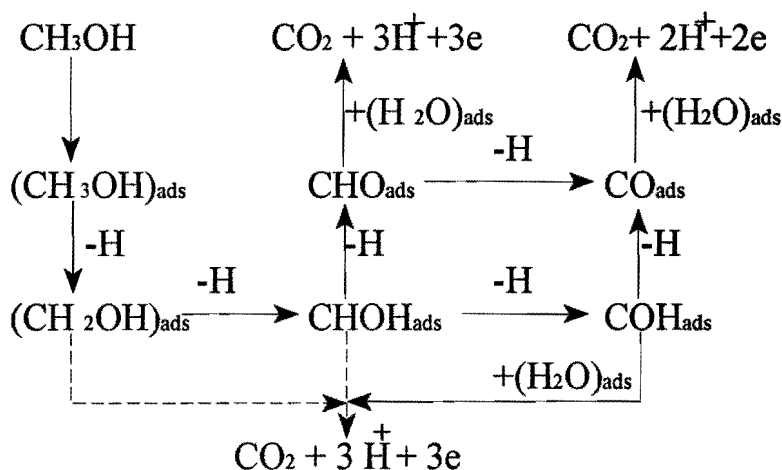


Figure 1 Mechanism of the electrocatalytic oxidation of methanol.

Mechanism for the electrooxidation of methanol.

The general mechanism for the electrochemical oxidation of methanol is given in figure 1.

From aqueous solution methanol is adsorbed to the surface via the carbon atom. Franaszcuk et al.[6] suggest that hydrogen bonding takes place between the alcohol-group and the water molecules. This is in contrast with gas-phase adsorption at low temperatures for which they[6] and others[7] have shown that a methoxy species is formed at the catalyst surface; here the bonding occurs via oxygen.

The methanol residue is oxidized to CO_2 by adsorbed hydroxy species. The presence of these hydroxy species appears to be essential for the methanol electrooxidation. The problem is that these species are only formed in appreciable amounts at relatively high potentials (>0.74 V vs RHE). On the other hand methanol cannot adsorb on the platinum oxides which are formed as well at these potentials. Burke and co-workers[8],[9] suggest that a hydrous-oxide is the oxygen-delivering species. This hydrous-oxide is however not very likely to play a role in the methanol oxidation in the fuel cell, because of the extreme conditions which are necessary to generate these species. Vassiliev et al.[10] conclude on the basis of measurements in pure methanol that water molecules are needed for the dehydrogenation of the methanol molecule, because no dehydrogenation takes place in pure methanol.

Type of intermediates

The identity of the adsorbed species and of the reaction intermediate in the methanol electrooxidation has been the subject of considerable controversy over the past 20 years. The detection and identification of adsorbed intermediates became possible in recent years due to the development of in-situ IR and MS techniques. The IR techniques all give the possibility of detecting an intermediate as a function of the electrode potential, although the various methods differ in the way to achieve this. The techniques most used are EMIRS[11] (Electrochemically Modulated Infrared Spectroscopy), SNIFTIRS[12] (Subtractively Normalized FTIRS), PMIRRAS[13] (Polarization Modulated IR Reflection Absorption Spectroscopy), SPAIRS[14] (Single Potential Alteration IRS) and LPSIRS[15] (Linear Polarized Sweep IRS). With the MS techniques the intermediates can be either detected indirectly by on-line determination of products as a function of potential (Differential Electrochemical Mass Spectroscopy[16]), or directly by transferring the electrode to a vacuum chamber and perform temperature programmed desorption (Electrochemical Thermal Desorption Mass Spectroscopy [17]).

Other in-situ measurement techniques that have been used for the study of the electrooxidation of methanol are: Electrochemical Quartz Crystal Microbalance (EQCMB)[18],[19], Sum Frequency Generation (SFG)[20] and Surface Enhanced Raman Scattering (SERS)[21].

Polycrystalline Pt surfaces

Most results have been obtained with polycrystalline Pt. Chandrakesaran et al.[22] state that in steady state measurements only CO is present and that "what cannot be seen, cannot be present". Their IR measurements suggest that CO is the intermediate and that linear CO is converted to bridge bonded species above 0.4 V vs RHE. There is however substantial evidence that CO cannot be an intermediate in the oxidation process: for example, Podlovchenko et al.[23] determined the methanol adsorption stoichiometry using an electrochemical method and found that three protons are lost upon chemisorption of methanol, which implies that the adsorbed residue should be $\equiv\text{COH}$ or $-\text{CHO}$. This was supported by DEMS experiments of Wolter et al.[24], who used this technique not only to detect the different reaction products, but also to establish the ratio between the amount of charge required and the amount of CO_2 molecules produced in the methanol electrooxidation. It is thus possible to distinguish between CO, where the ratio is 2, and COH/CHO , where the ratio is 3, as adsorbates. Wolter et al. found that three electrons are required for the oxidation of the adsorbate to CO_2 and concluded that CO cannot be the intermediate. This was also a possible explanation for the results of the SPAIRS experiments of Weaver et al.[25]. They studied the replenishment of an adsorbed ^{12}CO layer by $^{13}\text{CH}_3\text{OH}$ during the oxidation of the CO, by looking at the shift in the IR frequency. No ^{13}CO band was found while the oxidation of methanol continued.

The general opinion now held is that on polycrystalline Pt surfaces CO is not an intermediate but a poisoning species which only can be removed by oxidation at higher potentials.

To determine whether the intermediate is $-\text{CHO}$ or $\equiv\text{COH}$, DEMS experiments were carried out with deuterated methanol and D_2O [26],[27]. After adsorption of methanol, the adsorbed intermediate is electrochemically oxidized in H_2O (at 0.8 V vs RHE); in this process H^+ -ions are liberated. Immediately thereafter the potential is lowered to 0 V vs RHE in order to reduce these H^+ to H_2 ; in case of deuterated species D_2 and HD are formed as well. The evolving gas is analyzed for HD.

In experiments with adsorption of CH_3OH , followed by oxidation of the intermediate in D_2O , Willsau and Heitbaum[26] found HD. However when CH_3OD was adsorbed in D_2O (yielding $\equiv\text{COD}$ or $-\text{CHO}$) and the intermediate was oxidized in D-free electrolyte, no HD was detected. Since in the latter case HD could only be formed if the adsorbate is $\equiv\text{COD}$, they concluded that the intermediate must be $-\text{CHO}$. Vielstich et al.[27] established rather surprisingly that also if CD_3OD is adsorbed (yielding CDO or $\equiv\text{COD}$) and the adsorbate is subsequently oxidized in H_2O , no HD is formed. This could only be explained by a rapid exchange of the hydroxylic D with H_2O ; therefore they concluded indirectly that the intermediate is $\equiv\text{COH}$.

The Vielstich group found further evidence for $\equiv\text{COH}$ as an intermediate by combining Thermal Desorption Measurements of adsorbed methanol residues with the measurement of

the ratio of adsorption and oxidation charge of methanol [17],[28],[29]. This ratio was found to be one, so an equal amount of electrons must be involved in the adsorption and oxidation of methanol; this however does not discriminate between -CHO and $\equiv\text{COH}$.

Until 1987 these results could not be supported by any of the in-situ IR techniques, because the spectra only showed the presence of linearly and small amounts of bridge-bonded CO[30],[31],[22]. With EMIRS, Beden et al.[32] for the first time claimed evidence for the presence of an adsorbed -CHO species. A band at 1690 cm^{-1} , assigned to the C=O stretch vibration of this species, could be seen at methanol concentrations lower than $5 \cdot 10^{-3}\text{ M}$; at higher concentrations, the linearly adsorbed CO was predominant. This is in agreement with ECTDMS[33] results, which showed that other adsorbates than CO are favoured at low adsorbate coverage and CO at high coverage and cyclic voltammetric studies[34],[35],[36] where different adsorbate oxidation peaks were attributed to different adsorbed species. SFG[37] studies confirmed the presence of linearly bonded CO at high surface coverages and furthermore suggest that at low adsorbate coverages multibonded CO is the major species. A C=O stretching mode at ca. 1700 cm^{-1} is often reported in recent studies, however the assignments range from -COOH, -CHO to H_3COOCH [38],[39],[40]. Lopes et al.[41],[42], by comparing formate, methanol and methylformate adsorbates, found a whole set of adsorbed species ranging from -CO and -HCO to methoxy radicals. Direct evidence for a hydrogen atom bound to a carbon atom in the adsorbate was never found. It was however shown[43] that there is a difference in the adsorbate from CO and from methanol, since the former is capable of removing the latter from the surface.

IR evidence for a $\equiv\text{COH}$ group has been reported by several groups, although based on IR absorption at slightly different frequencies. Iwasita and co-workers[44] observed a band at 1270 cm^{-1} , which did not change upon use of CD_3OH and was thus attributed to $\equiv\text{COH}$. Nichols et al.[45], who used HClO_4 as a supporting electrolyte, assigned bands found between 1215 and 1425 cm^{-1} to a $\equiv\text{COH}$ species. Pham et al.[39] find on rough Pt that both the -CHO- (1716 - 1741 cm^{-1}) and the $\equiv\text{COH}$ (1253 - 1266 cm^{-1}) intermediate are present at $E=0.3\text{ V}$. The potentials at which these intermediates are observed seem to be reasonable in view of the CO_2 production potential. However Nichols and Bewick[45] do not find an intermediate at $E=0.44\text{ V}$, but only at $E=0.70\text{ V}$ vs RHE, which seems to be rather high.

It can thus be said that the IR measurements described here agree on the presence of linearly bonded CO on the Pt surface. The presence of multibonded CO is confirmed too, although only in very small amounts. Cyclic voltammetric studies [19],[34],[43],[46],[52] however show that the number of electrons per Pt site necessary to oxidise the methanol adsorbate is between 1 and 2, implying that considerable amounts of bridge and or multi-bonded CO are present. These results make it less probable that CHO is formed, since for this species the

number of electrons per site would be 3. There is thus a discrepancy between IR and the cyclic voltammetric studies, since the latter suggest that bridged- or multi-bonded CO is present in fairly large amounts, whereas in the IR measurements only small amounts can be found. In a recent study Weaver et al.[47] showed that this discrepancy may be due to the smaller cross-section of the multi-bonded species, leading to an underestimation of the amount of this species on the surface.

Single Crystal Surfaces.

Research on Pt single crystal surfaces (which has been extensively reviewed, see for example ref.[48] and [2]) has shown that the behavior of Pt(111) differs markedly from Pt(110) and Pt(100).

On repetitive oxidation and reduction cycling noticeable decreases in the current are observed on Pt(100) and Pt(110), but not on Pt(111)[49]; this agrees with the fact that less CO can be seen on Pt(111)[48], assuming that this is indeed a poisoning species. Lamy et al. [50] suggested multibonded CO to be the poisoning species, this species is preferentially bonded on Pt(110), the surface which shows the fastest deactivation[51].

Electrolyte dependence

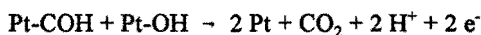
Anion adsorption is known to take place on Pt catalysts in electrolytes. The activity of Pt for methanol oxidation in H_2SO_4 is well below that in HClO_4 [48],[52],[53]; this effect is strongest for Pt(111)[49],[54], while no effect is found for Pt(110)[51]. Castro Luna et al.[55] have shown that the values of $\theta_{\text{org}}^{\text{max}}$, for electrodispersed Pt, attained in different electrolytes are 0.82, 0.74 and 0.62 for 1 M HClO_4 , 0.5 M H_2SO_4 and 0.3 M H_3PO_4 respectively, thus showing the influence of the electrolyte anion on the maximum available surface coverage. In HClO_4 a higher coverage of the poison is reached and the rate of poisoning is faster, so on the whole there is no clear advantage of HClO_4 over 0.5 M H_2SO_4 . The concentration of the sulphuric acid has a great influence on the catalytic activity for the methanol electrooxidation and a concentration of about 0.5 M is the optimum. For the high current densities required in fuel cell applications, however, a compromise is necessary between activity and solution conductivity; in this case the optimum is at a concentration of about 3 M.[4],[56]. Surface-oxide formation is also influenced by the nature of the acid-anion. It has been shown[36, 53],[52] that in HClO_4 the surface oxidation starts at lower potentials than in H_2SO_4 , leading to a lower potential for the start of the methanol oxidation.

Concluding we can say that, in spite of the extensive research still no total consensus is

reached on the intermediate of the methanol electrooxidation over Pt (mono- or polycrystalline). Although IR, DEMS and electrochemical methods all show that CO (either linear- or bridge- bonded) and/or COH are present, it is still not clear under what circumstances which adsorbate is present. With IR measurements, the presence of CHO has been claimed too. The small amounts of bridge/multi-bonded CO found with IR seems to be due to the small cross-section of these species. It has still to be determined why either CO or COH or both are found to be present on the electrode surface.

The adsorbed species form directly CO₂ under influence of adsorbed hydroxy groups. There is thus agreement on the fact that methanol first rapidly loses two protons from the methyl group, the third proton then to be lost, comes from either the methyl or the alcohol group under formation of COH or CHO respectively. The reaction may then proceed via either oxidation of the intermediate or the formation of a poisoning species.

It has been determined that the methanol oxidation rate is, in the absence of mass transport limitations, zero-order in methanol[57] (this also goes for electrodeposited Pt). This implies that the rate determining step involves either the removal of an adsorbed intermediate from the Pt surface or the formation of the species necessary for this removal to take place, viz. OH_{ad}, e.g.,



Methanol adsorbs easily at relatively low potentials, $E \geq 0.3 \text{ V}$, i.e. as soon as the Pt surface is substantially free from adsorbed H[58],[59]. The formation of hydroxy groups, on the other hand, is appreciable only at higher potentials, activation of water starting in earnest at $E=0.6-0.7 \text{ V}$, and this, as mentioned before is why the electrooxidation of methanol becomes measurable only at relatively high potential, $E=0.5 \text{ V}$.

Carbon supported platinum.

In order to use Pt as a catalyst in practical fuel cells, the surface area has to be large, which can be achieved by depositing small Pt particles on a conducting support. Different supports can be used for this purpose.

It is well known that by decreasing the particle size, one may, apart from increasing the surface area, also change the catalytic behavior of the material. Furthermore, the type of the carbon support can affect the catalytic behavior, because of possible metal-support interaction. Therefore we will first look at the behavior of electrochemically roughened Pt surfaces, after which the influence of the Pt/C preparation techniques and the particle size will be discussed.

Electrochemically Roughened Platinum Surfaces.

EMIR spectra[38],[60] show that with increasing roughness of the platinum surface, the

amount of adsorbed CO decreases, even at potentials (0.3 V vs RHE) at which smooth Pt is known to be covered nearly completely by CO. Pham et al.[39] suggest that a band at 1942 cm^{-1} on a sputtered Pt electrode is due to linear CO at 0.3 V, which is however highly unlikely. The amount of adsorbed CO appears to decrease with increasing electrode roughness. Beden et al.[38] suggest that this is due to the presence of mainly Pt(111) faces (see above), and the development of these faces has indeed been deduced from X-ray diffraction on electrodispersed electrodes[61].

The amount of linear CO increases with increasing methanol concentration[38]. The concentration for which CO can be seen is however much higher than for smooth Pt surfaces ($1 \cdot 10^{-1}\text{ M}$ vs $5 \cdot 10^{-3}\text{ M}$). The intensity of a band at $1650\text{-}1700\text{ cm}^{-1}$ (assigned to -CHO) decreases with increasing methanol concentration, and consequently with increasing amounts of linear CO present. Thus it may be anticipated, that high surface area Pt is much less prone to deactivation by adsorbed CO than the essentially flat Pt electrodes discussed before. A study by Christensen et al.[62] suggests that cycling in a methanol containing solution generates a roughened surface, whose kinetic properties are substantially different from those of Pt without cycling in methanol. The rate of methanol oxidation at low potentials is found to be far higher on this surface. This suggests that methanol "creates its own catalyst".

Particle Size Effects

The study of particle size effects is complicated by the fact that they may be influenced by metal support interactions, which may in turn depend on the Pt/C preparation method. The following five methods of preparation for supported Pt catalysts are widely used:

1. The impregnation method: the support is impregnated with H_2PtCl_6 which is then reduced with a strong reductor such as NaBH_4 [63].
2. The ion-exchange method: the carbon support is oxidized to form carboxylic acid groups and then ion-exchanged with $\text{Pt}(\text{NH}_3)_4(\text{OH})_2$ [64].
3. The colloidal method: a monodisperse Pt sol (prepared by reducing H_2PtCl_6 with e.g. sodium citrate) is added to the support[65].
4. Chemical Vapor Deposition: the platinum is vaporized on a substrate, e.g. glassy carbon[66].
5. Electrodeposition of Pt on a Teflon bonded carbon support[67].

Carbon blacks, active carbon and sometimes graphite are used as carbon supports. Most popular for fundamental studies is a high surface area carbon black: Vulcan XC-72 with a specific surface area of $300\text{ m}^2/\text{g}$. On the basis of ESR and XPS studies[68],[69] it has been concluded that electron donation by platinum to the carbon support takes place, and it is

believed that the extent of this donation is influenced by the particle size of the platinum. Differences in carbon pretreatment or the kind of carbon support may lead to appreciable differences in electrocatalyst support interactions and thus to different conclusions concerning the particle size effect for oxidation and/or reduction reactions. Carbon supported platinum electrodes show a much lower overpotential in the electrooxidation of methanol than polycrystalline Pt and are capable of higher current densities[70]. This cannot only be due to the enlargement of the surface area, because in that case one should only expect a larger overall current, and not per unit Pt surface. So there appears to be an additional effect due to the decrease of the Pt particle size or to a metal support interaction. As argued above it is difficult to distinguish between those two effects, because a different preparation method might lead to a smaller particle size, but it can also change the metal-support interaction.

In the previous section it was indicated that the high overpotential on smooth Pt electrodes is mainly due to the high formation potential of hydroxy surface species. The lowering of the overpotential i.e. the fact that the methanol oxidation starts at a lower potential on carbon supported Pt, could therefore very well be due to the lower formation potential of these hydroxy species on Pt/C catalysts. Indeed it is known that upon going from unsupported Pt to supported Pt the oxide formation potential is lowered, and that the oxide reduction peak shifts with changing Pt particle size[71]. A change in oxygen binding behavior with particle size has also been reported by Parmigiani et al.[72]. They investigated with XPS the interaction of oxygen with small Pt particles sputtered on Teflon, and their results show that small Pt particles are more easily oxidized than large ones, in agreement with electrochemical, TPD[73] and calorimetric[74] measurements.

With the higher performance of carbon-supported Pt, then, probably being due to a relatively low potential of formation for an adsorbed hydroxy species, one should also expect a particle size effect for the methanol electrooxidation. Such an effect has in fact been reported by McNicol et al.[75] employing Pt catalysts prepared in a variety of ways (impregnation and ion-exchange with different pretreated supports). The activity decreases for very small and very large particles. The cyclic voltammograms of the Pt/C catalysts in pure acid clearly show a stronger oxygen adsorption with decrease of the particle size. The variation in specific methanol oxidation activity can now be explained as follows. For larger particles, the activation of water still takes place at a relatively high potential, so that θ_{OH} is still relatively low at the potential at which the comparison is made. Decreasing the particle size results in OH formation at lower potentials, and so enhances the reaction rate. However, for very small particles activation of water takes place at such low potentials, that even at relatively low overpotentials the surface coverage with OH is already so substantial, that the CH_3OH adsorption step begins to suffer. That is, decreasing the Pt particle size too much results in a

change of rate-determining step with a concomitant decrease in the specific activity. However, as already mentioned, McNicol et al. used different preparation methods to arrive at different particle sizes, so that unfortunately the particle size effect cannot be fully separated from a metal-support effect, which has indeed been found to influence the methanol oxidation activity[76]. On the other hand, Matsuda et al.[77] have used the same preparation method (Chemical Vapor Deposition) and the same support to prepare catalysts with different particle sizes, and they found that the current density decreases with smaller platinum particles. These particle sizes (between 1.5 nm and 2.3 nm) are in the same range as the Pt particles for which McNicol observed a decrease, thus corroborating the view that the particle size effect is indeed the primary one. The overall methanol currents at these small particles are lower than on the larger particles, although the surface area has become larger. Machida et al.[78] used platinum-carbonyl clusters with different amounts of platinum atoms to prepare carbon supported catalysts. They found that the smallest clusters, with nine Pt atoms gave a catalyst with a smaller activity for the methanol electrooxidation than the clusters with fifteen Pt atoms. It was suggested that there exists an optimum size of the platinum particles larger than fifteen atoms, in agreement with the results of McNicol et al. Further confirmation for the presence of a particle size effect in the methanol oxidation comes from a study by Kabbabi et al.[79], who showed that it is the more easy oxidation of the Pt that causes the lower activity for the methanol oxidation at smaller Pt particles.

A very different result was however obtained by Watanabe et al.[80] for carbon supports with specific areas ranging from 60 to 835 m²g⁻¹. By deposition of Pt colloids Pt specific areas ranging from 70 to 201 m²g⁻¹ were obtained, with particle sizes between 1.4 and 4.0 nm. It appears from their measurements that surprisingly there is no particle size effect. Unfortunately enough no cyclic voltammograms are shown for these catalysts, so there is no clue on the oxide formation behavior.

Apart from showing a higher specific activity, platinised carbon electrodes also appear to be much more stable during CH₃OH electrooxidation than unsupported Pt. Recently Christensen et al.[81] showed that there is CO present after methanol adsorption on small Pt particles (~15 nm). The presence of ≡COH as an intermediate on the platinised glassy carbon electrodes was indicated by a band at a frequency of about 1230 cm⁻¹[82]. Although this band only appeared at a higher potential than the onset potential of CO₂ formation, its intensity increased with increasing methanol oxidation rate, thus suggesting that it is due to the true intermediate.

Still, platinised carbon electrodes do deactivate, and the question arises how this comes about. Two obvious explanations discussed in the literature are: (1) progressive oxidation of the Pt particles leading to a steady lowering of the efficiency of the CH₃OH adsorption reaction (lower $\theta_{\text{CH}_3\text{OH}}$), and (2) blocking of the Pt surface by an accumulating carbonaceous residue,

which may be thought to result from a reaction between two or more adsorbed methanol fragments. In both cases, but not should CO_{ad} be the poisoning species after all, one should expect the activity to be restored after exposing the deactivated electrode to open circuit conditions: the potential returns to such low values that Pt-oxide will be reduced and a carbonaceous residue may be hydrogenated off (CO cannot be removed in this way). This restoring action of open-circuiting has in fact been observed[83], thus proving that CO_{ad} is indeed not the poisoning species in this case. Evidence in favour of the progressive oxidation hypothesis has been obtained by XPS. Although XPS is an ex-situ technique, which makes the interpretation of the results less than straightforward, it does appear that a deactivated Pt/C electrode contains much more oxidized Pt, mainly Pt(II), than a fresh one[70],[84],[83]. Since no positive evidence for the existence of a poisoning carbonaceous species residue has yet been reported -although the kinetic studies of Andrew et al.[93] did lead those authors to postulate such a species- overoxidation of the Pt particles may be considered to be the main deactivation mechanism in platinized carbon electrodes. It should be noted, however, that in some cases the long-time experiments were terminated before the potential had actually increased into the Pt-oxide formation region, so that one then has to conclude that oxide formation can be enhanced by methanol[83]. This should be further checked. Also, part of the deactivation may be due to Pt particle growth in some cases (this is of course irreversible): the gradual decrease in binding energy of Pt(0) which Hamnett and Kennedy[83] observe, is probably due to this, although it was not taken into account by them.

In sum, it is clear that Pt/C catalysts do have a higher specific catalytic activity for the methanol oxidation than smooth Pt and that they are more stable. This is likely to be mainly due to a particle size on the effect of water activation, and to the absence of CO_{ad} poisoning. Whether a Pt-carbon interaction plays a role as well, remains to be seen. So far there has been no research on the change, if any, in CH_3OH adsorbate as a function of particle size.

Bimetallic catalysts.

The activity of Pt can be enhanced by introducing a second metal like Ru or Sn[85]. There is as yet no consensus about the actual mechanism of this promotion effect; different explanations have been proposed:

1. An electronic (ligand) effect[86], where the second metal alters the electronic state of the platinum in such a way that the activation of water is increased and/or the methanol residue is less strongly bonded.
2. A geometric (third-body) effect: the second metal blocks certain adsorption sites on the surface, so as to prevent/retard the build-up of poisoning species.

3. A bifunctional effect: the second metal specifically takes care of the activation of water, thus increasing the oxidation rate of the methanol residue.

4. A redox effect of the metal ion, where the oxidized form oxidises the methanol residue, upon which it is regenerated by water.

The geometric effect however can be discarded, because of the different metals with similar metal overlayer structures should have a similar effect on the methanol oxidation. This is not the case, as shown by Janssen and Moolhuysen[88] and Leiva and Giordano[36, 53].

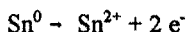
In the case of PtSn, supported and unsupported catalysts will be discussed together, but for PtRu it is more useful to discuss them separately.

Platinum/Tin Catalysts.

The modification of the activity of Pt for methanol electrooxidation by adding Sn has been the subject of intensive research. Strikingly however, neither the sign nor the size of the effect are clear yet. This may, at least in part, be due to the various measurement and preparation conditions employed, but a model explaining exactly why has not been forthcoming. The valence state of adsorbed Sn is another point of dispute.

Janssen and Moolhuysen[85],[87],[88], concluded that Sn has a very large effect on a Pt catalyst for methanol electrooxidation. They prepared electrodes by immersion, alloying and electrodeposition and found a 50-100 times increase in activity at low potentials (<0.5 V vs RHE) with respect to unpromoted Pt electrodes. For PtSn/C catalysts (which were prepared only by immersion) an enhancement with a factor 10 was found in the presence of Sn. For both the Pt grey and supported electrodes the optimum Sn coverage is about 10%. The redox mechanism for the Sn effect as previously suggested by Cathro[89] was abandoned by them, because no sign of a Sn redox couple was found in the cyclic voltammogram of a Sn modified Pt catalyst, and because the cathodic shift of the Pt-oxide reduction peak pointed into the direction of a mechanism where oxygen is bonded more strongly on the surface in the presence of Sn. Oxygen coverage measurements by Watanabe et al.[90] indeed show an increase in the amount of adsorbed oxygen in the presence of Sn at constant potential, the oxygen coverage increases linearly with increasing Sn coverage. This is consistent with explanation 1 and 3. There is also evidence for a change in mechanism. Apart from a change in Tafel slope in the presence of Sn, the number of electrons per Pt-site in the oxidation of the adsorbate has decreased and going from Pt to Pt-Sn the methanol reaction order changes from zero to values of about 0.5. This evidence points to a mechanism in which the oxidation of the adsorbate is no longer solely rate determining and in which the structure of the adsorbate has changed. The valence state of Sn was not actually determined by Janssen and Moolhuysen, but

they suggest Sn to be present in the zero-valence state and dissolution of Sn:



to take place above +0.8 V vs RHE. This last suggestion has been refuted by Stefenel et al.[91] who showed that an oxidation current is measured upon addition of Sn(II) to Pt at 0.8 V vs RHE, indicative of the reaction:



This might indicate that instead of Sn(0), Sn(II) is present in the potential range of methanol oxidation. The problem here is that this potential range is above the $\text{Sn}^{2+}/\text{Sn}^{4+}$ redox potential, and it is difficult to see where the adsorption stabilisation of Sn^{2+} should come from; this is less of a problem for Sn^0 , since PtSn forms very exothermic alloys, implying a very strong Pt-Sn⁰ interaction[87]. Also earlier Mössbauer studies[92],[93] indicate that in an acidic medium adsorbed tin is at least partly in the zero-valent state. It was suggested by McNicol et al.[94] that Sn is only in the zero-valent state under reaction conditions, implying that cyclic voltammetry in the absence of methanol cannot be used to determine the valence state of Sn.

The only authors who found an enhancement factor of the same order of magnitude as Janssen and Moolhuysen are Watanabe et al.[95]. With an Pt-Sn electrode, made by underpotential deposition, the highest activity (expressed in current per gram of catalyst) was found with the lowest Sn coverage they studied ($\theta_{\text{Sn}}=0.31$), the trend found is in agreement with the Janssen and Moolhuysen results. The relatively low value of the optimum Sn coverage, about one-tenth of a monolayer, is just what we should have expected in view of the fact that adsorbed Sn will reduce the number of Pt ensembles capable of adsorbing methanol, and that, as is discussed above for adsorbed oxygen, the CH_3OH adsorption reaction is already substantially hampered at a rather low coverage of adsorbed species. More evidence for a mechanism where Sn is responsible for a stronger oxygen adsorption on the surface, comes from XPS measurements[96] on a glass-supported Pt-SnO₂ electrode, which show that more oxidized Pt is present here than in glass-supported Pt (prepared in the same way). The only Sn species detected was Sn(IV). The steady state current on the 16% Pt-SnO₂ is 15 times higher than on smooth Pt, and in the long term Pt-SnO₂ keeps its high activity, whereas that of Pt rapidly decreases. It was concluded that a higher oxidation state of Pt is "frozen" by the presence of SnO₂ and thus the oxygen coverage is higher as compared to Pt alone. This may indeed account for the relatively high activity; the higher stability may on the other hand be just a consequence of smaller Pt particles being present, as discussed above for Pt/C catalysts. A cyclic voltammogram of the Pt/SnO₂ system[97] shows the presence of a redox couple, at 0.45 V vs RHE; according to the authors this is due to the Pt/Pt²⁺ redox couple but this conclusion was not further substantiated.

Wang and Fedkiw[98],[99] investigated the behavior of smooth and graphite supported Pt

with and without Sn modification using a pulsed potential method. Only very small enhancements in the rate of CH_3OH oxidation were observed. As before however, XPS measurements show an increase in the amount of oxidized Pt on the Sn modified electrodes, which would appear to imply that the presence of Sn is still leading to a ligand or electronic effect. Carbon supported Pt/Sn alloys with an enhancement factor of two[100] and Pt-Sn alloys supported on polymethylthiophene[101], where a cathodic shift of 150 mV of the CH_3OH oxidation onset potential was observed, are also thought to operate through a mechanism where the oxygen surface coverage is increased. XANES measurements[102], seem to indicate that there is some charge transfer from the Sn to Pt, in carbon supported catalysts. This charge transfer might not only account for the increase in oxygen surface coverage, but may also cause a weakened bonding of the adsorbate to the surface.

Several authors have investigated the behavior of Pt, when small amounts of a Sn salt are added to the electrolyte. The general conclusion is that this only gives a moderate enhancement with very small amounts of Sn ions ($<50 \mu\text{M}$). Bittins-Cattaneo et al.[103] showed that addition of Sn(II) to already adsorbed methanol has a far more pronounced effect than the addition of Sn(IV). In the presence of Sn(II) the oxidation potential of the methanol adsorbate was lowered by 0.15 V. They concluded that Sn acts through the formation of a hydroxy complex, which offers oxygen atoms to the methanol adsorbate. This result and conclusion is similar to the one previously published by Vassiliev et al.[104] A Sn hydroxy complex is also proposed by Norton-Haner and Ross[105], although these authors propose that this complex acts in solution through a mechanism which is comparable to the mechanism of Pt-Sn homogeneous catalysis[106].

Beden et al.[107], using both SnSO_4 in solution and upd Sn (source SnCl_2), likewise find a higher activity with low Sn concentrations. However, their conclusion that Sn decreases the number of adsorption sites for the strongly adsorbed residues can not be true because most metals should then show some enhancement, which is not the case. Upd Sn may also lower the activation energy for the methanol oxidation[108].

There is also a number of studies in which a negative Sn effect has been found. Gökagaç et al.[109] found a decrease in activity for carbon supported Pt+Sn catalysts, compared to Pt only, which they ascribe to depletion of Pt from the surface and enrichment of this surface with tin-oxide species. Inhibition of the methanol oxidation was also found by Campbell et al.[110] both for single crystal surfaces and carbon supported Pt after immersion in a SnSO_4 solution. Finally the single crystal PtSn alloys studied by Haner and Ross[105] also showed a decrease in activity.

From the results above it is clear that the effect of Sn on the methanol oxidation activity of Pt turns out to be rather variable. A point however on which there appears to be a consensus is

that in the presence of Sn a larger amount of oxygen is present on the surface. Whether this is due to the activation of water by Sn itself, or due to an electronic effect through which Pt can activate water more easily, is still a matter that is open for discussion. The difficulties in reaching consensus on the effect of Sn, may very well be connected with the unusual up behavior of Sn[111]. The valence state of Sn is another matter that still has to be clarified.

Platinum/Ruthenium Catalysts

Unsupported Platinum/Ruthenium catalysts.

In contrast to Sn, the effect of Ru on the activity of Pt in methanol electrooxidation is a very consistent one and is not restricted to low Ru surface coverages. While Sn blocks the adsorption of methanol, this is not necessarily so for Ru (it can accept H_{ad}). All research has shown a substantial increase in activity for a Ru promoted catalyst in agreement with earlier work[112].

From potential difference IR spectroscopy it appears that on a Pt-Ru alloy very little CO is present in comparison with pure platinum[40],[113],[120]. The higher frequencies for C-O stretch at comparable surface coverage indicate that the CO adsorption strength is weaker on the alloy[40], this effect was however only found for methanol adsorption and not for CO adsorption[114]. The weakening of the CO adsorption strength points to an electronic (ligand) effect. Smaller changes in the H_{ad} region of the CV in the presence of CH_3OH also point to a lower surface coverage by methanolic adsorbates. This would mean that this electrode is far less sensitive to poisoning phenomena. Life time measurements show indeed that the electrode is extremely stable, operating for 1000 hours at a current density of 250 mA/cm² [115].

The overpotential of Pt-Ru catalyst for methanol oxidation is much lower than for pure Pt: at a 85:15 Pt-Ru alloy CO₂ production begins already at 0.3 V vs RHE, and this was ascribed to the ability of Ru to form adsorbed OH at much lower potentials than Pt, which is in agreement with ellipsometry results[116]. Ru is the more oxophilic element in the alloy. At higher potentials however (0.7 V) more CO₂ is produced on Pt than on Pt-Ru. As discussed earlier, this is probably due to the oxygen surface coverage on the PtRu alloy becoming too high for easy CH₃OH adsorption.

Exactly why the addition of Ru to Pt enhances the methanol oxidation activity is still not completely clear. As described above, there is some evidence of the existence of a ligand effect resulting in a weakening of the bond between Pt and the methanolic adsorbate. On the other hand, there is now increasing evidence for an increased facility of water activation[117],[118],[119],[120],[121]. Prima facie evidence for the latter view is provided by Fra-

$$i_{ox} = nFk_{ox} \theta_{Ru} \theta_{CH_3OH} \exp(\beta F(E-E^0/RT)) \quad (1)$$

naszczuk et al.[122] who reported that the reaction rate is proportional to the amount of Ru present on the surface (cf eq. 1), and by the fact that at higher potentials PtRu is actually less efficient than Pt itself, the effect of Ru is found to increase with a decrease in potential[118]. However the absence of a poisoning term in eq(1) could well be due to the above mentioned ligand effect, thus suggesting that Ru plays a double role[113]. The work of Gasteiger et al. [117-120] on perfectly smooth alloys with well defined surface composition shows that the optimum in methanol oxidation activity in the presence of Ru, can be found with a ca 10% Ru surface coverage. This is further corroborated by a statistical analysis[117]. At lower potentials and higher temperatures the optimum amount of Ru increases[118], the latter effect being due to the adsorption of methanol on Ru, an effect which is absent at room temperature. These results are in agreement with the earlier results by Petrii et al.[123],[124].

In spite of the increasing evidence for the bifunctional effect of Ru, still some effects are found, which cannot be explained on basis of this, such as the facilitated adsorption of methanol on PtRu electrodes[125]. It must furthermore be mentioned that there is no enhancement in activity when Ru is present on a Pt(111) surface[121], which as discussed before, is free of poisoning adsorbates.

As to the valence state of the ruthenium, a combined Mössbauer/XPS study indicated that it is present as a Ru(IV) species in the fresh electrode, though not as the rutile RuO₂[115]. Based, e.g., on the combined TPR/CV study of Mahmood et al.[126], one should expect Ru to be reduced to Ru(0) in the initial stages of the CH₃OH oxidation run (i.e. at low potentials). Satisfyingly, an XPS study by Goodenough et al.[113] showed that upon use the B.E. of the Ru 3d_{5/2} peak decreased from 281.0 eV to 280.2 eV, which is close to the value expected for metallic Ru (279.9 eV). Thus, in the working electrode Ru is probably in its zero valent state.

Carbon supported Platinum/Ruthenium catalysts.

PtRu/C catalysts are more active for the methanol electrooxidation than Pt/C only or PtSn/C[127]. As has been discussed before, Pt/C seems to be quite optimal concerning the water activation. In view of this, it would seem to be at least strange that the effect of Ru is only through water activation. There should be an additional electronic (ligand) effect.

The preparation method is again of considerable influence on the catalyst performance. Buckley and Kennedy[128] studied the composition of the catalyst and the valence state of Pt and Ru as a function of the preparation method, sadly enough however, methanol oxidation activities were not reported. Their results show that a different preparation method results in a different particle size and a different amount of Ru present on the surface. From the XPS[129] and ⁹⁹Ru Mössbauer measurements[115], it is deduced that Ru is present as an oxidised species, probably Ru(IV). This Ru(IV) species is however not the rutile RuO₂, which was

shown to be inactive for the methanol oxidation[130]. In addition to this, Goodenough et al.[131] found evidence for a Ru(III) species from ESR and EXAFS measurements. Oddly enough there are no signs of a Ru(0) species.

The mechanism proposed by Hamnett et al.[83],[132] supposes that the primary effect of Ru is coming from water activation, something which was confirmed in some other studies[133],[134]. As we discussed before however, unsupported Pt/C catalysts seem to be fairly capable in activating water, it is thus strange that the effect of Ru is due to only water activation. Some work still needs to be done in this area.

A final point of concern for the PtRu/C catalysts is their stability during methanol oxidation, on which point no consensus is found in the literature. Both stable and unstable behavior has been reported. It is still not clear what is the cause of this variation in behavior. It is possible that fast decrease in activity is due to the formation of RuO₂, which is inactive for the methanol electrooxidation as has been noted before.

Other Bimetallic Systems

Other metals have been suggested as a promotor too. Small increases of activity were found for Mo[135],[136],[137], Nb₂O₅, TiO₂[138], ZrO₂[139] and platinum containing Ni-Nb alloys[140]. Furthermore it has been shown that Au[141], Cu[54], Ag, As, Pb[36, 53], Bi[142],[143] and Sb[144] result in a decrease in the methanol oxidation activity.

Supports other than carbon

SPE supported platinum electrodes.

The introduction of Solid Polymer Electrolyte (SPE) membranes as electrolyte and support system has led to extensive investigations on Pt-SPE electrodes for methanol oxidation[145],[146]. Although Pt supported by SPE shows less activity per real cm² than Pt-Pt, Aramata and Veersai[147],[148] found that the activity of the SPE supported catalyst does not decrease. As with carbon supported Pt, the activity was found to increase substantially with the addition of Sn or Ru[149],[150] the highest activity being obtained with a PtRuSn alloy[151].

A reasonable explanation for the long-term stability is the stabilisation of Pt-oxides. From XPS spectra it appears that the ratio of Pt²⁺/Pt is greater on Pt-SPE than on platinumised platinum[148]. It is suggested that the Pt²⁺ species is stabilized by the SPE matrix; this is the same effect as previously reported for Pt-SnO₂.

Tungsten Oxide Supported Pt Electrodes.

Tungsten oxides have been examined as a supporting material for platinum based electrodes,

both as pure tungsten oxides and as rare-earth metal tungsten bronze (Ln_xWO_3). WO_3 codeposited with Pt on carbon appears to act as an inhibitor for methanol oxidation[152], and Machida et al.[153] found the pure rare earth tungsten bronzes do not show any activity, Pt doped systems ($\text{PtDy}_{0.1}\text{WO}_3$) however do. Tseung et al. [154],[155] reported an increase in the methanol oxidation activity for co-deposited Pt- WO_3 systems compared to Pt-Pt. A 200 mV cathodic shift was reported, the formation of CO_2 already starting at +0.25 V vs RHE. The effect of the WO_3 was ascribed to an increased water activation. It has been furthermore suggested[153] that the higher activity is due to the removal of the strongly adsorbed species (CO) by a $\text{WO}_3/\text{WO}_3^+$ redox couple; however no clear relationship between the redox potential of this couple and the specific activity was found.

W(VI,V) oxide films with low loadings of platinum were investigated by Kulesza and Faulkner[156]. A substantial increase in the methanol oxidation current was found when the scan was initiated at a potential sufficiently negative to form hydrogen tungsten bronzes. It is likely that those bronzes reduce the adsorbates that accumulate on the electrode surface[156]. It is clear that hydrogen- as well as metal tungsten bronzes could be promising as a support for platinum in methanol electrooxidation. To improve the activity, more insight is required in the mechanism by which these systems work.

Polyaniline and polypyrrole

Considerable interest[157],[158],[159] has also arisen in polyaniline as a support for Pt. The first results show that with methanol oxidation the main product is HCHO. Furthermore addition of Ru[160] and Sn[161] result in a more efficient oxidation and an increase in activity, where PtRu in polyaniline is the most active. A higher activity than Pt alone was also reported for Pt in polypyrrole[162], the activity however being given for the geometric surface area.

Tungsten carbide.

According to Levy and Boudart[163] the electronic structure of WC is similar to that of Pt, which implies that WC could be a catalyst for methanol oxidation. The major problem is that WC does not easily adsorb methanol, whereas water is adsorbed very strongly[164], which is just the opposite behavior of platinum itself. Some methanol oxidation activity[165],[166] was however found, especially in the presence of Mo[167],[168].

It is clear that WC has an activity that is far too low for practical purposes. It might however be suitable as a support for platinum based catalysts.

Conclusions

On pure, smooth Pt the activation of water is the most difficult step. The methanolic adsorbates are usually divided into poisons and true reaction intermediates. Adsorbed CO is universally regarded as a poison, blocking the surface for further methanol adsorption. On the nature of the true intermediate(s) opinion is still divided, despite the advent of powerful in-situ spectroscopic methods: the most promising candidates are $\equiv\text{COH}$ and $-\text{CHO}$.

On small Pt particles water activation is much easier than on low surface area Pt. In fact, the smaller the particles the easier they are oxidised. This could well explain the often, but not always!, observed volcano-shaped relationship between specific methanol oxidation current and the particle size. Whether there is any Pt/support interaction is difficult to determine: no dedicated studies have been devoted to this subject, and only vague indications exist.

Promotion of Pt with Sn has often been claimed, but there is no consensus at all on the magnitude of the effect, some workers even reporting a negative one. Curiously, more unanimity exists as to the result of physical measurements. From XPS, e.g., it is deduced that the presence of Sn makes Pt more oxidisable. The valence state of Sn_{ad} , on the other hand, is not known beyond reasonable doubt. Optimum levels of Sn are always low, because it blocks the surface for methanol adsorption.

The promoting effect of Ru is consistently reported to be large, and not restricted to low Ru:Pt surface ratios. The action of Ru is probably through increased water activation compared to Pt alone, and through a ligand effect resulting in a weaker Pt-methanolic residue bond. This latter point follows from in-situ IR spectra and from the fact that Pt/C catalysts with optimal size as far as water activation is concerned, can still be promoted by Ru.

As to long-term stability: it is low for smooth Pt electrodes, and this is attributed to the accumulation of adsorbed CO. The stability of small Pt particles supported on carbon is much higher. The deactivation that does occur is probably due to adsorbed oxygen accumulating on the surface, although the formation of carbonaceous residues can not be completely excluded. The stability of PtSn and PtRu electrodes can be very high (relatively speaking) and seems to be ultimately limited by the formation of SnO_2 and RuO_2 , which block the Pt surface.

Acknowledgement.

We gratefully thank Paul Christensen for providing the papers on the in-situ IR work.

REFERENCES

- 1.R. Parsons, T. VanderNoot *J. Electroanal. Chem.* **257**, 9 (1988).
- 2.J.M. Leger, C. Lamy *Ber. Bunsenges. Phys. Chem.* **94**, 1021 (1990).
- 3.T. Iwasita-Vielstich in *Advances in Electrochemical Science and Engineering*, Vol.1 127-171, VCH New York 1990.
- 4.B.D. McNicol *J. Electroanal. Chem.* **118**, 71 (1981).

5. T. Frelink, W. Visscher, J.A.R. van Veen *in preparation*.
6. K. Franaszcuk, E. Herrera, P. Zelenay, A. Wieckowski, J. Wang, R.I. Masel *J. Phys. Chem.* **96**, 8509 (1992).
7. B.A. Sexton *Surf. Sci.* **102**, 271 (1981).
8. L.D. Burke, J.K. Casey *Electrochim. Acta.* **37**, 1817 (1992).
9. L.D. Burke, J.F. Healy, K.J. O'Dwyer, W.A. O'Leary *J. Electrochem. Soc.* **136**, 1015 (1989).
10. Yu.B. Vassiliev, B.M. Lotvin *Electrochim. Acta.* **30**, 1345 (1985).
11. A. Bewick, K. Kunimatsu, B.S. Pons, J.W. Russel *J. Electroanal. Chem.* **160**, 47 (1984).
12. S. Pons, T. Davidson, A. Bewick *J. Electroanal. Chem.* **160**, 63 (1984).
13. K. Kunimatsu *J. Electroanal. Chem.* **213**, 149 (1986).
14. D.S. Corrigan, M.J. Weaver *J. Electroanal. Chem.* **241**, 143 (1988).
15. K. Kunimatsu *J. Electron Spectrosc.* **30**, 215 (1983).
16. O. Wolter, J. Heitbaum *Ber. Bunsenges. Phys. Chem.* **88**, 2 (1984).
17. S. Wilhelm, W. Vielstich, H.W. Buschmann, T. Iwasita *J. Electroanal. Chem.* **229**, 377 (1987).
18. C.P. Wilde, M. Zhang *Electrochim. Acta* **39**, 347 (1994).
19. K. Shimazu, K. Kaneda, H. Kita *Bull. Chem. Soc. Jpn.* **67**, 2069 (1994).
20. A. Peremans, A. Tadjedinne, M. Suhren, R. Prazeres, F. Glotin, D. Jaroszinsky, J.M. Ortega *J. Electron Spectrosc. Relat. Phen.* **64**, 391 (1993).
21. Y. Zhang, M.J. Weaver *Langmuir* **9**, 1397 (1993).
22. K. Chandrakesaran, J.C. Wass, J.O'M. Bockris *J. Electrochem. Soc.* **137**, 518 (1990).
23. B.I. Podlovchenko, E.P. Gorgonova *Dokl. Akad. Nauk. SSSR* **156**, 673 (1964).
24. J. Willsau, O. Wolter, J. Heitbaum *J. Electroanal. Chem.* **185**, 163 (1985)
25. L-W. H. Leung, M.J. Weaver *Langmuir* **6**, 323 (1990).
26. J. Willsau, J. Heitbaum *J. Electroanal. Chem.* **185**, 181 (1985).
27. T. Iwasita, W. Vielstich, E. Santos *J. Electroanal. Chem.* **229**, 367 (1987).
28. S. Wilhelm, T. Iwasita, W. Vielstich *J. Electroanal. Chem.* **238**, 383 (1987).
29. T. Iwasita, U. Vogel *Electrochim. Acta* **33**, 557 (1988).
30. B. Beden, F. Kardigan, C. Lamy, J.M. Leger *J. Electroanal. Chem.* **121**, 343 (1981)
31. K. Kunimatsu *Ber. Bunsenges. Phys. Chem.* **94**, 1025 (1990).
32. B. Beden, F. Hahn, S. Juanto, C. Lamy, J.M. Leger *J. Electroanal. Chem.* **225**, 215 (1987)
33. W. Vielstich, P.A. Christensen, S.A. Weeks, A. Hamnett *J. Electroanal. Chem.* **242**, 327 (1988).
34. A. Papoutsis, J.M. Leger, C. Lamy *J. Electroanal. Chem.* **359**, 141 (1993).
35. J. A. Caram, C. Gutierrez *J. Electroanal. Chem.* **323**, 213 (1992).
36. E.P.M. Leiva, M.C. Giordano *J. Electroanal. Chem.* **158**, 115 (1983).
37. A. Peremans, A. Tadjedinne *Chem. Phys. Lett.* **220**, 481 (1994).
38. B. Beden, F. Hahn, J.M. Leger, C. Lamy, C.L. Perdriel, N.R. De Tacconi, R.O. Lezna, A.J. Arvia *J. Electroanal. Chem.* **301**, 129 (1991).
39. M.C. Pham, J. Moslih, M. Simon, P.C. Lacaze *J. Electroanal. Chem.* **282**, 287 (1990).

Chapter 2

40. T. Iwasita, F.C. Nart, W. Vielstich *Ber. Bunsenges. Phys. Chem.* **94**, 1030 (1990).
41. M.I.S. Lopes, B. Beden, F. Hahn, J.M. Leger, C. Lamy *J. Electroanal. Chem.* **313**, 323 (1991).
42. M.I. Lopes, I. Fonseca, P. Olivi, B. Beden, F. Hahn, J.M. Leger, C. Lamy *J. Electroanal. Chem.* **346**, 415 (1993).
43. M.C. Arevalo, A.M. Castro-Luna, A. Arevalo, A.J. Arvia *J. Electroanal. Chem.* **330**, 595 (1992).
44. T. Iwasita, F.C. Nart, B. Lopez, W. Vielstich *Electrochim. Acta* **37**, 2361 (1992).
45. R.J. Nichols, A. Bewick *Electrochim. Acta* **33**, 1691 (1981).
46. B. Bittins-Cattaneo, E. Santos, W. Vielstich, U. Linke *Electrochim. Acta* **33**, 1499 (1988).
47. I. Villegas, M.J. Weaver *J. Chem. Phys.* **101**, 1648 (1994).
48. C. Lamy, J.M. Leger *J. Chim. Phys.* **88**, 1649 (1991).
49. E. Herrero, K. Franaszczuk, A. Wieckowski *J. Phys. Chem.* **98**, 5074 (1994).
50. C. Lamy, J.M. Leger, J. Clavilier, R. Parsons *J. electroanal. Chem.* **150**, 71 (1983).
51. H. Kita, Y. Gao, T. Nakato, H. Hattori *J. Electroanal. Chem.* **373**, 177 (1994).
52. J. Sobkowski, K. Franaszczuk, K. Dobrowolska *J. Electroanal. Chem.* **330**, 529 (1992).
53. E.P.M. Leiva, M.C. Giordano *J. Electrochem. Soc.* **130**, 1305 (1983).
54. N. Markovic, P.N. Ross *J. Electroanal. Chem.* **330**, 499 (1992).
55. A.M. Castro Luna, M.C. Giordano, A.J. Arvia *J. Electroanal. Chem.* **259**, 173 (1989).
56. D.S. Cameron, G.A. Hards, B. Harrison, R.J. Potter *Plat. Met. Rev.* **31**, 173 (1987).
57. R. Inada, K. Shimazu, H. Kita *J. Electroanal. Chem.* **277**, 315 (1990).
58. T. Biegler, D.F.A. Koch *J. Electrochem. Soc.* **114**, 904 (1967).
59. V.S. Bagotzky, Yu.B. Vassiliev *Electrochim. Acta* **11**, 1439 (1966).
60. B. Beden, F. Hahn, C. Lamy, J.M. Leger, N.R. de Tacconi, R.O. Lezna, A.J. Arvia *J. Electroanal. Chem.* **261**, 401 (1989).
61. A.C. Chialvo, W.E. Tracia, A.J. Arvia *J. Electroanal. Chem.* **146**, 93 (1983).
62. P.A. Christensen, A. Hamnett, G.L. Troughton *To be published in J. Electroanal. Chem.*
63. H.E. v. Dam, H. v. Bekkum *J. Catal.* **131**, 335 (1991).
64. D. Richard, P. Gallezot in *Preparation of Catalysts IV* B. Delmon, P. Grange, P.A. Jacobs and G. Poncelet (Editors). Elsevier 1987, Amsterdam.
65. K. Aika, L.L. Ban, I. Okura, S. Namba, J. Turkevich *J. Res. Inst. Catalysis Hokkaido Univ.* **24**, 54 (1976).
66. K. Yahikozawa, Y. Fujii, Y. Matsuda, K. Nishimura, Y. Takasu *Electrochim. Acta* **36**, 973 (1991).
67. M. Hogarth, J. Munk, A.K. Shukla, A. Hamnett *J. Appl. Electrochem.* **24**, 85 (1994).
68. L.J. Hillenbrand, J.W. Lacksonen *J. Electrochem. Soc.* **112**, 249 (1965).
69. J. Escard, C. Leclerc, J.P. Contour *J. Catal.* **29**, 31 (1973).
70. J.B. Goodenough, A. Hamnett, B.J. Kennedy, S.A. Weeks *Electrochimica Acta* **32**, 1233 (1987).
71. Y. Takasu, Y. Fujii, K. Yasuda, Y. Iwanaga, Y. Matsuda *Electrochim. Acta* **34**, 453 (1989).
72. F. Parmigiani, E. Kay, P.S. Bagus *J. Electron. Spectrosc. Relat. Phenom.* **50**, 39 (1990).
73. N.I. Jaeger, A.L. Jourdan, G. Schulz-Ekloff *J. Chem. Soc. Faraday Trans.* **87**, 1251 (1991).
74. B. Sen, M. Vannice *J. Catal.* **129**, 31 (1991).

75. P.A. Attwood, B.D. McNicol, R.T. Short *J. Appl. Electrochem.* **10**, 213 (1980).
76. A.K. Shukla, M.K. Ravikumar, A. Roy, S.R. Barman, D.D. Sarma, A.S. Arico, V. Antonucci, L. Pino, N. Giordano *J. Electrochem. Soc.* **141**, 1517 (1994).
77. Y. Matsuda, Y. Fujii, Y. Matsuda *Bull. Chem. Soc. Jpn.* **59**, 3973 (1986).
78. K.I. Machida, A. Fukuoka, M. Ichikawa, M. Enyo *J. Electrochem. Soc.* **138**, 1958 (1991).
79. A. Kabbabi, F. Gloaguen, F. Andolfatto, R. Durand *J. Electroanal. Chem.* **373**, 251 (1994).
80. M. Watanabe, S. Saegusa, P. Stonehart *J. Electroanal. Chem.* **271**, 213 (1989).
81. P.A. Christensen, A. Hamnett, J. Munk *To be published in J. Electroanal. Chem.*.
82. P.A. Christensen, A. Hamnett, S.A. Weeks *J. Electroanal. Chem.* **250**, 127 (1988).
83. B.J. Kennedy, A. Hamnett *J. Electroanal. Chem.* **283**, 271 (1990).
84. J.B. Goodenough, A. Hamnett, B.J. Kennedy, R. Manoharan, S.A. Weeks *Electrochim. Acta* **35**, 199 (1990).
85. M.M.P. Janssen, J. Moolhuysen *Electrochim. Acta* **21**, 869 (1976).
86. N. Kizhakevariam, M.J. Weaver *Surf. Sci.* **310**, 183 (1994).
87. M.M.P. Janssen, J. Moolhuysen *J. Catal.* **46**, 289 (1977).
88. M.M.P. Janssen, J. Moolhuysen *Electrochim. Act.* **21**, 861 (1976).
89. K.J. Cathro *J. Electrochem. Soc.* **116**, 1608 (1969).
90. M. Watanabe, M. Shibata, S. Motoo *J. Electroanal. Chem.* **187**, 161 (1985).
91. M.M. Stefanel, T. Chierchie, C. Mayer *Zeit. Phys. Chem.* **135**, 251 (1983).
92. B.J. Bowles, T.E. Cranshaw *Phys. Lett.* **17**, 258 (1965).
93. M.R. Andrew, J.S. Drury, B.D. McNicol, C. Pinnington, R.T. Short *J. Appl. Electrochem.* **6**, 99 (1976).
94. B.D. McNicol, R.T. Short, A.G. Chapman *J. Chem. Soc. Far. Trans* **72**, 2735 (1976).
95. M. Watanabe, Y. Furuuchi, S. Motoo *J. Electroanal. Chem.* **191**, 367 (1985).
96. A. Katayama *J. Phys. Chem.* **84**, 376 (1980).
97. A. Aramata, I. Toyoshima, M. Enyo *Electrochim. Acta* **37**, 1317 (1992).
98. S.R. Wang, P.S. Fedkiw *J. Electrochem. Soc.* **139**, 2519 (1992).
99. S.R. Wang, P.S. Fedkiw *J. Electrochem. Soc.* **139**, 3151 (1992).
100. G.L. Throughton, A. Hamnett *Bull. Electrochem.* **7**, 488 (1991).
101. S. Swathirajan, Y.M. Mikhail *J. Electrochem. Soc.* **139**, 2105 (1992).
102. A.S. Arico, V. Antonucci, N. Giordano, A.K. Shukla, M.K. Ravikumar, A. Roy, S.R. Barman, D.D. Sarma *J. Pow. Sourc.* **50**, 295 (1994).
103. B. Bittins-Cattaneo, T. Iwasita *J. Electroanal. Chem.* **238**, 151 (1987).
104. Yu. B. Vassiliev, V.S. Bagotzky, N.V. Osetrova, A.A. Mikhailova *J. Electroanal. Chem.* **97**, 63 (1979).
105. A. Norton-Haner, P.N. Ross *J. Phys. Chem.* **95**, 3740 (1991).
106. M. Kubota *Inorg. Chem.* **29**, 574 (1990).
107. B. Beden, F. Kadirgan, C. Lamy, J.M. Leger *J. Electroanal. Chem.* **127**, 75 (1981).
108. T.E. Villar, T. Rabockai *J. Braz. Chem. Soc.* **2**, 86 (1991).
109. G. Gökgağaç, B.J. Kennedy, J.D. Cashion, L.J. Brown *J. Chem. Soc. Faraday Trans.* **89**, 151 (1993).

Chapter 2

- 110.S.A. Campbell, R. Parsons *J. Chem. Soc. Faraday. Trans.* **88**, 833 (1992).
- 111.E. Lamy-Pitara, L.F. Ouazzani-Benhima, J. Barbier, M. Cahoreau, J. Caisso *J. Electroanal. Chem.* **372**, 233 (1994).
- 112.B. D. McNicol in *Catalysis, A specialist Periodical Report* Vol. 2 The Chemical Society London, 1978 p 243-267.
- 113..J.B. Goodenough, A. Hamnett, R. Manoharan, B.J. Kennedy, S.A. Weeks *J. Electroanal. Chem.* **240**, 133 (1988).
- 114.R. Iannelo, V.M. Schmidt, U. Stimming, J. Stumper, A. Wallau *Electrochim. Acta* **39**, 1863 (1994).
- 115.A. Hamnett, B.J. Kennedy, F.E. Wagner *J. Catal.* **124**, 30 (1990).
- 116.E. Ticianelli, J.G. Beery, M.T. Paffet, S. Gottesfeld *J. Electroanal. Chem.* **258**, 61 (1989).
- 117.H.A. Gasteiger, N. Markovic, P.N. Ross, E.J. Cairns *J. Phys. Chem.* **97**, 12020 (1993).
- 118.H.A. Gasteiger, N. Markovic, P.N. Ross, E.J. Cairns *J. Electrochem. Soc.* **141**, 1795 (1994).
- 119.H. A. Gasteiger, N. Markovic, P.N. Ross, E.J. Cairns *Electrochim. Acta* **39**, 1825 (1994).
- 120.N.R. Markovic, H.A. Gasteiger, P.N. Ross, X. Jiang, I. Villegas, M.J. Weaver *Electrochim. Acta* **40**, 91 (1995).
- 121.E. Herrero, K. Francaszczuk, A. Wieckowski *J. Electroanal. Chem.* **361**, 269 (1993).
- 122.K. Francaszczuk, J. Sobkowski *J. Electroanal. Chem.* **327**, 235 (1992).
- 123.V.S. Entina, O.A. Petrii *Elektrokhimiya* **4**, 111 and 678 (1968).
- 124.O.A. Petrii *Dokl. Nauk. Akad. SSSR* **160**, 871 (1965).
- 125.M. Krausa, W. Vielstich *J. Electroanal. Chem.* **379**, 307 (1994).
- 126.T. Mahmood, J.O. Williams, R. Miles, B.D. McNicol *J. Catal.* **72**, 218 (1981).
- 127.S. Surampudi, S.R. Naranayan, E. Vamos, H. Frank, G. Halpert, A. LaConti, J. Kosek, G.K. Surya Prakash, G.A. Olah *J. Pow. Sourc.* **47**, 377 (1994).
- 128.A.N. Buckley, B.J. Kennedy *J. Electroanal. Chem.* **302**, 261 (1991).
- 129.M. Watanabe, M. Uchida, S. Motoo *J. Electroanal. Chem.* **229**, 395(1987).
- 130.B.J. Kennedy, A.W. Smith *J. Electroanal. Chem.* **293**, 103 (1990).
- 131.J.B. Goodenough, R. Manoharan, A.K. Shukla *Chem. Mater.* **1**, 391 (1989).
- 132.A. Hamnett, S.A. Weeks, B.J. Kennedy, G. Troughton, P. Christensen *Ber. Bunsenges. Phys. Chem.* **94**, 1014 (1990).
- 133.S. Wasmus, W. Vielstich *J. Appl. Electrochem.* **23**, 120 (1993).
- 134.S. Swathirajan, Y.M. Mikhail . *J. Electrochem. Soc.* **138**, 1321 (1991).
- 135.J.A. Shropshire *J. Electrochem. Soc.* **112**, 465 (1965).
- 136.H. Nakajima, H. Kita *Electrochim. Acta* **35**, 849 (1990).
- 137.H. Kita, H. Nakajima, K. Shimazu *J. Electroanal. Chem.* **248**, 181 (1988).
- 138.A. Hamnett, B.J. Kennedy, S.A. Weeks *J. Electroanal. Chem.* **240**, 349 (1988).
- 139.A. Hamnett, P. Stevens, G.L. Troughton *Cat. Tod.* **7**, 219 (1990).
- 140.A. Kawashima, T. Kanda, K Hashimoto *Mat. Sci. Eng.* **92**, 521 (1988).
- 141.M. Watanabe, S. Motoo *J. Electroanal. Chem.* **60**, 259 (1975).
- 142.S.C. Chang, Y. Ho, M.J. Weaver *Surf. Sci.* **265**, 81 (1992).

143. E. Herrero, A. Fernandez-Vega, J.M. Feliu, A. Aldaz *J. Electroanal. Chem.* **350**, 73 (1993).
144. S.G. Sun, J. Lipkowski, Z. Latounian *J. Electrochem. Soc.* **137**, 2443 (1990).
145. H. Takenaka, E. Torikai *Kokai Tokkyo Koho (Japan Patent)* **55**, 38934 (1980).
146. A. Katayama, H. Nakajima, K. Fujikawa, H. Kita *Electrochim. Acta* **28**, 777 (1983).
147. A. Aramata, W. Veersai *Electrochim. Acta* **36**, 1043 (1991).
148. A. Aramata *J. Electroanal. Chem.* **162**, 153 (1984).
149. A. Aramata, T. Kodera, M. Masuda *J. Appl. Electrochem.* **18**, 577 (1988).
150. G. Meli, J.M. Leger, C. Lamy, R. Durand *J. Appl. Electrochem.* **23**, 197 (1993).
151. A. Aramata, M. Masuda *J. Electrochem. Soc.* **138**, 1949 (1991).
152. P.A. Christensen, A. Hamnett, B.J. Kennedy, S.A. Weeks *Proc. C.E.C. Contractors 1988*.
153. K.I. Machida, M. Enyo, G.Y. Adachi, J. Shiokawa *J. Electrochem. Soc.* **135**, 1955 (1988).
154. P.K. Shen, K. Chen, A.C.C. Tseung *J. Chem. Soc. Far. Trans* **90**, 3089 (1994).
155. P.K. Shen, A.C. Tseung *J. Electrochem. Soc.* **141**, 3083 (1994).
156. P.J. Kulesza, L.R. Faulkner *J. Electroanal. Chem.* **259**, 81 (1989).
157. P. Ocon-Esteban, J.M. Leger, C. Lamy, E. Genies *J. Appl. Electrochem.* **19**, 462 (1989).
158. H. Laborde, J.M. Leger, C. Lamy *J. Appl. Electrochem.* **24**, 219 (1994).
159. K.M. Kost, D.E. Bartak, B. Kazee, T. Kuwana *Anal. Chem.* **60**, 2379 (1988).
160. H. Laborde, J.M. Leger, C. Lamy *J. Appl. Electrochem.* **24**, 1019 (1994).
161. C.T. Hable, M.S. Wrighton *Langmuir* **9**, 3284 (1993).
162. D.J. Strike, N.F. de Rooy, M. Koudhelka-Hep, M. Ullmann, J. Augustinsky *J. Appl. Electrochem.* **22**, 922 (1992).
163. R.B. Levy, M. Boudart *Science* **181**, 547 (1973).
164. G. Schulz-Ekloff *Coll. Czech. Chem. Comm.* **36**, 928 (1971).
165. H. Okamoto, G. Kawamura, A. Ishikawa, T. Kudo *J. Electrochem. Soc.* **134**, 1645 (1987); **134**, 1649 (1987)
166. K. Machida, M. Enyo *J. Electrochem. Soc.* **137**, 871 (1990).
167. H. Scholl, B. Hofman *Elektrokhimiya* **26**, 769 (1990).
168. G. Bronoel, S. Besse, N. Tassin *Electrochim. Acta* **37**, 1351 (1992).

Chapter 2

CHAPTER 3

Experimental Methods.

Introduction.

In this chapter the measurement techniques that have been used will be described. First of all cyclic voltammetry is discussed, then the in-situ electrochemical techniques are discussed; Differential Electrochemical Mass Spectroscopy, Electrochemical Quartz Crystal Microbalance, and Ellipsometry.

Cyclic Voltammetry.

Cyclic voltammetry is probably the most widely used technique for the electrochemical characterization of catalysts.

The theoretical as well as experimental aspects have been extensively covered[see for example refs. 1,2,3]. A short description will be given here, with attention to the application of this technique for the characterization of, and the study of the methanol electrooxidation on, Pt based catalysts.

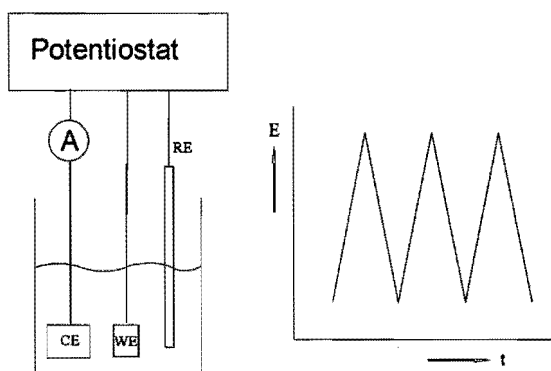


Figure 1 Three electrode system for cyclic voltammetry (left) and the potential program for cyclic voltammetry (right). WE=Work electrode; CE=Counter Electrode; RE=Reference electrode.

A schematic representation of the electrochemical cell that is used for cyclic voltammetry is given in Figure 1. A three electrode system is used, where the potential of the work electrode is changed, with respect to the fixed potential of the reference electrode, according to a potential program in Figure 1. In the experiments described in this thesis, mostly a $\text{Hg}/\text{Hg}_2\text{SO}_4$ reference electrode has been used. This reference electrode, which is denoted as MSE, has a potential of $E = +0.68 \text{ V}$ vs RHE (Reversible Hydrogen Electrode), which has by convention a

Chapter 3

potential of $E = 0.0$ V at room temperature and $a_{H^+} = 1$. Throughout this thesis both electrodes will be used in the description of the experiments.

Characterization of Pt [4,5,6].

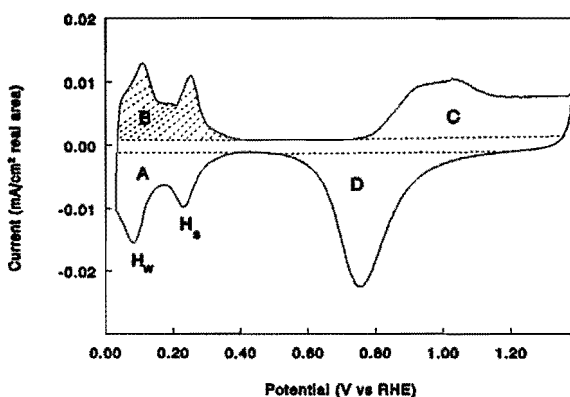


Figure 2 Example of a cyclic voltammogram of a Pt electrode in 0.5 M H_2SO_4 . $v=10$ mV/s

Cyclic voltammetry was for the first time used to study Pt in a acidic electrolyte by Will and Knorr[7]. The result of a cyclic voltammetric experiment on Pt in 0.5 M H_2SO_4 is shown in Figure 2. Four regions can be distinguished.

In region A, two reduction peaks are observed, which are due to the adsorption of hydrogen; the so-called strongly bonded hydrogen (H_s) and the weakly bonded hydrogen (H_w). Upon scan reversal at 0.03 V vs RHE, in region B two oxidation peaks are seen, due to the desorption of the adsorbed hydrogen, again in two steps. At a potential in between the H_s and H_w peaks in the positive going sweep, a third peak is often found, which we have shown to be due to the desorption of adsorbed molecular hydrogen[8]. At the end of the hydrogen adsorption region ($E=0.03$ V vs RHE), every Pt atom is covered by an adsorbed hydrogen atom. The charge used during the hydrogen adsorption or desorption thus gives the possibility of calculating the amount of Pt surface atoms and thus the real surface area of the Pt catalyst. For a polycrystalline Pt surface it is generally accepted that a charge of $Q_H=210\mu C$ corresponds to 1 cm^2 of Pt[9].

At higher potentials, in region C oxidation currents are found due to the oxidation of the Pt electrode surface, which takes place in two steps[10,11]:





where the second step only happens at potentials above 0.88 V vs RHE.

After scan reversal, in the cathodic scan a reduction peak is found (region D), which is due to the reduction of the Pt-oxide, which occurs in one step. The end potential in the cyclic voltammetric experiment determines the amount of Pt-oxide that is formed; the higher the end potential the more oxide is formed. Extensive scanning into the oxide region will cause surface roughening[12,13,14].

Between the so-called "hydrogen" and "oxide" regions there is the double layer region in which no faradaic processes occur, here water- and anion-adsorption are the major processes.

Methanol oxidation.

In Figure 3 the result of a cyclic voltammogram is given for Pt in 0.5 M H₂SO₄, in the presence

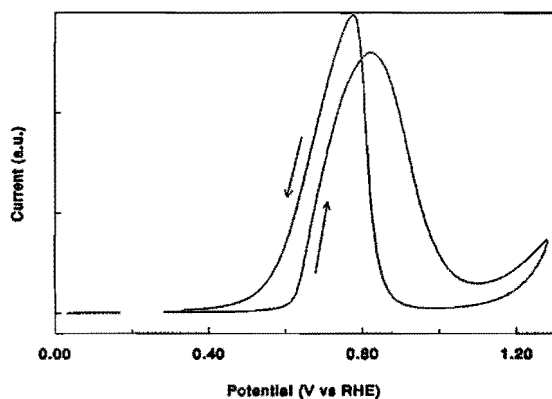


Figure 3 Example of a cyclic voltammogram of a Pt electrode in the presence of methanol. 0.5 M H₂SO₄, 0.1 M CH₃OH, $v=10$ mV/s.

of 0.1 M CH₃OH. It is first of all noted that the hydrogen adsorption/desorption region is suppressed considerably, due to the formation of adsorbed methanolic residues which block the surface for hydrogen adsorption. Furthermore in the anodic direction a current peak is seen due to the oxidation of methanol, this potential of this peak coincides with the potential of oxide formation (eq (2)) in the absence of CH₃OH. The oxides block the surface for further methanol adsorption and the current due to methanol oxidation will diminish until the surface is totally blocked by oxides. In the reverse scan the methanol oxidation starts at the potential where the Pt-oxide is reduced; there free Pt sites for methanol adsorption are created and

Chapter 3

methanol is oxidized again, until the potential is too low for the formation of an oxygen delivering species which is necessary for the oxidation of the methanol adsorbates. Although the peak in the cathodic scan has often been considered to be due to a poisoning species, an experiment in which methanol is added at the most anodic potential, after which the potential is scanned in cathodic direction, shows that the peak is due to freshly adsorbing CH_3OH [15].

In the positive going sweep, the oxidation of CH_3OH starts at ca. 0.48 V vs RHE. Considering the mechanism, discussed in chapter 2, a PtOH group is needed to oxidise the adsorbed methanolic residue. At these potentials however, no current due to PtOH formation is visible in the absence of methanol. Two explanations are possible:

(i) It is not PtOH that oxidises the methanol, but its precursor, an adsorbed water molecule $\text{Pt}(\text{H}_2\text{O})_{\text{ad}}$. This molecule then being adsorbed with the oxygen downwards. This idea was first suggested by Biegler[11], but is still not very generally accepted.

(ii) Methanol adsorbates induce the formation of PtOH, the methanol oxidation reaction now becoming semi-autocatalytic (which might lead to oscillations[16]). The adsorbed residue needs a PtOH group to get oxidized and the PtOH group needs methanolic residues to be formed. There is however some evidence against this explanation, since no change in Pt-oxide formation is found in the presence of methanol (as will be discussed in Chapter 7 and 10).

Considering this there is a slight preference for the first explanation.

Cyclic voltammetry is a dynamic technique. One of the implications is that the activities (or currents) that are measured for the methanol oxidation depend on the rate with which the potential is changed. Activities for the methanol oxidation are always measured by us in a semi-steady state experiment, i.e. a cyclic voltammogram measured with a low sweep rate between 1 and 5 mV/s. It was established that there is no change in activity with a change in scan rate, when the latter is below 5mV/s.

Differential Electrochemical Mass Spectroscopy.

Differential Electrochemical Mass Spectroscopy (DEMS) is based on the simultaneous measurement of volatile products and the current response of an electrode reaction as a function of the potential. This is achieved by attaching a porous electrode system directly to the ionization chamber of a Mass Spectrometer. The technique was developed by Heitbaum and co-workers[17,18] as an improvement of the proposal by Bruckenstein[19].

Here, first the electrochemical setup will be described, whereafter the calibration of the mass intensity measurements will be discussed.

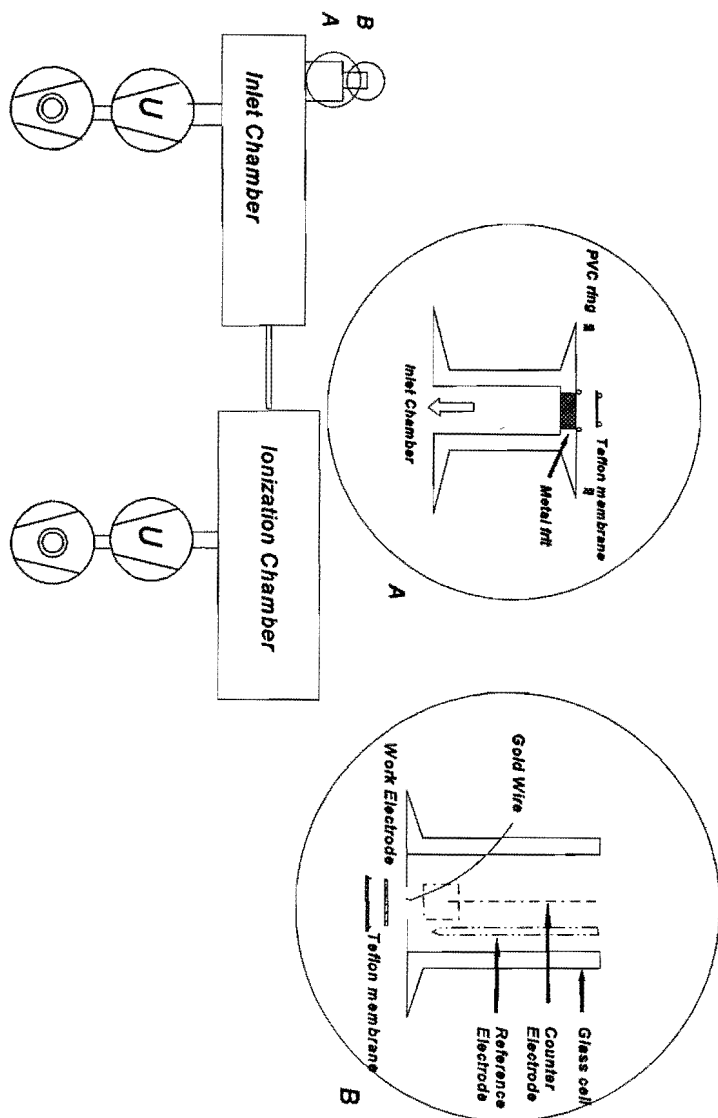


Figure 4 Schematic overview of DEMS. Inserts: (A) The inlet system; (B) The electrochemical Cell. Gas and electrolyte in- and outlet have been omitted for clarity.

Chapter 3

Experimental setup.

An schematic overview of the total setup, as it was built in our laboratory is given in Figure 4. The ionization chamber of a mass-spectrometer (Leyboldt PGA 100) is connected to an inlet system via a small tube. The connection can be closed with a pneumatic valve. The amount of gas flowing through the tube into the ionization chamber can be tuned with the valve between the inlet chamber and the first turbo-molecular pump.

The inlet system of the setup is shown enlarged in Figure 4A. It is placed on top of a pneumatic valve, which is necessary to be able to separate the "wet" part of the setup from the UHV part. It consists of a stainless steel part with a metal frit (which is necessary to withstand the atmospheric pressure) centered on top. On this frit a Teflon membrane (Schleicher and Schuell 0.02 μm) is placed, which is kept in place by two viton O-rings. The working electrode (which consists of either a platinum or gold gauze) is placed on top of the membrane.

The glass electrochemical cell, which is positioned on the inlet system with a PVC ring, is shown in Figure 4B. The volatile products formed during a reaction at the electrode will now directly flow into the inlet chamber, while the electrolyte is kept in the cell due to the small pores of the membrane. In the bottom of the cell is a circular opening of the size of the working electrode. Electrical connection to the working electrode is made via a gold wire, which is shielded from the solution by a Teflon sleeve. In the upper part of the cell are connections for electrolyte- and gas- inlet and outlet (not shown). Aside from the cell an electrolyte exchange system was built, in order to be able to exchange and keep three types of electrolyte under argon atmosphere.

Mass intensity measurements.

The mass-intensity(M) of a species is proportional to its partial pressure in the ionization chamber and thus also to its incoming flow:

$$M = K^0 \cdot J \quad (3)$$

where K^0 includes all the mass-spectrometer constants, electron emission current, multiplier voltage, pumping speed, etc. and J is the incoming flow in mol/s.

The flow rate can be correlated to the total current at the electrode through:

$$J = \frac{1}{nF} \cdot N \cdot A \cdot I \quad (4)$$

with n =the number of electrons transferred to produce one product molecule, F =the Faraday constant, A =current efficiency, I is the current and N is a collection efficiency. The mass-

intensity of a species can thus be found by combining equations 3 and 4:

$$M = C \cdot \frac{1}{n} \cdot A \cdot I \quad (5)$$

where C includes all the constants which are not specific for a given electrochemical process.



This constant has to be determined experimentally. In case of the methanol oxidation, the oxidation of adsorbed CO (eq 6) is used to calibrate the system. This can be done since for this reaction it is known that $A=1$. Measuring I and M during CO oxidation then gives C .

Although the strength of this technique is the direct determination of volatile reaction products, it of course suffers from a time delay ($t \leq 2s$), between the product being made at the electrode and it reaching the ionization chamber of the mass-spectrometer. Because of this delay time, the sweep rate in the cyclic voltammetric experiments has to be low, i.e. ≤ 2 mV/s.

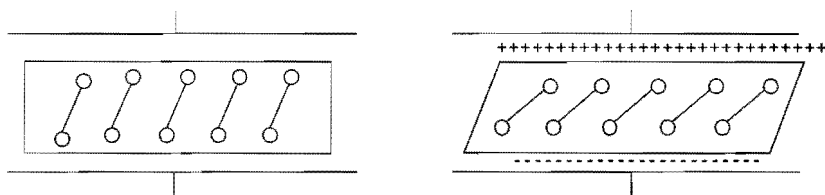


Figure 5 The effect of applying a voltage across a quartz crystal.

The Electrochemical Quartz Crystal Microbalance[20].

The Electrochemical Quartz Crystal Microbalance(EQCMB) is based on the inverse piezo-electric effect.

The piezo-electric effect was discovered by Jacques and Pierre Curie in 1880[21]. When mechanical stress is applied to the surface of for example quartz, an electric potential is afforded across the crystal, which is proportional to the applied stress. The electric potential is the results of shifting of the dipoles in the crystal.

The inverse piezo-electric effect also exists. Applying a voltage across the crystal, affords a corresponding mechanical strain, as depicted in Figure 5. Since the deformation in quartz is

Chapter 3

elastic and the strain induced by a potential of opposite polarity, is equal in magnitude and opposite in direction, an alternating current will cause a vibrational motion in the crystal.

The result of this vibrational motion is the establishment of a transverse acoustic wave across the crystal, reflecting back at the surfaces (Figure 6). This is essentially what the EQCMB technique is based on.

The frequency of the acoustic wave shown in Figure 6 is given by:

$$f_0 = v_{tr} / 2t_q \quad (7)$$

where v_{tr} is the transverse velocity of sound, given by:

$$v_{tr} = \sqrt{(\mu_q / \rho_q)} \quad (8)$$

ρ_q is the density of quartz, μ_q is the shear modulus of quartz and t is the thickness of the quartz crystal.

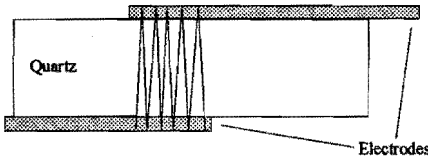


Figure 6 Reflection of an acoustic wave at the electrodes on a quartz crystal.

When there is a fractional change in thickness of the crystal, Δt , there will be a fractional change in frequency Δf . Thus:

$$f/f_0 = -\Delta t/t_q = -2f_0\Delta t/v_t \quad (9)$$

and:

$$\Delta f = \frac{-2nf_0^2\Delta m}{A\sqrt{(\mu_q\rho_q)}} = \frac{-\Delta m}{S} \quad (10)$$

which is the well known Sauerbrey[22] equation, where n stands for the n th overtone. The change in electrode thickness Δt is now expressed as $\Delta m/\rho_q A$, where Δm is the change in mass, A is the piezo-electrically active area, and S is the Sauerbrey constant.

Equation (4) shows that a change in electrode mass is inverse proportional to the change in frequency. An increase in mass will thus result in a decrease in frequency.

Experimental setup.

To suppress the appearance of a multitude of different frequencies during the measurement, quartz crystals with specific crystallographic orientations are used. For measurements at room temperature these are AT-cut quartz crystals.

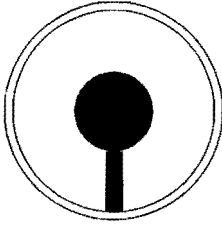


Figure 7 Electrode of a EQCMB; the Ti layer is shown in black.

On 5 MHz AT-cut quartz crystals a 5 nm Ti film was evaporated in a pattern as shown in Figure 7. The Ti film was used to improve the cohesion between the Pt (100 nm) and the quartz substrate.

The quartz crystals used had a diameter of 2.5 cm with an electrode of 0.9 cm diameter centered on top. On the back side the Ti pad had a diameter of 0.6 cm such that the edges of the electrode do not contribute to the frequency measurements. The crystals were used at their third harmonic overtone (15

MHz) so as to improve the mass sensitivity from ca 160 ng/Hzcm² to 18 ng/Hzcm² (cf eq.(10)). Since the resolution of the frequency measurement is ca 0.1 Hz, the minimum mass change detectable is ca 1.8 ng. A monolayer of for example Cu on 1 cm² of Pt weighs 147 ng, it is thus possible to detect close to 1 percent of a monolayer of Cu deposition.

Ellipsometry[23].

Ellipsometry is based on the change of polarization state of polarized light upon reflection at a surface. It is a very sensitive technique for the study of metal surfaces covered with thin films. When polarized light is reflected at a transparent surface, the parallel (p) component of the reflected light is more attenuated than the perpendicular (s) component, resulting in a change of polarization state of the light. This change depends on the angle of incidence (θ), the wavelength of the light, and the refractive index of the two media in question. In the case of a metal, instead of a transparent surface, also a phase shift (δ) is introduced between the incident and the reflected light, which is different for the p- and s- light. The reflected light is thus in general elliptically polarized light. In ellipsometry both the change in polarization state and the ellipticity are measured. The parameters concerned are $\Delta = \delta_p - \delta_s$ (phase shift) and $\tan\Psi$ (amplitude attenuation) which are given by:

$$\tan\Psi \exp(-i\Delta) = \frac{\hat{r}_p}{\hat{r}_s} \quad (11)$$

where r_p and r_s are the Fresnel reflection coefficients, which depend on the refractive indices of

Chapter 3

the two media (n) and the angle of incidence (θ)[24]. From the Fresnel coefficients, the refractive index of the metal can be calculated.

Ellipsometry is mostly used to measure the thickness (d) and the refractive index (n) of a thin film at a metal surface. Such a film changes the reflection behavior as is shown in Figure 8.

The reflected light from a film covered surface differs both in $\tan\Psi$ and Δ compared to the uncovered surface. The change in Δ and Ψ is a direct measure for the thickness and the

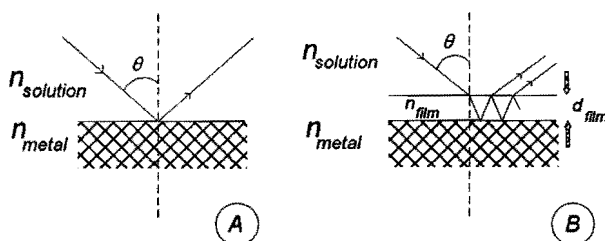


Figure 8 Reflection at a metal surface, and at a metal surface covered with a film of thickness d .

refractive index of the film. For very thin films ($d < 10$ nm) both Δ and Ψ change linearly with increasing film thickness. This even holds if the coverage with the film is less than a monolayer. The system then behaves as a system with an effective thickness.

Although the interpretation of ellipsometric results obtained for surface processes at metal electrodes at the submonolayer level is complex[24], changes in Δ and Ψ can be used to obtain information on the change in oxide formation behavior[25,26,27] and the presence of organic adsorbates[28] on smooth metal electrodes. The results obtained with ellipsometry will be discussed in chapters 8-10.

References

1. M. Noel, K. Vasu *Cyclic Voltammetry and the frontiers of Electrochemistry*, Aspect Publ. , London 1990.
2. G. Mabbott, *J. Chem. Ed.* **60**, 697 (1983).
3. A.J. Bard, L.J. Faulkner *Electrochemical Methods*, John Wiley and Sons, New York ,1980. Chapter 6.
4. S. Gilman in *Electroanalytical Chemistry*, A.J. Bard ed., Marcel Dekker New York, Vol. 2, 1967.
5. R. Woods in *Electroanalytical Chemistry*, A.J. Bard ed., Marcel Dekker New York Vol. 9, 1976.
6. H.E. Angerstein-Kozłowska, B.E. Conway, W.E. Sharp *J. Electroanal. Chem.* **43**, 9(1973).

- 7.F.G. Will, C.A. Knorr *Z. f. Elektrochem.* **64**, 258 (1960).
- 8.T. Frelink, W. Visscher, J.A.R. van Veen *Electrochim. Acta* **40**, 545 (1995).
- 9.T. Biegler, D.A.J. Rand, R. Woods *J. Electroanal. Chem.* **29**, 269 (1971).
- 10.B.E. Conway, H. Angerstein-Kozłowska *Acc. Chem. res.* **14**, 49 (1981).
- 11.T. Biegler *Aust. J. Chem.* **26**, 2571 (1973).
- 12.T. Frelink, T. Verhoeven, P. Gunther *unpublished AFM results*.
- 13.K. Yamamoto, D.M. Kolb, R. Kötz, G. Lemppühl *J. Electroanal. Chem.* **96**, 233 (1979).
- 14.H. You, Z. Nagy *Physica B* **198**, 187 (1994).
- 15.T. Frelink *unpublished results*.
- 16.M. Koper *PhD Thesis Univ. Utrecht*, 1994, Chapter 5.
- 17.O. Wolter, J. Heitbaum *Ber. Bunsenges. Phys. Chem.* **88**, 2, 6 (1984).
- 18.J. Willsau, O. Wolter, J. Heitbaum *J. Electroanal. Chem.* **185**, 163, 181 (1985).
- 19.S. Bruckenstein, R.R. Gadde *J. Am. Chem. Soc.* **93**, 793 (1971).
- 20.D.A. Buttry, M.D. Ward *Chem. Rev.* **92**, 1355 (1992).
- 21.P. Curie, J. Curie *C.R. Acad. Sci.* **91**, 294 (1880).
- 22.G. Sauerbrey *Z. Phys.* **155**, 206 (1955).
- 23.S. Gottesfeld in *Electroanalytical Chemistry*, A.J. Bard ed. Marcel Dekker New York Vol. 15, 1989 p143-266.
- 24.W. Visscher *J. of Materials Techn.* **4**, 303 (1973).
- 25.S. Shibata, M.P. Sumino *Electrochim Acta* **17**, 2215 (1972).
- 26.M. Peuckert, H.P. Bonzel *Surf. Sci.* **145**, 239 (1984).
- 27.J. Horkans, B.D. Cahan, E. Yeager *Surf. Sci.* **46**, 1 (1974).
- 28.P.J. Hyde, C.J. Maggiore, A. Redondo, S. Srinivasan, S. Gottesfeld *J. Electroanal. Chem.* **186**, 267 (1985).

Chapter 3

A DEMS Study on the Nature of the Adsorbate in the Electrooxidation of Methanol on Platinised Platinum.

Abstract

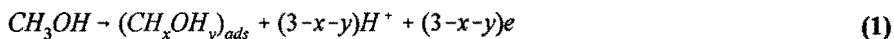
The adsorption and oxidation of methanol and CO on platinised Platinum were studied with DEMS. The number of electrons that is necessary to oxidise the formed adsorbate to CO₂, and the number of electrons per site upon oxidation were calculated. By comparing the oxidation behaviour for CO and methanol adsorbates, a proposition could then be made concerning the adsorbate structure. The influence of electrolyte anion, electrolyte concentration and adsorption potential on the adsorbate have been studied. Bridge- or multi-bonded CO seems to be the major adsorbed species, both for CO and CH₃OH, although differences between the two remain. These differences are discussed in terms of the adsorption geometry. Finally it was shown that activity for methanol oxidation increases with higher H_{strong}/H_{weak} ratio.

Introduction.

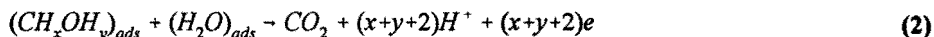
Exactly how methanol is electrooxidised over Pt in acid electrolyte continues to be an important research topic, mainly in the context of the development of direct methanol fuel cells.

Conceptually, two major steps can be distinguished in the oxidation process:

An adsorption step, in which there is a partial dehydrogenation of the methanol molecule:



and an oxidation step, in which the adsorbate is oxidised by an activated water molecule:



In spite of numerous investigations [1-25] on the nature of the adsorbed species, still no consensus has been reached on the values of x and y in the equations above. Many suggestions have been made.

With coulometric techniques [14,26,27] it was found that the adsorption and oxidation charge of methanol are equal and that the adsorbate should thus be -COH or -CHO. Although this conclusion was confirmed by studies involving Differential Electrochemical Mass Spectroscopy (DEMS)[1,2] and Electrochemical Thermal Desorption Mass Spectroscopy (ECTDMS)[16,17], it does not straightforwardly follow from in-situ IR measurements. IR experiments show

large amounts of linearly bonded CO[3] as adsorbate with small amounts of bridged bonded CO[5] and only sometimes -CHO[12] or -COH[5]. Villegas and Weaver[28] recently showed that the IR cross-section of bridge bonded CO is far smaller than that of linearly bonded CO, which may lead to an underestimation of the amount of bridge bonded CO species in IR experiments. It should also be stressed that, if detected at all, the amounts of -COH/-CHO always appear to be rather low, whereas the DEMS measurements suggest that -COH is the only intermediate present. ECTDMS however shows that with an increase in surface coverage -COH is transferred into CO. This is in agreement with the results of Beden et al.[9]; adsorbates other than CO only appear to be present at low methanol concentrations (i.e. at low surface coverages). As the adsorbate-surface bonding will vary with the type of adsorbate, one would expect a difference in oxidation potentials. It is therefore remarkable that no such strict correlation has been found with the in-situ techniques between the different adsorbate species and the position of the adsorbate oxidation peaks in cyclic voltammetry.

The possibility remains, however, that the apparent lack of consensus on the nature of the adsorbate is mainly due to the diversity of the experimental conditions, such as type of electrode, value of the adsorption potentials, and type and concentration of the background electrolyte.

Taking into account this possibility, the oxidation of the methanol adsorbate on platinised Platinum was studied with DEMS as a function of adsorbate surface coverage, adsorption potential, electrolyte concentration and electrolyte anion. For comparative purposes, the oxidation of the CO adsorbate was included as well. Also the influence of the ratio of weakly and strongly bonded hydrogen sites on the activity for methanol oxidation was studied. Although we are aware of the fact that the true intermediate of the methanol oxidation can only be established through in-situ detection of this species during continuous methanol oxidation, we have chosen to study the oxidation of the methanol adsorbate, as was also done in most of the papers cited [1-25]. At the end we will try to show what the implications of the results are for the intermediate during the continuous oxidation of methanol.

Experimental

Combined DEMS-Voltammetry measurements.

The experimental set-up of DEMS is similar to the one described previously [29]. Our mass-spectrometer system consisted of Leyboldt vacuum system coupled to a Leyboldt PGA 100 mass spectrometer. The DEMS cell was mounted on a stainless steel inlet system which consists of a metal frit with a Teflon membrane (Schleicher Schuell 0.02 μm pore size) on top. A platinised Pt gauze was placed on top of the membrane and was used as a working electrode, electrical contact was made via a gold wire. In this cell a Hg/Hg₂SO₄ reference and a Pt (sheet) counter electrode were used. The combined DEMS-voltammetry measurements were performed by a computer controlled Autolab (Eco Chemie) potentiostat, which is able to

record the mass-signal simultaneously with the current. All potentials are given vs RHE, taking $E_{MSE}=+0.68$ V.

The DEMS measurements were carried out with a platinised electrode, prepared from a 3×10^{-2} M H_2PtCl_6 solution, at a deposition current of 10 mA/cm² during 600 s, after which the electrode was thoroughly rinsed to remove possible chloride impurities.

All chemicals used in the DEMS experiments were of p.a. quality (Merck), all electrolyte solutions were made with ultrapure (18.2 M Ω , EcoStat) water.

Mass-intensity measurements.

The mass-intensity of CO₂ measured with the mass-spectrometer during CO or methanol adsorbate oxidation is related to the current by [1]:

$$M = K^0 \cdot J \quad (3)$$

where M=Mass-intensity, K^0 is a constant which includes all mass-spectrometer settings and J is the flux of CO₂ through the membrane into the ionization chamber. The flux is proportional to the faradaic current I by:

$$J = (1/nF) \cdot N \cdot A \cdot I \quad (4)$$

where n is the number of electrons necessary to produce one molecule of CO₂, F is the Faradaic constant, N is the collection efficiency and A is the current efficiency. A combination of these two equations gives a relation between the faradaic current and the CO₂ mass intensity:

$$M = C(1/n) \cdot A \cdot I \quad (5)$$

where C is the constant which represents all factors which are not specific for the electrochemical process. The oxidation of CO to CO₂ was used as calibration for the mass spectrometer signal. Assuming that the current efficiency is 1, for this reaction the value of n is known to be 2. The ratio between the total charge (Q_I) and the amount of CO (Q_M) produced upon oxidation of the adsorbate, then gives:

$$\frac{Q_I}{Q_M} = nK^* \quad (6)$$

By measuring this ratio for both CO and CH₃OH adsorbates, K_{CO}^* and $K_{CH_3OH}^*$ are obtained. From these data it is possible to determine the number of electrons necessary to oxidise the methanol adsorbate to CO₂, by calculating: $K^{**} = K_{CH_3OH}^* / K_{CO}^*$.

The number of electrons per Pt site (eps) released during adsorbate oxidation is calculated by:

$$eps = \frac{Q_{ox}}{Q_{H_0} - Q_{H_1}} \quad (7)$$

where (1) means in the presence of the adsorbate and (0) means without adsorbate. Furthermore the ratio between the adsorption and oxidation charge: Q_{ad}/Q_{ox} was calculated for methanol.

Calculated values for K^{**} , eps and Q_{ad}/Q_{ox} are given in Table 1 for a number of possible methanol adsorbate species.

Adsorbed Species	K^{**}	eps	Q_{ad}/Q_{ox}
-C=O	1	2	2
=C=O	1	1	2
≡C-O	1	0.67	2
≡COH	1.5	1	1
-CHO	1.5	3	1
-COOH	0.5	1	5

Table 1: Possible adsorbates, resulting from the methanol adsorption reaction and their theoretical values for K^{**} , eps, and Q_{ad}/Q_{ox} . The value of K^{**} is calculated on the basis of the fact that $K_{CO}^{*}=1$.

In particular the combination of K^{**} and eps is of interest: K^{**} gives information on the type of the intermediate and eps shows in which way the intermediate is bonded to the surface. The accuracy of the various measurements has been estimated to be as follows: For the K^{**} values, averages were taken over at least three measurements per surface coverage, and the deviation turns out to be $\pm 10\%$. The same deviation was found for the Q_{ad}/Q_{ox} ratio, although at low surface coverages it was difficult to determine Q_{ad} , therefore at low coverages data for this ratio have been omitted. For the eps values, averages over three measurements gave a deviation of $\pm 5\%$, but again at low coverages it was not possible to calculate these values accurately. All the deviations given here are the maximum deviations from the average.

CO adsorption and oxidation.

For each series of measurements CO was adsorbed at E_{ad} , during a given adsorption time from

a CO saturated solution, after which the solution was exchanged under Argon flow by fresh electrolyte. Then CO_{ad} was oxidized in a cyclic voltammetric scan starting either directly in the anodic direction or first in cathodic direction where the scan was reversed at 0.03 V in order to establish the surface coverage. By subtracting from the first scan, the second scan, in which adsorbate is no longer present, the CO oxidation charge could be obtained. Different surface coverages (θ) were obtained by varying the adsorption time.

The adsorption of CO was done from saturated CO solutions, in order to be able to obtain low as well as high CO coverages. Bubbling of CO gas did not give the possibility of obtaining low CO coverages. Furthermore the latter method may lead to non-homogeneous coverage of the electrode with CO, which will distort the measurement of K^* . Values of K^* from CO adsorbate oxidation experiments were also checked by calculating K^* from continuous CO oxidation experiments; both types of experiments were found to give the same value, thus confirming the validity of the CO adsorbate oxidation experiments. The disadvantage of adsorbing CO from saturated solutions turned out to be that CO coverages higher than 50% could not be obtained.

CH₃OH adsorption and oxidation.

For methanol a similar procedure was followed as for CO; in each series CH₃OH was adsorbed at the same potential as CO from a CH₃OH containing solution with different concentrations of methanol. After the adsorption the cell was flushed with electrolyte in order to remove all the methanol from the bulk. Then the oxidation of the methanol adsorbate was done in the same way as for the CO adsorbate.

Methanol activity measurements.

Platinised Pt electrodes with different amounts of strongly and weakly bonded hydrogen sites were prepared by electrodeposition onto a Pt sheet of 7 cm² area, using a solution with H₂PtCl₆ (Johnson and Matthey) in HCl and HClO₄ (Merck) and different deposition currents according to the method of Bakos and Horanyi[30].

For the three electrodes used here, the deposition solution consisted of 1×10^{-3} M H₂PtCl₆ and 1×10^{-1} M HCl. Deposition currents used were 5.3 mA/cm², 1.0 mA/cm², and 0.4 mA/cm². Deposition time was 1800 s. All chemicals used were of p.a. quality. The electrodes were characterized by recording the cyclic voltammogram in 0.5 M H₂SO₄ using a Wenking POS 73 potentiostat and a Philips PM 8041 X-Y recorder.

The electrochemical measurements were performed in a three compartment cell, with a Hg/Hg₂SO₄ reference electrode (+0.68 V vs RHE) and a Pt (sheet) counter electrode. All potentials, however are given with respect to RHE. The real surface area of the Pt-Pt electrode was measured by calculating the charge necessary to desorb the hydrogen atoms, assuming that 210 μC is needed for 1 real cm² of Pt.

The methanol activity measurements with the platinumised electrodes were carried out in a 0.1 M CH_3OH (Merck P.A.) in 0.5 M H_2SO_4 solution, with a linear sweep at a rate of 2 mVs^{-1} .

Results and discussion.

Since the oxidation of pre-adsorbed CO is used as a calibration system in our experiments, the results on CO oxidation will be discussed first.

Oxidation of pre-adsorbed CO.

The experiments with 0.5 M H_2SO_4 as electrolyte and adsorption potential $E_{\text{ad}}=0.38 \text{ V}$ vs RHE will be taken as the standard system. The results in other electrolytes and with other adsorption potentials will be compared to this.

0.5 M H_2SO_4 , $E_{\text{ad}}=0.38 \text{ V}$.

In figure 1 the oxidation of the CO adsorbate is shown at different surface coverages, which were achieved by varying the adsorption time. One major peak is seen, especially at higher coverages at $E_p=0.62 \text{ V}$, with a small shoulder at ca $E=0.68 \text{ V}$. The change in the hydrogen region due to the presence of CO clearly shows that all hydrogen adsorption sites are blocked to the same extent. At low surface coverages of CO the small shoulder on the positive side of the hydrogen region ($E=0.30 \text{ V}$) is blocked first; furthermore, at these coverages the oxidation

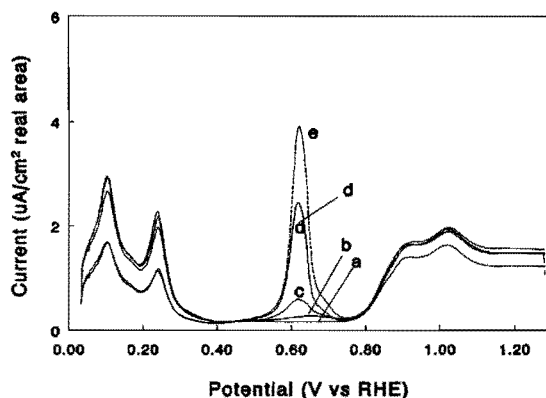


Figure 1: CO adsorbate oxidation in 0.5 M H_2SO_4 , $E_{\text{ad}}=0.38 \text{ V}$. Different surface coverages: (a) 0%; (b) 3%; (c) 10%; (d) 27%; and (e) 33%. $v=2 \text{ mV/s}$.

peak of the adsorbed CO is slightly asymmetric.

DEMS measurements yielded a K^* value which did not change with changing surface cover-

θ_{CO}	eps_{CO}	$\theta_{\text{CH}_3\text{OH}}$	$\text{eps}_{\text{CH}_3\text{OH}}$	$Q_{\text{ad}}/Q_{\text{ox}}$	K^{**}
0.03	0.84	0.03	0.94	?	1.00
0.10	1.08	0.11	0.86	?	0.89
0.14	1.15	0.18	1.04	1.82	0.96
0.27	1.27	0.26	1.04	1.91	0.91
0.33	1.32	0.37	0.95	1.83	0.96
0.39	1.39	0.43	1.05	1.78	1.10
0.44	1.31	0.49	1.17	1.86	1.04
		0.60	1.21	1.96	0.92
		0.72	1.25	2.15	0.91
		0.75	1.28	2.13	0.97

Table 2. Results for CO and CH₃OH with $E_{\text{ad}}=0.38$ V vs RHE in 0.5 M H₂SO₄. The values for K^{**} have been calculated by $K^{**} = K_{\text{CH}_3\text{OH}}^*/K_{\text{CO}}^*$.

age, indicating that CO is the only adsorbate. Neither did the values of K^* , nor the oxidation peak-shape and -position change, if the first scan direction after adsorption was anodic instead of cathodic, indicating that adsorbed CO is in the same state before and after surface coverage determination. The values for eps however, summarized in Table 2, do change from 0.84 at low coverages to 1.39 for the higher coverages, thus indicating that CO is initially present as a bridge-(CO_B) or multi-bonded(CO_M) species and that only at higher coverages some linearly bonded CO (CO_L) is formed.

These findings agree with results obtained by others[31,32,33] with cyclic voltammetry. In contrast, with in-situ IR spectroscopy [e.g.5,34,35] mainly linearly bonded CO (CO_L) is found as the adsorbed species. Recently, however, as mentioned in the introduction, Villegas and Weaver[28] showed that this discrepancy may arise from the large difference in IR cross-section between bridge and linearly bonded CO, thus resulting in a strong underestimation of the amount of bridge-bonded CO. We can therefore conclude that at the highest coverage ($\Theta=0.44$), about half of the total amount of CO is still bridge and/or multi bonded. With decreasing coverage a decrease in the amount of CO_L is seen. In the cyclic voltammogram, on the other hand, the oxidation peak is always found at the same position(except at the lowest $\Theta=0.03$), implying that unexpectedly there is no difference in oxidation potential between the different types of CO_{ad}. The shoulder in the oxidation peak at about 0.68 V, which is the small

oxidation peak found at the lowest coverage, might account for the oxidation of multi-bonded CO, since at the very low coverages at which only this peak is observed, ϵ_{ps} values are clearly below 1. CO_M is thus formed only in very small amounts and is the most difficult species to oxidise.

In sum, at $E_{ad}=0.38$ V vs RHE, CO adsorbs as CO_B and CO_M at low surface coverages. With increasing surface coverage, CO_L is formed, resulting in approximately 50 % of the total amount of CO, being CO_L at a surface coverage of $\Theta=0.44$. When the surface coverage with the CO species is considered, of course not 50 % of the total coverage is due to CO_L , since a CO_B species needs the double amount of Pt sites. This results thus in 1/3 of the total CO coverage being due to CO_L in this case.

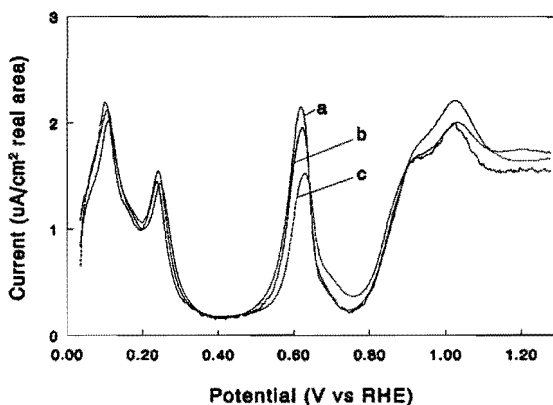


Figure 2: CO adsorbate oxidation in 0.5 M H_2SO_4 as a function of adsorption potential. Surface coverage $\theta=26\%$. Adsorption potential: (a) 0.38 V; (b) 0.43 V; (c) 0.28 V. $v=2$ mV/s.

Changing the adsorption potential.

Figure 2 shows the oxidation of the CO adsorbate ($\Theta=0.26$) after adsorption at 0.43, 0.38 and 0.28 V. It can be seen that the changes in the oxidation peak are small. A distinct change in the ϵ_{ps} value is observed however, ranging from 1.04 for $E_{ad}=0.28$ V to 1.32 for $E_{ad}=0.43$ V. A lower ϵ_{ps} value at the lower E_{ad} is found for all $\Theta_{CO} \geq 0.10$, as is apparent from Tables 2, 3 and 4. No changes in K^* were found. A lower adsorption potential thus results in the formation of relatively more bridged and multi-bonded species, at equal surface coverage. This was previously reported[36] for CO on Pt(100) single crystals, and was ascribed to the diminishing influence of the $d\pi-2\pi^*$ back bonding at higher potentials, which results in destabilisation of the bridge bonded CO[37].

θ_{CO}	eps_{CO}	$\theta_{\text{CH}_3\text{OH}}$	$\text{eps}_{\text{CH}_3\text{OH}}$	$Q_{\text{ad}}/Q_{\text{ox}}$	K^{**}
0.04	1.03	0.05	?	2.00	0.94
0.07	1.14	0.07	1.01	?	1.04
0.10	1.28	0.14	1.15	1.82	1.0
0.15	1.26	0.17	1.10	1.95	1.0
0.27	1.32	0.29	1.13	2.10	0.98
0.31	1.26	0.39	1.05	2.01	0.98
0.40	1.46	0.43	1.13	2.05	0.93
0.51	1.46	0.63	1.34	2.20	0.91
		0.76	1.49	2.64	1.0
		0.79	1.43	2.35	0.96

Table 3. Results for CO and CH₃OH with $E_{\text{ad}}=0.43$ V vs RHE in 0.5 M H₂SO₄. The values for K^{**} have been calculated by $K^{**} = K_{\text{CH}_3\text{OH}}^*/K_{\text{CO}}^*$.

Supporting electrolyte.

In figure 3 the effect of the supporting electrolyte on the oxidation of the CO adsorbate is shown. In 1 M HClO₄, the peak potential of CO is shifted to lower values compared with 0.5 M H₂SO₄, due to the well-known phenomenon[38] of sulphate anion adsorption. This is furthermore confirmed by the shift of the peak potential in 3 M H₂SO₄ to higher potentials. It may also be seen that the same shift occurs for the Pt-oxide formation. Both the same[39] and the opposite[40] effect on the oxidation potential of the CO adsorbate have been reported, going from H₂SO₄ to HClO₄.

The eps values also change with a change in electrolyte (cf Tables 2, 5 and 6), the lowest values are found in HClO₄; as discussed above the presence of adsorbed SO₄²⁻ might result in a compression of the CO adsorbates resulting in more linearly bonded CO and a higher eps value in SO₄²⁻ containing electrolytes.

One might thus conclude that the electrolyte anion influences the water activation (which is evident from the shift in Pt-oxide formation), resulting in a change in oxidation potential of the CO adsorbate, and through compression of the adsorbate influences the way in which it is bonded to the surface.

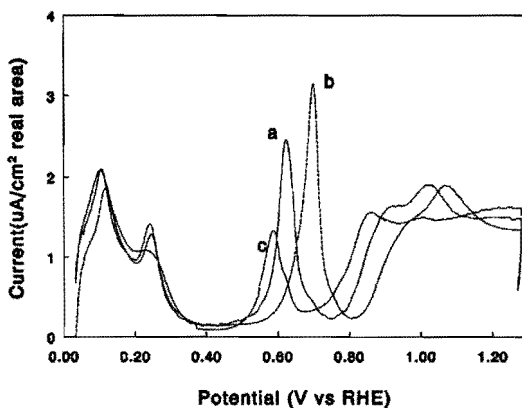


Figure 3: CO adsorbate oxidation in different supporting electrolytes. Adsorption potential $E_{ad} = 0.38$ V. $\theta = 26\%$. Electrolytes: (a) 0.5 M H_2SO_4 ; (b) 3 M H_2SO_4 ; (c) 1 M $HClO_4$.

θ_{CO}	$\epsilon_{ps_{CO}}$	θ_{CH_3OH}	$\epsilon_{ps_{CH_3OH}}$	Q_{ad}/Q_{ox}	K^{**}
0.05	1.29	0.02	0.88	?	1.45
0.07	1.03	0.03	?	1.50	1.37
0.10	0.97	0.08	0.99	1.63	1.35
0.16	1.00	0.13	0.97	?	0.91
0.25	1.04	0.28	0.91	1.73	1.10
0.49	1.18	0.34	0.93	1.49	1.20
0.52	1.22	0.43	1.12	1.60	0.88
		0.62	1.20	1.54	0.93
		0.67	1.15	1.58	0.98

Table 4. Results for CO and CH_3OH with $E_{ad} = 0.28$ V vs RHE in 0.5 M H_2SO_4 . The values for K^{**} have been calculated by $K^{**} = K_{CH_3OH}^*/K_{CO}^*$.

Oxidation of pre-adsorbed CH₃OH.

The different methanol surface coverages were achieved by using different methanol concentrations, methanol was adsorbed until the adsorption current decayed to zero. This gave the adsorption isotherms shown in figure 4, for the different adsorption potentials at room temperature. The linear correlation found between Θ and $\log C$, implies that methanol adsorption shows Frumkin behaviour, which is in agreement with the results found by others[41,42].

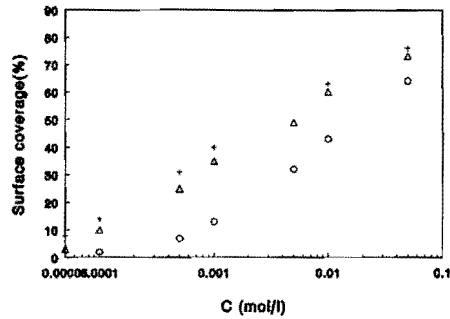


Figure 4: Methanol adsorption isotherms, for three different adsorption potentials. (+) 0.43 V; (Δ) 0.38 V; (○) 0.28 V.

θ_{CO}	$\epsilon_{ps_{CO}}$	θ_{CH_3OH}	$\epsilon_{ps_{CH_3OH}}$	Q_{ad}/Q_{ox}	K^{**}
0.05	?	0.04	0.95	1.70	1.02
0.08	?	0.15	?	1.76	0.96
0.16	0.85	0.21	1.17	1.94	0.91
0.20	0.92	0.27	0.93	1.94	1.00
0.55	1.30	0.40	1.11	1.88	1.06
		0.53	1.27	1.70	0.96
		0.61	1.24	1.78	0.88
		0.68	1.22	2.04	0.91
		0.72	1.35	1.87	0.93

Table 5. Results for CO and CH₃OH with $E_{ad}=0.38$ V vs RHE in 1 M HClO₄. The values for K^{**} have been calculated by $K^{**} = K_{CH_3OH}^*/K_{CO}^*$.

0.5 M H₂SO₄, E_{ad}=0.38 V.

In figure 5 the oxidation of the methanol adsorbates is shown for different surface coverages. At very low ($\Theta=0.03$) coverage a broad assymmetric peak is found at $E=0.63$ V. As the coverage increases ($\Theta=0.09$) the peak gets broader, which is due to a second oxidation peak at $E=0.58$ V. The latter grows further with increasing coverage and gradually shifts to higher potentials, while the first peak (originally at 0.63 V) appears only as a shoulder at ca 0.68 V for $\Theta \geq 0.18$.

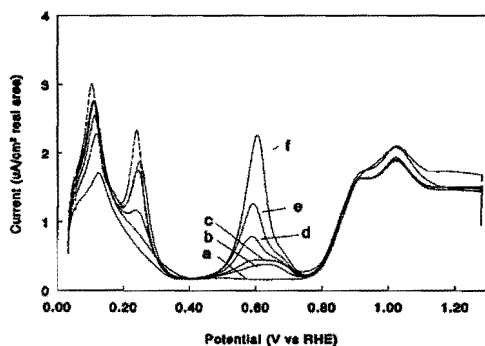


Figure 5A CH₃OH adsorbate oxidation in 0.5 M H₂SO₄, after adsorption at $E=0.38$ V. Different surface coverages: (a) 0%; (b) 3%; (c) 9%; (d) 18%; (e) 27%; (f) 43%.

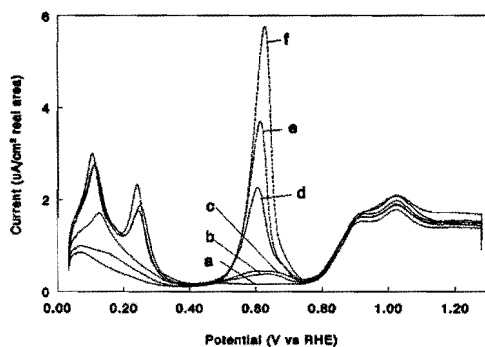


Figure 5B The same as for (A), surface coverages: (a) 0%; (b) 3%; (c) 9%; (d) 43%; (e) 60%; (f) 76%.

The voltammogram also indicates some interesting features with respect to the blocking of the hydrogen adsorption sites. First of all, as with CO, the shoulder in the hydrogen desorption area (at $E=0.30$ V) already disappears at very low surface coverages. Secondly, it can be seen that there is a preferential blocking of the strong hydrogen adsorption sites by the methanol adsorbate; at a coverage of $\Theta=0.4$ all strong hydrogen adsorption sites are blocked, whereas a considerable amount of weakly bonded hydrogen is still present. Thirdly, the peak potential of the desorption of the remaining weakly bonded hydrogen is shifted to more positive values in the presence of methanol, in sharp contrast with the results obtained with adsorbed CO. This shift in peak potential might point to an electronic effect of the methanolic adsorbate on the state of the adsorbed hydrogen. A similar effect, with the same explanation, of adsorbed methane on the state of co-adsorbed hydrogen has been reported recently in a UHV study[43].

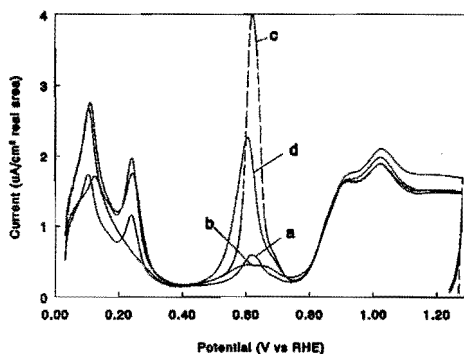


Figure 6: Comparison of the CO and CH₃OH adsorbate after adsorption at $E=0.38$ V in 0.5 M H₂SO₄. Surface coverages: (a) 10% after CO adsorption; (b) 9% after CH₃OH adsorption; (d) 44% after CO adsorption; (d) 43 % after CH₃OH adsorption.

In figure 6 the voltammograms for the oxidation of the methanol adsorbate are compared with those for the oxidation of the CO adsorbates at the same coverage. At low coverages the oxidation peak is much broader in the case of methanol than it is in the case of CO. At intermediate coverages the peak potential for the methanol adsorbate is shifted to cathodic values with respect to the CO_{ad} peak and it is only at the highest coverages that it approaches the value characteristic for CO_{ad} (cf fig. 5B). This suggests that the methanolic adsorbate is not a form of adsorbed CO over most of the coverage range. In order to check whether this is indeed so, the values of K^{**} for different surface coverages were calculated. The results are collected in Table 2. It can be seen that:

-There is no significant change in the K^{**} as a function of the adsorbate surface coverage and K^{**} is close to 1, i.e. $K_{CH_3OH}^{**}$ is essentially equal to K_{CO}^{**} .

-The eps values for the methanol adsorbate oxidation increase from 1 to 1.3, going from low to high surface coverages, and are similar, though not identical, to those obtained in the CO case.

-The Q_{ad}/Q_{ox} values are in reasonable agreement with the K^{**} values, $K^{**} = 1$ implying $Q_{ad}/Q_{ox} = 2$.

It must therefore be concluded that the adsorbate formed upon methanol adsorption at $E=0.38$ V is a CO species. Depending on the surface coverage this CO species is present in a mixture of multi- or bridge-bonded and linearly bonded CO, thus resulting in an eps value between 1 and 2.

Thus the striking fact is that although, it follows from DEMS measurements that both methanol and CO yield CO as an adsorbed species, the oxidation behaviour of both adsorbates is different. First of all, the peak potential at low and intermediate adsorbate coverages, for the oxidation of the methanol adsorbate is shifted to more cathodic values compared with CO, implying that the former is more easily oxidised. Only at higher coverages the peak potentials for both adsorbates are the same. Secondly the methanol oxidation peak is broader and has more of the shoulder at $E=0.63$ V. Thirdly the methanol adsorbate oxidation peak potential shifts to more anodic values with increasing coverages(cf fig. 5), whereas no shift is observed for the CO adsorbate oxidation peak(cf fig. 1).

The difference in adsorbed CO from methanol and adsorbed CO from CO was already noted by Kunimatsu[3], who observed with IR spectroscopy that the linearly bonded CO from methanol adsorption is at a lower wave number than linearly bonded CO from CO.

For adsorbed CO on Pt, Chang and Weaver[44] observed that patches or islands of CO are formed. This might explain why there is no shift in the CO adsorbate oxidation potential with increasing adsorbate coverage. It was shown[44] that upon island formation there was only a small change, if any, in the wave number for the linearly bonded CO with changing coverage.

Let us now assume that CH_3OH upon adsorption does not yield CO in island geometry, but CO homogeneously distributed across the surface. (This in agreement with the fact that methanol needs relatively large ensembles to adsorb.) The homogeneous distribution across the surface might lead to a larger spreading in the adsorption strengths than in the island geometry, leading to a broader adsorbate oxidation peak. With increasing adsorbate coverage, the differences between the homogeneous and the island geometry will get smaller, which can explain why the potential for the methanol adsorbate oxidation becomes equal to that of the CO adsorbate oxidation only at high coverages of the methanol adsorbate(cf fig. 1 and 5), where the differences between island and homogeneous geometry have vanished.

The difference in the oxidation potential might then be due to a kinetic effect. Because of the island geometry the interaction between a CO adsorbate and an activated water molecule at a neighbouring Pt site will be more difficult in the CO case than in the methanol case, this leading to a slower oxidation of the adsorbate in the case of CO. In order to check this explanation, an experiment was done where a CO and a CH_3OH adsorbate were oxidised in a potential step;

After adsorption at $E=0.33$ V, the potential was stepped to $E=0.68$ V and the current decay with time was recorded. It was observed that it takes more time to oxidise the CO adsorbate than the methanol adsorbate, thus confirming that the oxidation of the CO adsorbate is kinetically slower. This is a further indication for the idea that the difference in CO and CH_3OH adsorbates (although both are found to be CO) is due to the fact that the former is present in an island geometry, whereas the latter is not. In a second experiment, the potential was stopped, at a potential just before the peak potential, both for CO and CH_3OH adsorbate. After 100 sec, the cyclic voltammetric scan was continued. For CO adsorbate, almost no adsorbate was left after 100 sec, as was indicated by the absence of the oxidation peak in the rest of the cyclic voltammogram. This confirmed that the width of the CO peak is due to the kinetics of the adsorbate oxidation, and not to adsorbates with different adsorption strength. For the CH_3OH adsorbate, still a considerable amount of adsorbate (ca 50 %) was found after 100 sec; the rest of the oxidation peak still showed the same characteristics as the peak without the 100 s stop. This shows that in contrast to the CO case the width of the CH_3OH adsorbate oxidation is not due to slow kinetics but to thermodynamically different adsorption sites.

Further indications that methanol in contrast to CO does not adsorb in an island geometry, comes from the suppression of the hydrogen adsorption. The methanol adsorbate mainly blocks the strongly bonded hydrogen sites; It is unlikely that one type of sites is located in one region of the surface, it is far more likely that the sites are distributed across the surface. Adsorbed CO suppresses all hydrogen adsorption to an equal extent; in an island of CO probably all sites are present, meaning that adsorption of CO in an island will suppress all hydrogen adsorption sites. Furthermore methanol adsorbates shift the weakly bonded hydrogen desorption to more positive potentials, whereas CO adsorbates do not. It is imagineable that an adsorbate in an island geometry has little contact with co-adsorbed hydrogen, thus resulting in a weaker interaction of CO adsorbates with co-adsorbed hydrogen.

Although we are aware of the fact that this discussion is rather speculative, since we have no direct evidence for the homogeneous distribution of the methanol adsorbate, the explanation given above appears to be the only way to fully explain our results.

Changing the adsorption potential.

In Table 3 and 4 respectively, the results for the adsorption potentials $E=0.43$ V and $E=0.28$ V are shown. From the results in the Tables it is clear, that there is no change in K^{**} , and thus no difference in the type of adsorbate for adsorption potentials of 0.43 V and 0.38 V. The adsorbate formed at 0.28 V, however, gives $K^{**}>1$ at low coverages, implying that more than 2 electrons are needed for the oxidation of one molecule. At higher coverages $K^{**}\approx 1$, but Q_{ad}/Q_{ox} is still ca. 1.5. It is not clear why there is a discrepancy between the K^{**} and Q_{ad}/Q_{ox} . The eps values remain close to 1 for adsorbate coverages up to 67%. We surmise that at higher coverages no essential differences exist between the adsorbates formed at the various

adsorption potentials. But the results at $E_{ad}=0.28$ V apparently imply that, at the lower coverages up to ca. 30 %, next to CO (mostly bridge- or multi-bonded) one or more additional adsorbate species exist which require more than 2 electrons to be oxidised to CO_2 . Since there is a mixture of adsorbates on the surface, it is not possible to draw conclusions on the composition of the additional adsorbate(s), but the most probable candidate seems to be COH(cf Table 1). CHO as an additional adsorbate may be discarded since that would result in ϵ_{ps} values clearly higher than $\epsilon_{ps}=1$.

Figure 7 gives the cyclic voltammetric curves for an intermediate adsorbate coverage, upon methanol adsorption at the three different potentials. It can be seen that the oxidation peak for the adsorbate formed at $E=0.28$ V is shifted to more positive potentials and the shoulder at the positive side of the peak, is more pronounced. One might thus conclude that the adsorbates formed at this potential are more difficult to oxidise, although the differences in potential are rather small. The change in peak shape and position are essentially the same for the CO and the methanol adsorbate (cf fig. 2 and 7). No differences between the different adsorption potentials were found for the blocking of the hydrogen adsorption sites by the methanol adsorbate.

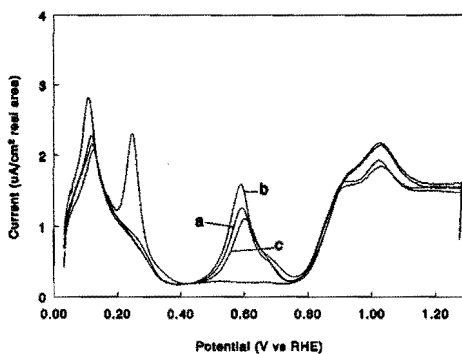


Figure 7: CH_3OH adsorbate oxidation in 0.5 M H_2SO_4 as a function of the adsorption potential. (a) $E=0.38$ V; (b) $E=0.43$ V; (c) $E=0.28$ V. $\theta=26\%$.

Supporting electrolyte.

In figure 8 the effect of the supporting electrolyte on the oxidation of the methanol adsorbate is presented. The pertinent data are summarized in Tables 2, 5 and 6. Both K^{**} and ϵ_{ps} values do not show significant differences. Hence it can be concluded that there is no difference in the type of adsorbate between the different electrolytes. The implication of this is then, that as in the case of CO, the electrolyte anion and concentration can only influence the water activation mechanism or the adsorbate binding strength, since, as is shown in figure 8, there is a considerable difference in oxidation peak potential. This is in agreement with results reported

previously by Castro-Luna et al.[39].

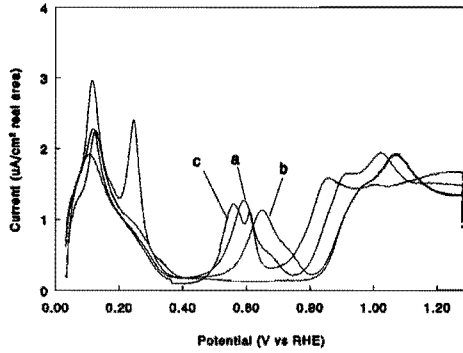


Figure 8 CH₃OH adsorbate oxidation after adsorption at $E=0.38$ V in different supporting electrolytes: (a) 0.5 M H₂SO₄; (b) 3 M H₂SO₄; (c) 1 M HClO₄

θ_{CO}	eps_{CO}	θ_{CH_3OH}	eps_{CH_3OH}	Q_{ad}/Q_{ox}	K^{**}
0.01	1.22	0.01	?	?	1.05
0.03	0.81	0.03	1.09	?	0.98
0.06	1.12	0.06	1.25	?	1.00
0.10	1.24	0.13	1.19	1.70	0.98
0.36	1.28	0.15	1.02	1.83	0.86
		0.25	1.09	1.85	0.92
		0.28	1.10	1.89	0.95
		0.40	1.14	1.69	1.06
		0.60	1.16	2.00	0.98
		0.67	1.24	1.91	1.05

Table 6. Results for CO and CH₃OH with $E_{ad}=0.38$ V vs RHE in 3 M H₂SO₄. The values for K^{**} have been calculated by $K^{**} = K_{CH_3OH}^+ / K_{CO}^+$.

Activity measurements.

Since it was observed that methanol preferentially adsorbs on the strongly bonded hydrogen sites, we wanted to reveal the effect of the percentage of strongly bonded hydrogen sites on the activity for the methanol oxidation. The activity of the electrodes was measured as a function of the H_s/H_w ratio. Results are given in figure 9. It is clear that the activity increases

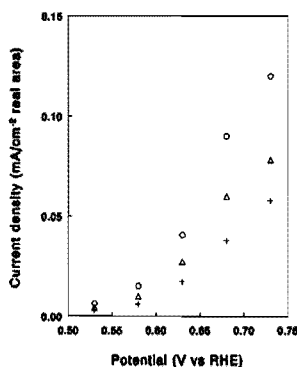


Figure 9 Activity for the methanol electrooxidation of electrodes with a different ratio of strongly bonded (H_s) and weakly bonded (H_w) hydrogen sites. 0.5 M H_2SO_4 /0.1 M CH_3OH . (+) $H_s/H_w=1$; (Δ) $H_s/H_w=1.10$; (\circ) $H_s/H_w=1.19$.

with an increase in the H_s/H_w ratio. Increasing the number of preferential adsorption sites thus yields an increase in methanol oxidation activity, because the adsorbates formed at these adsorption sites are more easy to oxidise, as can be seen from the cyclic voltammetric curves in figure 5.

General Discussion.

To facilitate the discussion, we will first present the picture of the formation of methanol adsorbates on platinumised platinum that we have deduced from our results described above, and then discuss how our data support this picture.

Upon adsorption on platinumised Pt at low potentials ($E=0.28$ V vs RHE), CH_3OH first loses its three methylic protons under formation of a $-COH$ species. Depending on the adsorption potential and the concentration of methanol in the electrolyte, the following may then happen: (1) At low potential and coverage $-COH$ will only be partly converted to CO_{ad} . (2) At higher surface coverage and constant potential, the adsorbate will also lose its alcoholic proton, partly due to compression effects, and form a CO species. At first this CO species will be

present as multi- and bridge-bonded CO. A further increase in surface coverage however will result in a further compression of adsorbates resulting in the formation of linearly bonded CO in addition to the multi- and bridge bonded CO. (3) At higher potentials and equal surface coverage the adsorbate will also lose its alcoholic proton, under formation of a CO species. Whether this CO species is now multi-, bridge- or linear-bonded, depends on the surface coverage, the fraction Θ_L increases with Θ .

The surface coverage itself is influenced by the concentration of methanol in the electrolyte and the adsorption potential. Increase in methanol concentration and increase in adsorption potential (up to a maximum) both lead to higher surface coverages.

The role of the electrolyte anion is not decisive in the formation of the type of adsorbate, but merely influences the water activation ability of the platinised Platinum. The same holds for the concentration of the electrolyte anion, this however in addition causes a compression of the adsorbate, and thus increases the amount of linearly bonded CO, as is apparent from the lower eps values in HClO_4 compared to H_2SO_4 .

Let us now see what evidence we have for the picture presented above.

At $E=0.28$ V and low surface coverages, the values for K^{**} show that the adsorbate consists of a mixture of -CO and -COH. Furthermore the eps values show that multi- and/or bridge bonded CO are present and not linearly bonded CO, since the latter would result in eps values >1 . Increasing the coverage at this potential, by increasing the methanol concentration, results in a decrease in K^{**} , whereas there is no change in eps, showing that the -COH loses its proton, to form -CO, all of which is multi- and or bridge bonded, linearly bonded CO only being formed above $\Theta=0.43$. Increasing the potential to $E=0.38$ V and going back to low surface coverages, we see that from the values for K^{**} , there is no indication for an adsorbate other than CO. It is thus not only the surface coverage that determines whether COH loses its proton but also the potential, $E=0.38$ V being high enough to break the CO-H bond. Higher surface coverages at this potentials again result in an increase in eps, showing that above $\Theta=0.45$, linearly bonded CO is formed in addition to multi- and bridge-bonded CO. Increasing the potential even further to $E=0.43$ V, does not further influence the type of adsorbate, again here it can be seen that above $\Theta=0.43$, considerable amounts of linearly bonded CO are formed.

These results all support the picture we presented and show that the surface coverage (in forcing the formation of linearly bonded CO) and the adsorption potential (in breaking the CO-H bond) are the critical parameters that determine the type of adsorbate.

The nature of the electrolyte anion does not influence the type of adsorbate, as can be seen from Tables 2 and 5. The fact that the adsorbate is oxidised more easily in HClO_4 , must then be due to either an increased water activation ability, or a decrease in Pt-CO bond strength. Since it can be seen from figure 8, that oxide formation in HClO_4 also starts at lower

potentials, it is reasonable to assume that the more easy water activation causes the shift in adsorbate oxidation potential. Essentially the same view holds for the concentration of the sulphate anion, which by blocking the surface hinders water activation, thus giving an increase in Pt and adsorbate oxidation potential.

It can therefore be concluded that the picture presented, is supported by the results: formation of -COH at low coverages and low potentials and formation of -CO at higher coverages and higher potentials, where linearly bonded CO only appears above $\Theta=0.45$.

However, a comparison of the methanol adsorbate with the adsorbate resulting after CO adsorption, shows that, although both are considered to form CO as an adsorbate, some differences still remain. First of all there is a small difference in the oxidation potential of both adsorbates, which shows that the methanolic CO is more easily oxidised. The difference between the two adsorbates may arise from the difference in adsorption geometry, where the oxidation of the CO adsorbate is kinetically slower than that of the methanol adsorbate, as was discussed above. CO is known to adsorb in island geometry, the differences between the methanol and CO adsorbate can now be explained, assuming that the methanol adsorbate is distributed homogeneously across the surface (vide supra). The fact that CH₃OH upon adsorption gives less linearly bonded CO than CO is probably also connected to the difference in island and homogeneous geometry.

The second major difference is the difference in the blocking of the hydrogen adsorption sites. The fact that CH₃OH adsorbs preferentially on the sites responsible for the strongly bonded hydrogen, and the shift in the desorption potential of the weakly bonded hydrogen in the presence of the methanol adsorbate may both be connected with the difference in adsorption geometry, as was discussed above.

The implication of all this, for the intermediate is then, that upon continuous oxidation of methanol at $E > 0.28$ V the intermediate will probably be CO, which will be largely in the linearly adsorbed form at potentials $E > 0.38$ V. It should however still be checked by doing in-situ experiments, that is try to identify the adsorbate during bulk methanol oxidation experiments.

Conclusions.

Methanol adsorbs on Pt preferentially on strongly bonded hydrogen sites, resulting in the formation of a -COH species at low adsorption potential and low surface coverage. At higher adsorption potentials and higher surface coverages, CO species are formed. At coverages above ca. 45% multi- or bridge- bonded CO progressively changes into linearly bonded CO due to compression effects.

The methanolic CO differs in oxidation behaviour from the CO formed after CO adsorption, in that it is more easily oxidised and it shifts the desorption potential of adsorbed hydrogen to higher values, this difference is explained with the difference in adsorption geometry; CO forms

adsorbed CO in islands, whereas the CO adsorbate from methanol does not.

The different adsorbates formed after methanol adsorption cannot be distinguished solely on the basis of their oxidation potentials. The results presented here show that the difference in measurement conditions can perfectly well account for the different results that have been presented in the literature; both adsorption potential and the nature and concentration of the anion being of influence on the type of adsorbate that is formed.

References.

1. J. Willsau, O. Wolter, J. Heitbaum *J. Electroanal. Chem.* **185**, 163, 181, (1985).
2. T. Iwasita, W. Vielstich, E. Santos *J. Electroanal. Chem.* **229**, 367 (1987).
3. K. Kunimatsu *J. Electroanal. Chem.* **213**, 149 (1986).
4. D.S. Corrigan, M.J. Weaver *J. Electroanal. Chem.* **241**, 143 (1988).
5. T. Iwasita, F.C. Nart, B. Lopez, W. Vielstich *Electrochim. Acta* **37**, 2361 (1992).
6. B. Beden, F. Hahn, S. Juanto, C. Lamy, J.M. Leger *J. Electroanal. Chem.* **225**, 215 (1987).
7. B. Beden, S. Juanto, J.M. Leger, C. Lamy *J. Electroanal. Chem.* **238**, 323 (1987).
8. B. Beden, F. Hahn, C. Lamy, J.M. Leger, N.R. de Tacconi, R.O. Lezna, A.J. Arvia *J. Electroanal. Chem.* **261**, 401 (1989).
9. B. Beden, F. Hahn, J.M. Leger, C. Lamy, C.L. Perdriel, N.R. de Tacconi, R.O. Lezna, A.J. Arvia *J. Electroanal. Chem.* **301**, 129 (1991).
10. M.I.S. Lopes, B. Beden, F. Hahn, J.M. Leger, C. Lamy *J. Electroanal. Chem.* **313**, 323 (1991).
11. E.P.M. Leiva, M.C. Giordano *J. Electroanal. Chem.* **158**, 115 (1983).
12. M.C. Pham, J. Moslih, M. Simon, P.C. Lacaze *J. Electroanal. Chem.* **282**, 287 (1990).
13. J.A. Caram, C. Gutierrez *J. Electroanal. Chem.* **323**, 213 (1992).
14. B. Bittins-Cattaneo, E. Santos, W. Vielstich, U. Linke *Electrochim. Acta* **33**, 1499 (1988).
15. R.J. Nichols, A. Bewick *Electrochim. Acta* **33**, 1691 (1988).
16. S. Wilhelm, T. Iwasita, W. Vielstich *J. Electroanal. Chem.* **238**, 383 (1987).
17. S. Wilhelm, W. Vielstich, H.W. Buschmann, T. Iwasita *J. Electroanal. Chem.* **229**, 377 (1987).
18. S.G. Sun, J. Clavilier *J. Electroanal. Chem.* **236**, 95 (1987).
19. M.I. Lopes, I. Fonseca, P. Olivi, B. Beden, F. Hahn, J.M. Leger, C. Lamy *J. Electroanal. Chem.* **346**, 415 (1993).
20. A. Peremans, A. Tadjidine *Chem. Phys. Lett.* **220**, 481 (1994).
21. Y. Zhang, M.J. Weaver *Langmuir* **9**, 1397 (1993).
22. J. Sobkowski, K. Franaszczuk, K. Dobrowolska *J. Electroanal. Chem.* **330**, 529 (1992).
23. K. Shimazu, K. Kaneda, H. Kita *Bull. Chem. Soc. Jpn.* **67**, 2069 (1994).
24. C.P. Wilde, M. Zhang *Electrochim. Acta* **39**, 347 (1994).
25. A. Papoutsis, J.M. Leger, C. Lamy *J. Electroanal. Chem.* **352**, 141 (1993).
26. B.I. Podlovchenko, E.P. Gorgonova *Dokl. Akad. Nauk. SSSR* **156**, 673 (1964).
27. T. Iwasita, W. Vielstich, E. Santos *J. Electroanal. Chem.* **229**, 367 (1989).
28. I. Villegas, M.J. Weaver *J. Chem. Phys.* **101**, 1648 (1994).
29. O. Wolter, J. Heitbaum *Ber. Bunsenges. Phys. Chem.* **88**, 2 (1984).
30. I. Bakos, G. Horanyi *J. Electroanal. Chem.* **332**, 147 (1992).

Chapter 4

31. J. Sobkowski, A. Czerwinski *J. Phys. Chem.* **89**, 365(1985).
32. O. Wolter, J. Heitbaum *Ber. Bunsenges. Phys. Chem.* **88**, 6(1984).
33. M. Watanabe, S. Motoo *J. Electroanal. Chem.* **206**, 197(1986).
34. C.S. Kim, C. Korzeniewski, W.J. Tornquist *J. Chem. Phys.* **100**, 628 (1994).
35. S. Watanabe, J. Inukai, M. Ito *Surf. Sci.* **293**, 1(1993).
36. S.C. Chang, M.J. Weaver *J. Phys. Chem.* **94**, 5095 (1990)
37. S.P. Mehandru, A.B. Anderson *J. Phys. Chem.* **93**, 2044 (1989).
38. E. Herrero, K. Franaszczuk, A. Wieckowski *J. Phys. Chem.* **98**, 5074(1994).
39. A.M. Castro Luna, M.C. Giordano, A.J. Arvia *J. Electroanal. Chem.* **259**, 173 (1989).
40. K. Kunimatsu, W.G. Golden, H. Seki, M.R. Philpott *Langmuir* **1**, 245 (1985).
41. T. Biegler, D.F.A. Koch *J. Electrochem. Soc.* **114**, 904 (1967).
42. S.S. Beskorovainiya, Yu.B. Vassiliev, V.S. Bagotskii *Elektrokhimiya* **1**, 1029 1965).
43. W.S. Lisowski, R. Dus *Appl. Surf. Sci.* **78**, 363(1994).
44. S.C. Chang, M.J. Weaver *J. Chem. Phys.* **92**, 4582 (1990).

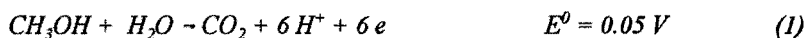
On the particle size effect of carbon supported Pt catalysts for the electrooxidation of methanol.

Abstract

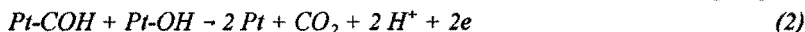
In this paper the effect of particle size of carbon-supported Pt catalysts on the electrooxidation of methanol is presented. Different methods were used to prepare Pt/C catalysts with particle sizes ranging between 1.2 and 10 nm. Also the possible interaction of Pt with carbon surface groups was investigated by preparing catalysts on oxidized and non-oxidized carbon supports. The specific activity is found to decrease with decreasing particle size in the range 4.5 to 1.2 nm. Carbon supported Pt particles appear to be more active than non-supported ones and the presence of an acidic group on the support slightly enhances this effect. The dependence of the activity on the particle size can be explained either in terms of its effect on the formation of an adsorbed hydroxy species or its effect on the number of methanol adsorption sites.

Introduction.

The electrooxidation of methanol is a matter of intensive research in the context of the development of the direct methanol fuel cell. Though the reaction proceeds faster in alkaline than in acidic media, an acid electrolyte is generally preferred for practical application since carbonate residues are not formed in this electrolyte. The choice of the electrocatalyst material is then however confined to Pt, which has a rather low activity for the methanol electrooxidation:



It is generally accepted [1][2] that the crucial and rate limiting step in this reaction is the oxidation of a methanol adsorbate by an adsorbed hydroxy species or activated water group. When it is assumed that -COH is the methanol adsorbate, the rate determining step is:



The problem is generally recognized to be the lack of a suitable Pt surface-oxide species in the potential region 0-0.6 V[3], where methanol is adsorbed. The Pt-oxide that is formed at and above +0.75 V blocks the surface and impedes the methanol oxidation. The electrooxidation of methanol begins at 0.45 V; therefore adsorbed hydroxy species or activated water-groups must be the reaction partner. The rate of reaction (2) depends on coverage with θ_{COH} and θ_{OH} . Since $\theta_{COH} + \theta_{OH} \leq 1$ it implies that a high θ of either one will decrease the amount of Pt-sites that are available for the formation of respectively an adsorbed methanol or hydroxy species, and the reaction rate will consequently be low. Hence it is obvious that the efficiency of the Pt catalyst would be improved if a well balanced co-adsorption of methanol and water could be

realized at low potential.

The Pt electrocatalyst in fuel cells usually consists of Pt particles on a carbon support. The surface area of this electrocatalyst increases with smaller particles; however it is known that by decreasing the particle size, the catalytic behaviour of the material can be altered [4],[5]. Watanabe et al.[4] argued that the inter-particle distance can affect the catalytic behaviour as well. In a later paper, however, Giordano et al.[6] could not find conclusive evidence for such an effect.

In their investigation of the oxygen interaction with Pt particles sputtered on Teflon, Parmignani et al.[7] found with XPS measurements that Pt is more easily oxidized when the particle size is decreased. This is confirmed by the electrochemical measurement of Pt-oxide reduction by Takasu[8], who observed a potential shift in the cathodic direction with a decrease in Pt particle size. This could imply that also the oxidation occurs at lower potentials for smaller Pt particles. For electrocatalytic reactions such as the O_2 reduction, several workers observed a decrease in specific activity with smaller particles in the range from 12 to 1 nm [9], which again could be related to the increased difficulty of reducing Pt-O species. Peuckert et al.[10] investigated the oxygen reduction on highly dispersed platinum on carbon and concluded that there is a maximum in the activity expressed per unit weight of platinum for particle sizes between 3 and 5 nm. The results of Giordano [6] however reveal no clear evidence for such a maximum, but there is a sharp increase with smaller particles (<5nm).

So if in fact the onset of Pt oxidation is enhanced at smaller particles, one should expect Pt-OH species to be present on the catalyst surface at lower potentials. For the range of particle sizes where θ_{OH} does not become too high, one should therefore expect a positive effect on the activity of methanol oxidation. Such an effect has indeed been reported: Attwood et al.[11], employing Pt/C catalysts prepared in a variety of ways, found an optimum in the specific activity at a specific surface area of $140 \text{ m}^2/\text{g}$, corresponding to a Pt particle size of about 3nm. However, different preparation methods and different carbon supports were used, so the metal-support interaction could have been changed as well. Indeed in a recent paper[12] it is pointed out that carbon surface groups influence the electronic nature of the supported platinum. Enyo et al.[13] observed for small Pt clusters (Pt_2 and Pt_4), deposited on carbon, that the activity decreases for the smaller Pt clusters (these Pt aggregates, derived from platinum-carbonyl cluster anions below 1 nm in size, still exhibit a higher activity than smooth Pt). Watanabe et al.[14] prepared Pt catalysts with different particle sizes on several carbon supports, using one and the same preparation method. The surface area of these catalysts range from $70 \text{ m}^2/\text{g}$ to $201 \text{ m}^2/\text{g}$, thus covering approximately the same range as those of Attwood et al.[11]. Surprisingly enough however, they did not find a particle size effect, the specific activity for the methanol oxidation appeared to be the same for all Pt particle sizes. They also concluded that there was no intercrystallite distance effect. On the contrary Yahikozawa et al.[15] who prepared catalysts by Chemical Vapor Deposition found a decrease in activity with smaller

particles (1.5 to 2.3 nm).

Considering all these results, it is not yet clear to what extent the performance of carbon supported Pt for the methanol oxidation is influenced by the particle size and by the nature of carbon surface groups. In this paper results will be presented for the methanol oxidation at Pt/C catalysts with different particle sizes. The catalysts were obtained not only by different preparation methods, but also by a variation of a single preparation method. Furthermore to investigate a possible carbon support interaction colloidal Pt was deposited on carbon as well as on oxidized carbon.

Experimental.

Catalyst preparation.

Carbon black (Vulcan XC-72/Cabot International) with a specific surface BET area of 340 m²/gr was used as support for all catalysts.

The following carbon-supported Pt catalysts were prepared by ion-exchange, impregnation or colloidal precipitation; the Pt loading was 3.5 - 5.5 wt%. Furthermore some of the catalysts were modified by potential cycling, details are given in the text.

1) Ion-exchanged catalyst: Carbon was oxidized with HNO₃ and then ion-exchanged [16] with Pt(NH₃)₄(OH)₂ (Johnson and Matthey). The ion-exchanged catalyst was reduced in H₂ at 200 °C for 2 hours.

2) Impregnated catalyst: Carbon was impregnated with H₂PtCl₆ (Drijfhout) in water by refluxing for two hours, and then reduced with formaldehyde. After one more hour of reflux, the catalyst was filtered, extensively washed in order to remove chloride ions and dried at 125 °C.

3) Colloidal catalyst: two preparation methods were employed:

3a) Colloidal Pt was prepared by the method of Turkevich et al. [17], in which an aqueous H₂PtCl₆ solution is reduced with sodium-citrate under reflux until a black Pt-sol is formed. This sol is then added to the carbon suspended in water. After filtration, extensive washing with hot water and drying at 125 °C, the Pt/C catalyst is obtained. The carbon was used either as received or in the oxidized form.

3b) Colloidal Pt on a carbon support (carbon as received or oxidized) was prepared for us by Prof. Bönnemann [18]. PtCl₂ is suspended in THF and reduced with (N(octyl)₄BEt₃H), where the ammonium salt functions as a stabilizer for the colloidal metal particles.

4) Impregnated-sintered catalyst: Sintered Pt/C was prepared by impregnating carbon with an aqueous H₂PtCl₆ solution, followed by filtration, washing and drying at 125 °C. The catalyst was thereafter reduced by H₂ at 700 °C for 2 hours.

5) Ageing of catalyst: potential cycling can modify the particle size of Pt/C [19]; therefore repeated potential cycling was applied as well on Pt/C catalysts.

Electrode preparation.

Pt/C electrodes were prepared by pressing a mixture of the catalyst and a Teflon (Fluon GP1; DPI) suspension on a Pt or Au gauze. The electrode was dried at 125 °C and then sintered in Ar atmosphere at 325 °C during two hours. The total amount of catalyst used always was ca. 10 mg on a gauze of ca 2 cm² geometric area. The final Teflon content is 20 % (by weight).

Catalyst characterization.

The Pt particle size of the catalysts was determined with Transmission Electron Microscopy on a Jeol (JEM 2000FX) microscope.

The Pt/C electrodes were characterized by cyclic voltammetry using a computer controlled Autolab (Eco Chemie) potentiostat. Cyclic voltammetric scans were obtained in 0.5 M H₂SO₄ between -0.65 V and +0.6 V versus a Hg/Hg₂SO₄ electrode (+0.68 V vs RHE), against which all potentials are given. Platinum specific surface areas were determined from the hydrogen desorption area in the anodic voltammogram, assuming that 1 cm² of smooth Pt required 210 μC [20].

Methanol oxidation.

The activity for methanol oxidation was measured in 0.1 M CH₃OH + 0.5 M H₂SO₄ by applying a sweep at a scan rate of 5 mVs⁻¹, starting at open circuit potential. It was established that the results did not change significantly at lower scanrates. The activities per real surface area were obtained from the forward scan of the second sweep. All activity measurements were at least done in duplo with a freshly prepared electrode for each new measurement. The activities are given in mA/cm², where 0.1 mA/cm² corresponds to a turn-over frequency off TOF=0.07 s⁻¹.

Catalyst/Support	Pt Loading	Particle size (nm)
Ion-exchanged/ox. C	3.5 %	1.2± 0.4
Impregnated/C	4.4 %	1.7± 0.5
Colloïdal Turkevich/C	5.5 %	2.5± 0.9
Colloïdal Bönemann/C	3.7 %	2.1± 1
Sintered impregnated/C	4.0 %	7.8± 2.5

Table I: Mean particle size as measured by TEM.

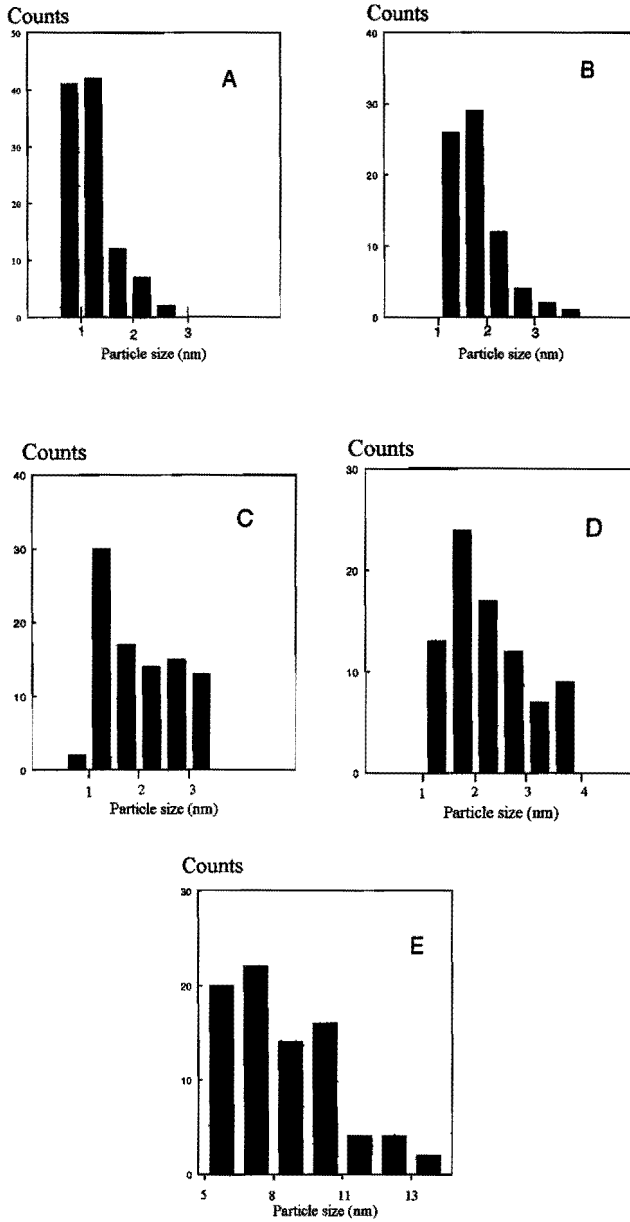


Figure 1 Histograms obtained from TEM photo's for the Pt/C catalysts. (a) Ion-exchanged; (b) Impregnated; (c) Colloidal Turkevich; (d) Colloidal Bönemann; (e) Sintered.

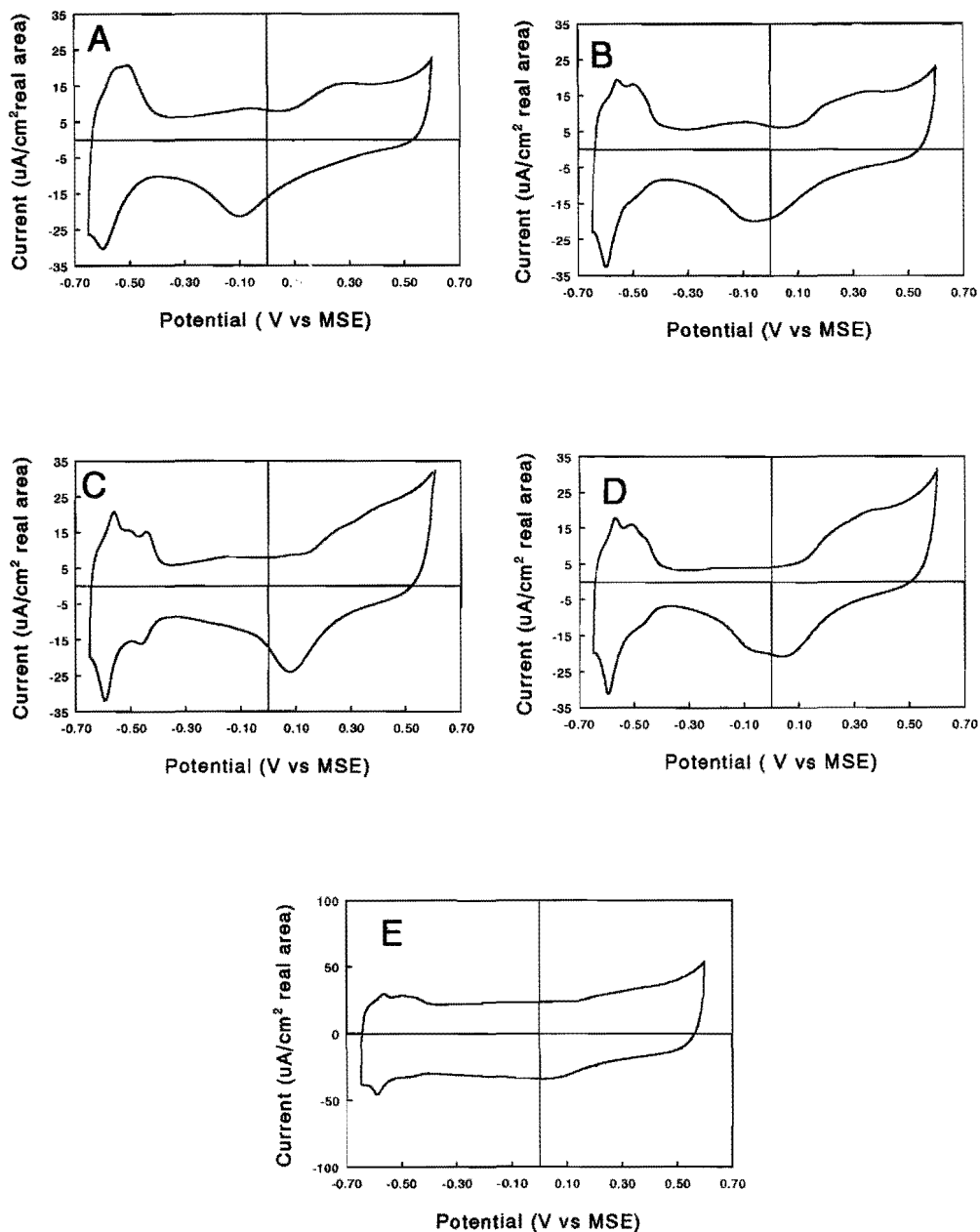


Figure 2 Cyclic voltammograms of catalysts in figure 1 in 0.5 M H_2SO_4 . Scan rate 10 mV/s.

Results

TEM characterization.

Figure 1 shows the histograms of the particle size distribution for all catalysts. The mean particle sizes are summarized in table 1; they range from 1.2 to ca 10 nm.

The smallest Pt particles were obtained by the ion-exchange method on an oxidized carbon support. The Pt loading for the catalysts is also given in this table.

Electrochemical characterization.

The cyclic voltammograms of the catalysts in 0.5 M H₂SO₄ are given in figure 2. The voltammogram of the Turkevich catalyst and the sintered Pt/C catalyst show the well known hydrogen adsorption/desorption characteristics for Pt; two cathodic adsorption peaks and three anodic desorption peaks, usually assigned to respectively weakly-, intermediate- and strongly bonded hydrogen. The result that there are only two adsorption peaks while there are three desorption peaks is also found for polycrystalline Pt[21]. The shape of the hydrogen area for the colloidal catalysts is comparable, except that the ratio of weakly/strongly bonded adsorbed hydrogen is somewhat higher for the "Bönnemann" catalyst than for the "Turkevich" catalyst. For the ion-exchanged and impregnated catalysts (fig.2a and b), it appears that the strongly bonded hydrogen peak is totally absent, only two desorption peaks and one adsorption peak are seen.

Comparing the oxide reduction peaks for the catalysts clearly shows that the peak potential shifts to higher values going from ion-exchanged catalysts (fig.2a) to impregnated (fig.2b) to colloidal (fig.2c). In figure 3 the peak potential for the oxide reduction is plotted as a function of the (mean) particle size of the catalysts; this shows that the peak potential increases with increasing particle size in the range upto ca 4.5 nm, to the value of smooth- and platinised- Pt. In voltammogram 2d ("Bönnemann" catalyst) two oxide reduction peaks seem to be present, which could point to a mixture of smaller and larger particles.

Catalyst/Support	Particle size (nm)
Impregnated/C	2.9± 1.4
Colloidal Turkevich/C	4.3± 1.9
Colloidal Bönnemann/C	3.9± 1.4

Table II Mean particle size after repeated scanning, as measured by TEM.

The effect of repeated potential cycling is shown in figure 4 for an impregnated catalyst. Both the oxide peak potential and the onset of oxidation are shifted to higher potentials with increasing number of potential cycles. TEM photo's taken after 60 cycles show an increase in particle size; this is shown in Table 2.

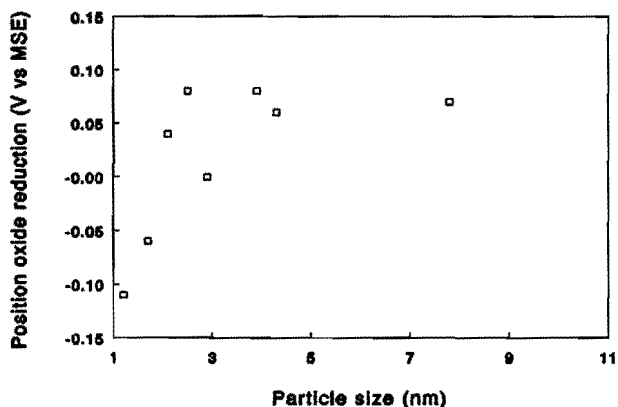


Figure 3 Peak potential for the oxide reduction for the different catalysts in relation to their particle size.

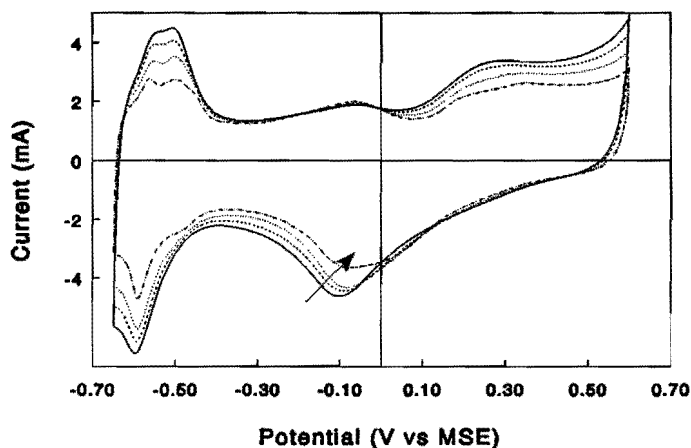


Figure 4 Effect of repeated cycling in 0.5 M H_2SO_4 on the impregnated catalyst. The oxide reduction peak is seen to shift to higher potentials, with an increasing number of scans. Last scan is the 62th. Arrow indicates increase in number of scans.

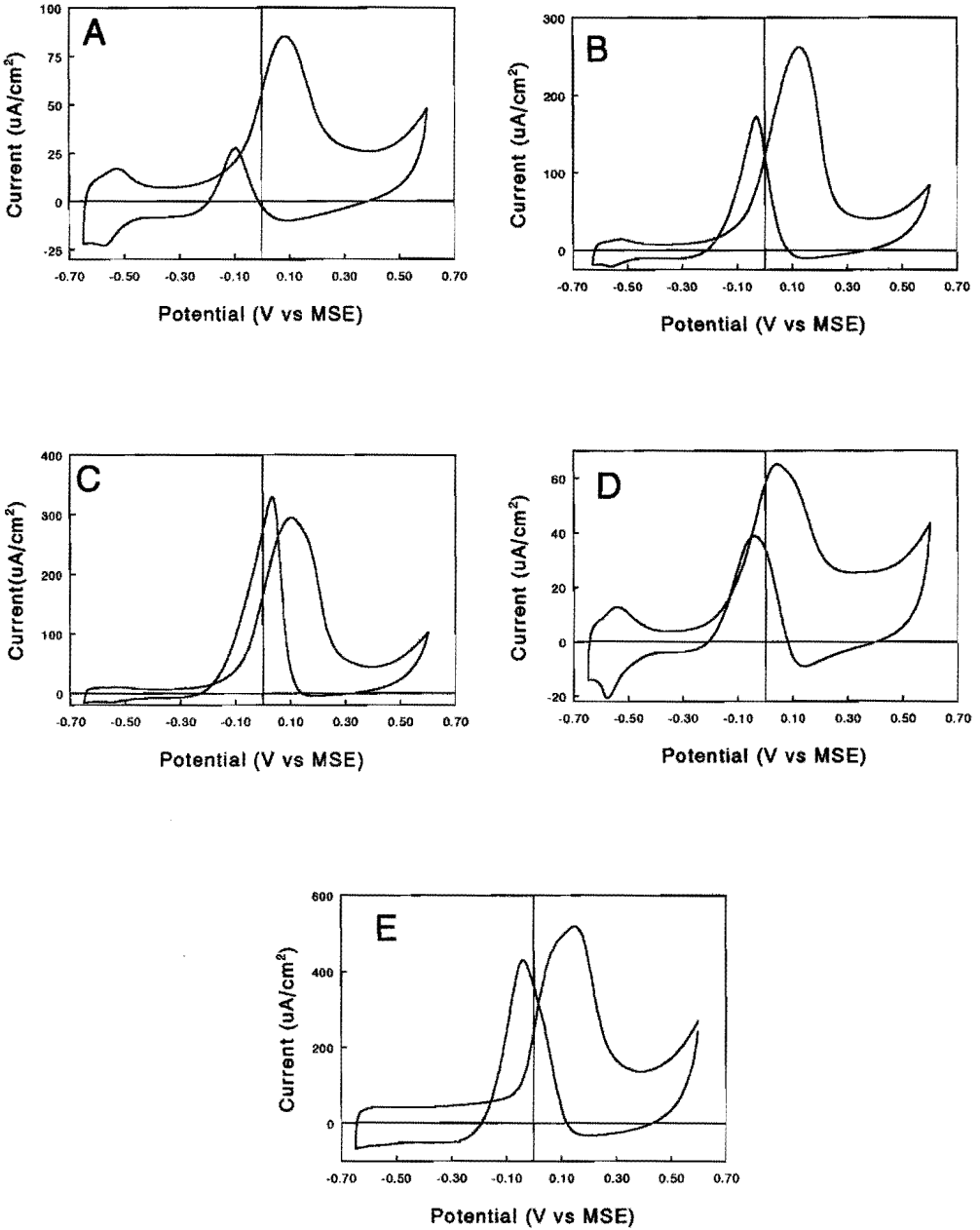


Figure 5 Cyclic voltammograms of catalysts in figure 1 in 0.5 M $H_2SO_4/0.1$ M CH_3OH . Scan rate 5 mV/s.

Oxidation of methanol.

In figure 5 the cyclic voltammograms (second scan) of all catalysts in 0.1 M CH₃OH/0.5 M H₂SO₄ are presented. The catalysts show different specific activities for the methanol oxidation. The position of the peak potentials changes: there is a small difference in the forward scan between the different catalysts, but in the backward scan a larger shift is noted; this is of course related to the position of the oxide reduction potential. In table 3 the specific activities of all catalysts for the methanol oxidation at a potential of -0.05 V vs MSE are summarized. These data were taken from the forward scan of the cyclic voltammetric curves in figure 5.

Figure 6 shows the effect of repeated potential cycling of the catalyst in 0.5 M H₂SO₄ on the methanol oxidation. In all cases this led to an increase in specific activity; in table 3 the activities at -0.05 V vs MSE are given.

Catalyst/Support	Activity (mA/cm ²)	Activity after particle size growth (mA/cm ²)
Ion-exchanged/ox. C	0.032	0.071
Impregnated/C	0.055	0.071
Colloidal Turkevich/C	0.080	0.110
Colloidal Bönemann/C	0.060	0.086
Colloidal Turkevich/ox.C	0.085	-
Colloidal Bönemann/ox.C	0.073	-

Table III Specific activity for methanol oxidation at -0.05 V vs MSE in 0.5 M H₂SO₄ and 0.1 M CH₃OH at 23 °C.

Carbon support effect.

The possible synergetic effect of the carbon support was studied by comparing the activity of the two colloidal catalysts on oxidized and non-oxidized carbon. TEM-measurements revealed no change in particle size for the oxidized and non-oxidized carbon systems; the electrochemical characterization of the hydrogen area does not reveal significant differences either (figure 7). The specific activity for the methanol oxidation was higher for the oxidized catalyst

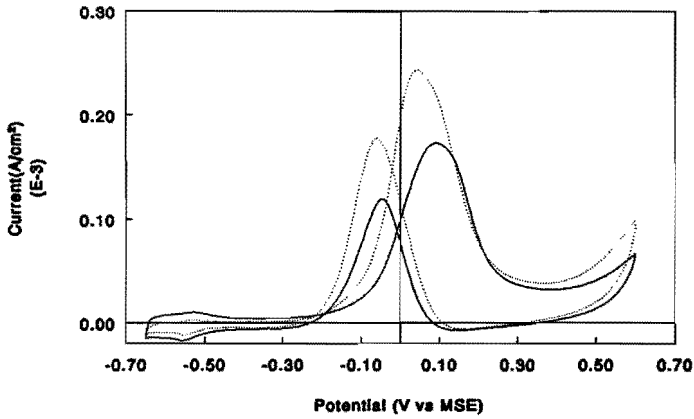


Figure 6 Effect of scanning on the methanol oxidation of the impregnated catalyst Q after 5 scans in $0.5 \text{ M H}_2\text{SO}_4$; (....) after 50 scans in $0.5 \text{ M H}_2\text{SO}_4$. Scan rate 5 mV/s in $0.1 \text{ M CH}_3\text{OH}/0.5 \text{ M H}_2\text{SO}_4$.

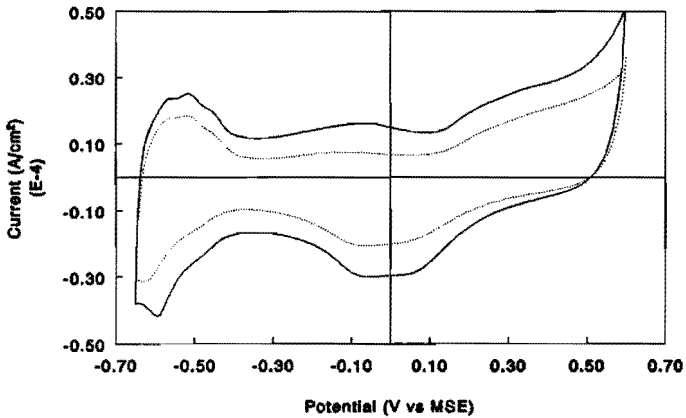


Figure 7 Voltammogram of the Bönemann catalyst on a non-oxidised (....) and an oxidised carbon support. $0.5 \text{ M H}_2\text{SO}_4$, 10 mV/s .

as is shown in figure 8 for the Bönemann preparation. Similar results were obtained with the "Turkevich" preparation.

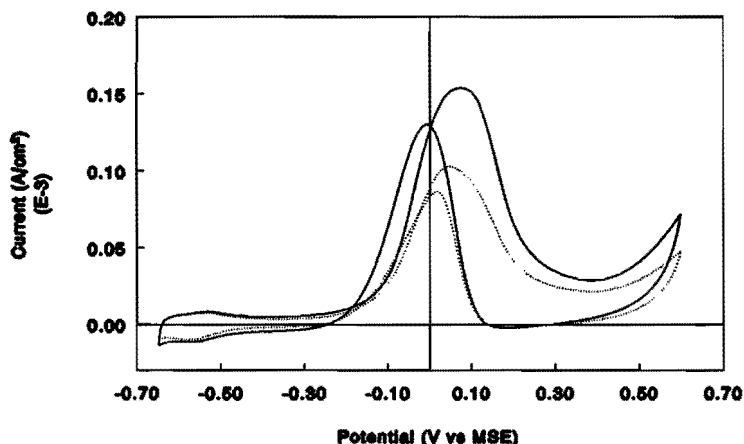


Figure 8 Cyclic voltammetric curves for methanol oxidation of catalysts in figure 7. 0.1 M $\text{CH}_3\text{OH}/0.5 \text{ M H}_2\text{SO}_4$, 5 mV/s.

Discussion.

Repeated oxidation and reduction of the carbon supported Pt catalyst causes a growth of the Pt particles (compare table 1 and 2). This is in agreement with Kinoshita[19]. The accompanying shift to higher potentials for the Pt-oxide reduction with increasing particle size is in agreement with results of Takasu[8]. Also the onset of oxidation is shifted to higher potentials, cf figure 4. This is indicative of a lower Pt-O affinity for larger Pt particles and implies that the ability to activate water, i.e. to break a H-O-H binding with formation of a Pt-OH species proceeds at a lower potential for smaller particles. Hence we assume that the smaller sized ion-exchanged catalyst will contain more Pt-OH groups at a given potential than a colloidal catalyst which in turn should contain more Pt-OH groups than smooth Pt. In view of reaction (2) we therefore expect an increase in specific activity for the methanol oxidation with a decrease in particle size. However this is not observed as can be deduced from figure 9 in which the specific activities (per real surface area) are presented for all of the Pt/C catalysts. In the figure the activity for platinized Pt (electrodeposited from H_2PtCl_6 at 10 mA/cm^2 during 5 min.) and smooth Pt (polycrystalline) are also included. For particle sizes in the range 10 - 4.5 nm, the activity is constant, for particles in the range 4.5 - 1.2 nm the activity decreases with smaller sizes.

At first sight these results would appear to imply that the oxygen affinity of very small particles is so high that the catalyst surface is largely covered with Pt-OH, thus leaving insufficient sites for methanol adsorbates. Due to the low amount of methanol adsorbates, the activity of the small Pt particles is low. The implication then is that water activation is already optimal for large platinum particles, contrary to the general view set out in the introduction.

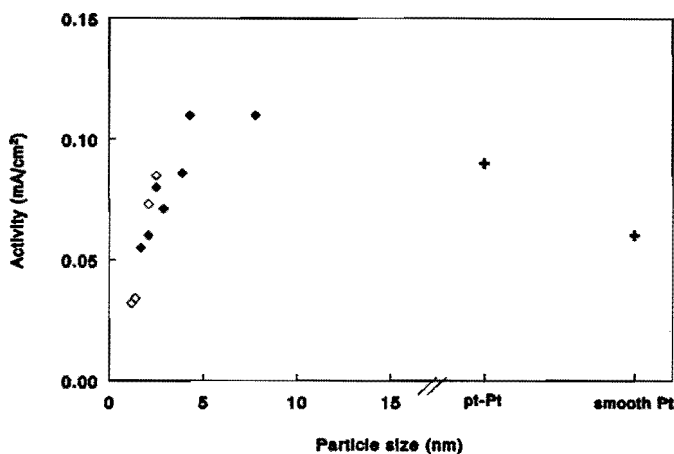


Figure 9 Specific activity for the methanol oxidation of all Pt/C catalysts, ptPt and smooth Pt at -0.05 V vs MSE. Open symbols refer to Pt/C catalysts on an oxidised carbon support.

There is however an alternative possible interpretation: when the particle size decreases, the number of methanol adsorption sites decreases. It can be deduced from figure 2 that the ratio amount of weakly bonded H to strongly bonded H increases with decreasing particle size. At platinized Pt electrodes we observed that when the amount of strongly adsorbed hydrogen sites increases, also the methanol oxidation activity increases [22]. Beden et al[23] also reported that methanol preferentially adsorbs on the sites that can strongly bind hydrogen. Thus the relative decrease in strongly bonded H features can be seen as indicative of a decrease in the preferred methanol adsorption sites. On this view, then, the change in methanol adsorption characteristics dominates over the increased water activation. At present we cannot distinguish between the two explanations.

In figure 10 the activity for the methanol oxidation expressed per unit Pt weight is plotted vs the Pt particle size; the results might indicate a slight maximum at ca 1.8 nm. Such a maximum occurs due to the mixed influence of decreasing specific surface area and increasing specific activity with increasing particle size. With our catalysts no substantial differences were found in the intercrystalline distances. The variation in this distance within one catalyst is at least comparable to the variation between the different catalysts.

The observed difference in specific activity between smooth and platinised Pt is difficult to explain. In the cyclic voltammetric curves in 0.5 M H_2SO_4 , no difference was observed for the oxide-formation or oxide-reduction potential. The difference in methanol oxidation activity for these two catalysts thus may not be attributed to a different oxygen binding of the platinum. Furthermore as there is almost no difference between the H_w/H_s ratios for both systems, it may be assumed that the adsorption sites for methanol also do not differ substantially. At present it

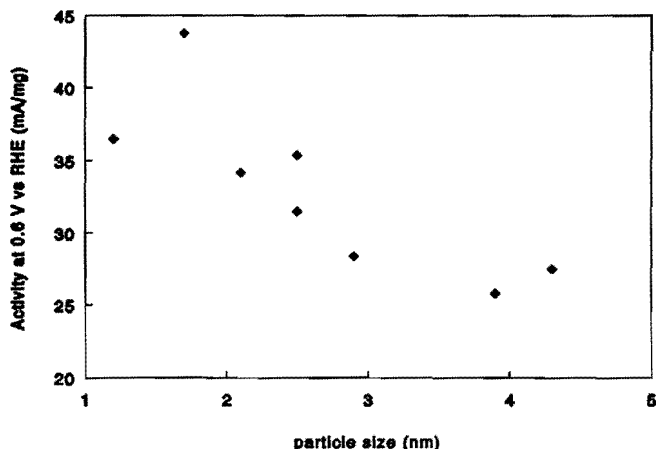


Figure 10 Specific activity per weight of Pt, for the Pt/C catalyst of figure 9.

is therefore not clear why platinumized platinum has a higher activity for the methanol oxidation. It is seen in figure 9 that upon introduction of a carbon support, a further increase in methanol oxidation activity is found. This suggests a metal support interaction, i.e. a ligand effect due to the carbon support. Using an oxidized carbon support, instead of a non-oxidized support, increases the activity even further, which confirms the presence of a metal support interaction. The results presented here differ from those of Attwood[11] who observed a maximum in specific activity vs platinum area. Estimation of the particle size from the specific surface area reveals that the sizes used by Attwood are in the same range (1.5-4 nm) as those presented here. One can therefore conclude that the different preparation methods used by Attwood et al. should have a considerable influence on the behavior of the Pt catalyst. The results by Watanabe et al.[14] and Enyo[13] cannot be compared with our results since we do not know if their catalysts give a shift in oxide reduction potential with change in particle size.

Conclusions

The Pt particle size clearly affects the methanol oxidation activity. For particle sizes in the range 1.2-4.5 nm a decreasing size results in a decrease in methanol oxidation activity; for sizes larger than ca 4.5 nm the methanol oxidation activity remains almost constant. Furthermore a close relationship between particle size and the oxide reduction potential for particles in the range 1.2 to 4.5 nm is observed. This would imply that a higher coverage of OH species can be obtained on Pt if the particle size is decreased to values below 4.5 nm. However the expected increase of the specific activity of Pt/C for the methanol oxidation is not observed. Apparently the coverage ratio OH/methanolic species has become unfavourable. This may be due to: (1) A surface coverage of OH_{ads} that is too high and results in a decrease in COH_{ads} . (2)

A decrease in the amount of preferred adsorption sites for methanol with a decrease in Pt particle size. For particle sizes >5 nm the specific activity reaches a limiting value which is about twice that of smooth Pt.

Finally, it is found that a metal-support interaction exists for Pt/C catalysts; Pt on oxidized carbon shows a higher activity due to the introduction of an acidic group.

Acknowledgements

We would like to thank Prof. Dr. H. Bönemann (Max Planck Institut für Kohleforschung, Mülheim an der Ruhr) for the preparation of one of the colloidal catalysts. Ing D. Klepper is thanked for the electron microscopy measurements.

References

1. B.D. McNicol, *J. Electroanal. Chem.* **118**, 71 (1981)
2. R. Parsons and T. vander Noot *J. Electroanal. Chem.* **257**, 9 (1988)
3. J. Sobkowsky, K. Franaszuk, K. Dobrowolska, *J. Electroanal. Chem.* **330**, 529 (1992)
4. M. Watanabe, S. Saegusa, P. Stonehart *Chem. Lett.* 1487 (1988).
5. M. Watanabe, H. Sei, P. Stonehart *J. Electroanal. Chem.* **261**, 375 (1989).
6. N. Giordano, E. Passalacqua, L. Pino, A.S. Arico, V. Antonucci, M. Vivaldi, K. Kinoshita, *Electrochim. Acta* **36** 1979 (1991)
7. F. Parmigiani, E. Kay, P.S. Bagus *J. Electron Spectrosc. Relat. Phenom.* **50**, 39 (1990).
8. Y. Takasu, Y. Fujii, K. Yasuda, Y. Iwanaga, Y. Matsuda *Electrochim. Acta* **34**, 453 (1989).
9. S. Mukerjee, *J. Appl. Electrochem.* **20**, 537 (1990)
10. M. Peuckert, T. Yoneda, R.A. Dalla Betta, M. Boudart *J. Electrochem. Soc.* **113**, 944 (1986)
11. P.A. Attwood, B.D. McNicol, R.T. Short *J. Appl. Electrochem.* **10**, 213 (1980).
12. P.L. Antonucci, V. Alderucci, N. Giordano, D.L. Cocke, H. Kim, *J. Appl. Electrochem.* **24**, 58 (1994)
13. M. Enyo, K. Machida, A. Fukuoka, M. Ichikawa *Electrochemistry in Transition* ed. by O.J. Murphy Plenum Press, New York. p. 359-369.
14. M. Watanabe, S. Saegusa, P. Stonehart *J. Electroanal. Chem.* **271**, 213 (1989).
15. K. Yahikozawa, Y. Fujii, Y. Matsuda, K. Nishimura, Y. Takasu *Electrochim. Acta* **36**, 973 (1991).
16. D. Richard and P. Gallezot in *Preparation of Catalysts IV*. B. Delmon, P. Grange, P.A. Jacobs, G. Poncelet editors. Elsevier Amsterdam 1987.
17. K. Aika, L.L. Ban, I. Okura, S. Namba, J. Turkevich *J. Res. Inst. Catalysis Hokkaido Univ.* **24**, 54 (1976).
18. H. Bönemann, W. Brijoux, R. Brinkman, E. Dinjus, T. Jousen, B. Korall *Angew. Chem.* **103**, 1344 (1991).
19. K. Kinoshita, J. Lundquist, P. Stonehart, *J. Electroanal. Chem.* **48**, 157 (1973)
20. T. Biegler, D.A.J. Rand, R. Woods *J. Electroanal. Chem.* **22**, 269 (1973).
21. R.M. Cervino, W.E. Tracia, A.J. Arvia *J. Electroanal. Chem.* **182**, 51 (1985).
22. T. Frelink, W. Visscher, J.A.R. van Veen. to be published.
23. B. Beden, F. Kadirgan, C. Lamy, J.M. Leger, *J. Electroanal. Chem.* **142**, 171 (1982)

Chapter 5

The Adsorbate in Methanol and CO Electrooxidation over Carbon Supported Pt. A DEMS Study

Abstract

An analysis of the methanol and CO adsorbate on carbon supported Pt is given. It is shown with DEMS that there is no influence of the Pt particle size on the structure of both adsorbates. The adsorption of methanol is more difficult at smaller particles. The difference in oxidation peak shape and position between CO and CH₃OH is similar to that found on platinised Pt and is explained in terms of adsorption geometry.

Introduction

It is generally accepted[Chapter 2] that the oxidation of methanol proceeds via the formation of an adsorbed intermediate (eq. 1), here represented as COH, which is then oxidised in a subsequent step(eq. 2).



The type of methanol adsorbate on platinised Platinum, depends both on the potential and on the surface coverage and is a mixture of linearly and bridge bonded CO and at lower potentials COH[Chapter 4].

Until now, there is only one paper in which the structure of the methanol adsorbate on small carbon supported Pt particles is studied[1]. The IR spectra in that study show that the adsorbate mainly consists of CO. Furthermore as far as we know, there is also only one investigation[2] on the Pt particle size effect on the oxidation of CO on carbon supported Pt. It is shown with cyclic voltammetry that the oxidation peak of dissolved CO shifts to higher values with a decrease in particle size. There are no studies on the oxidation of pre-adsorbed CO on Pt/C.

The major problem in studying the methanol- or CO adsorbate on carbon supported systems is the difficulty of applying most of the standard in-situ techniques, especially the IR techniques. We[3] and others[4] however, have shown that it is possible to study processes at carbon supported Pt with Differential Electrochemical Mass Spectroscopy (DEMS).

As was shown in the previous chapter of this thesis and in some other papers[5,6,7], the Pt particle size determines the activity for the methanol oxidation. At particles smaller than ca. 4 nm the specific activity decreases with decreasing particle size. In view of this fact, and the apparent lack of literature on the structure of the methanol and CO adsorbate on carbon supported Pt, in this chapter results on the oxidation of adsorbed CO and CH₃OH on Pt/C as studied with DEMS, will be given. The oxidation of both adsorbates is studied as a function of the Pt particle size.

Experimental

Catalyst preparation and characterization.

The Pt/C catalysts used here are identical to the catalysts described in chapter 5. In addition to these catalysts, a commercial 10 % Pt/C (EICHEM) was used. The characterization of these catalysts, with TEM and Cyclic Voltammetry is described in chapter 5. The particle sizes are given in table 1. The mean particle size of the "Echem" catalyst was found to be the same as

Catalyst/Support	Pt Loading	Particle size (nm)
Ion-exchanged/ox. C (A)	3.5 %	1.2± 0.4
Impregnated/C (B)	4.4 %	1.7± 0.5
Colloidal Turkevich/C (D)	5.5 %	2.5± 0.9
Colloidal Bönemann/C (C)	3.7 %	2.1± 1
Echem catalyst (E)	9.0 %	2.7

Table 1: Mean particle size as measured by TEM.

that of the Turkevich catalyst (i.e. 2.7nm).

Electrode preparation.

The catalyst is mixed with a Teflon suspension (Fluon, DPG) and then pressed on a Au current collector. After drying at 80°C, the electrode is sintered for two hours at 320°C under Ar atmosphere. The final Teflon content in all electrodes was 18%. In the DEMS cell (described in chapter 3) the contact to the Au current collector is made via a Au wire.

Analysis of the methanol adsorbate

In order to be able to determine the structure of the methanol adsorbate with DEMS, here the

same method is used as described in chapter 4 for platinised Pt. The ratio between the total charge (Q_I) and the amount of CO_2 (Q_M) produced upon oxidation of the adsorbate is determined (eq 1).

$$nK^* = \frac{Q_I}{Q_M} \quad (3)$$

By measuring this ratio for both the CO and CH_3OH adsorbate oxidation, we can, by comparing these ratios, determine the number of electrons necessary to oxidise the methanol adsorbate to CO_2 (eq. 2).

$$K^{**} = \frac{K^*_{\text{CH}_3\text{OH}}}{K^*_{\text{CO}}} = \frac{n_{\text{CH}_3\text{OH}}}{n_{\text{CO}}} \quad (4)$$

Furthermore the number of electrons per Pt site (eps) released during adsorbate oxidation is also determined for both the methanol and CO adsorbate. As is shown in table 2 this can give additional information on the structure of the adsorbate.

Adsorbed Species	K^{**}	eps	$Q_{\text{ad}}/Q_{\text{ox}}$
-C=O	1	2	2
=C=O	1	1	2
≡C=O	1	0.67	2
≡COH	1.5	1	1
-CHO	1.5	3	1
-COOH	0.5	1	5

Table 2: Possible adsorbates, resulting from the methanol adsorption reaction and their theoretical values for K^{**} , eps, and $Q_{\text{ad}}/Q_{\text{ox}}$. The value of K^{**} is calculated on the basis of the fact that $K^*_{\text{CO}}=1$.

CO and CH_3OH adsorption and oxidation

For each catalyst CO was adsorbed from a CO saturated solution for a given adsorption time

at a given adsorption potential (E_{ad}), after which the solution was exchanged under Argon flow with fresh electrolyte. Different surface coverages were obtained by changing the adsorption time.

At each catalyst CH_3OH was adsorbed from methanol containing electrolyte until the adsorption current reached zero. Then the solution was replaced with fresh electrolyte. Different surface coverages with the methanol adsorbate were obtained by varying the methanol concentration in the adsorption solution.

After obtaining an adsorbate covered catalyst, the potential was in both cases swept from E_{ad} to 0.03 V vs RHE, where the scan was reversed and swept to 1.2 V to oxidise the adsorbate. From the decrease in the hydrogen desorption area, the surface coverage (θ) was calculated. The charge for the oxidation of the adsorbate was calculated by subtracting a scan without adsorbate.

All experiments were carried out in 0.5 M H_2SO_4 , made from p.a. H_2SO_4 (Merck) and ultrapure water (EcoStat). Methanol containing solutions were prepared with p.a. CH_3OH (Merck). A Pt counter electrode and a $\text{Hg}/\text{Hg}_2\text{SO}_4$ ($E=+0.68$ V vs RHE) reference electrode was used. All potentials are given with respect to the RHE. Argon (99.99 %) was used to provide oxygen free conditions.

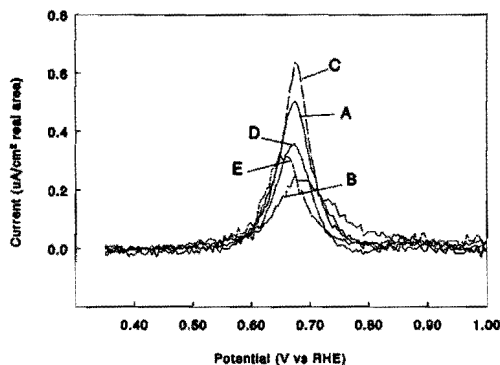


Figure 1 Oxidation of the CO adsorbate at the catalysts from table 1. Background subtracted cyclic voltammograms are shown. Low CO coverage (ca 10%) 0.5 M H_2SO_4 , $v=2\text{mV/s}$.

Results and discussion

Oxidation of adsorbed CO.

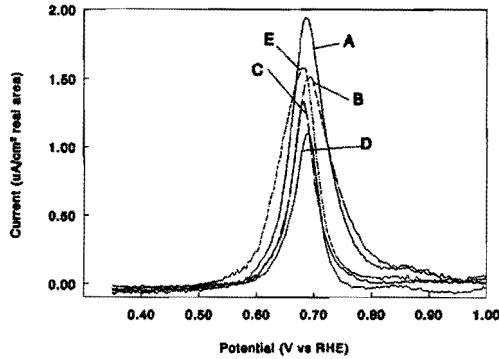


Figure 2 Same as for figure 1, but medium CO coverage (ca 22%).

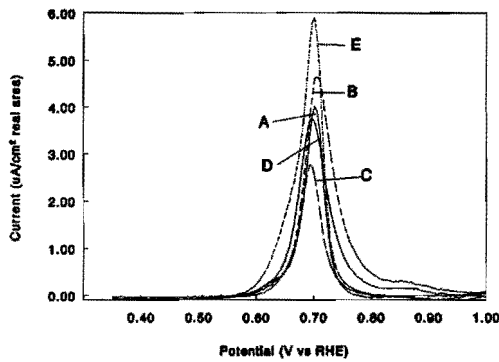


Figure 3 Same as for figures 1 and 2, but high CO coverage (ca 40%).

The oxidation of pre-adsorbed CO at Pt/C, after adsorption at $E_{ad}=0.38$ V, with different particle sizes is shown in Figures 1-3. At low CO coverage ($\theta_{CO}=0.1$) no big differences are seen (Fig. 1) between the different catalysts, there is no appreciable shift in peak-potential, nor in the start of the CO oxidation. Only for the impregnated catalyst(B) a slight shift to higher potentials and a somewhat broader peak is observed. At medium coverage($\theta_{CO}=0.22$) of CO, a shift of the peak potential to more positive values is observed at all catalysts (Fig. 2). It is striking that the CO oxidation at the 'Echem catalyst'(E) at this coverage is clearly more active at lower potentials than the other catalysts. This difference is also observed at higher coverages($\theta_{CO}=0.40$) (Fig. 3) where the peak potential for all catalysts is seen to have shifted

further to more positive values, but again no substantial differences are observed between the catalysts. In table 3, the eps values for the different catalysts at different surface coverages of CO are given. No appreciable changes can be seen, not as a function of the particle size and not as a function of the surface coverage. The value of 1.5-1.7 for eps indicates that the CO adsorbate is dominantly present in the linearly bonded form, with small amounts of bridge- and/or multi-bonded CO. During the adsorption of CO, a small negative adsorption current was observed on all catalysts. This was also observed by Clavilier et al. [8] and Bilmes et al. [9] for adsorption of CO on Pt single crystals and was ascribed to the displacement of anions from the surface. By varying the adsorption potential, we found that at low potentials ($E_{ad}=0.18$ V) the negative adsorption current was no longer observed, in agreement with the results in [8]. No change in K^* was observed for a CO adsorbate formed at different adsorption potentials, the negative adsorption current can therefore not be due to a change in adsorbate structure and must be attributed to anion displacement.

θ	A(1.2 nm)	B(1.7 nm)	C(2.1 nm)	D(2.5 nm)	E(2.7 nm)
3	-	-	-	1.56	1.43
6	1.62	1.26	1.60	1.60	1.30
8	1.56	1.39	1.76	1.43	1.34
20	1.77	1.77	1.70	1.65	1.47
33	1.88	-	1.78	1.69	-
47	-	1.75	-	-	1.86

Table 3: Eps values for CO oxidation at five different catalysts as a function of the surface coverage. $E_{ad}=0.38$ V vs RHE

Finally we observed a gradual decrease in the amount of adsorbed hydrogen, after adsorption and oxidation of the CO. In order to check whether this is due to the presence of CO, a blank adsorption experiment, without CO, was done. In this case no decrease in hydrogen adsorption charge was observed. This implies that the decrease in Pt surface area is due to the presence of the CO adsorbate. We further checked if this decrease in surface area was due to the formation of carbonaceous species. By applying a cathodic potential pulse, it should be possible to hydrogenate such species of the surface [10]. After adsorption of CO, the potential was stepped to 0.03 V, no methane formation was found with DEMS however.

As we will see in the next section, the phenomenon of the surface area decrease, however smaller, was also observed for CH_3OH .

Although the particle size thus seems to have no influence on the peak-shape and position nor

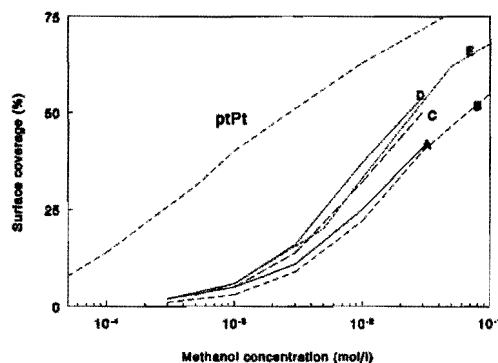


Figure 4 Adsorption isotherms at room temperature for methanol on the Pt/C catalysts from table 1, ptPt is shown for comparison. Letters point to the catalysts.

on the binding geometry of the CO on the Pt, two interesting features remain. First of all the eps values found here are substantially higher than those found for platinumised platinum (chapter 4), indicating that at carbon supported Pt more linearly bonded CO is formed. Secondly the peak potential increases with increasing CO surface coverage, which phenomenon was not observed for the oxidation of CO over platinumised platinum. At platinumised Pt we also found that a change in adsorption potential gave a change in eps values; more bridge-bonded CO was formed at lower adsorption potentials. This particular aspect was checked for the 'Turkevich catalyst', but no differences in eps values were found.

The results we presented in the previous chapter for platinumised platinum, were explained with CO being present in an island geometry, and the adsorption potential influencing the adsorption geometry by a change in $d\pi-2\pi^*$ back-bonding[11]. We must conclude then that at the catalysts used here, it is more difficult to form bridge- or multi-bonded CO, since even at lower adsorption potentials where bridge-bonded CO is more favourable, the eps values stay close to two. This is probably due to the small particles. The same holds for the island formation upon CO adsorption; at small particles it is less probable that CO islands are formed, especially at low CO coverages. With increasing CO coverages, islands will be formed, resulting in a slower oxidation of the CO (as explained in the previous chapter) and thus in a shift in peak potential to higher values.

Oxidation of adsorbed methanol.

In figure 4 the adsorption isotherm of methanol at different Pt/C catalysts is shown and compared with ptPt. It appears that the catalysts with the smaller particles (Exchange(curve A) and Impregnated(curve B)) have a smaller surface coverage at the same methanol concentration;

the adsorption of methanol at these catalysts is thus more difficult. This is in agreement with the conclusions of chapter 5, where the decrease in methanol oxidation activity with a decrease in particle size was ascribed to a lower amount of methanol adsorbate.

Figures 5-7 show the oxidation of methanol adsorbates formed at $E=0.38$ V, for different surface coverages at different Pt catalysts. Again, as with CO, it appears that no substantial differences exist between the different catalysts, although at higher coverages the peak potential seems to be shifted to somewhat higher potentials for the impregnated and exchange catalysts. The most striking feature in Fig. 5-7 is the shift of the adsorbate oxidation peak potential to lower values with an increase in surface coverage, implying that at higher coverages the methanol adsorbate is oxidised more easily. This is opposite to what was found for the oxidation of the methanol adsorbate at platinised Platinum (chapter 4) and the oxidation of CO at Pt/C (vide supra).

The eps values for the methanol adsorbate are given in table 4, together with the values for K^{**} obtained with DEMS. These results show that the K^{**} remains close to 1 for all catalysts, meaning that the methanol adsorbate is identical to that of CO. The eps values, however, are in the range 1.1-1.8, which is lower than for CO, and indicate that upon methanol adsorption more bridge- and multi-bonded CO is formed than upon CO adsorption.

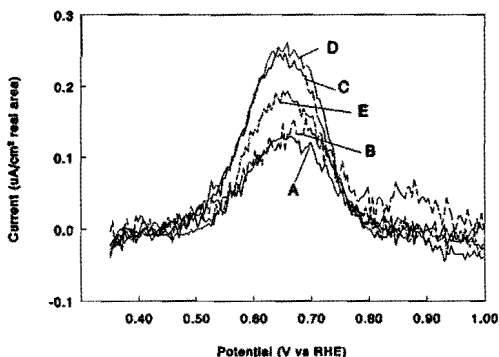


Figure 5 Oxidation of the methanol adsorbate at the catalysts from table 1. Background subtracted cyclic voltammograms. Low methanol coverage (ca 10%) 0.5 M H_2SO_4 , $v=2$ mV/s.

During methanol adsorption at 0.38 V CO_2 formation was detected in the mass-spectrometer, especially at higher methanol concentrations. At this same potential on platinised platinum, no CO_2 formation was found (Chapter 5). This confirms that methanol is more easily oxidised on carbon supported Pt catalysts. Furthermore it was found that at smaller Pt particles, CO_2 was formed more easily during methanol adsorption. This again confirms the conclusions of Chapter 5 that with a decrease in Pt particle size, the oxidisability of the Pt increases.

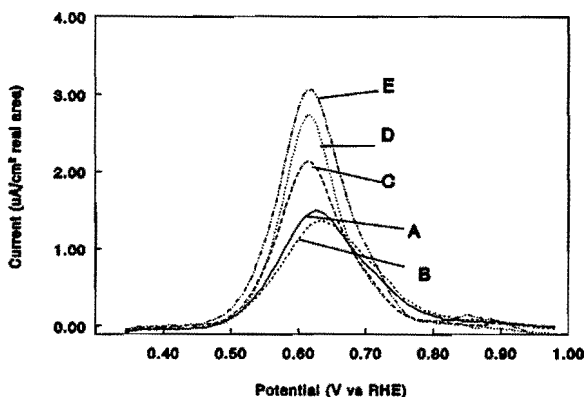


Figure 6 Same as for figure 5, but medium coverage (ca 20%).

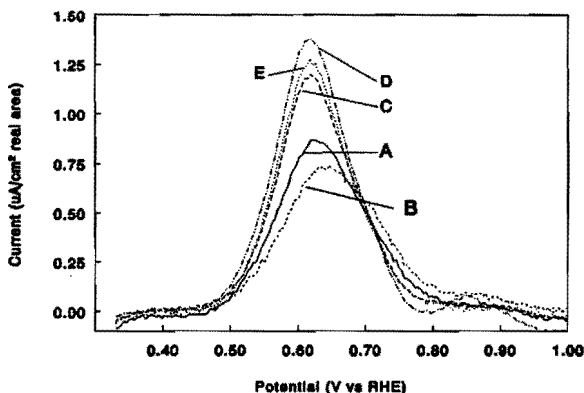


Figure 7 Same as for figure 5, but high coverage (ca 50%).

In order to check whether adsorption at a potential where CO_2 is formed, has an influence on the adsorbate structure, methanol adsorption was performed at different potentials in the range 0.18 V - 0.43 V. At potentials lower than +0.28 V vs RHE no CO_2 formation could be detected during methanol adsorption. The value for K^{**} was the same for all adsorption potentials, implying that there is no change in adsorbate structure with changing potential. This in contrast with platinumised Pt, where CO was found to be the major adsorbate, but at potentials below +0.28 V, substantial amounts of COH were formed.

In Figure 8 the oxidation peak of pre-adsorbed CO is compared to that for the oxidation of the methanol adsorbate. It is shown that the later is found at lower potentials and the peak is more broad, as was also found for platinumised platinum.

As for CO, a gradual decrease in the hydrogen adsorption charge was found after methanol

adsorption and oxidation, although the effect was smaller than for CO. Since it seems to be unlikely that this decrease is caused by the presence of a strongly bonded residue, we suggest that the Pt particle size grows in the presence of an adsorbate. Christensen et al. [12] showed that there is a change in roughness for Pt in the presence of a methanol adsorbate, although this study was performed with smooth Pt, it seems, as our results here, to confirm that the surface morphology of a Pt catalyst may change in the presence of an adsorbate.

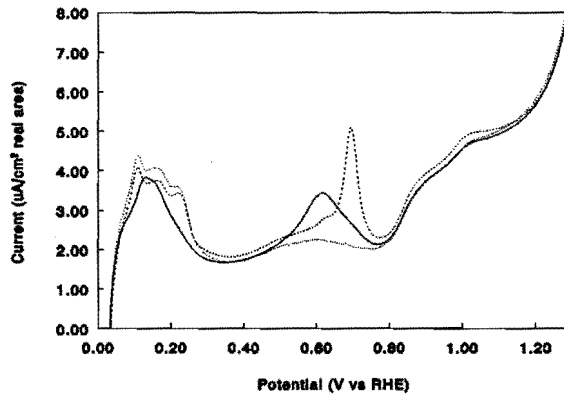


Figure 8 Comparison of the oxidation of a methanol and a CO adsorbate at the Bönemann catalyst. Solid curve: methanol adsorbate; dashed curve: CO adsorbate; dotted curve: blank.

θ	A(1.2 nm)		B(1.7 nm)		C(2.1 nm)		D(2.5 nm)		E(2.7 nm)	
	K^{**}	eps	K^{**}	eps	K^{**}	eps	K^{**}	eps	K^{**}	eps
3	1.0	-	0.87	1.44	0.86	1.40	0.68	1.56	0.84	-
8	-	-	0.94	1.40	0.91	1.60	0.82	1.61	0.84	1.84
11	0.90	1.37	0.94	1.17	0.68	1.18	-	-	-	-
22	0.94	1.27	0.94	1.23	-	-	0.89	1.24	1.05	1.41
40	0.94	1.33	0.94	1.28	0.80	1.29	0.90	1.29	1.0	1.36
55	-	-	0.94	1.31	0.86	1.27	0.90	1.29	1.05	1.54

Table 4: K^{**} and eps values for methanol adsorbate oxidation at five different catalysts. $E_{ad}=0.38$ V vs RHE.

General Discussion

The Pt particle size of carbon supported Pt catalysts is only of influence on the amount of adsorption of methanol but not on the type of adsorbate that is formed. The surface coverage with methanol adsorbate decreases with a decrease in particle size. This is in general agreement with the observations we made before[13], that the activity decreases with decreasing particle size as a result of hindered methanol adsorption.

The results show that there is a difference between the methanol and CO adsorbate, with respect to peak-position and peak-shape. These differences are similar to those observed for platinised platinum [Chapter 4]. Furthermore there is a difference in the blocking of hydrogen adsorption sites upon methanol or CO adsorption. Methanol preferentially blocks the strongly adsorbed hydrogen sites, whereas CO blocks all sites to an equal extent. This difference was also observed at platinised Platinum electrodes.

It is known that CO forms islands upon adsorption[14]. As we have discussed in chapter 4, the oxidation of CO is slower due to this island formation. Reaction between an adsorbed water molecule and CO only takes place at the island edges. For methanol, which is assumed to adsorb homogeneously across the surface, the reaction between the adsorbate and an adsorbed water molecule is more easy and the reaction is thus faster. The shift of the oxidation peak of the CO adsorbate to higher potentials with increasing adsorbate coverage, is due to the kinetic slowness of the reaction.

The difference in the blocking of the hydrogen adsorption sites is probably also due to the difference in adsorption geometry. Methanol adsorbs preferentially on strongly bonded hydrogen sites, which will not be located in an island, but will be homogeneously spread across the surface. It is easily imaginable that adsorption in an island geometry will cover all different hydrogen sites, which is actually observed for the adsorption of CO.

Conclusion

There is no influence of the Pt particle size on the type of adsorbate that is formed upon adsorption of methanol. Generally more linearly bonded CO is formed at small particles than at platinised Platinum. Adsorption of methanol gives more bridge-bonded CO than the adsorption of CO. The oxidation of the adsorbate from CO is kinetically slower than the oxidation of the adsorbate from methanol.

References

- 1.P.A. Christensen, A. Hamnett, J. Munk, G.L. Troughton *J. Electroanal. Chem.* **370**, 251 (1994).
- 2.K. Yahikozawa, N. Tateishi, K. Nishimura, Y. Takasu *Chemistry Express* **7**, 437 (1992).
- 3.T. Frelink, W. Visscher, J.A.R. van Veen *Electrochim. Acta* **39**, 1871 (1994).
- 4.S. Wasmus, W. Vielstich *J. Appl. Electrochem.* **23**, 120 (1993).

Chapter 6

5. P.A. Attwood, B.D. McNicol, R.T. Short *J. Appl. Electrochem.* **10**, 213 (1980)
6. Y. Matsuda, Y. Fujii, Y. Matsuda *Bull. Chem. Soc. Jpn.* **59**, 3973 (1986)
7. A. Kabbabi, F. Gloaguen, F. Andolfatto, R. Durand *J. Electroanal. Chem.* **373**, 251 (1994)
8. J. Clavilier, R. Albalat, R. Gomez, J.M. Orts, J.M. Feliu, A. Aldaz *J. Electroanal. Chem.* **330**, 489 (1992).
9. S.A. Bilmes, A.J. Arvia *J. Electroanal. Chem.* **361**, 159 (1993).
10. U. Schiemann, U. Müller, H. Baltruschrat *Electrochim. Acta* **40**, 99 (1995).
11. S.C. Chang, M.J. Weaver *J. Phys. Chem.* **94**, 5095 (1990).
12. P.A. Christensen, A. Hamnett, G.L. Troughton *J. Electroanal. Chem.* **362**, 201 (1993).
13. T. Frelink, W. Visscher, J.A.R. van Veen *J. Electroanal. Chem.* **382**, 65 (1995).
14. S.C. Chang, M.J. Weaver *J. Chem. Phys.* **92**, 4582 (1990).

Ellipsometry and DEMS study of the electrooxidation of methanol at Pt and Ru- and Sn- promoted Pt.

Abstract

The oxidation of submonolayers of Ru and Sn on Pt in sulfuric acid was monitored with ellipsometry. In the presence of methanol the oxides on Ru and Sn disappear but the Pt-oxide is not affected by methanol. This signifies that Ru and Sn are present in their zero valent state during the methanol oxidation.

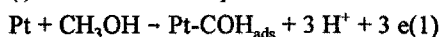
DEMS measurements showed that both metals enhance methanol oxidation. The promoting role of these metals is explained with the bifunctional mechanism.

Introduction

The investigation of methanol oxidation is of importance because of its possible application in the direct methanol fuel cell. Because of the necessity of an acid electrolyte the choice of the catalyst is confined to noble metals of which Pt has the highest activity. This metal, however, has a high overpotential for this reaction and deactivates rapidly. Therefore several efforts have been made to modify its electrocatalytic behaviour[1,2].

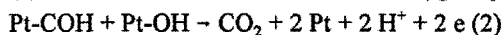
The oxidation of methanol at Pt is generally accepted to proceed via two major steps:

(i) dissociative adsorption of methanol:



in which the adsorbate can be $(\text{COH})_{\text{ads}}$ or CO_{ads} [3].

(ii) oxidation of the adsorbate with an oxygen species that is present on Pt:



Here the oxygen supplying species is represented as Pt-OH. It is still a moot question whether the oxygen originates from an adsorbed hydroxy species or from activated water. The main reason for the low activity of Pt for the methanol oxidation is its inability to provide an oxygen species at low potential; Pt-OH is formed at relatively high potentials.

It is well known [4,5,6] that the activity of Pt can be improved by addition of metals like Sn or Ru. Since neither Ru[7] nor Sn[8] are active for the methanol oxidation, the promoting metal should only partially cover the Pt surface. If the coverage with the promoting metal is too high, the number of methanol adsorption sites becomes too small and thus the oxidation activity decreases. The promoting effect of these metals is usually attributed to either a

bifunctional[9] or to a ligand[10] effect. The bifunctional effect involves the forming of an oxygenated species at the promoting metal at a less anodic potential than at Pt, with the result that the methanol adsorbate can be oxidised at a lower potential. According to the ligand theory the promoting metal changes the electronic state of the Pt, thus influencing the reactivity of the Pt. Other explanations, which are sometimes mentioned in the literature[10] for the electrocatalytic action of adatoms, viz. a geometric (third-body) effect and a redox effect are not likely: the geometric effect would imply that other (geometrically similar) metals are also active as promoters which has not been observed for methanol oxidation. If the promoting action were due to a redox effect[11], a redox couple should be observed in the cyclic voltammetric measurements.

The promoting metal can be electrochemically deposited as an adatom or applied via immersion[12] onto Pt; in both cases a submonolayer is formed. Another method is to prepare a Pt/M (M=Sn or Ru) alloy via electrocodeposition[13]. The electrocatalytic behaviour of an adatom layer was found to be similar to that of the codeposited alloy, both for Ru and for Sn [6,9,13]. The adsorbed methanolic intermediates have been extensively investigated with a large variety of surface detection methods. Ellipsometry is an optical method for the characterization of the metal/electrolyte interface[14] and is often applied to monitor the formation of thin films at a metal surface. The technique is based on the changes in the polarization state of monochromatic light upon reflection at the surface; the measuring parameters are Δ and Ψ which are related to phase retardation and relative amplitude. Since ellipsometry is an in situ technique we applied this method in combination with Differential Electrochemical Mass Spectroscopy (DEMS) to get more insight into the role of Ru and Sn promoters on the methanol oxidation at Pt. The results will be discussed in the view of a bifunctional or ligand effect of the promoting metal.

Experimental

Combined cyclic voltammetry and ellipsometry experiments were carried out at a smooth Pt disc electrode (area 0.5 cm^2) using a Wenking potentiostan POS 73 with Philips PM 8043 recorder and an automated ellipsometer Rudolph RR 2200 with tungsten iodine light source and monochromatic filter resulting in light with a wavelength of 546.1 nm. The optical cell is cylindrical and supplied with windows arranged for an angle of incidence of 70° at the substrate.

Combined voltammetric and DEMS experiments were performed at a platinized gauze electrode (real area 60 cm^2) using a mass spectrometer system (Leybold PGA 100) and computer controlled AutoLab potentiostat (Eco Chemie) which is arranged for simultaneous recording of current- and mass response. The setup is similar to that of Vielstich et al.[15]. In both electrochemical cells the counter electrode is a Pt foil and the reference electrode a Hg/Hg₂SO₄ electrode (MSE); E = +0.68 V vs RHE.

The experiments were carried out in 0.5 M H_2SO_4 (or 1 M HClO_4) with or without CH_3OH (Merck) (up to 0.33 M); submonolayers of Ru or Sn were deposited by potential cycling in solutions containing low concentrations of ruthenium(III)-nitrosyl nitrate (Johnson Matthey) or SnSO_4 (Janssen Chimica) in 0.5 M H_2SO_4 . All chemicals are p.a. grade. All solutions were prepared with Ecostat water (18.2 M Ω). Argon (99.99%) was used to provide oxygen free electrolyte. The Pt disc was polished with 0.05 μm alumina paste.

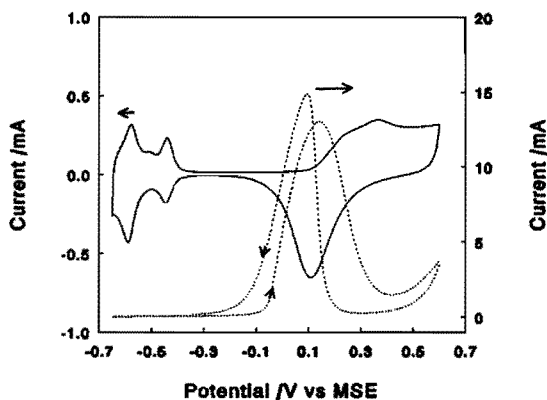


Figure 1 Voltammogram of Pt in 0.5 M H_2SO_4 (-) and in 0.5 M H_2SO_4 /0.1 M CH_3OH (-); scanrate 10 mV/s.

Results and discussion

Methanol adsorption

Figure 1 gives the voltammogram of Pt in 0.5 M H_2SO_4 in the presence and absence of methanol. Comparison of both the anodic scans shows that methanol oxidation starts at a potential at which no oxide formation on Pt is yet found. This fact, often noted in the literature, makes it plausible that an activated water molecule takes part in the electrooxidation of methanol (cf eq.2) and not a Pt-oxide or -hydroxide. Furthermore the peak potential of methanol oxidation is seen to coincide with the onset of the Pt-oxide formation, which shows that Pt-oxides are inactive for the oxidation of methanol. In the cathodic scan methanol oxidation restarts at a potential at which the Pt-oxide is partially reduced. Figure 2 shows the corresponding optical Δ -E curves in 0.5 M H_2SO_4 ; the Ψ -E curves show similar behaviour and are therefore not given. Without methanol a steep decrease of Δ is seen during the anodic scan at potentials higher than +0.1 V vs MSE, this is indicative of the growth of Pt-oxide and coincides with the potential region where Pt oxidation is observed in the cyclic voltammogram (cf fig 1). Furthermore, a slight decrease in Δ is found in the potential region from -0.6 V to

+0.1 V; in the presence of methanol however, Δ remains virtually constant in the same potential region.

The decrease of Δ in the double layer region was also observed by Hyde et al.[16] and attributed to a restructuring of the water layer causing a higher density. If the optical curve is

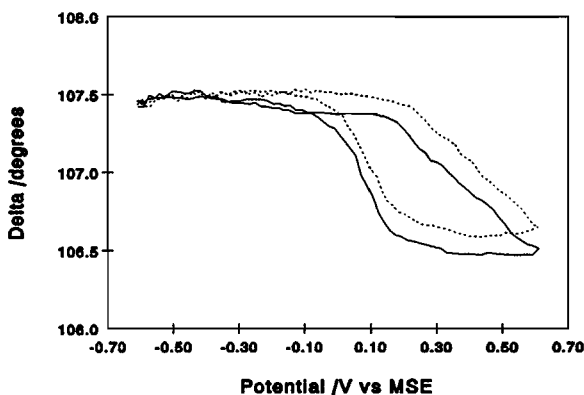


Figure 2 Variation of ellipsometric parameter Δ with potential at Pt in 0.5 M H_2SO_4 (-) and 0.5 M $\text{H}_2\text{SO}_4/0.1$ M CH_3OH (--); scanrate 10 mV/s.

measured in 1 M HClO_4 , a similar behaviour is found, only the decrease of Δ in the double layer region is smaller. This small difference between sulfate and perchlorate electrolyte is probably due to the stronger adsorption of sulfate ions. According to Horanyi[17], the adsorption of bisulfate increases with potential and reaches a maximum at -0.05 V vs MSE.

The fact that in the presence of methanol Δ becomes virtually constant indicates that the adsorbed water layer on the electrode is modified. It is known [18,19,20,21] that methanol (depending on the concentration) adsorbs in the potential range -0.60 V to +0.1 V vs MSE. The flattening of the Δ -E curve must therefore be due to the presence of adsorbed methanolic species, which have (partially) replaced both the adsorbed electrolyte anions and adsorbed water molecules. The replacement of the adsorbed sulfate anions is in agreement with the data of Horanyi[17] which show that less sulfate is detected in the presence of methanol.

Figure 2 provides only indirect evidence for the presence of an adsorbed methanolic species; no direct evidence for this adsorbate is found with ellipsometry. This however offers us a great advantage; now we are able to detect possible changes in the Pt surface oxidation in the presence of methanol. The potential at which the oxide coverage begins is seen to shift to a slightly higher potential in the presence of methanol; however the total Δ and Ψ changes up to the potential of reversal (+0.65 V vs MSE) are virtually the same with and without methanol.

One might state that the onset of Pt-oxide formation is only slightly retarded by the presence of methanolic species. This is in agreement with the quartz-microbalance results of Wilde et al.[21]. The fact that the total changes in Δ and Ψ are not affected by the presence of methanol implies that Pt-oxides do not take part in the oxidation of methanol and that at higher potentials no more methanolic adsorbates are present.

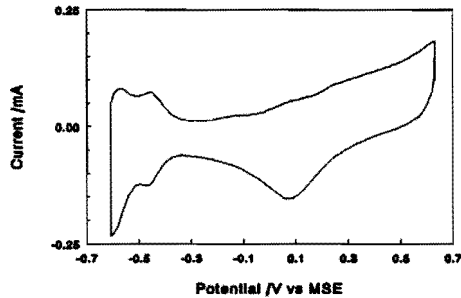


Figure 3 Voltammogram of Pt in 0.5 M H_2SO_4 + $1.35 \cdot 10^{-5}$ M $\text{Ru}(\text{NO})(\text{NO}_3)_3$; scanrate 10 mV/s.

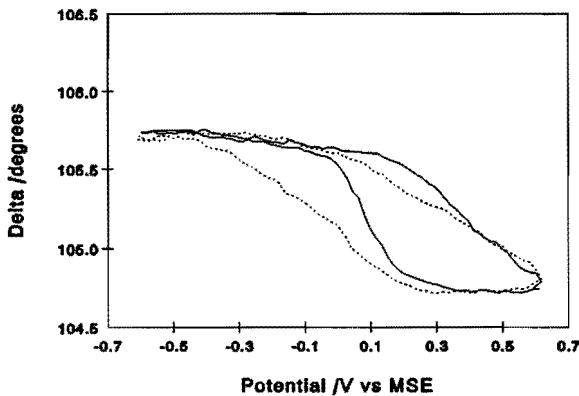


Figure 4 Ellipsometric Δ -E curve of Pt in 0.5 M H_2SO_4 (-) and in the presence of $1.35 \cdot 10^{-5}$ M $\text{Ru}(\text{NO})(\text{NO}_3)_3$ (--); scanrate 10 mV/s.

Pt-Ru system

Figure 3 shows the cyclic voltammogram for Pt in the presence of $1.35 \cdot 10^{-5}$ M Ru ions in the electrolyte. The current in the hydrogen adsorption region has decreased compared with the

voltammogram in the absence of Ru and an anodic hump at ca +0.05 V vs MSE is observed which points to the presence of a Ru species. In the cathodic scan the current in the double layer region has increased due to Ru deposition. Calculation of the Ru coverage by measuring the change in the hydrogen adsorption region is not fully reliable since Ru itself is known to adsorb hydrogen[22]. We therefore calculated the Ru coverage from the anodic Ru peak following the method of Watanabe and Motoo[9]. This gave $\Theta_{\text{Ru}}=0.50$ on the basis of one electron transfer. Figure 4 gives the corresponding Δ -E curves before and after Ru addition. A rather drastic change in the Δ -E curve is seen. In the presence of Ru Δ already starts to decrease at ca -0.3 V in the anodic scan; furthermore in the cathodic scan the change in Δ is extended over a wider potential range. This potential range is extended even further at higher

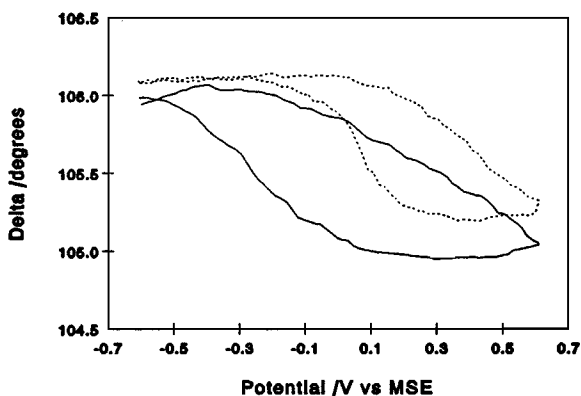


Figure 5 Ellipsometric Δ -E curve of Pt in 0.5 M H_2SO_4 + $2.7 \cdot 10^{-5}$ M $\text{Ru}(\text{NO})(\text{NO}_3)_3$ (-) and in the presence of 0.16 M CH_3OH (--); scanrate 10 mV/s.

Ru concentrations as shown by the full line in figure 5 for $2.7 \cdot 10^{-5}$ M. The Ψ -E curves show similar changes. For comparison both the voltammetric and ellipsometric responses of a Ru electrode were measured. The optical curve is given in figure 6 and shows that Δ starts to decrease in the anodic scan at ca -0.3 V. It is known that the Ru surface is oxidized[22,23] at $E > -0.3$ V, hence the Δ change in figure 6 indicates oxide growth. It is noted that the Pt/Ru electrode behaviour (figure 4 or 5) closely resembles the Δ -E curve for Ru and thus shows predominantly the Ru features. One can therefore confirm that the peak at +0.05 V in the anodic voltammogram is due to the oxidation of Ru atoms on the Pt surface which are reduced in the cathodic scan.

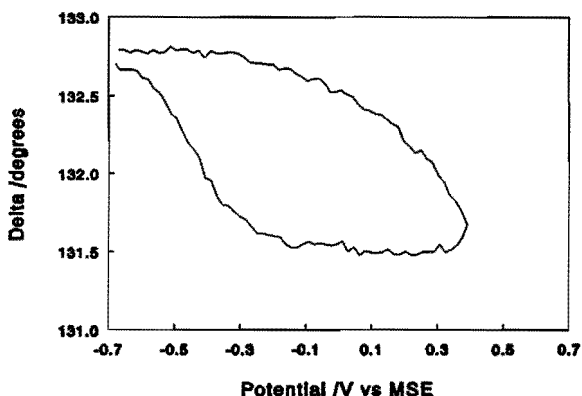


Figure 6 Ellipsometric Δ -E curve of Ru in 0.5 M H_2SO_4 ; scanrate 10 mV/s.

With the pure Ru electrode it is found that Ru dissolves with repeated scanning to potentials higher than +0.2 V; this confirms the work of Beden et al.[13] on Pt-Ru.

In the presence of methanol (0.167 M) the ellipsometric curve of the Pt/Ru system ($2.7 \cdot 10^{-5}$ M Ru ions) changes significantly (Figure 5 dashed line); the Ru features have become less distinct. At higher methanol concentration (0.33 M) they are totally absent and the Δ -E curve is now virtually identical to the ellipsometric curve of Pt without Ru; the only difference is the shift in Δ by 0.25 over the whole potential region. Though the observed change in Δ seems now only due to oxidation and reduction of Pt, there is still Ru present at the surface as can be deduced from the Δ shift with respect to that of the Ru-free Pt (cf figure 5). We further demonstrated this by an experiment in which after methanol oxidation the electrolyte was replaced by fresh sulfuric acid without Ru-salt and methanol. The optical diagram still showed the characteristic Ru features.

In another experiment a Pt-Ru electrode was prepared by potential scanning in a Ru containing electrolyte outside the optical cell. Optical measurements in a Ru-free electrolyte showed the characteristic Ru features. After addition of methanol again similar optical changes were observed as for the Ru containing electrolyte.

The ellipsometric curve of Ru itself does not alter in the presence of methanol. This is in accordance with Franaszczuk et al.[24] who did not find methanol adsorption on Ru.

The voltammogram of the Pt-Ru-methanol system in 0.5 M H_2SO_4 + 0.33 M CH_3OH is given in figure 7A for different Ru concentrations. These data show that in the anodic scan the methanol oxidation is enhanced in the presence of Ru-ions in the potential region up to 0 V vs MSE, while at higher potentials the activity decreases. To verify that the increase in oxidation current is indeed due to methanol oxidation, simultaneous DEMS measurements were carried out. The results are given in figure 7B and demonstrate that in the potential region -0.3 to 0 V

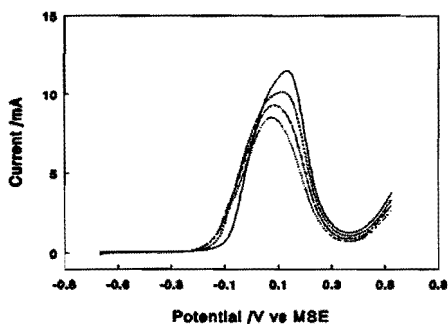


Figure 7a I-E curve of Pt in 0.5 M $\text{H}_2\text{SO}_4/0.33$ M CH_3OH and (-) 0M; (--) 5×10^{-5} M; (-.) 1×10^{-4} M; (...) 1.5×10^{-4} M $\text{Ru}(\text{NO})(\text{NO}_3)_3$.

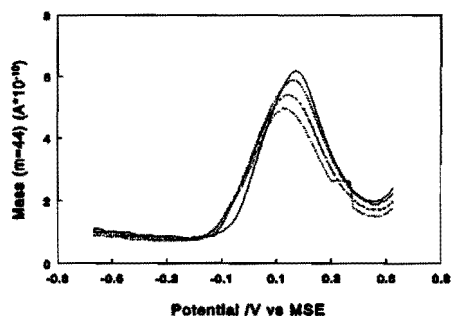
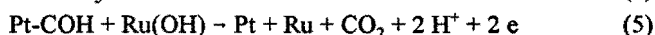
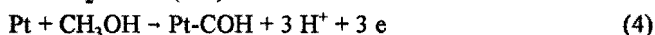
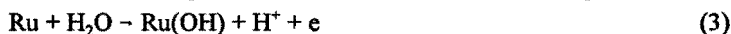


Figure 7b Same as for A, but M-E curve.

vs MSE the CO_2 production increases with higher Ru concentration.

The results of the Pt-Ru system may be summarized as follows: Ru, which is present in submonolayer form on Pt, is oxidized at potentials ≥ -0.3 V vs MSE. This oxide growth can be followed with ellipsometry and appears to be virtually the same as that found on Ru metal. The Ru-oxides are found to disappear in the presence of methanol whereas those on a Ru electrode do not. In the same potential region where the oxides are formed, an enhancement in the methanol oxidation activity is observed.

We may thus conclude that the disappearance of the Ru-oxide is caused by the reaction with an adsorbed methanolic species on Pt. This leads to the following reaction scheme:



This mechanism was first proposed by Watanabe and Motoo[9] and represents the bifunctional model. They assume that monovalent $\text{Ru}(\text{OH})$ is the active Ru species; this is also supposed by Herrero et al.[25]. With ellipsometry the exact nature of the Ru-oxide species cannot be established, RuO_2 however may be excluded because this was found [26] to be inactive for the methanol oxidation.

The ellipsometric data indicate that Ru is present in the metallic state during the methanol oxidation, which implies that the reactions (eqs 3-5) are rapid. The conclusion that Ru is zero-valent was also postulated by Janssen and Moolhuysen[6] but contradicts the XPS and Mössbauer measurements of Hamnett and Kennedy[27,28] which show that all Ru is present

as Ru(IV). They concluded that the actual processes must take place at Pt via a Ru-Pt oxide species. These measurements were however carried out *ex-situ* and are thus not fully relevant for the actual situation at the surface during methanol oxidation.

Pt-Sn system

Figure 8 gives the cyclic voltammograms for Pt in the presence of different SnSO_4 concentrations. It shows the same characteristics as the voltammogram for Pt-Ru (figure 3). The hydrogen region is partially suppressed and the current increase around -0.2 V in the cathodic scan indicates the reduction of a Sn species. The anodic peak at $+0.05$ V indicates the oxidation of a Sn species. At higher anodic potentials Sn is found to dissolve from the surface. The Sn coverage was calculated from the difference between the hydrogen adsorption area (Q_H) in the absence and presence of Sn; $\Theta_{\text{Sn}} = (Q_H^0 - Q_H^{\text{Sn}})/Q_H^0$. For the three presented curves of figure 8 these coverages are respectively $\Theta_{\text{Sn}}=0.20$; $\Theta_{\text{Sn}}=0.52$ and $\Theta_{\text{Sn}}=0.72$. The corresponding Δ -E curves are shown in figure 9 for Sn coverages of $\Theta_{\text{Sn}}=0.20$ and $\Theta_{\text{Sn}}=0.72$. Compared to the Δ -E curve of Pt (cf figure 2) a change in Δ is seen in the low potential region during the cathodic scan, this indicates the upd of Sn; with increasing Sn coverage the changes in Δ are more pronounced.

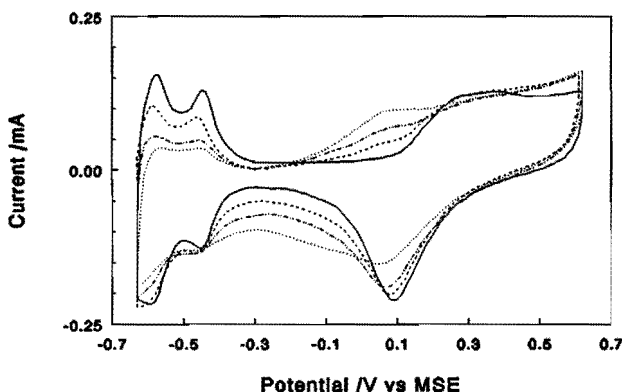


Figure 8 Voltammogram of Pt in $0.5 \text{ M H}_2\text{SO}_4$ and (-) 0; (--) $2.7 \cdot 10^{-5}$; (·) $5.4 \cdot 10^{-5}$; (-·) $8.1 \cdot 10^{-5} \text{ M SnSO}_4$; scanrate 100 mV/s .

During the anodic scan Δ decreases only slightly with potential in the low potential region. The larger decrease of Δ at $E > \text{ca } 0.3 \text{ V}$ indicates the growth of a layer which is most likely oxidation of Pt that is not covered with Sn. The Ψ -E curves gave a different pattern. This is demonstrated by figure 10 which represents the change of Ψ vs Δ during a full scan for the Pt-

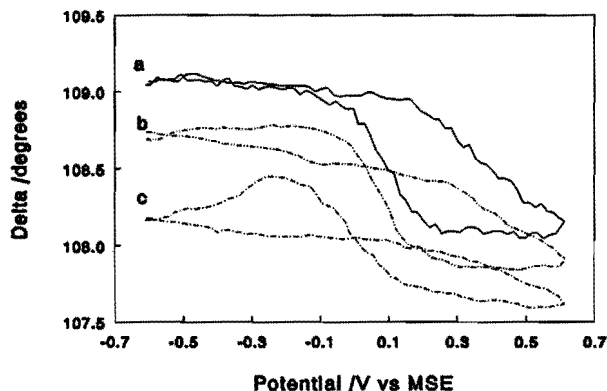


Figure 9 Ellipsometric curve of Pt in 0.5 M H_2SO_4 and (a) 0; (b) $2.7 \cdot 10^{-5}$; (c) $8.1 \cdot 10^{-6}$ M SnSO_4 . Scanrate 10 mV/s.

Sn system with $\Theta_{\text{Sn}} = 0.20$. It follows from the theory of ellipsometry[14] that the growth of a very thin film with constant refractive index is represented by a linear Ψ - Δ curve. For the cathodic scan the Ψ vs Δ curve is linear in the potential range from 0.6 V to ca 0 V; this line signifies the decrease in oxide coverage during reduction, while around -0.05 V the slope of the line changes indicating the onset of another process viz. Sn upd. After scan reversal at -0.6 V it is noted that the curve turns around until at ca 0.1 V Ψ reaches a maximum. In the potential range 0.2 to 0.6 V the curve is again linear and virtually retraces the oxide reduction line. This behaviour can be explained as follows: Pt is oxidized and reduced in the potential region 0.2 to 0.6 V and Sn that is deposited on Pt is oxidized in the potential region -0.2 to 0.2 V. Hence the anodic peak at 0.05 V in the voltammogram of figure 8 represents the surface oxidation of Sn.

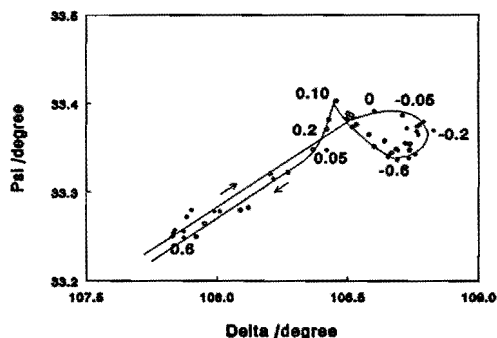


Figure 10 Plot of ellipsometric parameters Ψ vs Δ for the Pt-Sn ($\theta_{\text{Sn}}=0.2$) system of figure 9. (•) increasing potential; (◦) decreasing potential. Numbers indicate potential (V vs MSE).

It was observed that with repeated scanning in the Sn-containing electrolyte the optical behaviour of the Pt electrode changed. This was established by taking optical measurements at the Pt electrode in a Sn-free electrolyte. The Δ , Ψ data differ from the values obtained at Pt before Sn addition. This change of the Pt substrate indicates that some Sn dissolves into platinum as was also noted by others[29,30,31]. With prolonged oxidation at high potential Δ and Ψ return slowly to the original values.

In the presence of 0.16 M methanol the ellipsometric curve for the Pt-Sn ($\Theta=0.72$) electrode changes as shown in figure 11. The Sn features have become less dominant in the potential range -0.5 to ca 0.3 V; with 0.33 M methanol the original Δ -E plot for Pt is obtained. It was concluded above that Sn-oxides are formed in the potential region up to 0.2 V vs MSE. The optical change of figure 11 then implies that the Sn-oxide disappears due to reaction with methanol. It is possible that also some removal of Sn species from the surface is involved. It is known that at higher potentials some dissolution of Sn-oxide occurs [6,31], which could be enhanced by methanol. Vassiliev et al.[29] concluded from radiotracer experiments that the Sn coverage is lower in the presence of methanol; they found that Sn already disappears at -0.35 V. We however found that after methanol oxidation there is still Sn present on the electrode surface.

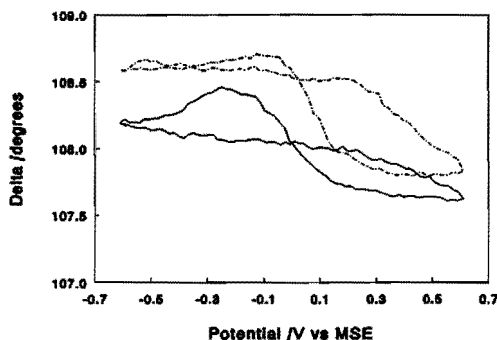
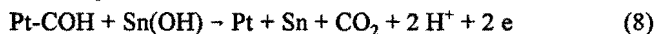
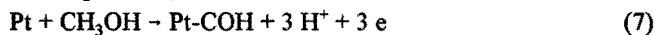


Figure 11 Ellipsometric curve of Pt in 0.5 M H_2SO_4 + $8 \cdot 10^{-5}\text{M}$ SnSO_4 (-) and in the presence of 0.16 M methanol (--). Scanrate 10 mV/s.

Voltammetry and DEMS measurements of methanol oxidation at Pt with different Sn concentrations are presented in Figures 12A and 12B. The results, as with Ru, show a simultaneous increase of current and CO_2 in the presence of Sn at potentials -0.15 to 0 V, signifying an enhanced methanol oxidation. Thus the Sn surface species enhances the methanol oxidation in the same potential region as where it is oxidized in the absence of methanol.

The behaviour of the Pt-Sn system is thus similar to the Pt-Ru system. The bifunctional mechanism as was discussed for Ru, will therefore also apply for Sn.



Sn(OH) is used here as a formal notation. According to Iwasita[2] Sn is present in different redox states depending on the potential; Janssen and Moolhuysen[32] favor a zero-valent state and Sobkowski et al.[11] concluded to an adsorbed divalent hydroxy- or sulfate tin

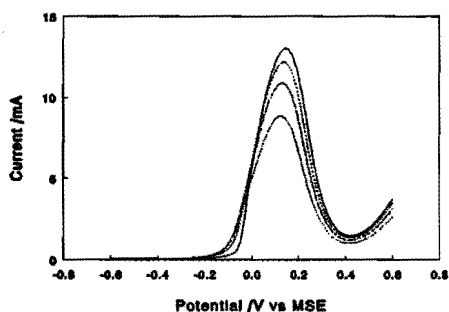


Figure 12a Voltammometry of PtPt in 0.5 M $\text{H}_2\text{SO}_4/0.33 \text{ M CH}_3\text{OH}$ and (-) 0; (-) $5 \cdot 10^{-5}$; (-) $1 \cdot 10^{-4}$; (...) $1.5 \cdot 10^{-4} \text{ M SnSO}_4$; scanrate 2 mV/s.

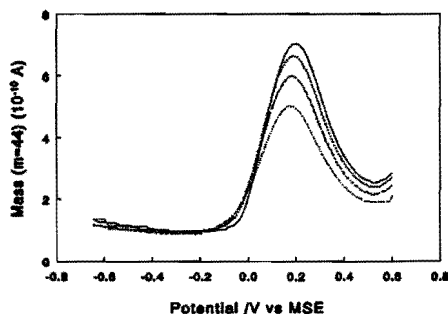


Figure 12b Same as for (a), but CO_2 mass-E, instead of I-E.

complex. The ellipsometric results presented here seem to indicate that Sn is zero valent during the methanol oxidation, which again implies that all reactions (eqs 6-8) must be very rapid.

Conclusions

- The amount of Pt-oxide formed during a potential scan is not affected by the presence of methanol, but the onset potential of Pt oxidation is shifted to slightly higher potentials in the presence of methanol.
- The oxidation of Ru and Sn, deposited on the Pt surface in submonolayer coverage, can be followed with ellipsometry.
- In the presence of methanol the oxide coverage of Ru and Sn disappears. Therefore both metals must be present in the zero-valent state at Pt during the methanol oxidation.

-DEMS and voltammetric measurements show that Ru and Sn enhance the methanol oxidation in the same potential region where these metals are covered with an oxide layer in the absence of methanol.

-A bifunctional mechanism is proposed for the effect of both Sn and Ru, although an additional ligand effect can not be excluded on the basis of these measurements.

References

1. R. Parsons and T. Vandermoot *J. Electroanal. Chem.* **257**, 9 (1988)
2. T. Iwasita-Vielstich in *Advances in Electrochemical Science and Engineering*, Vol.1, p.127 ed H. Gerischer and Ch. W. Tobias, VCH Publishers, New York, 1990
3. T. Iwasita, F.C. Nart, B. Lopez and W. Vielstich *Electrochim. Acta* **37**, 2361 (1992)
4. V.S. Entina and O.A. Petrii *Elektrokhimiya* **4**, 678 (1968)
5. A.A. Mikhailova, N.V. Osetrova and Yu.V. Vassiliev *Elektrokhimiya* **13**, 518 (1978)
6. M.M.P. Janssen and J. Moolhuysen *Electrochim. Acta* **21**, 869 (1976)
7. H.A. Gasteiger, N. Markovic, P.N. Ross and E.J. Cairns *J. Phys. Chem.* **97**, 12020 (1993)
8. S.A. Campbell and R. Parsons *J. Chem. Soc. Faraday Trans.* **88**, 833 (1992)
9. M. Watanabe and S. Motoo *J. Electroanal. Chem.* **60**, 267 (1975)
10. R.R. Adzic in *Advances in Electrochemistry and Electrochemical Engineering*, Vol. 13 p. 159. Ed. H. Gerischer, J. Wiley, New York, 1984
11. J. Sobkowski, K. Franaszczuk and A. Piasecki *J. Electroanal. Chem.* **196**, 145 (1985)
12. M.M.P. Janssen and J. Moolhuysen *Electrochim. Acta* **21**, 861 (1976)
13. B. Beden, F. Kadirgan, C. Lamy and J.M. Leger *J. Electroanal. Chem.* **127**, 75 (1981)
14. R.H. Muller in *Advances in Electrochemistry and Electrochemical Engineering*, Vol.9, p.167 ed H. Gerischer and Ch. W. Tobias, J. Wiley, New York, 1973
15. T. Iwasita, W. Vielstich and E. Santos *J. Electroanal. Chem.* **229**, 367 (1987)
16. P.J. Hyde, C.J. Maggiore, A. Redondo, S. Srinivasan and S. Gottesfeld *J. Electroanal. Chem.* **186**, 267 (1985)
17. G. Horanyi and A. Wieckowski *Proc. Workshop on Direct Methanol Air Fuel Cell*. Ed. A.R. Landgrebe et al. Proc. Vol. 92-14 Electrochem. Soc. p.70 (1992).
18. V.S. Bagotsky and Yu.B. Vassiliev *Electrochim. Acta* **11**, 1439 (1966).
19. J. Sobkowski, K. Franaszczuk and K. Dobrowolska *J. Electroanal. Chem.* **330**, 529 (1992)
20. A. Papoutsis, J.M. Leger and C. Lamy *J. Electroanal. Chem.* **234**, 315 (1987)
21. C.P. Wilde and M. Zhang *Electrochim. Acta* **39**, 347 (1994)
22. S. Hadri-Jordanov, H. Angerstein-Kozłowska, M. Vukovic and B.E. Conway *J. Electrochem. Soc.* **125**, 1471 (1978)
23. E. Ticanelli, J.G. Beery, M.T. Paffett and S. Gottesfeld *J. Electroanal. Chem.* **258**, 61 (1989)
24. K. Franaszczuk and J. Sobkowski *J. Electroanal. Chem.* **327**, 235 (1992)
25. E. Herrero, K. Franaszczuk and A. Wieckowski *J. Electroanal. Chem.* **361**, 269 (1993)
26. B.J. Kennedy and A.W. Smith *J. Electroanal. Chem.* **293**, 103 (1990)
27. A. Hamnett, B.J. Kennedy and F.E. Wagner *J. Catal.* **124**, 30 (1990)
28. B.J. Kennedy and A. Hamnett *J. Electroanal. Chem.* **283**, 271 (1990)

Chapter 7

29. Yu. B. Vassiliev, V.S. Bagotsky, N.V. Osetrova and A.A. Mikhailova *J. Electroanal. Chem.* 97, 63 (1979)
30. M.M. Stefanel, T. Chiechie and C. Mayer *Z. f. Physik. Chem. NF* 135, 251 (1983)
31. E. Lamy-Pitara, L. El Ouazzani-Benhima, J. Barbier, M. Cahoreau and J. Caisso *J. Electroanal. Chem.* 372, 233 (1994)
32. M.M.P. Janssen and J. Moolhuysen *J. Catal.* 46, 289 (1977)

The role of surface oxides in the electrooxidation of Methanol, Formic Acid and CO on Pt, Ru and codeposited Pt-Ru.

Abstract

The growth of an oxide layer on Pt, Ru and codeposited Pt-Ru was monitored ellipsometrically during the electrooxidation of CH_3OH , HCOOH and adsorbed CO. The results show that no oxide is present at the Pt-Ru surface in the potential region where these molecules are oxidized. This supports the bifunctional mechanism that has been proposed for the promoting role of Ru on Pt. The oxide at Pt is not involved in the HCOOH and CO_{ads} oxidation. The adsorbed CO layer on Pt and on Pt-Ru could also be observed with ellipsometry.

Introduction

Platinum is considered to be the most suitable catalyst for the electrooxidation of methanol in acid electrolyte. Its activity, however, is too low for application in a direct methanol fuel cell; moreover, the catalyst rapidly deactivates. One of the causes for this deactivation is the formation of a CO intermediate that is only oxidised at relatively high potentials. Since molecules like CO or HCOOH are oxidized at the same potentials, show similar current-potential profiles and are believed to react via similar intermediates, the behaviour of these molecules has also been explored extensively [1,2,3,4]. The nature of the adsorbed species (and/or intermediates) has been investigated with a wide variety of in-situ surface techniques, though it is surprising that rather few investigations have employed in situ reflectance spectroscopy or ellipsometry.

It is generally accepted that an oxygen species or activated water molecule must be present at the surface to enable the oxidation of the adsorbed intermediates. The Pt-oxide itself is not involved in the oxidation of methanol, but the onset of the surface oxidation was found to be slightly retarded by the presence of adsorbed methanolic species. This was established with ellipsometry [5] and electrochemical quartz crystal microbalance measurements [6].

Ruthenium is the best promotor for the oxidation of small organic molecules over Pt. This is generally attributed to the lower oxidation potential of Ru with respect to that of Pt such that Ru-oxides now supply the oxygen necessary to oxidise the adsorbate. At Pt-Ru_{ad} we found that Ru-oxides take part in the oxidation, they disappear from the surface during the methanol oxidation [5]. This finding supports the bifunctional mechanism that has been proposed for Ru in the methanol oxidation over Pt [7]. The Ru surface coverage that gives the highest activity, varies for the different molecules: for HCOOH and CO the highest activity is found at ca 46% [8,9], for methanol it is ca 7% at 25 °C but ca 33% at 60 °C [10]. The differences between the

different molecules are related to the fact that CH_3OH needs a large Pt ensemble to adsorb, whereas HCOOH and CO do not, as was explained by Gasteiger et al.[10].

In this paper we have further investigated with ellipsometry the role of surface oxides in the electrooxidation of CO , HCOOH and CH_3OH at Pt and codeposited Pt-Ru electrodes of varying composition. Results for Ru will be shown for comparison.

Experimental

Combined cyclic voltammetry and ellipsometry measurements were carried out at a smooth disc electrode using a Wenking potentiostat POS 73 with Philips PM 8043 recorder and an automated ellipsometer Rudolph RR 2200 with tungsten iodine light source and monochromatic filter resulting in light with a wavelength of 546.1 nm.

The optical cell is cylindrical and supplied with windows arranged for an angle of incidence of 70° at the substrate. The counter electrode is a Pt foil and the reference electrode a $\text{Hg}/\text{Hg}_2\text{SO}_4$ electrode ($E_{\text{MSE}} = +0.68$ V vs RHE). The applied scanrate is 10 mV/s.

The disc electrode is smooth Pt (area 0.5 cm^2) or Ru (area 0.785 cm^2). Electrodeposited PtRu electrodes with different Ru/Pt ratio were prepared by deposition onto Pt or Ru at constant current or potential from solutions containing low concentrations of ruthenium (III)-nitrosyl-nitrate (Johnson Matthey) and H_2PtCl_6 in $0.5 \text{ M H}_2\text{SO}_4$.

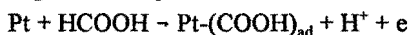
The experiments were carried out in $0.5 \text{ M H}_2\text{SO}_4$ to which CH_3OH (Merck) (up to 0.33 M) or HCOOH (0.09 M) was added. The electrolyte was deoxygenated with argon (99.99%). Experiments with CO were performed by keeping the potential at -0.3 V and adsorbing CO for 5 min, thereafter argon was passed through for 10 min. All chemicals are p.a. grade. All solutions were prepared with ultrapure water (Ecostat 18.2 M Ω).

Results and discussion

Oxidation of HCOOH and CO over Platinum

The oxidation of formic acid follows a dual path mechanism [11] viz.

a dehydrogenation step:



and a dehydration step:



The cyclic voltammogram of HCOOH oxidation at Pt in $0.5 \text{ M H}_2\text{SO}_4$ is given in Fig.1 and shows the well known profile with current maxima at -0.1 and $+0.15 \text{ V}$ (main peak) in the positive sweep [12,13]. The oxidation starts immediately after the hydrogen desorption region and reaches its maximum at the potential where Pt-oxide formation starts in the absence of HCOOH . In the reverse scan, the oxidation starts at the onset of the Pt-oxide reduction and reaches higher currents than in the forward scan at the same potentials. The oxidation current falls back to zero again as the hydrogen adsorption starts. In the simultaneously recorded

ellipsometric curves of Fig.2 the variation of the optical parameter Δ in the absence and presence of HCOOH is given. In the presence of HCOOH the value of Δ is virtually constant going from -0.6 V up to +0.2 V while in the supporting electrolyte Δ decreases slightly in this region. This behaviour was earlier also noted for the electrooxidation of CH₃OH over Pt [5] and it was postulated that this is probably due to the presence of organic adsorbates which replace adsorbed water and sulphate anions. Above +0.2 V Δ decreases due to oxide growth on Pt. The onset of oxide formation virtually coincides with the main oxidation peak in the voltammogram and is not shifted considerably in the presence of HCOOH. In the reverse sweep the Δ increase at 0.25 V, both in absence and in presence of HCOOH, indicates the start of the oxide reduction; this is accompanied by a rapid current increase to higher values than in the forward scan and shows that the presence of HCOOH does not influence the onset of oxide formation or reduction.

No significant change in Pt-oxide formation and/or reduction is thus be found in the presence

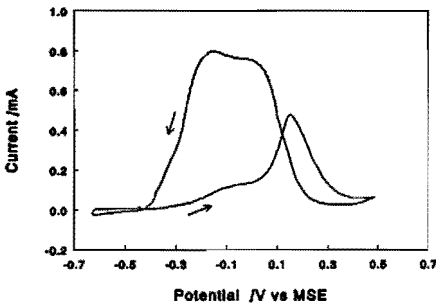


Figure 1 Voltammogram of Pt in 0.5 M H₂SO₄/0.09 M HCOOH.

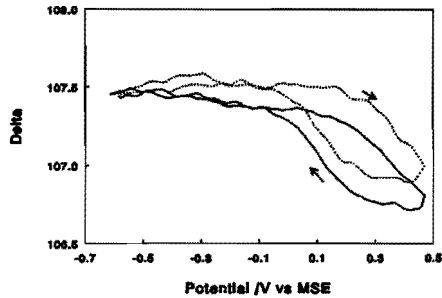
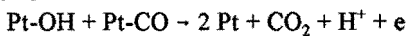


Figure 2 Δ -E curve of Pt in 0.5 M H₂SO₄ (-); and with 0.09 M HCOOH.

of HCOOH; also the total change in Δ due to Pt-oxide film is the same both with and without HCOOH, and indicates that Pt-oxide does not play a role in the HCOOH oxidation as was also observed for CH₃OH[5].

The CO oxidation was measured by monitoring the behaviour of the Pt/CO_{ad} system in CO-free electrolyte. The voltammogram of Fig.3 shows in the positive potential sweep an oxidation current peak at +0.03 V, in agreement with [2,13,14,15]. This current maximum corresponds with the oxidation of an adsorbed CO molecule with an activated water or hydroxy species:



The surface coverage with CO_{ad}, calculated from the hydrogen desorption area, is 87%. The eps (electron per site) value is found to be 1.4 indicating that both linearly and bridge bonded

CO are present. The optical response is given in Fig.4 together with the curve before CO adsorption and reveals a remarkable difference. The initial Δ value in the case of CO_{ad} is distinctly lower than for Pt alone. During the positive going potential scan Δ remains constant up to -0.15 V, then increases until at ca 0.1 V, Δ begins to decrease due to Pt-oxide growth.

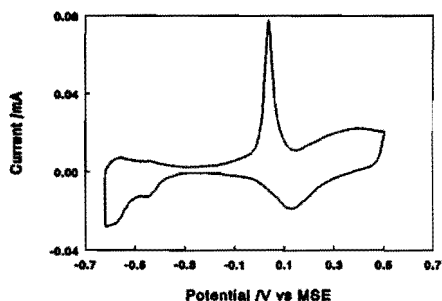


Figure 3 Voltammogram of CO_{ad} on Pt in $0.5 \text{ M H}_2\text{SO}_4$.

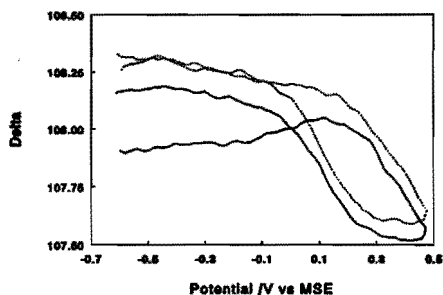


Figure 4 Δ -E curve of Pt in $0.5 \text{ M H}_2\text{SO}_4$, before (--) and after (-) CO adsorption.

The shift in Δ in the low potential region indicates the presence of an adsorbed layer, this is most likely CO, which starts to be oxidised from the surface at -0.20 V, in agreement with the start of the CO-oxidation current in the voltammogram. The maximum in Δ is reached at the potential where almost all CO is oxidised from the surface as again can be seen in the voltammogram. In the reverse scan Δ starts to increase at 0.2 V due to oxide reduction and rises to approximately the same value as in the CO free system. This means that the adsorbed CO is indeed removed by the oxidation cycle. The results show clearly that the oxidation of CO_{ad} starts effectively as soon as CO_{ad} begins to react and disappears from the surface. This corroborates with the conclusions of Corrigan and Weaver[16] based on SPAIR results. With in situ reflectance spectroscopy measurements [17,18,19] coverage dependent reflectivity changes have been found. The observed shift in Δ in the low potential region must thus be attributed to an adsorbed CO layer, however the magnitude of this shift raises a problem. No significant optical shift was observed for CH_3OH and HCOOH although the reaction mechanisms for these molecules are known to proceed via a CO intermediate. If we calculate the thickness of the adsorbed film from the difference in Δ at -0.6 V for Pt- CO_{ad} and bare Pt, a value of 0.54 nm with a refractive index $n - ik = 1.55 - 0i$ is obtained. This is far larger than would be expected for an adsorbed CO layer (ca. 0.3 nm). Although such large thickness might be explained by a hydrated CO layer, as was proposed by Stonehart[20], this does not seem to be very likely because CO_{ad} from CH_3OH or HCOOH must then be expected to be hydrated also. Caram and Gutierrez [21] suggest that a Pt-CO surface complex is formed, as it has been noted [22] that the $\text{Pt}_{24}\text{CO}_{30}$ cluster exhibits the same IR behaviour at chemisorbed

CO on Pt. Kunimatsu[4] found with IR a small difference between CO_{ad} from CH_3OH or HCOOH and CO_{ad} from CO; this effect is too small to explain the difference observed here. It was however noted by Ikezawa et al.[19] that only part of the CO on the surface was visible with IR and the rest was IR inactive. Recently [23] similar large change in reflectivity at wavelength 250 nm upon CO adsorption was reported; it is suggested that this is due to a charge transfer transition of CO-Pt surface complex. A possible explanation for the ellipsometric result might be that the effect is caused by a structural difference between the adsorbed layer from CO and that from methanol or formic acid. By comparing IR spectra of CO_{ad} layers formed by dosing from solution and by partial electrooxidative stripping of the saturated adsorbed layer, Chang and Weaver [24] have concluded that CO is adsorbed as islands in which CO is present at high local coverage. If we may assume that this does not occur in the case of methanol, which is in agreement with reactivity differences between CO and methanol, or formic acid, then the adsorbate layer resulting from these molecules can be a homogeneously adsorbed film. Such a structural difference between the layers could imply a difference in optical density and hence in a larger Δ change for the adsorbed layer from CO.

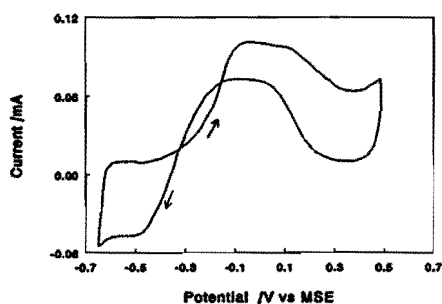


Figure 5 Voltammogram of Ru in 0.5 M $\text{H}_2\text{SO}_4/0.09$ M HCOOH .

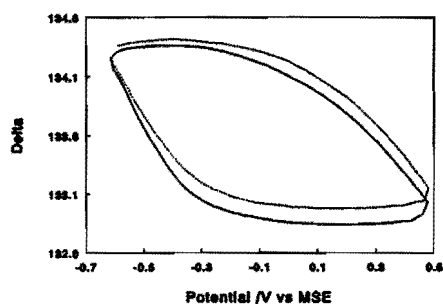


Figure 6 Δ -E curve of Ru in 0.5 M H_2SO_4 (-); and with 0.09 M HCOOH (--).

Oxidation of HCOOH and CO over Ruthenium.

Ruthenium itself has only low activity for the oxidation of HCOOH and CO [8,25]. Its behaviour will be presented here in order to compare the results with those for Pt-Ru. Ru shows no activity at all for oxidation of CH_3OH [9,26]; ellipsometric measurements [5] likewise do not reveal a change in the presence of methanol.

The voltammogram of the oxidation of HCOOH at Ru is given in Fig. 5 and shows a current due to the oxidation of HCOOH in the potential region -0.4 to 0.4 V. The shape of the

voltammogram resembles that of Pt, though the activity over Ru is much less than over Pt. In Fig. 6 the ellipsometric curves are given for Ru in the presence and absence of HCOOH. In the supporting electrolyte alone the beginning of the surface oxidization is observed by the decrease of Δ at -0.3 V, this has been attributed to Ru-oxide, which is known to form at $E > -0.3$ V [5,27,28,29]. In the presence of HCOOH the Ru oxidation sets in at slightly higher potential. It is strange to note, that although Ru-oxide in the reverse scan is not reduced until -0.5 V, HCOOH oxidation already proceeds below $+0.25$ V. No free Ru is thus necessary for the oxidation of HCOOH. Although the cyclic voltammogram suggests that HCOOH oxidation occurs over Ru-oxide, it is not likely that the oxides do react with HCOOH, since no change in the amount of oxide formed is found. This might indicate that no oxygen supply is necessary for the oxidation of HCOOH. This is furthermore corroborated by the fact that the oxidation

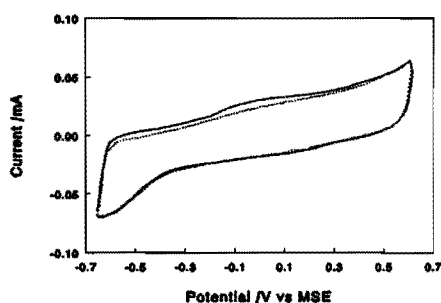


Figure 7 Voltammogram of Ru in 0.5 M H_2SO_4 , with (-) and without CO_{ad} (---).

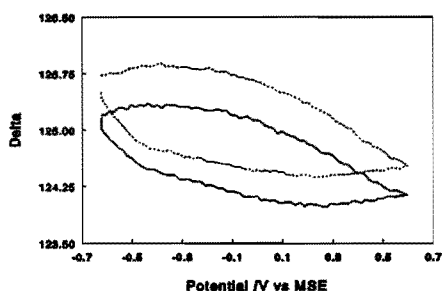


Figure 8 Δ -E curves for the systems in figure 7.

starts at the same potential both on Pt and Ru; at $E = -0.4$ V, a potential at which on a Pt electrode no oxide species are present on the surface.

The behaviour of Ru/ CO_{ad} is presented in the voltammogram of Fig. 7, the oxidation starts at -0.25 V and reaches a maximum at -0.05 V. As can be seen in the optical response of Fig. 8 the onset of Ru-oxidation occurs virtually at the same potential as without CO_{ad} but the total Δ difference between the positive and negative going potential sweep is less compared to Ru alone. This might point either to blocking of the surface by an adsorbate (possibly CO) which cannot be removed by oxidation and thus prevents part of the surface of getting oxidised, or it might point to the reaction of the oxide with the CO adsorbates, thus removing part of the surface oxides.

The different activity of Ru for oxidation of HCOOH and CH_3OH was attributed by Gasteiger et al. [8] to a difference in adsorption path: at Ru HCOOH follows only the dehydration route

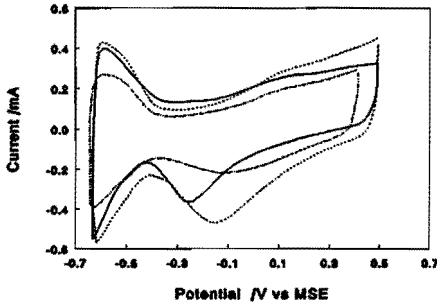


Figure 9 Voltammograms of PtRu (-) $\theta_{\text{Ru}}=0.50$; (--) $\theta_{\text{Ru}}=0.32$; (-.) $\theta_{\text{Ru}}=0.21$ in 0.5 M H_2SO_4 .

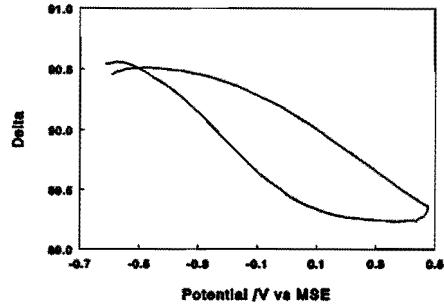


Figure 10 Δ -E curve of PtRu ($\theta_{\text{Ru}}=0.5$) in 0.5 M H_2SO_4 .

resulting in CO_{ad} , whereas CH_3OH can not be dehydrogenated at Ru. From our experiments however it remains to be seen whether a surface oxide species is involved in the oxidation of HCOOH on Ru, this would then imply that the adsorbate is not be CO since the oxidation of this species requires an oxide species.

Codeposited Pt-Ru films

Figure 9 shows the voltammograms of codeposited PtRu electrodes with $\theta_{\text{Ru}}=0.50$, $\theta_{\text{Ru}}=0.32$ and $\theta_{\text{Ru}}=0.21$ in 0.5 M H_2SO_4 . There is no difference between Pt-Ru films deposited on Pt or on Ru. The Ru surface content of the deposited film is determined from the peakpotential at which the surface oxide is reduced; we found earlier [30] that a linear relationship exists between the reduction potential of the surface oxide and the Ru surface content in the

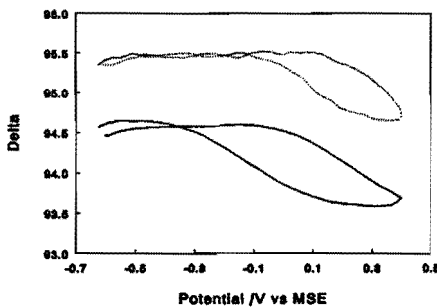


Figure 11 Δ -E curve of PtRu ($\theta_{\text{Ru}}=0.21$) in 0.5 M $\text{H}_2\text{SO}_4/0.16$ M CH_3OH . (-) 1st scan; (--) 18th scan.

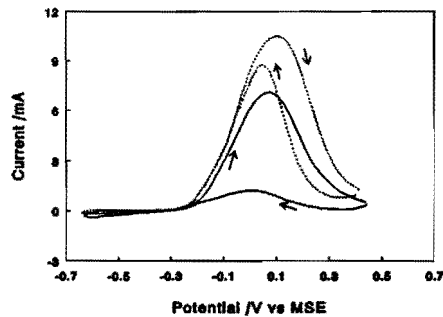


Figure 12 Voltammogram of system in figure 11.

electrodeposited PtRu films. The ellipsometric response to a potential sweep is given in Fig.10 for PtRu($\theta_{Ru}=50$). The decrease of Δ at ca -0.3 V indicates the beginning of the surface oxidation; similar curves were found at other Ru coverages.

The activity for the oxidation of CH₃OH at the different Pt-Ru electrodes depends on the Ru surface content, a typical diagram is given in Fig.11 for PtRu($\theta_{Ru}=0.21$) in 0.16 M methanol (full line). The much smaller current during the reverse part of the scan is indicative of the presence of PtRu-oxides which block the surface such that only a small amount of free Pt sites are available on which CH₃OH can re-adsorb. In the corresponding optical curves of Fig.12 no Ru oxide formation is detected in the potential region -0.3 to 0 V, in agreement with our earlier results at PtRu_{ad} [5]. The start of the oxide growth at $E \geq 0$ V virtually coincides with the

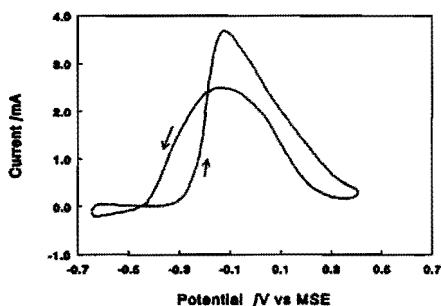


Figure 13 PtRu ($\theta_{Ru}=0.21$) in 0.5 M H₂SO₄/0.09 M HCOOH.

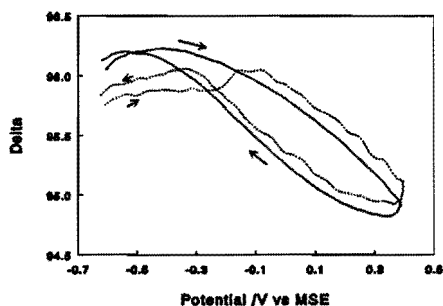


Figure 14 Δ -E curve of the system in figure 13; solid curve without HCOOH.

current maximum for the methanol oxidation. The slight Δ increase at the start of the positive potential sweep was observed at most PtRu electrodes. A similar behaviour was found by Velikodnyi et al.[29] and is due to desorption of absorbed hydrogen from Ru. With repeated cycling up to 0.4 V, Ru is leached out and the surface gradually becomes more rich in Pt as shown by the dashed line in Fig.12, which resembles a Pt profile (onset of oxide growth at higher potential) and by the increased current for the methanol oxidation in the reverse scan of the voltammogram (dashed line in Fig.11).

The oxidation of HCOOH at PtRu electrodes is characterized by a single maximum at -0.12 V, as can be seen in the voltammogram of Fig.13 for PtRu($\theta_{Ru}=0.21$), in agreement with measurements at PtRu alloys [31]. In Fig.14 the optical results obtained at this electrode with and without HCOOH are given. In the presence of HCOOH no change in Δ is found between -0.6 V and -0.25 V, as was also observed for Pt alone. At -0.25 V a slight increase in Δ is found up to -0.2 V, this effect is similar, though far smaller than that found for CO_{ad} on Pt.

Furthermore the decrease of Δ due to PtRu-oxide formation starts at higher potential (-0.06 V). In the negative going sweep the behavior of Δ is the same as without HCOOH, while the current for HCOOH oxidation is much smaller than in the forward scan. The PtRu electrodes with $\theta_{\text{Ru}}=0.50, 0.32$ and <0.05 show similar behaviour: at all electrodes the oxide is apparently not any more present in the potential region -0.30 to -0.10 V since the start of the Δ decrease due to oxide growth is shifted to higher potentials. This change in Δ sets in at the same

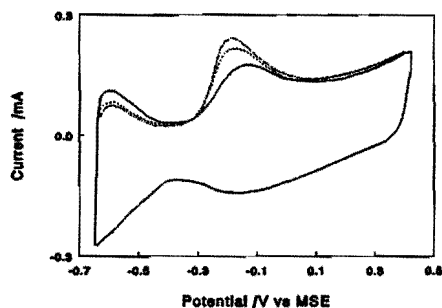


Figure 15 PtRu ($\theta_{\text{Ru}}=0.32$) with adsorbed CO. $\theta_{\text{CO}}=0.44(-)$; $0.63(- -)$; $0.73(- \cdot)$. $0.5 \text{ M H}_2\text{SO}_4$.

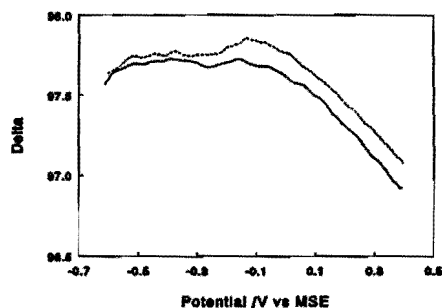


Figure 16 Δ -E curve for the system in fig. 15. $\theta_{\text{CO}}=0.63 (-)$; $0.73 (- -)$.

potential as the potential of the current maximum in the voltammogram. The hump in the Δ change around -0.2 V is most pronounced for the PtRu($\theta_{\text{Ru}}=0.21$) electrode and is not observed a PtRu($\theta_{\text{Ru}}=0.50$). This Δ change is concomitant with the current rise and suggest therefore removal of an adsorbed layer of HCOOH or an intermediate.

Although the Δ -E curve still shows considerable Ru character, part of the Ru-oxide that is present without HCOOH is no longer seen in the presence of HCOOH. Furthermore the surface oxide seems to be reduced somewhat easier in the presence of HCOOH, as can be seen in the reverse scans with and without HCOOH.

The results of the oxidation of CO_{ad} at PtRu are shown in the voltammogram of Fig.15 for different amounts of CO at PtRu($\theta_{\text{Ru}}=0.32$); this was achieved by varying the adsorption time und using a dilute (10%) CO - Argon gas mixture. The oxidation peak is at $E=-0.15 \text{ V}$ for $\theta_{\text{CO}} = 0.44$ and shifts slightly to lower potentials with increasing CO. The eps values are close to 2 for all curves, which means that CO is linearly bonded. This is contrary to CO_{ad} at pure Pt, where large amounts of bridge bonded CO are found. The corresponding ellipsometric curves are given in Fig. 16 for $\theta_{\text{CO}} = 0.63$ and 0.73 and show that the Δ decrease starts at ca. -0.05 V i.e. the onset of oxide growth is shifted to higher potential. Thus no Ru-oxide is present in a

large part of the potential region where CO_{ad} is oxidized. The current maximum is reached ca 100 mV before the oxide formation in the presence of CO_{ad} is observed. Between -0.25 and -0.15 V a small Δ increase is noted which indicates the disappearance of CO_{ad} due to oxidation, this is the same as for CO_{ad} oxidation on Pt. There is however a significant difference between

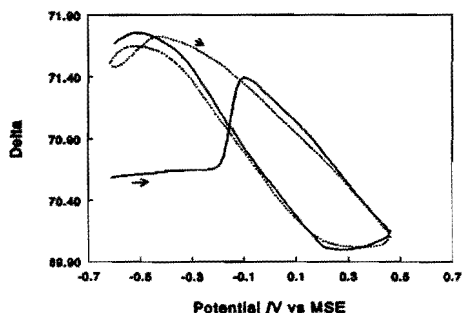


Figure 17 Δ -E curve of adsorbed CO on PtRu ($\theta_{\text{Ru}} < 0.05$) in 0.5 M H_2SO_4 . Solid curve is without CO.

the codeposited electrodes and Pt. The change in Δ over PtRu indicates that CO is removed from the surface at ca -0.25 V, whereas in the cyclic voltammogram the CO oxidation already starts at ca -0.4 V. For CO_{ad} oxidation over pure Pt the potentials deduced from the Δ -E and the I-E curve coincided. Furthermore the maximum in the Δ -E curve (fig.16) is reached at potentials at which according to the voltammogram not yet all the CO is removed from the surface. The potential region where the change in Δ takes place is thus far smaller than the CO oxidation region in the cyclic voltammogram. For low Ru surface coverages the optical changes due to CO_{ad} are more pronounced as shown by Fig.17 for PtRu ($\theta_{\text{Ru}} < 0.05$), the effect here is even larger than for Pt alone! There is a sharp Δ increase in the potential region -0.2 V to -0.1 V, which coincides with the current increase the voltammogram. The region in which Δ increases is again smaller than the CO oxidation peak in the cyclic voltammogram.

Summarizing / Conclusions

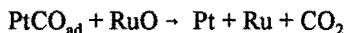
The presence of an oxide layer on Pt, Ru and PtRu can be detected with ellipsometry. This enables us to monitor the Pt-Ru surface during the oxidation of CH_3OH , HCOOH and CO_{ad} . The results show that PtRu-oxide is indeed involved in the reaction of CH_3OH and CO_{ad} ; whether this also holds for HCOOH remains to be seen. For all molecules it appears that no oxide is present at the PtRu surface in the potential region where the molecule (or its intermediate) is oxidized. The oxides at Ru and Pt alone do not seem to play a significant role

in the oxidation of HCOOH[?].

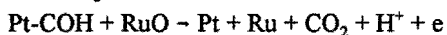
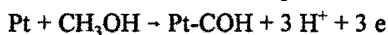
The optical results support the bifunctional mechanism that has been proposed to explain the role of Ru [7]. The Ru-oxide in the potential region of the methanol oxidation is divalent, this was established with EQCM [32] So we can describe the process by the following reactions:



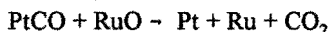
In the case of oxidation of CO_{ad} :



and in the case of oxidation of CH_3OH



or $\text{Pt} + \text{CH}_3\text{OH} \rightarrow \text{Pt-CO} + 2 \text{H}^+ + 2 \text{e}$



The oxide growth on the PtRu electrodes for both HCOOH and CO oxidation begins at some 50 - 100 mV higher potential than the maximum in the voltammogram, whereas for CH_3OH the potential of the current maximum coincides with the start of the oxide growth.

At Pt and PtRu the adsorbed CO layer can be clearly observed with ellipsometry. Its disappearance from the surface however does not exactly coincide with the oxidation peak in the cyclic voltammogram.

By comparing the activities for the electrooxidation of CO_{ad} , HCOOH and CH_3OH at the Pt-Ru electrodes, it appears that the optimal Ru coverage is < 30 % for all molecules. This is lower than has been reported for HCOOH and CO by Gasteiger et al.[8]. We found an optimum of ca 15% for the oxidation of CH_3OH and CO, this will be published in another paper [32].

References

1. R. Parsons and T. Vandermoot *J. Electroanal. Chem.* **257**, 9 (1988).
2. B. Beden, C. Lamy, N.R. de Tacconi and A.J. Arvia *Electrochim. Acta* **35**, 691 (1990).
3. T. Iwasita, in: *Advances in Electrochemical Science and Engineering*, vol.1 (ed. by C. Tobias and H. Gerischer) VCH, Weinheim, 1990, p.127
4. K. Kunitatsu *J. Electroanal. Chem.* **213**, 149 (1986).
5. T. Frelink, W. Visscher, A.P. Cox and J.A.R. van Veen *Electrochim. Acta*, accepted for publication
6. C.P. Wilde and M. Zhang *Electrochim. Acta* **39**, 347 (1994).
7. M. Watanabe and S. Motoo *J. Electroanal. Chem.* **60**, 267 (1975).
8. H.A. Gasteiger, N.M. Markovic, P.N. Ross and E.J. Cairns *Electrochim. Acta* **39**, 1825 (1994).
9. H.A. Gasteiger, N.M. Markovic, P.N. Ross and E.J. Cairns *J. Phys. Chem.* **97**, 12020 (1993).
10. H.A. Gasteiger, N.M. Markovic, P.N. Ross and E.J. Cairns *J. Electrochem. Soc.* **141**, 1795 (1994).
11. A. Capon and R. Parsons *J. Electroanal. Chem.* **45**, 205(1973).

Chapter 8

12. A. Capon and R. Parsons *J. Electroanal. Chem.* **44**, 239(1973).
13. J. Sobkowsky and A. Czerwinski *J. Phys. Chem.* **89**, 365(1985).
14. K. Kunimatsu, W.G. Golden, H. Seki and M.R. Philpott *Langmuir* **1**, 245 (1985).
15. K. Kunimatsu, H. Seki, W.G. Golden, J.G. Gordon II and M.R. Philpott *Langmuir* **2**, 464(1986).
16. D.S. Corrigan and M.J. Weaver *J. Electroanal. Chem.* **241**, 143 (1988).
17. N. Collas, B. Beden, J.M. Leger and C. Lamy *J. Electroanal. Chem.* **186**, 287(1985).
18. B. Beden, N. Collas, C. Lamy, J.M. Leger and V. Solis *Surf. Sci.* **162**(1985).
19. Y. Ikezawa, N. Nagashima, T. Shibata and T. Takamura *J. Electroanal. Chem.* **365**, 261(1994).
20. P. Stonehart *Electrochim. Acta* **18**, 63(1973).
21. J.A. Caram and C. Gutierrez *J. Electroanal. Chem.* **305**, 259(1991).
22. G.N. Lewis, J.D. Roth, R.A. Montag, L.K. Safford, X. Gao, S.-C. Chang, L.F. Dahl and M.J. Weaver *J. Am. Chem. Soc.* **112**, 2831(1990).
23. A. Cuesta and C. Gutierrez *J. Electroanal. Chem.* **383**, 195(1995).
24. S.-C. Chang and M.J. Weaver *J. Chem. Phys.* **92**, 4582(1990).
25. M. Krausa and W. Vielstich *J. Electroanal. Chem.* **379**, 307 (1994).
26. K. Franaszczuk and J. Sobkowski *J. Electroanal. Chem.* **327**, 235(1992).
27. S. Hadri-Jordanov, H. Angerstein-Kozłowska, M. Vukovic and B.E. Conway *J. Electrochem. Soc.* **125**, 1471 (1978).
28. E. Ticanelli, J.G. Beery, M.T. Paffett and S. Gottesfeld *J. Electroanal. Chem.* **258**, 61(1989).
29. L.N. Velikodnyi, V.A. Shepelin and E.V. Kasatkin *Elektrokhimiya* **18**, 1134 (1982).
30. T. Frelink, W. Visscher and J.A.R. van Veen *Surf. Science*, accepted for publication.
31. N.M. Markovic, H.A. Gasteiger, P.N. Ross, X. Jiang, I. Villegas and M.J. Weaver *Electrochim. Acta* **40**, 91(1995).
32. T. Frelink, W. Visscher and J.A.R. van Veen *Submitted for publication*.

On the Role of Ru and Sn as Promoters of Methanol Electrooxidation over Pt.

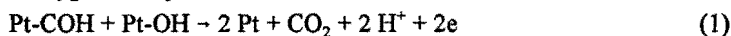
Abstract

The role of Ru and Sn on the methanol oxidation over Pt was investigated for three different systems viz. Pt covered with adatom layer of Ru and Sn, electrocodeposited Pt-Ru and carbon supported Pt-Ru. By following the oxide growth on the Pt-promoter metal electrodes with ellipsometry it was found that in the presence of methanol the surface oxides of the promoter metal are no longer present on the surface. This supports the bifunctional model of the promoter action. DEMS measurements at Pt with submonolayer coverage of Ru or Sn revealed that the current efficiency of the methanol oxidation to CO₂ is increased in the presence of Ru or Sn and that the onset potential of the oxidation keeps lowering with increasing amounts of the promoting metal. On electrodeposited Pt-Ru systems the adsorption of methanol already takes place at potentials in the hydrogen range. These results seem to point to an electronic (ligand) effect. This is further corroborated by activity measurements at carbon supported Pt-Ru with very small particles, which show a tenfold higher activity compared with the Ru free system.

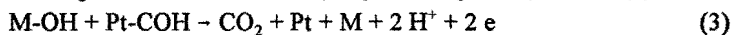
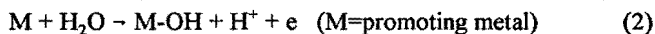
It is concluded that the promoting action of Ru and Sn may involve both a bifunctional and an electronic (ligand) effect.

Introduction.

Although it is quite well known that Sn and Ru can promote the electrochemical oxidation of methanol over Pt electrodes, it is still less well known by what mechanism they actually act. The electrooxidation of methanol over Pt proceeds via an adsorbed methanolic species, for example Pt-COH[1] or Pt-CO[2] at high methanol concentrations, which is oxidized by an adsorbed oxygenated species or activated water:



At present the most popular view is that the promoters act by supplying the oxygen atom:



The formation of an oxygenated species on Pt is reputedly difficult, as Pt-OH groups are only formed, in substantial quantities, above ca. +0.7 V vs RHE. The idea is that both Ru and Sn are more easily oxidised than Pt and thus are able to oxidise the methanol adsorbate at a lower potential. The promoters act via a so-called bi-functional mechanism, as was suggested for both Sn[3] and Ru[4]. An alternative explanation however, is that the Pt properties themselves are modified by Sn[5] and Ru[6,7] (the so-called ligand or electronic effect). Such an effect was for example observed in gas-phase adsorption of CO on Sn/Pt(111)[8], where the Pt-CO bond strength was found to weaken in the presence of Sn.

Taking into account that ensembles of Pt surface atoms are required for the adsorption of methanol on Pt[9] and that methanol does not adsorb on Sn or Ru[10], it follows that the promotor atoms should be present in low amounts, although this is not yet the general opinion. The optimal ratio M/Pt is still not definitely established, but it was confirmed by several authors[9,11,12] that a Pt-Ru electrode with a low Ru content (ca. 10%) has the highest activity for the methanol electrooxidation. This was also found for Sn [5]. The activity of Ru for the methanol adsorption appears to be strongly temperature dependent. In a recent article Gasteiger et al.[13] showed that at 60 °C the optimum Ru composition is about 30%. We have tried to obtain further evidence for either a bifunctional or a ligand effect through ellipsometry, Differential Electrochemical Mass Spectroscopy (DEMS) and activity measurements. Three different systems were used for these measurements; (i) smooth Pt with adatom coverage of Sn and Ru, (ii) electrocodeposited Pt-Ru and (iii) carbon supported Pt-Ru systems.

Experimental

Electrode Preparation.

Platinum electrodes with submonolayer coverage of Sn or Ru were prepared by potential cycling between -0.65 V and +0.6 V vs MSE in 0.5 M H₂SO₄ containing small ($<1 \cdot 10^{-3}$ M) amounts of SnSO₄ (Aldrich) or Ru(NO)(NO₃)₃ (Johnson and Matthey) respectively. Electrocodeposited Pt-Ru electrodes were prepared from a solution containing $2.4 \cdot 10^{-3}$ M H₂PtCl₆ and $1.2 \cdot 10^{-3}$ M Ru(NO)(NO₃)₃ using different deposition-times and -currents. The Ru/Pt atom ratio, measured with SEM/EDX, increases with higher deposition current.

Carbon supported Pt-Ru catalysts were prepared by depositing a Pt-Ru colloid on Vulcan XC-72 carbon support. The colloid was prepared via the Turkevich method[14]. The catalyst was mixed with PTFE suspension and the mixture was pressed on a Pt current collector. After drying at 125 °C, the electrode was sintered at 325 °C for two hours under argon atmosphere. The final Teflon content was 17 %.

Measurements.

Ellipsometry experiments were carried out using an automated ellipsometer Rudolph RR 2200 with tungsten iodine light source and monochromatic filter resulting in light with a wavelength of 546.1 nm. The optical cell is cylindrical and supplied with windows arranged for an angle of incidence of 70° at the substrate. The optical measurements were performed during potential scanning at disk electrodes of Pt (area 0.5 cm²) and of Ru (area 0.79 cm²) covered with electrodeposited Pt-Ru. The potential scan was supplied by a Wenking potentiostat POS 73 with Philips PM 8043 recorder. The activity for the methanol oxidation was determined from voltammetry measurements at low sweep rate (2 mVs⁻¹). Combined voltammetric and DEMS experiments were performed at a platinized platinum gauze electrode (specific area 60 cm²)

using a computer controlled AutoLab potentiostat (Eco Chemie) suitable for simultaneous recording of current- and mass response. The experimental setup of the mass-spectrometer system (Leybold) is similar to that of Vielstich et al.[15].

In all electrochemical cells the counter electrode is a Pt foil; the reference electrode is a Hg/Hg₂SO₄ electrode (MSE); E = +0.68 V vs RHE. The measurements were performed in 0.5 M H₂SO₄. The methanol concentration was either 0.1 M or 0.33 M.(Merck). All chemicals are p.a. grade. The solutions were prepared with Ecostat water(18.2 MΩ). Argon (99.99%) was used to provide oxygen free electrolyte.

Results and Discussion.

Ellipsometry

Figure 1A shows the change in the ellipsometric parameter Δ during a potentialscan at Pt in

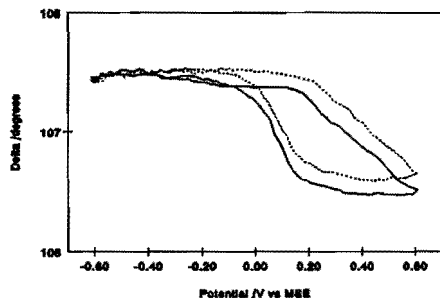


Figure 1A Δ -E curve for Pt. (-) 0.5 M H₂SO₄; (--) with 0.33 M CH₃OH.

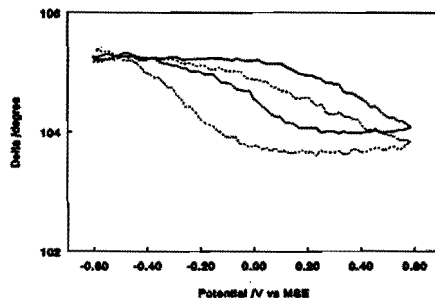


Figure 2B Δ -E curve for PtRu. (-) 0.5 M H₂SO₄; (--) with 0.33 M CH₃OH.

0.5 M H₂SO₄. The growth of the oxide layer during the anodic scan and its subsequent reduction during the cathodic scan is observed as a decrease respectively increase of Δ . Upon addition of methanol the curve is virtually the same (cf dashed line in figure 1A) hence no change in the Pt-oxide formation occurs in the presence of methanol.

Figure 1B (drawn line) gives the optical change observed at an electrocodeposited Pt-Ru electrode (30% Ru, estimated bulk content) in 0.5 M H₂SO₄. Here the change in Δ reflects the oxide film growth on Pt-Ru. It is seen that the surface is oxidised more easily in the presence of Ru (it is known that oxidation of Ru begins at -0.3 V vs MSE[16]) and that the oxide is reduced over a larger potential range compared with Pt. This behaviour is in agreement with the results found for bulk Pt_{0.5}Ru_{0.5} alloy[17]. The optical response alters in the presence of methanol (0.33 M) as shown by the dashed curve of figure 1B. The curve is shifted to higher Δ values and the total Δ change is smaller. In the anodic scan the decrease of Δ begins at a higher potential; in the cathodic scan the Δ increase begins at higher potential than without

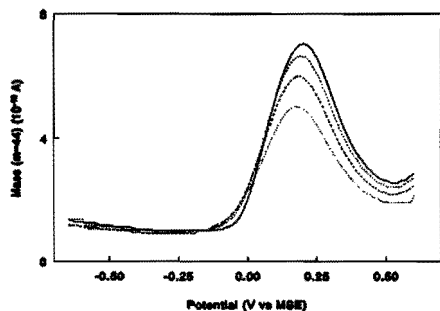


Figure 2A CO_2 production in the presence of Ru. (-) 0 M; (--) $5 \cdot 10^{-5}$; (·) $1 \cdot 10^{-4}$; (...) $1.5 \cdot 10^{-4}$ M $\text{Ru}(\text{NO})(\text{NO}_3)_3$.

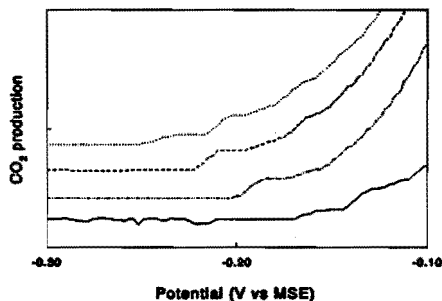


Figure 2B Enlarged part of (A). 0.5 M $\text{H}_2\text{SO}_4/0.33$ M CH_3OH .

methanol. Apparently in the presence of methanol less Ru-oxide film is "seen" on the surface, which implies that it is removed by reaction with methanol. For Pt partially covered with Ru adatoms or with upd Sn we found a similar effect[18]; in both systems the adatom-oxide features diminish or are completely absent. The disappearance of the metal-oxide layer in the presence of methanol supports the bifunctional mechanism in which the promoting metal transfers oxygen to Pt-COH, cf eqn (2) and (3); the rate of reaction (3) is apparently much higher than that of reaction (2).

Concentration	Onset-Potential of CO_2 production
0 M Sn	-0.135 V
$1 \cdot 10^{-4}$ M Sn	-0.197 V
$2 \cdot 10^{-4}$ M Sn	-0.282 V
0 M Ru	-0.135 V
$1 \cdot 10^{-4}$ M Ru	-0.222 V
$2 \cdot 10^{-4}$ M Ru	-0.276 V

Table 1 Change of the onset potential for CO_2 production during methanol oxidation on Pt in the presence of Sn and Ru.

DEMS at Pt with submonolayer coverage of Sn and Ru.

With DEMS the methanol oxidation was measured on Pt in the presence of different amounts of SnSO_4 and $\text{Ru}(\text{NO})(\text{NO}_3)_3$ in the electrolyte. The results are given in figure 2 for the Pt-Ru system. It can be concluded that Ru indeed enhances the CO_2 production in the potential region up to 0 V vs MSE and also that the onset potential for CO_2 production (and thus CH_3OH oxidation) decreases with increasing amount of the promotor metal. For Pt-Sn similar results were obtained. In Table 1 the onset potentials for the Pt-Ru and Pt-Sn systems are summarized, these data were evaluated from the mass-potential curves, as the currents at the onset of the methanol oxidation are extremely small. The lowering of the onset potential is quite remarkable; however this must be distinguished from the overall activity. At higher potentials the methanol oxidation current decreases with increasing amount of promotor metal, due to blocking of the Pt surface. It is furthermore striking that the peak potential of the methanol oxidation decreases in the presence of Ru, but does not change in the presence of Sn. Determination of the ratio between the current(I) and the mass-current(M) -which is di-

I/M ratio	E=-0.1 V.	E=0 V.	E=+0.1 V
0 M Sn	1	1	1
$1 \cdot 10^{-4}$ M Sn	0.46	0.72	0.93
$2 \cdot 10^{-4}$ M Sn	0.45	0.67	0.93
0 M Ru	1	1	1
$1 \cdot 10^{-4}$ M Ru	0.80	0.74	0.84
$2 \cdot 10^{-4}$ M Ru	0.67	0.70	0.76

Table 2 Ratio between the current(I) and mass-current(M) for the electrooxidation of methanol on Pt in the presence of Sn or Ru. The ratios without metals were set to 1.

rectly related to amount of CO_2 molecules[19]- showed that for the dynamic measurements the ratio becomes smaller in the presence of Sn or Ru. The I/M ratio values, calculated at three different potentials, are presented in Table 2; the ratio without promoting metal is set to 1. A decrease of the I/M ratio means an increase of the current-efficiency for CO_2 . Shibata et al.[20] also reported a higher current-efficiency in the presence of Ru, however they found a lower current-efficiency in the presence of Sn.

Although a change in current-efficiency can be explained on the basis of the bifunctional model where the role of the promotor is solely to donate an oxygen species, it is difficult to see how the continuous lowering of the onset potential with increasing promotor metal fits in this

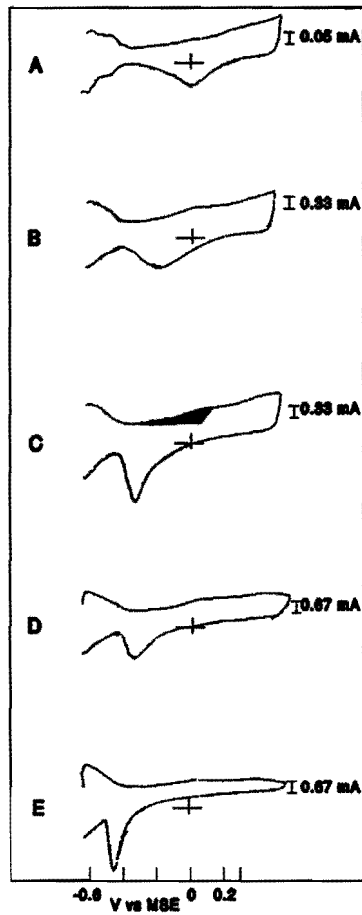


Figure 3 Pt-Ru codeposits in 0.5 M H₂SO₄. (A) 13% Ru; (B) 18% Ru; (C) 25% Ru; (D) 27% Ru; (E) 28% Ru. In (C) the are for Ru oxidation is indicated.

model. This phenomenon may therefore indicate that the promotor metals also evoke a ligand effect, i.e. the strength of the Pt-adsorbate bond is weakened by increasing amounts of promotor metal which results in a lowering of the oxidation potential of the adsorbate.

Codeposited Pt-Ru electrodes.

Figure 3 gives the cyclic voltammograms for codeposited Pt-Ru electrodes with different Ru contents. For all electrodes only one oxide reduction peak is observed, implying that only one type of oxide is formed. Platinum and ruthenium therefore may be assumed to be present as one phase. The position of the oxide reduction peak shifts to lower potentials for electrodes

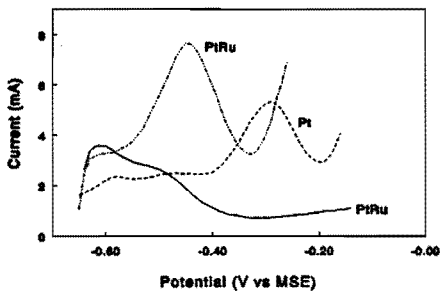


Figure 4A Codeposited PtRu (27% Ru) and Pt in 0.5 M $\text{H}_2\text{SO}_4/0.1$ M CH_3OH . Blank of PtRu is shown for comparison.

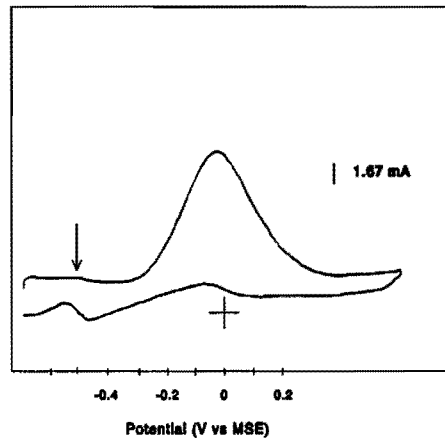


Figure 4B PtRu of (A) in 0.5 M $\text{H}_2\text{SO}_4/0.1$ M CH_3OH . Arrow indicates methanol adsorption peak. Scanrate 5 mV/s.

deposited with higher current, i.e. with higher Ru content. This agrees well with the results of McNicol et al.[21,22] who found that the oxide reduction peak of Pt-Ru alloys shifts to lower potentials with an increase in Ru content of the alloys. At electrodes with a bulk Ru content of 28% the oxide reduction can no longer be distinguished from the hydrogen reduction as was also observed by Entina et al.[23].

The voltammetric scan during methanol oxidation changes with the Pt-Ru composition; with increasing Ru content the methanol oxidation peak in the cathodic scan decreases and disappears completely at high Ru contents. In figure 4A the methanol oxidation is shown for Pt-Ru(27%). It is noted that an oxide reduction peak appears at the same potential as without methanol. Also a new (small) peak emerges in the anodic scan at -0.5 V vs MSE; this is more

clearly seen in the enlargement in figure 4B, in which part of a cyclic voltammogram is shown for an electrode with a different geometric surface area than in 4A, but with the same Ru content(27%). A peak at this potential was also reported by Gasteiger et al.[9] for Pt-Ru(10-%) and by Caram et al.[24] for Pt. With DEMS we established that no CO₂ was produced during this peak. If the potential scan is reversed immediately after this peak, we found that the hydrogen coverage had diminished; this indicates that the -0.5 V peak is due to oxidative adsorption of methanol on the surface. Figure 4B shows also the methanol adsorption at Pt-Pt at the same methanol concentration; here the peak is observed at a higher potential. It thus appears that while methanol is adsorbed on Pt after virtually all adsorbed hydrogen has been removed from the surface, the methanol adsorption on Pt-Ru can already occur at potentials in the hydrogen region (cf full line in figure 4B). This could point to the formation of another adsorbate and might indicate that Ru does not solely act via the bifunctional mechanism.

	PtRu					Pt
	13%	18%	25%	27%	28%	-
SEM/EDX	13%	18%	25%	27%	28%	-
Coverage calculated via Ru-oxide charge ^a	11%	24%	33%	33%	28%	-
Coverage estimated from red.peak pot.	10%	30%	45%	48%	60%	-
Activity at -0.2 V in mA cm ⁻²	0.1	0.09	-	0.04	0.02	0.01

Table 3 PtRu codeposited electrodes; Ru content measured by different methods; activities for methanol electrooxidation at -0.2 V, in 0.1 M CH₃OH/0.5 M H₂SO₄.

In order to compare the activities of the different electrodes for the methanol oxidation, it is necessary to know the amount of Ru present on the surface and the specific surface area. The SEM/EDX data present bulk values and may differ from the surface values due to surface segregation. For adatom Ru-Pt systems Watanabe et al.[4] measured the charge necessary to oxidise Ru and calculated the Ru coverage by assuming that this charge corresponds with the formation of RuOH. We performed Electrochemical Quartz Crystal Microbalance experiments, in which the mass-change of a Pt electrode was monitored during Ru deposition and oxidation[25]. It was concluded from these measurements that the Ru-oxide is Ru(OH)₂. Furthermore a linear correlation was observed between the mass change of the electrode and

the shift of the oxide reduction peak. The coverage, obtained by measuring the electrode-mass change during Ru deposition ($\theta=0.20$), was found to be fairly close to the coverage established from the decrease in the amount of adsorbed hydrogen ($\theta=0.23$), although it is recognized that this measurement of the surface content gives only an upper limit of the amount of Ru, because Ru adsorbs hydrogen itself[16]. The Ru surface content of the codeposited electrodes was calculated from the charge corresponding with the Ru oxidation as indicated in voltammogram C of figure 3 with: $\theta_{Ru} = (Q_{Ru(OH)_2}) / (Q_{Ru(OH)_2} + 2 Q_H)$. The only assumption in this calculation is that one Ru atom replaces one Pt atom. The calculated coverages are summarized in Table 3 and agree reasonably well with the values obtained by SEM/EDX. In this table also another estimate of the Ru content is given; this was obtained from the position of the oxide reduction potential: if it is assumed that for codeposited electrodes the shift of the oxide reduction peak with increasing Ru content is the same as for adatom systems, the Ru content can be determined via the EQCMB measurements. This resulted in larger values in particular at higher Ru content; the difference may be due to surface segregation.

In Table 3 the activities of the different Pt-Ru electrodes for the methanol oxidation are compared at -0.2 V vs MSE. These activities are expressed with respect to the real(true) Pt surface area, calculated with the Ru coverages (a) from table 3 assuming that 1 cm² of real surface area contains $1.41 \cdot 10^{15}$ atoms and that the Pt surface structure is not distorted by the presence of Ru. The table shows that for these electrodes the highest activity is obtained with relatively low Ru content as was discussed in the introduction. Although it is obvious that there exists an optimum for the Ru coverage, the data do not allow to ascertain its exact value. Our results are in agreement with the results of Gasteiger et al.[9] on well characterized smooth Pt-Ru surfaces. Watanabe et al.[4] concluded that the maximum activity was obtained at $\theta_{Ru}=0.5$; this Ru coverage however was based on the assumption that RuOH is formed. With Ru(OH)₂ as oxide species this coverage is 0.25, which is in reasonable agreement with the result of us and others[9,11,12].

carbon supported catalyst	current density (mA cm ⁻²)
Pt	0.02
Pt-Ru (2:1)	0.15
Pt-Ru (8:1)	0.30

Table 4 Activity at -0.2 V vs MSE for methanol oxidation of carbon supported Pt and Pt-Ru catalysts in 0.5 M H₂SO₄/0.1 M CH₃OH.

Carbon supported Pt-Ru catalysts.

It is known that the onset of Pt oxidation can be enhanced by decreasing the Pt particle size. However we found[26] that the specific activity of carbon supported Pt for the methanol oxidation remains constant for Pt sizes down to about 4 nm and that below that value the specific activity decreases with smaller particles. We attributed this to the much stronger water activation by the smaller particles at low potentials, resulting in a thwarting of the methanol adsorption reaction. It is therefore of interest to measure the methanol oxidation at carbon supported Pt-Ru catalysts with very small particles. Pt-Ru/C catalysts (5 wt %) were prepared with different ratios of Pt:Ru viz. [2:1], [4:1], [8:1]; with TEM it was established that the Pt-Ru [8:1] catalyst consists of particles from 1 to 2 nm with both Pt and Ru; the [2:1] and [4:1] catalysts consist of particles of 3 to 4 nm. In Table 4 the activities for the methanol oxidation are compared at -0.2 V vs MSE; the activity of Pt/C is also included. The highest activity for the methanol oxidation was obtained for the Pt:Ru [8:1] catalyst. Again as with electrodeposited Pt-Ru the results here seem to indicate that the highest activities for the methanol oxidation are obtained with a low Ru content (ca 10 %), although the promotor effect still has to be separated from the Pt particle size effect, because in our preparation method the particle size increases with the Ru content. The potential of the oxide reduction peak for the carbon supported Pt-Ru electrodes is the same as without Ru.

The presence of Ru appears to be quite effective: the activity of these Pt-Ru particles in the potential region -0.2 to -0.05 V vs MSE was a factor 10 higher than for Pt/C catalysts with particles of the same size. As for such small particles water activation is already too effective, the role of Ru can hardly be simply that of an oxygen donor, but may rather be ascribed to its modification of the electronic properties of Pt.

Conclusions.

The ellipsometric measurements at codeposited Pt-Ru show that Ru-surface oxide disappears in the presence of methanol. This was also found both for adatom coverage of Ru and Sn on Pt. The absence of these oxides during the methanol oxidation indicates that the metals act via the bifunctional mechanism in which an oxygenated species of Ru or Sn oxidizes the methanolic adsorbate. With EQCMB it was established that on Pt-Ru(ad) $\text{Ru}(\text{OH})_2$ is formed.

Activity and DEMS measurements at Pt electrodes with partial coverage of Sn or Ru reveal that in the presence of the promoting metal not only the activity for the methanol oxidation changes but also the current efficiency for CO_2 production; moreover the onset potential for the methanol oxidation is lowered with increasing amounts of promotor metal. These phenomena are difficult to explain with a bifunctional mechanism and may indicate that the electronic properties of Pt are changed as well. This is further corroborated by the results at carbon supported Pt-Ru electrodes, which show that the methanol oxidation at very small particles can be enhanced by Ru in spite of the fact that Pt particles (<4 nm) alone are too

active for water activation. The activity for the methanol oxidation for the electrocodeposited Pt-Ru systems is found to be the highest for a low Ru content.

It seems clear then that the promoting action of Sn and Ru involves both water activation and platinum modification. Their relative importance in each particular case remains to be more accurately determined e.g. through in situ IR spectroscopy.

References

1. T. Iwasita, F.C. Nart, B. Lopez and W. Vielstich, *Electrochim. Acta* 37(1992), 2361.
2. R. Parsons and T. VanderNoot, *J. Electroanal. Chem.* 257(1988)9.
3. A.A. Mikhailova, N.N. Osetrova and Yu. B. Vassiliev, *Elektrokhimiya* 13(1977), 518.
4. M. Watanabe and S. Motoo, *J. Electroanal. Chem.* 60(1975), 267.
5. M.M.P. Janssen and J. Moolhuysen, *J. Catal.* 46(1977), 289.
6. H. Binder, A. Köhling and G. Sandstede, in "From Electrocatalysis to Fuel Cells", p. 43, Washington Univ. Press, Seattle, 1972.
7. T. Iwasita, F.C. Nart and W. Vielstich, *Ber. Bunsenges. Phys. Chem.* 94(1990), 1030.
8. M.T. Paffett, S.C. Gebhard, R.G. Windham and B.E. Koel, *J. Phys. Chem.* 94(1990), 6831.
9. H.A. Gasteiger, N. Markovic, P.N. Ross and E.J. Cairns, *J. Phys. Chem.* 97(1993), 12020.
10. K. Franzaszczuk and J. Sobkowski, *J. Electroanal. Chem.* 327(1992), 235.
11. O.A. Petrii, *Dokl. Akad. Nauk. SSSR* 160(1965), 871.
12. V.S. Entina and O.A. Petrii, *Elektrokhimiya* 4(1968), 678.
13. H.A. Gasteiger, N. Markovic, P.N. Ross and E.J. Cairns, *J. Electrochem. Soc.* 141 (1994), 1795
14. K. Aika, L.L. Ban, I. Okura, S. Namba and J. Turkevich, *J. Res. Inst. Catalysis Hokkaido Univ.* 24(1976), 54
15. T. Iwasita, W. Vielstich and E. Santos, *J. Electroanal. Chem.* 229(1987), 367
- [15] S. Hadri-Jordanov, A. Angerstein-Kozłowska, M. Vukovic and B.E. Conway, *J. Electrochem. Soc.* 125(1978), 1471.
17. E. Ticanelli, J.G. Beery, M.T. Paffet and S. Gottesfeld, *J. Electroanal. Chem.* 258(1989), 61.
18. T. Frelink, W. Visscher, A.P. Cox and J.A.R. van Veen, submitted for publication
19. O. Wolter and J. Heitbaum, *Ber. Bunsenges. Phys. Chem.* 88(1984), 2.
20. M. Shibata and S. Motoo, *J. Electroanal. Chem.* 209(1986), 151.
21. T. Mahmood, J.O. Williams, R. Miles and B.D. McNicol, *J. Catal.* 72(1981), 218.
22. B.D. McNicol and R.T. Short, *J. Electroanal. Chem.* 92(1978), 115.
23. V.S. Entina and O.A. Petrii, *Elektrokhimiya* 4(1968), 111.
24. J.A. Caram and C. Gutierrez, *J. Electroanal. Chem.* 323(1992), 213.
25. Chapter 10 of this thesis
26. Chapter 5 of this thesis

Chapter 9

Measurement of the Ru Surface Content of Electrodeposited PtRu

Electrodes with the Electrochemical Quartz Crystal Microbalance:

Implications for Methanol and CO Electrooxidation.

Abstract

To obtain the surface content of Ru in rough electrodeposited PtRu electrodes, the mass change of a Pt electrode during Ru deposition was measured with the Electrochemical Quartz Crystal Microbalance. It is shown that there is a correlation between the potential of the surface oxide reduction peak of the PtRu electrode and the surface Ru content. With EQCMB also the methanol oxidation and oxide formation both on Pt and PtRu were studied. Implications for the oxidation of CO and CH₃OH are discussed, in the context of which some IR experiments on CO on PtRu are presented as well.

Introduction

Ruthenium is generally regarded to be the best promotor of Pt in the electrooxidation of methanol. Higher activities in the presence of Ru have been reported since the 1960's[1,2,3]. The mechanism by which Ru actually acts has been much studied in recent years [4,5,6,7,8,9,10,11], but it is still not clear whether Ru acts via a bifunctional mechanism, where Ru is responsible for the activation of water necessary to oxidise the methanol adsorbate, a ligand effect, where the electronic properties of Pt itself are modified, or both. Another major discussion point is the optimum surface coverage with Ru; i.e. the surface coverage at which the maximum overall activity for the electrooxidation of methanol is obtained. Values for the surface coverages ranging from 10%[4] to 50%[11] have been reported. Comparison of data of different authors should be made on the basis of surface coverage of course, but these have most often been assumed rather than measured. Either the assumption has been made that the Ru surface coverage for the various samples is equal to the bulk content[3], or the composition of the electrode was taken to be equal to the composition of the deposition bath[12]; the latter method can lead to large discrepancies as is clear from our study on Pt-Ru electrodeposits[5]. Measurement of coverage via blocking of the hydrogen area is not a-priori applicable since Ru itself also adsorbs hydrogen. The only study, in which the real surface composition has been established, is that by Gasteiger et al.[4], who have used Low Energy Ion Scattering (LEIS) and Auger Electron Spectroscopy (AES) to measure the ratio between the amount of Ru and Pt on the surface of perfectly smooth alloys. They found a rather low optimum surface coverage viz. ca. 10%.

In order to determine Ru surface concentration in the case of electrodeposited or PtRu/C

electrodes, it would be advantageous to avail of a simple in-situ technique, such as cyclic voltammetry. Indeed McNicol et al.[9] already showed that the peak potential of the surface-oxide reduction shifts to lower values (compared to pure Pt) in the presence of Ru. In our previous paper[5], we tried to correlate the amount of Ru in the electrodeposited electrode(determined with EDX) to the peak potential of the oxide reduction(measured with CV). It was found however, with cyclic voltammetry, that the peak potential of the oxide reduction kept shifting, whereas EDX measurements indicated no further change in the amount of Ru. The discrepancy between both techniques (CV and EDX) should arise from the fact that EDX measures the amount of Ru present in the bulk, whereas CV only shows the behaviour of the outermost layer.

In trying to circumvent this problem, we switched in the first instance to electrodeposited Ru on Pt, where we could follow the deposition of Ru with the Electrochemical Quartz Crystal Microbalance(EQCMB), and hence correlate the amount of deposited Ru with the potential of oxide reduction. This technique has the advantage that the surface coverage of the deposited metal is measured by the mass-change of the electrode and it has been used extensively for the study of for example Cu, Bi and Pb upd on Au and Pt[13,14,15,16,17]. Furthermore the EQCMB offers the possibility of studying the oxide formation on the electrode in the presence and absence of methanol[18,19,20,21].

In this paper, then, the Ru surface coverage so determined with EQCMB will be correlated with the shift in surface-oxide reduction. Also the oxide formation both on Pt and PtRu and its implications for both CO and CH₃OH oxidation will be discussed. Furthermore, in order to obtain some information on the effect of Ru on the electronic properties of Pt, if any, a few in-situ IR measurements of CO adsorbed on PtRu have been performed as well. Similar measurements were previously done by Iwasita et al.[22], but in discussing the effect of Ru, not much attention has been given to these measurements in the literature.

Experimental

All experiments were performed in a 0.5 M H₂SO₄ supporting electrolyte solution, prepared from p.a.H₂SO₄ (Merck) and ultrapure (18.2 M Ω)water (Ecostat). The ruthenium salt solution, used for the Ru deposition was prepared from a concentrated Ru(NO)(NO₃)₃ solution (Aldrich). The 0.1 M CH₃OH solution was prepared with p.a. methanol (Merck).

Planar 2.5 cm diameter, 5 MHz AT-cut quartz crystals were operated at their third harmonic frequency in all experiments. Platinum film electrodes were evaporated onto one side of the crystal. A Ti film was used to improve the cohesion between the Pt and the Quartz substrate. The electrode was centred on the crystal and had a diameter of 0.95 cm. On the back side of the electrode the Ti pad had a diameter of 0.6 cm, such that the edges of the electrode do not contribute to the frequency measurements.

The surface of the electrode was cleaned with ethanol and hexane, thereafter the electrode was

exposed to UV-ozone for 10 minutes. Cyclic voltammetry and the frequency change during multiple scanning were used in order to check the cleanness of the electrode. The crystal was mounted in a Teflon electrochemical cell, with a Hg/Hg₂SO₄ (MSE) electrode as a reference ($E_{\text{MSE}} = +0.68$ V vs RHE) and a Pt counter electrode.

The frequency of the crystal was measured with a high precision frequency counter (Philips PM 6654). For the cyclic voltammetric experiments the potential was controlled by using a PAR 175 programmer and a PAR 176 potentiostat. Data were directly stored on a PC.

From the Sauerbrey equation[23] (eq. 1) where Δf_n is the frequency change of the electrode, Δm is the mass change, μ_q is the shear modulus, ρ_q is the density of quartz, A is the piezoelectrically active surface area of the electrode, f_0 is the harmonic frequency of the crystal and n stands for the n th overtone, the theoretical mass-sensitivity, S (= the "Sauerbrey constant") for this system was calculated to be 18 ng/Hzcm².

$$\Delta f_n = -\frac{2nf_0^2 \Delta m}{\sqrt{\mu_q \rho_q} A} = -\frac{\Delta m}{S} \quad (1)$$

The electrode roughness factor was calculated to be about 10, on the basis of the hydrogen desorption region.

Infrared experiments

For the IR experiments a BioRad FTS45-A1 IR apparatus was used with a home made electrochemical thin layer cell. A CaF₂ window was used in a 0.5 M H₂SO₄ solution. CO was adsorbed from a CO containing electrolyte solution at $E = -0.3$ V vs MSE. After adsorption the electrode was pushed against the window and a spectrum was taken. Each spectrum consisted of 64 scans. After each spectrum the potential was scanned to the anodic potential limit where a reference spectrum was taken. For the Pt experiment a smooth Pt electrode was used, to which for the PtRu experiment a small amount (ca 10%) of Ru was added by potential cycling. This strategy was chosen in order to exclude roughness differences between the two electrodes. The anodic potential limit was $E = 0.7$ V vs MSE for Pt and $E = 0.4$ V vs MSE for PtRu, this in order to avoid dissolution of Ru during the experiments.

Results and Discussion

Cu deposition on Pt in 0.5 M H₂SO₄

In order to check the reliability of the frequency measurements, it was decided to check the value of the Sauerbrey constant, by measuring the frequency change during dissolution of bulk Cu that had been deposited on Pt. (It was previously reported[13] that the electrosorption

valency is $\gamma=2$ for bulk Cu deposition.)

By measuring the total charge during bulk Cu dissolution, (with two electrons per Cu ion) and comparing this to the change in frequency, the Sauerbrey constant was calculated to be 18.8 ng/Hzcm^2 , which is close to the theoretical value of 18.

A more thorough discussion of EQCMB measurements of Cu (upd and bulk) on Pt will be given elsewhere[24].

Frequency response of Pt in 0.5 M H₂SO₄

In figure 1 the current and frequency response are given for a Pt electrode in 0.5 M H₂SO₄.

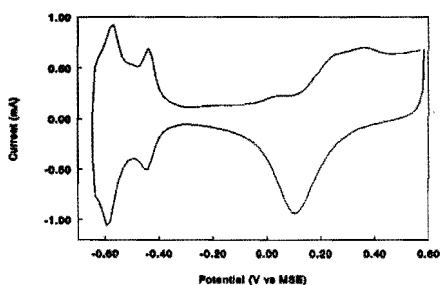


Figure 1A CV of Pt in 0.5 M H₂SO₄, $v=10 \text{ mV/s}$.

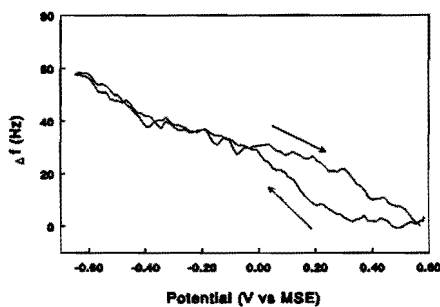


Figure 1B As for (A) but frequency response.

The frequency-potential curve is comparable to those that have been published previously[18,21]. Starting at the most cathodic potential (-0.65 V) a strong decrease in frequency and thus an increase in mass is observed during the positive scan through the hydrogen desorption region. This implies that as soon as the hydrogen desorbs, H₂O adsorption occurs: according to results by Wieckowski et al. [25] SO₄²⁻ adsorption will only take place after hydrogen has desorbed completely, so the mass increase in the hydrogen region must be due to H₂O adsorption. After the hydrogen region the decrease in frequency is smaller during the scan through the double layer region, this decrease then must be due to sulphate adsorption and maybe some additional water adsorption. Finally as the Pt-oxide formation starts the rate of decrease in frequency increases again. A plot of the frequency-change vs the charge (figure 2) during a cyclic voltammetric scan, analogous to the plots in [18], gives the possibility of establishing what kind of adsorption processes take place. By using the equation:

$$\Delta m_{\text{Pt}} = \frac{|\Delta f| \cdot S}{Q/F} \quad (2)$$

it is possible to calculate the mass change per mole of Pt surface atoms. Here Q is the charge for the hydrogen desorption region and $|\Delta f|$ is the absolute frequency change.

It can be seen that essentially four different regions exist[18]. First of all there is the hydrogen

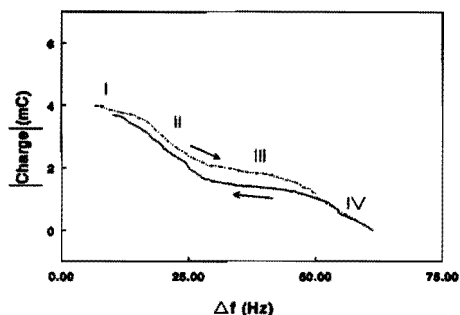


Figure 2 Frequency vs charge during a CV of Pt in 0.5 M H_2SO_4 .

region, where $\Delta m_{Pt}=9$ g/mol Pt, which is consistent with the view that water in this potential range is bonded to Pt via the H atoms, thus covering two Pt atoms with one water molecule. In the double layer region the weight change is ca 10 g/mol Pt, which together with the mass change in the hydrogen region results in a total change of 19 g/mol Pt, which is very close to the value expected for water adsorbed, as Pt-OH₂. Although there might be additional anion adsorption, according to Kita et al.[18] the contribution of the sulphate anion is only small, this is however in contradiction with other literature results[25]. Assuming then, that at the start of the oxide formation region the surface is totally covered with water molecules, the formation of surface oxides (PtO) or surface hydroxides(PtOH) would have to result in a mass-decrease! We and others however find that there is an ongoing decrease in the frequency and thus an increase in the mass.

Two possible explanations may be given for this ongoing decrease in frequency:

-Oxide formation on the Pt electrode does not result in PtO, but in Pt(OH)₂, leaving the charge required, to two electrons per Pt atom (which is close to the 1.6 electrons we measure), but increases the mass change by a factor of 2.

or:

-The mass change in the region from -0.65 V to the beginning of the oxide formation region, which was found to be $\Delta m_{Pt}= 19$ g/mol, is due to the adsorption of both, H₂O and SO₄²⁻(or HSO₄⁻). Upon oxide formation the electrode mass will then further increase due to additional water and sulphate adsorption until a layer of PtO with occluded sulphate is formed[26].

The first possibility may be discarded on the basis of literature results[21]. It was shown with in-situ Raman spectroscopy that platinum mainly forms PtO upon oxidation and not hydroxi-

des. Thus the total mass change of $\Delta m_{\text{Pt}}=35$ g/mol is due to a mixture of PtO formation and SO_4^{2-} adsorption. The fact that the value found here is somewhat higher than in [18] might be due to the fivefold higher concentration of SO_4^{2-} in our case. Since theoretically PtO formation results in a mass change of 16 g/mol, the additional 19 g/mol must be due to SO_4^{2-} adsorption, meaning one SO_4^{2-} ion per every 5 Pt atoms.

Although the interpretation is somewhat different, the results found here are in good agreement with those found elsewhere [18,21].

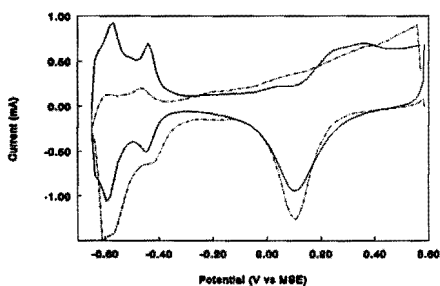


Figure 3A CV of Ru deposition on Pt. $[\text{Ru}]=2 \cdot 10^{-4}$ in 0.5 M H_2SO_4 .

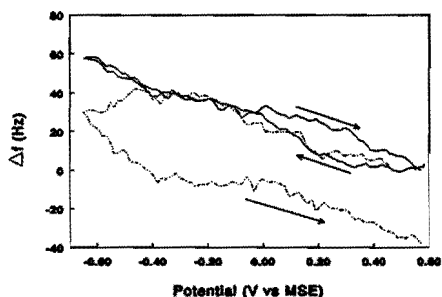


Figure 3B As for (A) but frequency curve.

Ruthenium deposition.

Ru deposition was achieved by potential scanning in a 0.5 M H_2SO_4 solution containing $2 \cdot 10^{-4}$ M $\text{Ru}(\text{NO})(\text{NO}_3)_3$. The cyclic voltammogram is shown in figure 3A. A reduction current due to Ru discharge is seen from -0.1 V to -0.65 V. The corresponding frequency curve (figure 3B), shows a deviation from the Ru-free behaviour from ca -0.4 V downwards, indicating the start of Ru deposition. Since the experiments were done with an anodic potential limit of 0.6 V vs MSE, Ru will dissolve from the electrode surface during extensive scanning, resulting in a decrease in electrode mass as is shown in figure 4. Since it is impossible to follow the change in Pt-oxide reduction potential during Ru deposition, the frequency change was followed during a number of cyclic voltammograms in the Ru containing electrolyte, the solution was then exchanged for 0.5 M H_2SO_4 , and the position of the oxide reduction peak was measured. An example of a cyclic voltammogram after electrolyte change is given in figure 5. From the frequency change at -0.65 V, the amount of Ru deposited is obtained.

Now, the mass change can directly be related to the shift in the oxide reduction potential. The result of these experiments is shown in figure 6, where it is seen that a linear relationship exists between the Ru coverage and the oxide reduction potential. The value for 100 % Ru [27] is added for comparison. The data points obtained upon deposition and upon subsequential

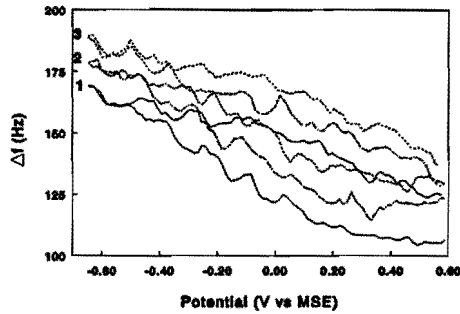


Figure 4 Frequency-potential curve during scanning of PtRu in 0.5 M H_2SO_4 . Sequence of scans as indicated.

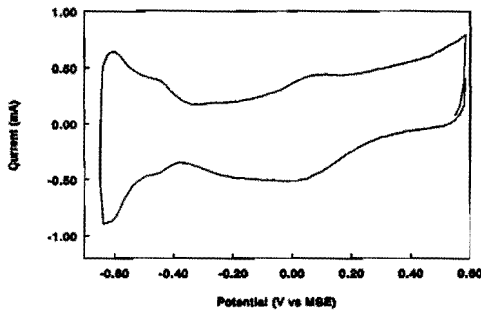


Figure 5 CV after Ru deposition and electrolyte exchange. 0.5 M H_2SO_4 , $v=10$ mV/s.

partial dissolution of Ru are found to fall on the same curve.

This now gives us a tool to determine the Ru surface coverages in rough electrocodeposited PtRu electrodes. By establishing the position of the PtRu-oxide reduction peak, it is possible to determine the Ru surface coverage. LEIS experiments were attempted to confirm these results, however the presence of oxides and sulphates made it impossible to determine the composition of the outermost layers. The Ru concentration, eventually measured with LEIS, gave approximately the same results as the EDX measurements, these being bulk values. At first it was found that the surface did not consist of pure Pt and Ru, but was covered with other species probably oxides and sulphates. Sputtering was thus necessary in order to clean the surface. Upon sputtering the total amount of Pt+Ru increased, showing that the surface was cleaned, but the Ru/Pt ratio decreased, suggesting that the outermost layers of the deposit are richer in Ru than the bulk. The Ru/Pt ratio measured with LEIS after extensive sputtering

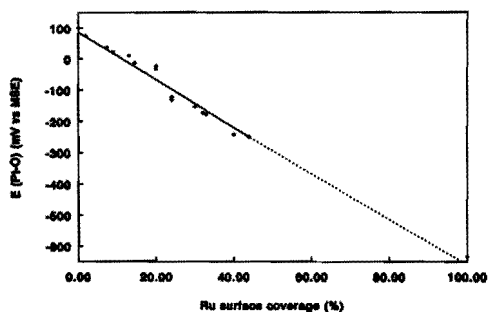


Figure 6 Surface oxide reduction potential vs Ru coverage. Peak potential after a scan to 0.6 V vs MSE.

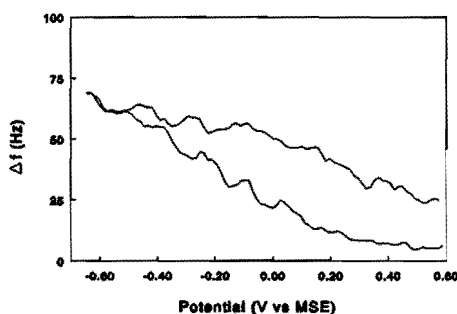


Figure 7 Frequency potential curve of PtRu. Ru surface coverage 40%.

were found to be equal to the ratio measured with EDX.

Frequency response during oxidation of PtRu.

In addition to the information obtained with the EQCMB during Ru deposition, it is also possible to study the frequency change during cyclic voltammetry of a PtRu electrode.

In figure 7 the frequency-potential curve for a PtRu ($\theta_{Ru}=40\%$) electrode is shown. This curve is consistent with the cyclic voltammogram and ellipsometry results[28] which show that the oxidation of the electrode surface in the anodic scan starts at ca -0.3 V; the reduction of the oxide in the cathodic scan start at lower potentials than at Pt itself. At ca -0.55 V vs MSE, the frequency change in the cathodic cycle coincides with the anodic scan, meaning that the oxide is only then completely reduced.

The frequency vs charge plot in figure 8, shows a difference with the same plot for Pt from

figure 2: for PtRu only one slope and thus one process is found after the hydrogen desorption region. One may thus conclude that only one type of oxide is formed on the electrode surface in the potential region from -0.3 V to +0.6 V, consistent with the fact that we see only one oxide reduction peak in the cyclic voltammogram. The total change in frequency due to oxide formation is equal to that on Pt. This implies that the same type of oxide (with the inclusion of SO_4^{2-}) is formed on Pt and on PtRu. At very low values of θ_{Ru} (<5%) however two reduction peaks were found, meaning that there two types of oxides were formed. This is to be understood on basis of the fact that 5% coverage with Ru is not enough to form a mixed oxide of Pt and Ru. With these low coverages, some Pt sites will remain without Ru neighbours,

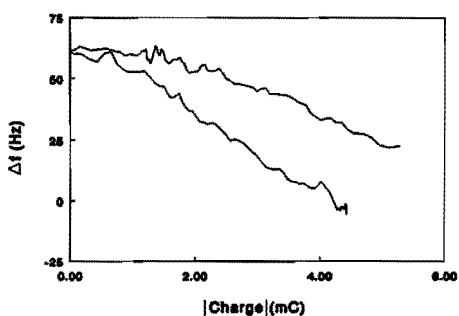


Figure 8 Frequency vs charge for a PtRu electrode in 0.5 M H_2SO_4 . Surface coverage of Ru 24%.

thus resulting in an oxide reduction for free Pt and one for PtRu.

At coverages with θ_{Ru} larger than 5% on a Pt-Ru electrode one surface oxide is formed, which has the same structure as the oxide formed on the Ru free surface and thus may be represented as $(\text{PtRu})\text{O}_x(\text{SO}_4)_y$, where $x \approx 2$ and $y \approx 0.4$. We[5] previously suggested $\text{Ru}(\text{OH})$ to be the species formed, this however was based on the assumption that at the start of the oxide formation region, the Pt surface is free of oxygen containing species, an assumption which was also made in other EQCMB measurements [18,21]. This assumption however is not legitimate as shown in the discussion on the formation of Pt oxides and in recent EXAFS measurements[29]. The mass change of the electrode as a result of oxide formation starts after the hydrogen desorption region and cannot be distinguished from the mass change due to sulphate adsorption. However the postulated valency change upon oxidation of Ru remains 2. The method used by Watanabe et al.[11] for the determination of the Ru surface coverage was based on the assumption that only one electron is involved in the oxidation of Ru. Taking into account our results the optimum surface coverage in their measurements is 25% , instead of

the reported 50%.

Frequency response during methanol oxidation.

As we reported before[28], ellipsometry shows that in the presence of methanol, no Ru-oxides are found during the methanol oxidation reaction. It was suggested that this was due to the reaction of the Ru-oxide and the methanol adsorbate.

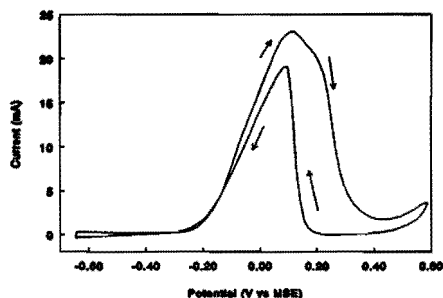


Figure 9A Methanol oxidation on PtRu (10%). 0.1 M CH₃OH/0.5 M H₂SO₄.

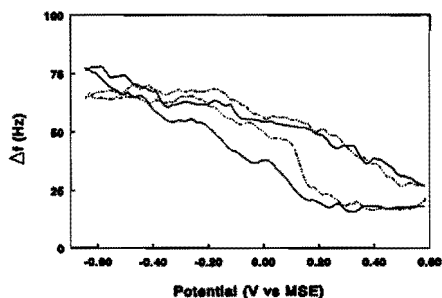
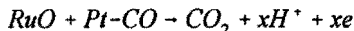


Figure 9B Frequency response of system in (A). Solid line is blank, for comparison.



Furthermore, the Pt-oxide formation was not influenced by the presence of methanol. To further substantiate this result, methanol oxidation experiments were done on a Pt-Ru electrode with low Ru content(10 %) and the frequency response was followed.

The results are shown in figure 9, where the cyclic voltammogram(figure 9A) shows that methanol oxidation starts at a potential below $E = -0.2$ V, thus confirming the promoting effect of Ru. In Fig. 9B, the frequency change is shown, with and without methanol in solution. Two striking differences may be seen: first of all the frequency decrease in the hydrogen desorption region is absent in the presence of methanol, which was also observed in other experiments[19,20]. Secondly, in the cathodic scan, at the potential where a sharp increase in the methanol oxidation current is recorded, we see a rapid increase in the frequency, implying a rapid reduction of the surface oxide.

The absence of the frequency decrease in the hydrogen desorption region can be explained by the fact that the Pt surface is blocked with methanol adsorbates, which prevent water adsorption. The rapid reduction of the surface oxide in the presence of methanol, tells us that methanol is capable of rapidly reducing the Pt-oxides in the cathodic scan. Finally no change in

the oxide formation is seen in the presence of methanol, which thus confirms the ellipsometry results.

On the optimal Ru surface coverage for methanol oxidation.

In our previous paper[5], we concluded that the optimum in the specific activity for methanol oxidation on electrocodeposited PtRu electrodes (measured with EDX), was at low Ru contents. Using the curve in figure 6 to determine the surface coverages with Ru shows that these appear to be somewhat higher than the bulk contents. The optimum in the methanol electrooxidation activity for these systems is then found to be at a surface coverage of ca 15%. This result on rough electrocodeposited PtRu electrodes thus confirms the results obtained on perfectly smooth alloys[4]. However the low optimum itself does not distinguish between the bifunctional and the ligand effect of the promotor. From the results in the previous section the bifunctional effect appears to be the most likely. We discussed before[5], however, that there are some experimental results which are not easily understood on the basis of the bifunctional mechanism alone. These results concern the facilitated adsorption of methanol on PtRu, compared with Pt and the decrease in onset potential for the methanol electrooxidation with increasing Ru content. To obtain more evidence in favour of either the bifunctional or the ligand effect, some in-situ IR experiments were done on CO adsorbed on PtRu. These results

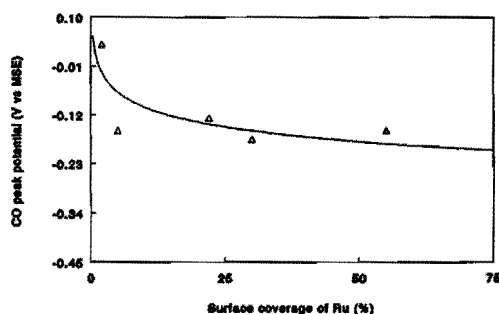


Figure 10 Peak potential of adsorbed CO oxidation on Pt in 0.5 M H₂SO₄ as a function of Ru surface coverage.

will be discussed later, after the results obtained for CO oxidation have been presented.

Implications for the CO oxidation.

In the CO oxidation experiments, CO was adsorbed at -0.35 V vs MSE for 2 min and the solution was then flushed with Argon for 15 min to remove gaseous CO. In a cyclic voltam-

metric scan the adsorbed CO was then oxidised. The results are summarized in figure 10, where the CO_{ads} oxidation peak potential is plotted as a function of the Ru content. It can be seen that a 150-200 mV shift to lower potentials occurs for low Ru contents; further increa-

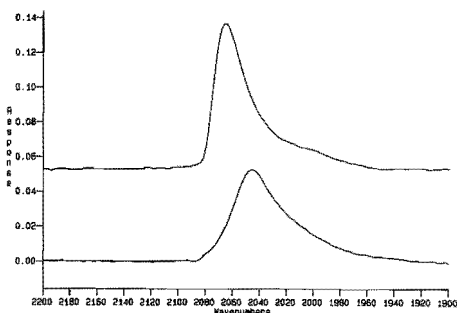


Figure 11A

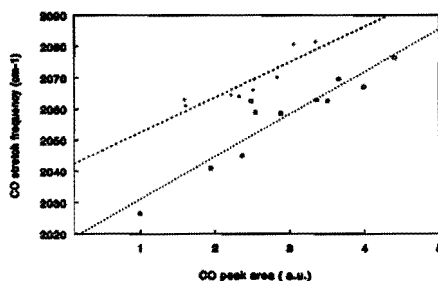


Figure 11B CO stretch freq. vs amount of CO. (+) CO on PtRu; (□) CO on Pt.

ing of the Ru content does not result in a larger shift. This implies that the optimum for CO oxidation at PtRu electrodes may, as for methanol oxidation, be considered to be at low Ru surface coverages; higher coverages appear only to block the surface and thus cause no further shift in the oxidation potential. This in contrast with the start of the methanol oxidation, which keeps shifting to lower potentials with increasing Ru content. This shift in the CO oxidation potential is in agreement with the maximum shift found by others[12], the surface coverage of Ru however at which the maximum shift is obtained is lower, ca. 15%, rather than at 50% [4].

In order to see whether Ru changes the CO binding strength to the surface, thus acting via a ligand effect, some IR experiments were performed. The linearly bonded CO stretching frequency[30] was measured as a function of the CO coverage in the presence and absence of Ru. An example is given in figure 11A, where the upper curve is for PtRu ($\theta_{\text{Ru}}=0.10$) and the lower for Pt. It can be seen that the CO stretching frequency is shifted to slightly higher values in the presence of Ru. For a range of CO surface coverages on Pt and PtRu, the results are plotted in figure 11B. The frequency is seen to shift to higher values in the presence of Ru, whereas the slope of the curve is the same for Pt and PtRu. These results are in perfect agreement with those of Iwasita et al.[31] on a 85:15 PtRu alloy, and show that the Pt-CO bond strength is weakened in the presence of Ru.

The peak area of the CO peak in the IR spectrum is taken as a measure for the CO coverage, this gives the total amount of CO molecules rather than the amount of surface that is blocked by CO. This method is valid only if we assume that the cross-section for CO is the same in

both cases and if the two electrodes used have the same roughness. In order to achieve this, the same Pt electrode was used in all experiments; a low coverage with Ru was chosen, since large surface coverages of Ru may cause compression effects, meaning that the CO adsorbates will be forced to be close to one another, thus causing an additional shift in the CO stretching frequency.

Since roughness and compression effects were minimised, we believe that the observed shift in CO stretching frequency is indeed due to the presence of Ru, implying that the Pt-CO bond is weakened in the presence of Ru. We may therefore conclude that the action of Ru is at least partly due to a ligand effect, as was proposed before[5].

The difference in the effect of Ru on the oxidation of CO and the oxidation of methanol is now that the CO oxidation potential does not shift to lower values if the Ru surface coverage is increased above the optimum value (cf Fig. 10), whereas the methanol oxidation potential does[5]. This effect can in our view only be explained by assuming that, in the presence of Ru CO is not the adsorbate in the methanol oxidation. A different reaction path, might account for the observed difference; this, however needs further study.

Conclusion

With the EQCMB technique the amount of Ru deposited on a Pt electrode can be determined. The Ru surface coverage appears to be related to the potential of the PtRu-oxide reduction peak; it is therefore possible to obtain a calibration curve for the determination of the Ru surface coverage in rough electrodeposited electrodes. Comparison with EDX data show that surface enrichment with Ru occurs. Oxide formation on a PtRu electrode results in one type of oxide: $(\text{PtRu})\text{O}_x(\text{SO}_4)_y$ where $x \approx 2$ and $y \approx 0.4$. The optimum amount of Ru surface coverage both for CO and CH_3OH oxidation is found to be low, about 15%. IR experiments show that Ru (partly) acts via a ligand effect in the oxidation of CO over Pt. In both CH_3OH and CO oxidation the bifunctional effect seems to play a role as well. The difference in the oxidation potential shift between CO and CH_3OH in the presence of Ru is suggested to be due to a difference in adsorbed species.

Acknowledgements

We are grateful to Philips Research in Eindhoven for giving one of us (T.F.) the opportunity to perform the EQCMB measurements and to Dr. J. Sondag-Huethorst and Dr. L.G.J. Fokkink for their assistance with the experiments and for the stimulating discussions. Ir. L.A. van de Oetelaar (Dep. of Physics, Eindhoven University of Technology) is thanked for performing the LEIS measurements and Drs J.F.E. Gootzen (Lab. for Inorganic Chemistry and Catalysis) for performing the in-situ IR experiments.

References

Chapter 10

- 1.O.A. Petrii, V.E. Kazarinov *Elektrokhimiya* 1, 1389(1965).
- 2.O.A. Petrii *Dokl. Akad. Nauk. SSSR* 160, 871(1965).
- 3.V.S. Entina, O.A. Petrii *Elektrokhimiya* 4, 111, 678 (1968).
- 4.H.A. Gasteiger, N. Markovic, P.N. Ross, E.J. Cairns *J. Phys. Chem.* 97, 12020 (1993).
- 5.T. Frelink, W. Visscher, J.A.R. van Veen, Accepted for publication in *Surf. Sci.*
- 6.H.A. Gasteiger, N. Markovic, P.N. Ross, E.J. Cairns *J. Phys. Chem.* 98, 617 (1994).
- 7.H.A. Gasteiger, N. Markovic, P.N. Ross, E.J. Cairns *J. Electrochem. Soc.* 141, 1795 (1994).
- 8.E. Herrero, K. Franzaszuk, A. Wieckowski *J. Electroanal. Chem.* 361, 269(1993).
- 9.B.D. McNicol, R.T. Short *J. Electroanal. Chem.* 92, 115(1978).
- 10.T. Mahmood, J.O. Williams, R. Miles, B.D. McNicol *J. Cat.* 72, 218(1981).
- 11.M. Watanabe, S. Motoo *J. Electroanal. Chem.* 60, 275(1975).
- 12.R. Ianniello, V.M. Schmidt, U. Stimming, J. Stumper, A. Wallau *Electrochim. Acta* 39, 1863 (1994).
- 13.M.R. Deakin, O. Melroy *J. Electroanal. Chem.* 239, 321(1988).
- 14.H.J. Schmidt, U. Pittermann, H. Schneider, K.G. Weil *Analytica Chim. Acta* 273, 561(1993).
- 15.G.L. Borges, K.K. Kanazawa, J.G. Gordon II, K. Ashley, J. Richer *J. Electroanal. Chem.* 364, 281(1994).
- 16.C.P. Wilde, M. Zhang *Langmuir* 10, 1600 (1994).
- 17.M. Watanabe, H. Uchida, N. Ikeda *J. Electroanal. Chem.* 380, 255 (1995).
- 18.K. Shimazu, H. Kita *J. Electroanal. Chem.* 341, 361(1992).
- 19.K. Shimazu, K. Kaneda, H. Kita *Bull. Chem. Soc. Jpn.* 67, 2069(1994).
- 20.C.P. Wilde, M. Zhang *Electrochim. Acta* 39, 347(1994).
- 21.V.I. Birrs, M. Chang, J. Segal *J. Electroanal. Chem.* 355, 181(1993).
- 22.T. Iwasita, F.C. Nart, W. Vielstich *Ber. Bunsenges. Phys. Chem.* 94, 1030 (1990).
- 23.D.A. Buttry, M.D. Ward *Chem. Rev.* 92, 1355 (1992).
- 24.T. Frelink, L.G.J.Fokkink, W. Visscher, J.A.R. van Veen *to be published*.
- 25.A. Wieckowski, P. Zelenay, K. Varga *J. Chim. Phys.* 88, 1247 (1991).
- 26.F.C. Nart, T. Iwasita *J. Electroanal. Chem.* 308, 277 (1991).
- 27.M. Vukovic, H. Angerstein-Kozlowska, B.E. Conway *J. Appl. Electrochem.* 12, 193 (1982).
- 28.T. Frelink, A.P. Cox, W. Visscher, J.A.R. van Veen, *accepted for publication in Electrochim. Acta*.
- 29.P.G. Allen, S.D. Conradson, M.S. Wilson, S. Gottesfeld, I.D. Raistrick, J. Valerio, M. Lovato *Electrochim. Acta* 39, 2415 (1994).
- 30.K. Kunimatsu *J. Electroanal. Chem.* 213, 149(1986).
- 31.T. Iwasita, W. Vielstich *Ber. Bunsenges. Phys. Chem.* 90, 1024 (1990).

The effect of Sn on Pt/C Catalysts for the Methanol Electrooxidation.

Abstract

The effect of Sn for the methanol oxidation in sulfuric acid is investigated using electrodeposited Pt and carbon supported Pt. The preparation has a considerable influence, as the Sn effects range from a small increase to a decrease in methanol oxidation activity. Sn is believed to act through the activation of H₂O. The optimum Sn surface coverage is found to be low; of the order of 10%.

Introduction

The direct methanol fuel cell has been designated as a candidate for electric power sources. Because of the use of an acid electrolyte the choice of the anode is confined to Pt. The performance of Pt for the methanol oxidation is still rather poor, but one of the possibilities to improve this performance is to promote the Pt based catalyst with another metal. The choice is not wide however. Usually Ru is taken as a promotor[1,2], but Sn is also mentioned frequently. In early papers[3,4] on the effect of Sn, large enhancement factors (50-100) were mentioned for smooth and electrodeposited Pt, while the effect for carbon supported Pt catalysts was substantially lower (ca. 10). Later, other authors found effects for Sn that were considerably smaller or sometimes even negative[5,6,7,8]. The positive effect of Sn, is mainly attributed to H₂O activation, that is, Sn is responsible for the deliverance of an oxygen atom to the methanol adsorbate to oxidise it to CO₂. Another explanation is the ligand effect, here Sn influences the Pt-oxide formation or the Pt-adsorbate binding. A complicating fact in the comparison of the literature data, is the large variety in preparation methods, which might be the cause of the different results. Moreover the influence of Pt particle size on the effect of Sn is not yet clear.

The aim of the present paper is: (i) Explore whether variations in the way in which Sn is incorporated do indeed lead to variations in its effect on the methanol oxidation activity of Pt based electrodes; (ii) Find out whether any positive effects are in fact consistent with the view of H₂O activation, taking into account that a carbon based catalyst with ~4 nm particles already appears to have optimum H₂O activation ability[9,10].

Experimental

Catalyst preparation.

Electrodeposited Pt was prepared on a smooth Pt electrode of 6 cm², from a 2 gr H₂PtCl₆/100 ml solution with a current of 5 mA/cm² for 15 minutes. The real Pt surface area was 101 cm² after electrodeposition, as measured from the hydrogen desorption area. Sn was added by immersing the electrode, which was electrochemically pre-covered with hydrogen, in 0.3 g/l SnO in 36% KOH at 80 °C.

All carbon supported catalysts were prepared with Vulcan XC-72R (325 m²/gr) (Cabot) as support. Three different catalysts were used.

A -Colloidal Pt/C was prepared by reducing H₂PtCl₆ (Drijfhout) with sodium-citrate under reflux as described previously[11]. The obtained Pt sol was then added to the suspended carbon support. After filtration, the filtrate was found to be colourless, indicating that all Pt was adsorbed on the support. After filtration the catalyst was washed and dried at 125 °C. TEM measurements showed that the mean Pt particle size is ca 4 nm.

B -PtSn sol was prepared by adding SnCl₂(Aldrich) to a boiling solution of H₂PtCl₆ and sodium-citrate in water, in a stoichiometry of Pt:Sn 10:1. The PtSn sol was then adsorbed on the carbon support, filtered, washed and dried at 125 °C.

C -Impregnated PtSn/C was prepared by mixing the carbon support with a dissolved 5:1 Pt-Sn chloride complex, this compound is used in the colorimetric detection of Pt[12]. The mixture was boiled for two hours; formaldehyde (Merck) was then added as a reductor. After one more hour of reflux the catalyst was filtered, washed with water and dried at 125 °C.

Electrode preparation.

Sn was added to catalyst A by immersion of the electrode(which was previously kept at a potential of E=-0.65 V vs MSE for 60 s) in a solution of either 0.3 g/l SnO(Aldrich) in 36% KOH(Merck) at 80 °C, or an aqueous solution of 10 g/l SnCl₄ at 23 °C. The amount of Sn on the electrode was varied by varying the adsorption time.

The electrodes of the carbon supported Pt catalysts were prepared by pressing a mixture of the catalyst and a Teflon suspension on a Pt current collector. The electrode was dried at 125 °C and sintered at 340 °C for two hours. The final Teflon content of all electrodes was ca 20%.

Electrochemical characterization.

The catalyst surfaces were characterized by cyclic voltammetry at room temperature using a computer controlled Autolab potentiostat(Eco chemie). Potentiodynamic cycling was generally carried out between -0.65 and +0.6 V vs MSE (E=0.65 V vs RHE) in 0.5 M H₂SO₄. A Pt sheet was used as a counter electrode. Pt surface areas and Sn surface coverages were determined from the hydrogen desorption area of the anodic cyclic voltammetric sweep

assuming that 1 cm² of Pt required 210 μC[13].

Activity measurements for the methanol oxidation were performed in 0.1 M CH₃OH(Merck)-/0.5 M H₂SO₄ with a potential sweep with a sweep rate of 5 mV/s, it was established that no significant different results were obtained with lower sweep rates. Differential Electrochemical Mass Spectroscopy measurements were carried out with an experimental setup similar to that of Vielstich et al.[14].

Results

Electrodeposited Pt.

Immersion (during 15 min) of electrodeposited Pt resulted in a Sn coverage of 20 %. The effect of this Sn coverage on the oxidation of methanol is shown in figure 1. In the low potential region the methanol oxidation activity is a factor 10 larger in the presence of Sn. Our result is in good agreement with the results of Iwasita et al.[15] who found an enhancement with a factor of 7.5. It is however substantially smaller than the 100 fold increase at -0.15 V found by Janssen and Moolhuysen[3]. It is further relevant to note that Sn does not influence the position of the Pt-O reduction peak. Measurements of the activity as a function of Sn surface coverage show that high Sn coverages (>50%) give a decrease in activity. All Sn coverages below 50% give an increase in activity in the low potential region. The optimum Sn coverage is below 20 %.

Catalyst A.

Figure 2a shows the cyclic voltammogram of the Pt/C catalyst(A) as prepared and after Sn

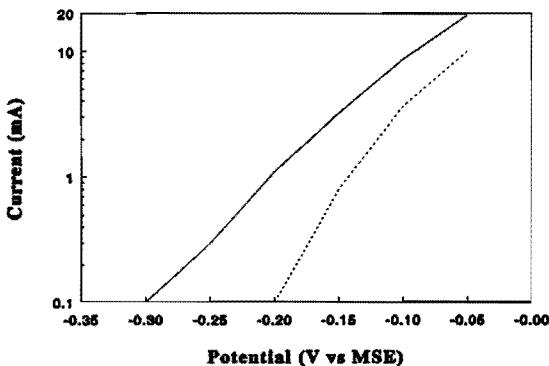


Figure 1 Methanol oxidation activity of Pt/C before and after Sn immersion. Solid curve with Sn immersion. 0.5 M H₂SO₄/0.1 M CH₃OH.

immersion. It is seen in the anodic hydrogen area that Sn preferentially covers the sites that strongly bind hydrogen. The hump at ca. 0 V indicates oxidation of Sn and no change in the Pt-oxide reduction is observed (figure 2b). The Sn surface coverages for two different

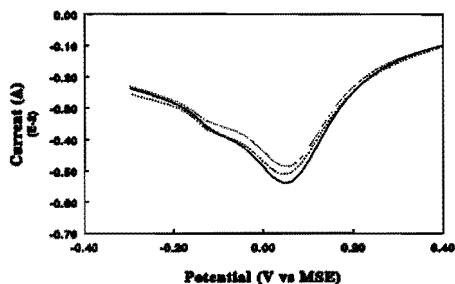
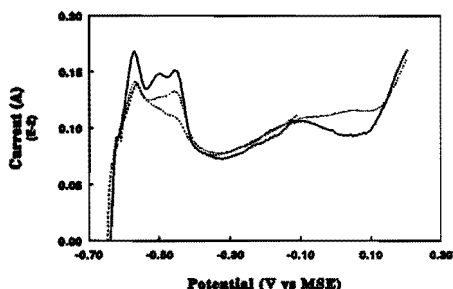


Figure 2A The effect of Sn coverage on CV of Pt in 0.5 M H_2SO_4 . (-) $\theta_{\text{Sn}}=0$; (--) 0.26; (...) 0.13. Hydrogen adsorption region. **Figure 2B** As for (A) but for the oxide reduction region.

preparations were calculated to be $\theta_{\text{Sn}}=0.26$ and $\theta_{\text{Sn}}=0.13$. The effect of these Sn coverages on the oxidation of methanol is shown in figure 3. In the low potential region, between -0.2 and 0 V, a higher methanol oxidation activity is obtained in the presence of Sn. The catalyst with 13% Sn is has the highest oxidation activity. At higher potentials however the activity is lower than that of pure Pt/C, even at this relatively low Sn loading, confirming that Sn is also a surface blocking agent vis-a-vis methanol adsorption[3]. Immersion in SnCl_4 solutions always

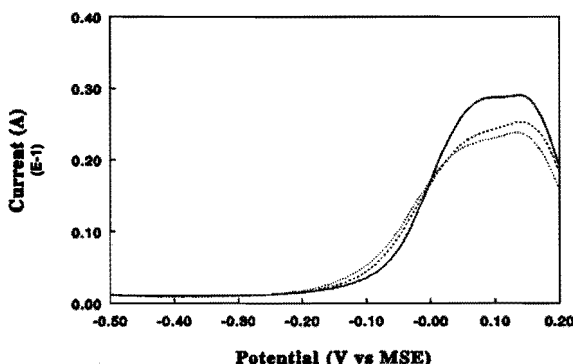


Figure 3 Effect of Sn on the methanol oxidation on Pt/C (A). (-) $\theta_{\text{Sn}}=0$; (--) 0.26; (-) 0.13. 0.5 M H_2SO_4 /0.1 M CH_3OH , $v=10$ mV/s.

resulted in a surface coverage higher than 50%. At this high coverage still some enhancement in methanol oxidation activity was found in the low potential region. DEMS measurements showed that the CO_2 production during the methanol oxidation, is indeed somewhat higher

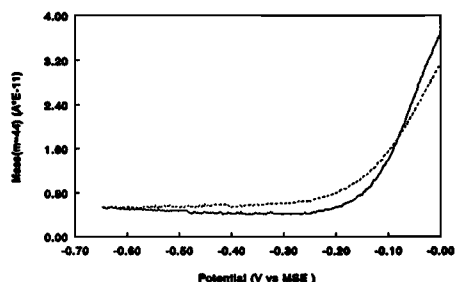
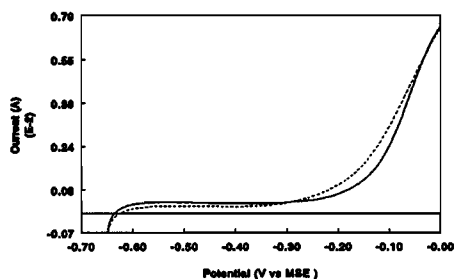


Figure 4A Effect of high Sn coverage on methanol oxidation. $\theta_{\text{Sn}}=0$ (-); 0.5 (- -). 0.5 M $\text{H}_2\text{SO}_4/0.1$ M CH_3OH .

Figure 4B Same as for A, but mass-potential curve.

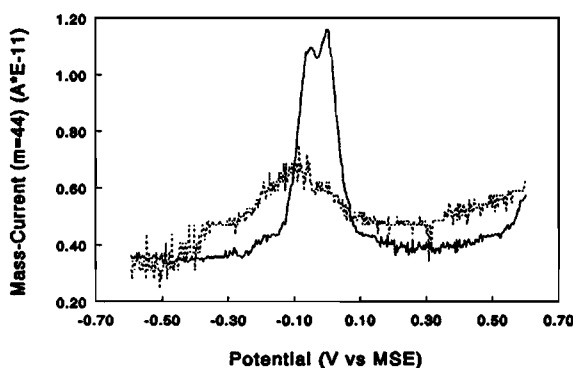


Figure 5 Effect of Sn coverage on the oxidation of adsorbed CO. Mass-potential curve. (-) $\theta_{\text{Sn}}=0$; (...)0.48. 0.5 M H_2SO_4 , $v=5$ mV/s.

and that there is a small cathodic shift in the CO_2 production potential (figure 4). Oxidation of a pre-adsorbed species (either from CO or CH_3OH) gives a cathodic shift of approximately 0.1 V in CO_2 production potential, as is shown in figure 5, again indicating that Sn promotes the oxidation of the adsorbed residue but also hampers the methanol adsorption.

Catalyst B.

XPS measurement of catalyst B shows the presence of mainly Pt metal, with a small amount of oxidised species. The Sn spectra show that only oxidised Sn is present. The Pt:Sn ratio was

found to be 8:1. The electrode of the colloidal PtSn/C catalyst gives the cyclic voltammogram shown in figure 6a. No change in the Pt-oxide reduction potential is found. Again a Sn oxidation is observed at ca. 0 V, which disappeared upon cycling of the electrode, indicating that Sn disappears from the catalyst surface. This is accompanied by an increase in the anodic hydrogen area. No preference for strongly bonded hydrogen is seen this time. As soon as the oxidation peak at 0 V was no longer observed and the surface area did not increase any further, we assumed that the surface was free of Sn. The methanol oxidation activity of this Sn free catalyst was found to be equal to the activity of a Pt/C catalyst without Sn, having the same cycling history. Estimation of the Sn surface coverage is hampered by the fact that we

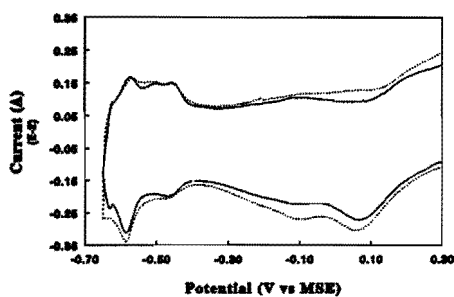


Figure 6A CV of catalyst B. Solid curve without Sn. 0.5 M H₂SO₄, $\nu=10$ mV/s.

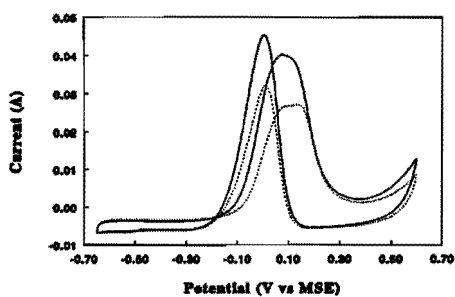


Figure 6B As for A, but in the presence of methanol. Solid curve, with Sn. 0.1 M CH₃OH

have found[9] that Pt particles on a carbon support grow during extensive cycling. However by assuming that no particle size growth takes place, we estimated a Sn surface coverage of at least $\theta_{\text{Sn}}=0.07$, which is close to the Pt:Sn ratio determined with XPS. This suggests that there is no strong Sn enrichment of the PtSn particle surface. The methanol oxidation activity on PtSn/C as given in figure 6b is about a factor two higher, than on the catalyst free of Sn.

Catalyst C.

XPS measurements of the impregnated catalyst show Pt metal with a relatively large amount of oxidised species; the Sn spectra show the presence of an oxidised Sn species. The ratio of Pt:Sn is found to be 4:3, which implies a very strong Sn enrichment of the surface.

No oxidation peak for Sn could be detected in the cyclic voltammogram of the impregnated catalyst. Upon cycling however the hydrogen area was found to increase and the methanol oxidation activity reached a value representative of an impregnated catalyst without Sn [9]. In contrast to both other catalysts the methanol oxidation activity was found to be lower in the presence of Sn (figure 7).

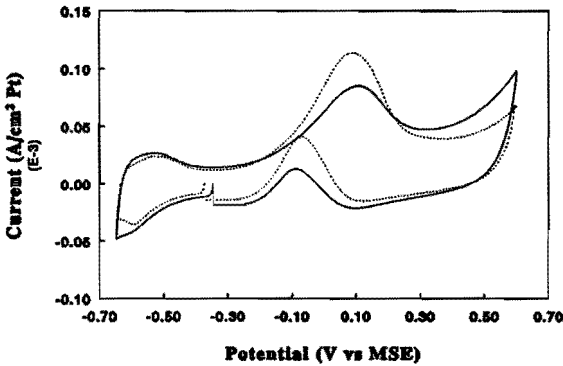
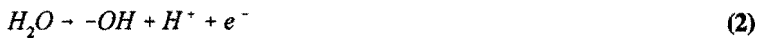


Figure 7 Methanol oxidation on catalyst C. Solid curve with Sn. 0.5 M H_2SO_4 /0.1 M CH_3OH .

General Discussion.

In contrast to the results of Janssen et al.[3] no change in the Pt-oxide reduction is observed in the presence of Sn for any of the Pt catalysts. Sn thus does not seem to have any influence on the Pt-oxide formation. A ligand effect of Sn therefore is not very likely. For the purpose of this discussion the methanol oxidation can be written as:



We take Sn to promote the activation of water, eq(2), which is difficult on Pt itself. A secondary effect of Sn is to impede the methanol adsorption reaction, so that optimal Sn coverages are low. Evidence exists that Sn covers two Pt sites[16], whereas methanol needs an ensemble of 5-6 Pt sites. The amount of these ensembles rapidly decreases with an increasing Sn coverage. This explains why at high Sn surface coverages, where a large cathodic shift for the oxidation of an adsorbate is observed the steady state activity is still low (low rate of formation of the adsorbate).

-The enhancement in methanol oxidation activity is highest for the largest Pt particles (electrodeposited Pt) where the H₂O activation is most difficult. The activity of the Sn promoted Pt is higher than that of colloidal Pt with optimum particle size.

-The enhancement in the case of colloidal Pt, of optimum particle size[9], is still about a factor 2, indicating that Sn transfers its oxygen to the adsorbed residue at a higher rate than Pt. No enhancement, on the contrary, is found for the smallest Pt particles.

We observed that Pt particles of ~4 nm have an optimal water activation ability[9]. Impregnated Pt particles are known to be substantially smaller (~2 nm) and thus "over-active" in water activation[9]. This over-activity diminishes the amount of free adsorption sites for methanol, addition of Sn will only decrease this amount further and thus lower the methanol oxidation activity. This could explain the decrease in activity for the impregnated PtSn catalyst, but incomplete reduction of the catalyst might also be of influence, as XPS spectra show higher oxidation states for Pt and Sn in the impregnated catalyst. The fact that XPS measurements show a high amount of Sn (~40%) should not be of any influence, as with immersed electrodes Sn coverages as high as 50% still show a small enhancement in activity.

Conclusion

It appears that different preparation methods may indeed account for the different results on the effect of Sn. A Pt particle size effect may play a role as well. There is no indication that Sn acts via a ligand effect, a water activation effect seems to be most likely.

References

1. T. Iwasita, F.C. Nart, W. Vielstich *Ber. Bunsenges. Phys. Chem.* **94**, 1030 (1990).
2. A. Hamnett, B.J. Kennedy, F.E. Wagner *J. of Catalysis* **124**, 30 (1990).
3. M.M.P. Janssen, J. Moolhuysen *Electrochim. Acta* **21**, 861 (1976).
4. S. Motoo, M. Watanabe *J. Electroanal. Chem.* **69**, 429 (1976).
5. M. Watanabe, Y. Furuchi, S. Motoo *J. Electroanal. Chem.* **191**, 367 (1985).
6. S.R. Wang, P.S. Fedkiw *J. Electrochem. Soc.* **139**, 3151 (1992).
7. B. Bittins-Cattaneo, T. Iwasita *J. Electroanal. Chem.* **238**, 151 (1987).
8. S.A. Campbell, R. Parsons *J. Chem. Soc. Faraday Trans.* **88**, 833 (1992).
9. T. Frelink, W. Visscher, J.A.R. van Veen *J. Electroanal. Chem.* **382**, 65 (1995).
10. P.A. Atwood, B.D. McNicol, R.T. Short *J. Appl. Electrochem.* **10**, 213 (1980).
11. K. Aika, L.L. Ban, I. Okura, S. Namba, J. Turkevich *J. Res. Inst. Catalysis Hokkaido Univ.* **24**, 54 (1976).
12. A.S. Meyer, G.H. Ayres *J. Am. Chem. Soc.* **77**, 2671 (1955).
13. T. Biegler, D.A.J. Rand, R. Woods *J. Electroanal. Chem.* **22**, 269 (1971).
14. T. Iwasita, W. Vielstich, E. Santos *J. Electroanal. Chem.* **229**, 367 (1987).
15. T. Iwasita-Vielstich in *Advances in Electrochemical Science and engineering* Vol 1., Page 127-170. H. Gerischer, C.W. Tobias editors, VCH New York 1990.

16. J. Sobkowski, K. Franaszcuk, A. Piasecki *J. Electroanal. Chem.* 196, 145 (1985).

Metal-oxide supported catalysts for the electrooxidation of Methanol.

Abstract

Results on alternative catalysts for the electrooxidation of methanol are presented. It is shown that the presence of both TiO_2 and WO_3 increases the methanol oxidation activity of Platinum. It is furthermore demonstrated that oxidation of methanol is also possible with AuRu/TiO_2 . The oxidation of methanol on Pt/WO_3 results in a decrease in the amount and a recrystallisation of WO_3 in the electrode.

Introduction

In the previous chapters it has been shown that Ru (and Sn) considerably increases the activity of platinum for the electrooxidation of methanol. The measured activities however, are too low for practical application in a fuel cell. Therefore some research has also been directed towards alternative catalysts to see if there are more promising systems. In this search for alternative materials for methanol electrooxidation catalysts, in recent years some attention has been paid to oxide supported systems. Most research has been done on WO_3 [1],[2],[3] supported Pt, but TiO_2 , ZrO_2 and Nb_2O_5 [4],[5] have also been considered as a support.

Both pure tungsten oxides and rare-earth metal tungsten bronzes (Ln_xWO_3) are inactive for the methanol oxidation, however, doped with Pt ($\text{PtDy}_{0.1}\text{WO}_3$) these materials do show some activity[1]. It was proposed[1] that the higher activity is due to the removal of CO by a $\text{WO}_3/\text{WO}_3^+$ redox couple or due to the reduction of strongly bonded adsorbates by hydrogen tungsten bronzes[6]. There is however no clear evidence in favor of one of these hypotheses. Tseung et al.[2,3] showed that codeposited Pt/WO_3 was more active than platinized Pt for the methanol oxidation: the current peak in the cyclic voltammogram was shifted 200 mV to more cathodic values in the presence of WO_3 . This shift was attributed to an increased water activation, the same effect as for other promotor metals (Chapter7-10).

It is generally recognized that the electrooxidation of methanol is retarded by the formation of CO like species [Chapter 2]. It would therefore be worthwhile to add or use a good CO oxidation catalyst in the methanol oxidation. It was reported by two research groups [7],[8] that Au/TiO_2 is a remarkable active catalyst in the gas-phase oxidation of CO, even at temperatures below 0°C .

Electrochemical studies have shown that CO can be oxidized at Au[9], but that Au is not active at all for the oxidation of methanol[10]. Both lower[11] and higher[12] activities for

PtAu for the methanol oxidation systems have been reported. PtAu/TiO₂ might also be considered as a catalyst for the electrooxidation of methanol because of the good CO oxidising properties of the Au/TiO₂.

Hammnett et al.[4] showed that there is a slight increase in activity for the electrooxidation of methanol when TiO₂ is used as a support for the Pt catalyst. TiQ has furthermore proven to be a good catalyst for the oxidation of formic acid[13].

In this chapter we will present some preliminary results on Au/TiO₂, PtAu/TiO₂, Pt/TiQ, AuRu/TiO₂ and Pt/WO₃. Since TiQ is a semi-conductor all catalysts containing this species are carbon supported. All WO₃ containing catalysts are unsupported.

Experimental

TiO₂/C

Carbon supported TiO₂ was prepared according to the method of Uchida et al.[14]. For a 20%(weight) TiO₂ catalyst, 3 ml titanium-tetra-isopropoxide (Janssen Chimica) was added to 9 ml HNO₃. The solution became transparent after 2 hours of stirring, then the pH is adjusted to 3 by adding the appropriate amount of 1 M NaOH. The colloid, which has then formed, is added to 4 g Vulcan XC-72. After filtration and washing the catalyst is dried at 80°C for one hour and heated at 300°C in air for another hour.

Au/TiO₂/C

To prepare the TiO₂/C supported metal catalysts, a method similar to that of Biswas et al.[15] was used. A Au-colloid was prepared according to the method of Turkevich[16]. HAuCl₄(Johnson/Matthey) was reduced with sodium-citrate to form after 1 hour of reflux a ruby-red Au colloid. This colloid was then added to the suspended TiO₂/C catalyst. After filtration the catalyst was washed with water and dried at 80°C. For preparation of the AuRu catalyst, Ru(NO)(NO₃)₃ (Johnson-Matthey) was added during Au colloid formation in the appropriate amount.

Pt/TiO₂/C

This catalyst was prepared in the same way as described above. H₂PtCl₆(Johnson/Matthey) was used to prepare the Pt colloid, which has a brownish-black color. Catalysts containing two metals were prepared in the same way; colloids were prepared using two metals instead of one.

Electrode preparation.

Electrodes were prepared by adding a Teflon suspension to the carbon (Vulcan XC-72) supported catalyst, pressing the catalyst on a Au current collector, drying the electrode for one hour at 125°C and sintering for two hours under Ar at 300°C. The final Teflon content was

always 20%.

Pt/WO₃

The codeposited Pt/WO₃ electrodes were prepared according to a method similar to that described by Tseung et al. [3]. Electrodeposition solutions were prepared by dissolving tungsten powder in 30% H₂O₂. After addition of water and ethanol up to the desired volume, the excess H₂O₂ was decomposed at platinised platinum, and the required amount of H₂ PtCl₆ was added. The final concentrations in the solution were: 0.1 M WO₃ and 8 mM H₂ PtCl₆. According to [3] this gives a stable deposition solution, from which no precipitation occurs. Electrodeposition was done on a Pt sheet or gauze with different current densities for 15 minutes. Thereafter the electrode was thoroughly rinsed with deionised water to remove chloride impurities.

Electrochemical characterization.

Cyclic voltammetry was carried out with a Wenking POS 73 potentiostat, using a Philips 8043 XY recorder. Hg/Hg₂SO₄ was used as a reference electrode and Pt as a counter electrode. Electrolyte solutions were prepared from p.a. H₂SO₄(Merck), p.a. CH₃OH and ultrapure water (EcoStat). Morphology and W/Pt ratio in the Pt/WO₃ electrodes were determined with SEM. Activities for the methanol oxidation were measured in the anodic part of a cyclic voltammetric sweep with 5 mV/s and are given with respect to the real Pt area, calculated from the hydrogen desorption charge.

Results and Discussion.

Au/C, Au/TiO₂/C, and AuRu/TiO₂/C.

Catalyst	10 % Au/C	20% Au/C	10%Au/ 20%TiO ₂ /C	20%Au/ 40%TiO ₂ /C
E _{CO} (V vs MSE)	-0.26	-0.37	-0.33	-0.42

Table I Onset-potentials for CO oxidation of different catalysts.

Both CO and CH₃OH oxidation were studied on these catalysts. The results for CO oxidation are shown in table 1, where it can be seen that the onset of CO oxidation shifts to more cathodic values in the presence of TiO₂. This is in agreement with the gas-phase studies [8] which reported that in the presence of TiO₂, CO can be oxidised at lower temperatures.

At none of the prepared electrodes any oxidation of methanol was observed, as might have

been expected from the fact that Au itself is inactive for this reaction. Weaver et al.[17] showed with Surface Enhanced Raman Spectroscopy that although methanol is not oxidised on Au, methanol adsorbates are formed on Au but cannot be oxidised.

In order to get some more insight in this, a AuRu/TiO₂ catalyst was prepared. As discussed in chapters 7-10 of this thesis, Ru forms oxides at rather low potentials, which are then capable of oxidising a methanol adsorbate on Pt, at a lower potential than Pt itself does.

Figure 1 shows the oxidation of methanol on the Ru containing catalyst. Although the currents are only very small it can be seen that in the presence of Ru methanol can be oxidised on Au at

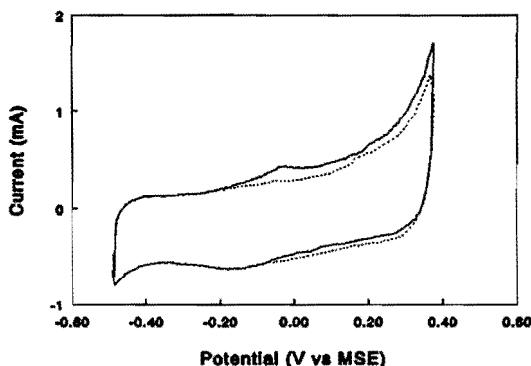


Figure 1 CV of AuRu/TiO₂/C in the presence and absence of methanol. Solid curve with methanol. 0.5 M H₂SO₄/0.1 M CH₃OH, $v=5$ mV/s.

potentials of ca -0.20 V vs MSE and higher. On Ru/C this potential was 0.5 V higher. This seems to confirm that methanol adsorbates are indeed formed on Au, but are only oxidised in the presence of Ru. The fact that Ru is necessary for the oxidation of the methanol adsorbate combined with the fact that Au itself is capable of oxidising CO, suggests that the adsorbate formed on Au in the presence of methanol can not be a CO-species.

Pt/TiO₂

Figure 2 shows that in the presence of TiO₂ a shoulder appears in the oxidation peak of pre-adsorbed CO on Pt, indicating that only a small part of the adsorbed CO is oxidised more easily. This is consistent with the results of Folkesson et al.[18] who did not find a CO frequency in their IR spectrum of methanol on Pt/TiO₂ and explained this absence by assuming that CO is oxidised by a Ti-oxide species. After all, interaction between a CO adsorbate and a

Ti-oxide species will occur only at the edges of a Pt particle. The amount of CO that can be oxidised by a Ti-oxide is thus small, resulting in a shoulder in the CO oxidation peak.

In figure 3 the methanol oxidation activities in the presence and absence of TiO_2 are

Dep. Current	$I_{\text{H}_2\text{WO}_3}/I_{\text{PtO}}$ [b]	W percentage (EDX) [a]
10.5	1.19	9.8 at. %
13.5	1.20	9.9 at. %
17.5	1.38	10.7 at. %

Table II Characterization of Pt/WO_3 electrodes as a function of deposition current.

compared. The figure shows that Pt/TiO_2 (curve B) gives higher current densities than Pt itself

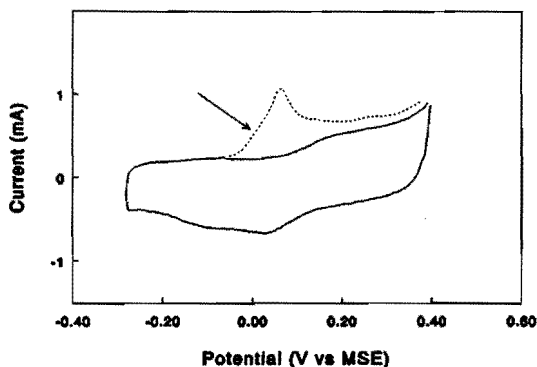


Figure 2 CO oxidation on $\text{Pt}/\text{TiO}_2/\text{C}$. CO was adsorbed at -0.3 V vs MSE. Solid curve is the blank.

(curve A). This was also observed by others[4]. It does not seem to be very likely that this increased activity is due to the direct oxidation of the methanol adsorbate by Ti-oxide species, because of the fact that this would only concern very few methanol adsorbates. Both Hamnett[4] and Biswas[15] ascribe the increase in activity to an increase in oxidisability of the Pt. As was discussed before in Chapter 5, an increased oxidisability of the Pt would result in a shift of the Pt-oxide reduction potential to lower values. Such a shift is indeed observed in the cyclic voltammetric curve of the Pt/TiO_2 catalyst, thus confirming the results of Hamnett[4]

and Biswas[15].

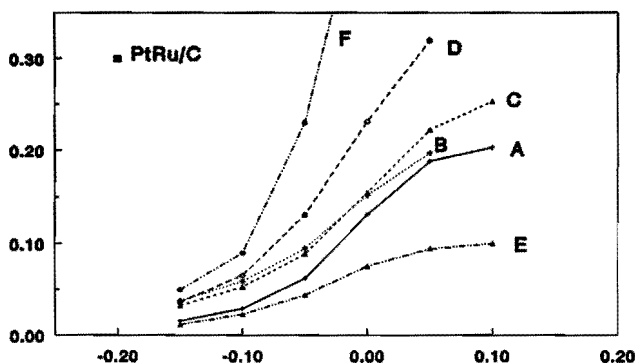


Figure 3 Specific activity for methanol oxidation. (A) Pt/C; (B)Pt/TiO₂/C; (C) PtAu(1:1); (D) PtAu(3:1); (E) PtAu/TiO₂/C; (F) Pt/WO₃. PtRu/C is added for comparison. 0.5 M H₂SO₄/0.1 M CH₃OH.

PtAu and PtAu/TiO₂

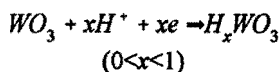
A PtAu/C catalyst was found to be more active for the methanol oxidation than Pt/C as is shown in Figure 3 (curves A,C and D). This is in agreement with results of Enyo et al.[12], who reported a higher activity for the methanol oxidation for small PtAu clusters on carbon; this was ascribed to the good CO oxidising properties of Au. Previously Watanabe et al.[11] reported a decrease in activity in the presence of Au.

Because of the increase in CO oxidising properties of Au when supported on TiO₂(vide supra), a PtAuTiO₂/C catalyst was also tested. Only a very low activity for the methanol oxidation was found, as may be seen in Figure 3(curve E). For the electrooxidation of CO, the results were similar;CO is oxidised at lower potentials on PtAu/C than on Pt/C, the presence of TiO₂ did not give an additional effect. It is not yet understood why the presence of both TiO₂ and Au results in a decrease in the methanol oxidation activity.

Pt/WO₃

Characterization

In figure 4, a typical voltammogram is given for a Pt/WO₃ electrode in 0.5 M H₂SO₄. In the potential region between -0.65 V and -0.35 V vs MSE, a typical shape (B) for these electrodes is observed in agreement with results by others[1,6]. The redox couple observed here is due to[19]:



Furthermore a small reduction peak (A) is observed at ca 0.1 V vs MSE due to the reduction of Pt-oxides. Sadly enough no comparison can be made with the results of Tseung et al.[3], because no cyclic voltammetric characterization is given in their study. In trying to establish the W/Pt ratio of the electrodes, the ratio of the peak-currents of the Pt-oxide reduction (I_{PtO}) and the H_xWO_3 ($I_{H_xWO_3}$) oxidation was calculated. The results are given in Table 2, together with the values obtained with the results from SEM/EDX measurements, only Pt and W were found in all samples.

The results in the table show that the trend in the SEM/EDX value is the same as the trend in

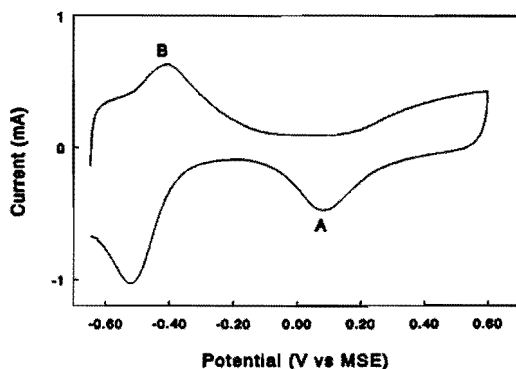


Figure 4 CV of Pt/ WO_3 in 0.5 M H_2SO_4 . For A and B see text.

the $I_{PtO}/I_{H_xWO_3}$ peak ratio; with increasing deposition current density there is an increase in the amount of W in the electrode. The current ratio (b) can thus also be used to estimate the Pt/W ratio in the electrode.

A typical SEM photograph is given in figure 5. In addition to the grey electrodeposit on the background, white particles are seen across the surface, EDX analysis shows that these particles contain ca 40 % W. Although the EDX measurements show that the grey electrodeposit is constant in composition across the surface, there are thus additional areas on the electrode where WO_3 is the major species. It must be noted that the W content is low probably because the deposited films are very thin. The Pt on which the film is deposited is then also measured with EDX.

The notion by Tseung et al.[3] that the electrodeposition solution is stable for a long period and that the Pt/W ratio is identical in each electrode could not be substantiated.

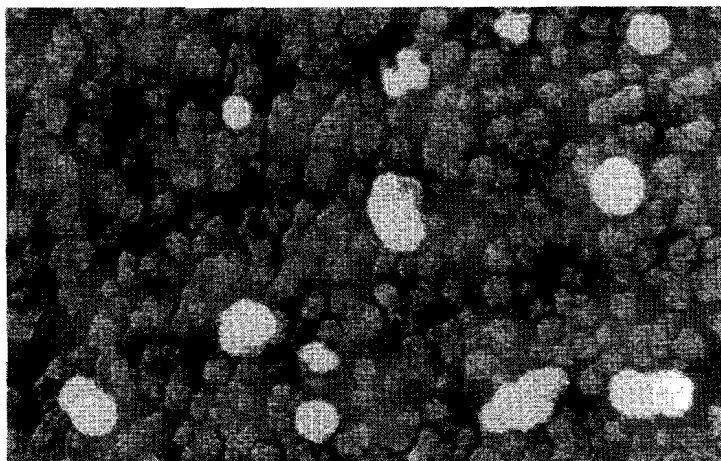


Figure 5 SEM image of an electrocodeposited Pt/WO₃ catalyst.

Methanol oxidation

A cyclic voltammogram of methanol oxidation on Pt/WO₃ is given in figure 6, together with the CO₂ production at the start of the methanol oxidation as measured with DEMS. The shift in methanol oxidation peak potential, which was observed by Tseung et al.[3] was not observed by us. It can also be seen that the start of the methanol oxidation, which is at -0.32 V vs MSE (dashed curve in Figure 6), is shifted to more negative potentials, when compared to PtPt (ca -0.25 V vs MSE). These results seem to be in agreement with the results in ref[6]. In Figure 3 (curve F), the activity for the methanol oxidation of a Pt/WO₃ electrode is compared to that of the other catalysts. It is seen the currents on the former are considerably higher. The presence of WO₃ thus has a positive influence on the methanol oxidation activity of Pt (curve A). Since the methanol oxidation also starts at a lower potential, the higher activity is probably due to a more easy oxidisability of the Pt, as was the case for the TiO₂ supported Pt.

To check whether there is an effect of performing methanol oxidation on the composition of the electrode, SEM/EDX measurements were also done after methanol oxidation. We found that not only the amount of W in the electrodes diminishes, but there is also a growth of the size of the white WO₃ enriched particles. A CH₃OH induced dissolution and precipitation of WO₃ thus seems to occur. It is furthermore found in the SEM pictures after methanol oxidation, that the WO₃ is now present as small needles, while before small particles were observed. This crystallization phenomenon was also observed by Tseung et al.[3].

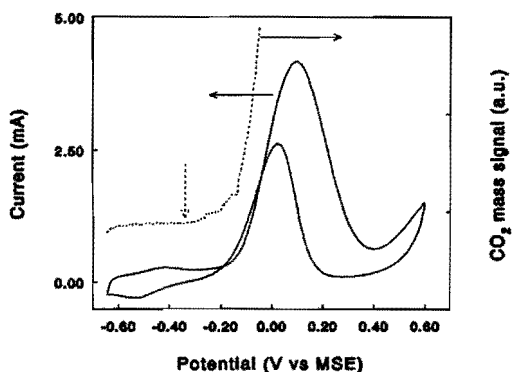


Figure 6 CV of methanol oxidation on the catalyst of figure 4. The dashed curve gives the CO_2 production, measured with DEMS. The dashed arrow indicates the start of methanol oxidation. $0.5 \text{ H}_2\text{SO}_4/0.1 \text{ M CH}_3\text{OH}$, $v=2\text{mV/s}$.

General Discussion

The results presented here show that both oxides, TiO_2 and WO_3 , have a positive influence on the methanol oxidation activity of Pt. Although there is some indication that Ti-oxide species directly oxidise the adsorbate, at least in the case of adsorbed CO, this cannot be the only effect.

In analogy with gas-phase studies we found that CO on Au/TiO_2 is oxidised more easily than on Au. With Ru added to this system, even methanol is oxidised although only in small amounts, which suggests that methanol adsorbates that differ from CO are formed on Au. In order to compare the activities found for the alternative catalysts, in Figure 3 the activity (at -0.2 V vs MSE) of the most active PtRu/C catalyst is added. Although the activity of these PtRu/C systems is still too low for practical applications, it is still considerably higher than that of the alternative catalysts presented in this chapter.

It is clear that these are only preliminary results on two (WO_3 and TiO_2 supported) relatively unknown systems for the oxidation of methanol, it seems worthwhile to study these and similar systems in more detail. Especially the addition of Ru to the Pt/ WO_3 system seems promising.

Acknowledgement

Two people deserve many thanks for producing most of the results presented in this chapter: Renee van Schijndel and Liane Schoonus. Furthermore Drs. Martien Haanepen is thanked for doing all SEM/EDX measurements.

References

I.K.I. Machida, M. Enyo, G.Y. Adachi, J. Shiokawa *J. Electrochem. Soc.* **135**, 1955 (1988).

Chapter 12

- 2.P.K. Shen, K. Chen, A.A.C. Tseung *J. Chem. Soc. Far. Trans.* 90, 3089 (1994).
- 3.P.K. Shen, A.A.C. Tseung *J. Electrochem. Soc.* 141, 3083 (1994).
- 4.A. Hamnett, B.J. Kennedy, S.A. Weeks *J. Electroanal. Chem.* 240, 349 (1988).
- 5.A. Hamnett, P. Stevens, G.L. Troughton *Cat. Tod.* 7, 219 (1990).
- 6.P.J. Kulesza, L.R. Faulkner *J. Electroanal. Chem.* 259, 81 (1989).
- 7.S.D. Lin, M. Bollinger, M.A. Vannice *Cat. Lett.* 17, 245 (1993).
- 8.M. Haruta, S. Tsubota, T. Kobayashi, H. Kageyama, M.J. Genet, B. Delmon *J. Cat.* 144, 175 (1993).
- 9.S.C. Chang, A. Hamelin, M.J. Weaver *J. Phys. Chem.* 95, 5560 (1991)
- 10.M.W. Breiter, *Electrochim. Acta* 8, 973 (1963).
- 11.M. Watanabe, S. Motoo *J. Electroanal. Chem.* 60, 259 (1975).
- 12.M. Enyo, K.I. Machida, A. Fukuoka, M. Ichikawa in *Electrochemistry in Transition* ed. O.J. Murphy, Plenum Press New York 1992. p. 359-369.
- 13.R.W. Matthews *J. Catal.* 100, 275 (1986).
- 14.H. Uchida, S. Itoh, H. Yoneyama *Chem. Lett.* 1995(1993)
- 15.P.C. Biswas, Y. Nodasaka, M. Enyo, M. Haruta *J. Electroanal. Chem.* 381, 167 (1995).
- 16.K. Aika, L.L. Ban, I. Okura, S. Namba, J. Turkevich *J. Res. Inst. Catal. Hokaido Univ.* 24, 54 (1976).
- 17.Y. Zhang, M.J. Weaver *Langmuir* 9, 1397 (1993).
- 18.B. Folkesson, R. Larsson, B. Rebenstorf *J. Electroanal. Chem.* 272, 231 (1989).
- 19.B. Reichman, A.J. Bard *J. Electrochem. Soc.* 126, 2133 (1979).

Summary

The Direct Methanol Fuel Cell is attractive as a source of power for vehicle traction. One of the major problems in the development of this fuel cell is, however, the electrocatalytic oxidation of methanol over a Pt catalyst. In this half reaction, methanol is oxidised to CO_2 by an on the catalyst adsorbed water molecule. Both the activity and the long term stability of the now known catalysts, are, in spite of more than 30 years of research, not good enough for practical applications however; on Pt the reaction is too slow and the catalyst deactivates rapidly. The work described in this thesis is aimed towards a better understanding of the electrooxidation of methanol over Pt and the influence of a promotor metal, like Sn or Ru on Pt.

A review of the research in the field of the electrocatalytic oxidation of methanol is given in Chapter 2. It is shown that in spite of the development of a number of in-situ techniques, still no consensus is reached on the type of adsorbed intermediates via which the methanol oxidation proceeds. Furthermore the effect of a change in Pt particle size, as well as the effect of a change in the Pt-carbon interaction are not clear yet, neither is the mechanism by which the promotor metals (of which Sn and Ru give the best results) actually act. Finally a short account is given of the search for alternative catalysts, of which tungsten-bronzes and tungsten-carbides seem to be the most promising.

Chapter 3 gives a short introduction in the in-situ electrochemical techniques that have been used. Of the three techniques that are described, Electrochemical Quartz Crystal Microbalance (EQCMB) and ellipsometry are relatively newcomers in this area. The third technique, Differential Electrochemical Mass Spectroscopy (DEMS) has already been proven to be a powerful technique for the study of adsorbed reaction intermediates.

In order to obtain a better insight in particle size- and promotor-effects, it is first of all necessary to have a clear view of the mechanism of the methanol electrooxidation over Pt. This is dealt with in Chapter 4. With DEMS, the adsorbed intermediates formed in the presence of methanol have been studied under a number of reaction conditions. Under most circumstances a mixture of linear- and bridge-bonded CO is formed on the surface. The ratio of these two species is found to depend on the type and the concentration of the anion of the supporting electrolyte, on the adsorption potential and on the surface coverage of the adsorbate. Furthermore a difference is found between adsorbed CO formed from CO and adsorbed CO formed from methanol; CO formed from methanol is homogeneously distributed across the surface, while CO from CO is adsorbed in an island geometry. At very low adsorbate coverage and low adsorption potential, the adsorbate formed from methanol appears to be COH. With increasing surface coverage and increase in potential this adsorbate immediately loses its proton under formation of adsorbed CO.

In order to make optimal use of the amount of Pt present in a catalyst, it is necessary to

Summary

decrease the Pt particle size. This may however, also change the properties of Pt, as is described in Chapter 5 and 6. The influence of the Pt particle size and the effect of a Pt-carbon interaction on the activity for the electrooxidation of methanol is described in Chapter 5. It appears that with a decrease in Pt particle size, the Pt surface is more easily oxidised. Below $d \approx 4$ nm there is a decrease in the specific activity for the methanol electrooxidation is found. This is due to a decrease in the number of free adsorption sites, either due to an overoxidation of the Pt surface (methanol does not adsorb on Pt-oxides) or due to a decrease in the number of by methanol favoured adsorption sites. It is furthermore shown that Pt deposited on an oxidised carbon surface gives a slightly higher activity for the methanol oxidation.

In Chapter 6, it is first of all confirmed that methanol adsorbs less easily on Pt particles below 4 nm. Furthermore DEMS results show that there is no influence of the Pt particle size on the type of adsorbate that is formed; only adsorbed CO, in both the linear and the bridge-bonded form could be detected.

With the insight in the methanol oxidation mechanism, obtained in Chapter 4-6, it is now possible to study the effect of a promoter metal (Ru or Sn) on the electrooxidation of methanol over Pt. This is the subject of the Chapters 7-11. The most simple model system for a promoted catalyst is smooth Pt metal with a submonolayer of the promoter (Chapter 7). First of all DEMS measurements confirm that CO₂ production, and hence methanol oxidation, starts at a lower potential in the presence of either Sn or Ru. With ellipsometry it was possible to follow oxide formation on the surface of the catalyst, either promoted- or bare Pt. It appears that without promoter the amount of Pt-oxide that is formed is not affected by the presence of methanol. Without methanol the oxide formation on Sn and Ru, present in a submonolayer on Pt could be followed. In the presence of methanol, however, the oxide coverage on both Sn and Ru disappears, indicating that the promoter-metaloxides are responsible for the increase in the methanol oxidation activity. Therefore a bifunctional mechanism, where the promoter metal is responsible for the delivery of the oxygen atom, is proposed for the effect of both Sn and Ru. This conclusion was further substantiated by the results on codeposited PtRu electrodes (Chapter 8). No oxides are present on the PtRu surface in the potential region where small organic molecules are oxidised. It was furthermore confirmed that the oxides of Pt do not participate in the oxidation of HCOOH, CO or CH₃OH. Although the results in these two chapters point to a bifunctional effect, a ligand effect, where the promoter metal modifies the properties of Pt itself, cannot be excluded on the basis of these measurements. Results in Chapter 9 even suggest that such a ligand effect is indeed present; (i) an increasing amount of the promoter metal results in a decrease of the onset potential of the methanol oxidation, (ii) methanol adsorbs more easily on PtRu than on Pt and (iii) the effect of Ru is still present on carbon supported Pt with small particles, which

are, as shown in Chapter 5, already overoxidised at low potentials. These results are not explainable directly on basis of the bifunctional mechanism and thus suggest the presence of a ligand effect. Further substantiation comes from in-situ IR measurements on CO adsorbed on PtRu (Chapter 10) which show that the linear bonded CO stretch frequency is shifted to more positive values in the presence of Ru.

In studying the behavior of a catalyst its exact composition must be known. This cannot be straightforwardly analysed however for codeposited PtRu systems. We therefore developed an electrochemical method using EQCMB. This method is described in Chapter 10. It is shown that the oxide reduction potential can be used as a measure for the amount of Ru that is present on the surface. By using a calibration curve, obtained with EQCMB, it is possible to determine the Ru surface coverage in a codeposited PtRu electrode.

Although Sn is also known to be a promotor for the methanol electrooxidation, the literature is less consistent than for the effect of Ru. We therefore investigated (Chapter 11) the effect of Sn on Pt/C catalysts as a function of the preparation method. It appears that the preparation method is indeed of influence, the effects range from a small increase to a decrease in activity. As for Ru, the optimum of the amount of Sn is always low, ca 10%.

The performance of the catalysts described so far is still too poor for a practical application. Therefore some research was directed towards the development of alternative catalysts. The results, which are described in Chapter 12, show that PtAu/C and Pt/WO₃ are both more active than Pt itself, although neither of them reaches the activity of a PtRu/C catalyst. Furthermore a catalyst without Pt, AuRuTiO₂/C, also seems to be capable of oxidising methanol. It is not yet clear via what mechanism these systems act.

Summary

Samenvatting

De directe methanol brandstofcel is aantrekkelijk als een vermogensbron in de transportsector. Één van de belangrijkste problemen in de ontwikkeling van deze brandstofcel is echter, de electrokatalytische oxidatie van methanol over een Pt katalysator. In deze halfreactie wordt methanol, door reactie met een op de katalysator geadsorbeerd water molecuul, geoxideerd tot CO_2 . Zowel de activiteit als de lange termijn stabiliteit van de nu bekende katalysatoren, zijn echter, ondanks meer dan 30 jaar onderzoek, niet goed genoeg voor praktische toepassingen; de reactie op Pt is te langzaam en de katalysator deactiveert snel. Het werk dat wordt beschreven in dit proefschrift is bedoeld om een beter begrip te krijgen van de electrooxidatie van methanol over Pt en de invloed daarop van een promotor metaal, zoals Sn of Ru.

In Hoofdstuk 2 wordt een overzicht gegeven van het onderzoek op het gebied van de electrokatalytische oxidatie van methanol. Daaruit blijkt dat er, ondanks de ontwikkeling van een aantal in-situ technieken, nog steeds geen consensus is over via wat voor een type geadsorbeerd intermediair de methanol oxidatie verloopt. Bovendien is niet duidelijk wat het effect is van verandering in deeltjesgrootte van Pt of van een verandering in Pt-drager interactie. Ook is het mechanisme van het promotor effect (waarbij Sn en Ru het beste resultaat geven) nog steeds niet opgehelderd. Tot slot wordt in hoofdstuk 2 een kort overzicht gegeven van het onderzoek naar alternatieve katalysatoren, waarbij wolfram-bronzen en wolfram-carbides het meest veel belovend lijken te zijn.

Hoofdstuk 3 geeft een korte inleiding in de in-situ electrochemische technieken die gebruikt zijn. Van de drie technieken die worden beschreven, zijn Ellipsometry en de Electrochemische Quartz Microbalans (EQCMB) relatieve nieuwkomers in het onderzoek naar de methanol oxidatie. Differentiele Electrochemische Massa Spectroscopie (DEMS) heeft al bewezen een krachtige techniek te zijn voor het onderzoek naar geadsorbeerde reactie-intermediaren.

Om een beter inzicht te kunnen krijgen in deeltjes grootte- en promotor-effecten, is het allereerst nodig om een duidelijk beeld te hebben van het mechanisme van de methanol oxidatie over Pt. Dit laatste is het onderwerp van hoofdstuk 4. Met behulp van DEMS zijn de geadsorbeerde intermediaren, gevormd in de aanwezigheid van methanol onder verschillende reactie-omstandigheden, onderzocht. In de meeste omstandigheden wordt er een mengsel van lineair- en gebuigd gebonden CO gevormd op het oppervlak. De verhouding tussen deze twee blijkt af te hangen van het type en de concentratie van het electrolyet, de adsorptie potentiaal en de oppervlakte bedekking van het adsorbaat. Bovendien wordt er een verschil gevonden tussen geadsorbeerd CO gevormd uit CO en geadsorbeerd CO gevormd uit methanol; CO gevormd uit methanol is homogeen over het oppervlak verdeeld, terwijl CO gevormd uit CO zich in een eiland geometrie bevindt. Bij hele lage adsorbaat bedekkingen en een lage adsorptie potentiaal blijkt het adsorbaat gevormd uit methanol COH te

zijn. Met een toename in adsorbaat bedekking en potentiaal verliest dit adsorbaat onmiddellijk een proton onder vorming van CO.

Om zo optimaal mogelijk gebruik te maken van de hoeveelheid Pt die aanwezig is in een katalysator, is het nodig om de Pt deeltjesgrootte te verkleinen. Dit kan echter ook gevolgen hebben voor de eigenschappen van het Pt, zoals wordt beschreven in hoofdstuk 5 en 6. De invloed van de Pt deeltjesgrootte en het effect van een Pt-kool interactie op de activiteit voor de methanol oxidatie wordt beschreven in Hoofdstuk 5. Het blijkt dat bij een afname in deeltjesgrootte het oppervlak makelijker wordt geoxideerd. Beneden $d \approx 4 \text{ nm}$ blijkt de specifieke activiteit voor de methanol electrooxidatie af te nemen. Dit is het gevolg van een afname in vrije adsorptie-plaatsen, ofwel door overoxidatie van het Pt oppervlak (methanol adsorbeert niet op Pt-oxide), of door een afname in het aantal, voor methanol gunstige adsorptie plaatsen. Verder wordt aangetoond dat Pt neergeslagen op een geoxideerde kool drager een iets hogere activiteit geeft voor de methanol oxidatie.

In Hoofdstuk 6 wordt allereerst het idee uit hoofdstuk 5 bevestigd, dat methanol minder gemakkelijk adsorbeert op Pt deeltjes die kleiner zijn dan 4 nm. Bovendien laten DEMS resultaten zien dat er geen invloed is van de deeltjesgrootte op het type adsorbaat dat wordt gevormd; alleen lineair en gebrugd gebonden CO werden waargenomen.

Met het inzicht in het methanol oxidatie mechanisme, verkregen in Hoofdstuk 4-6, is het nu mogelijk om het effect van een promotor metaal, (Ru of Sn) op de electrooxidatie van methanol over Pt, te bestuderen. Dit is het onderwerp van Hoofdstuk 7-11. Het meest simpele model voor een gepromoteerde katalysator is glad Pt metaal met een sub-mono-laag van de promotor (Hoofdstuk 7). DEMS metingen tonen aan dat de CO₂ productie, en dus de methanol oxidatie beginnen bij een lagere potentiaal in de aanwezigheid van Sn of Ru. Met ellipsometrie was het mogelijk om om de oxide vorming op de katalysator, met of zonder promotor, te volgen. Het blijkt dat op ongepromoteerd Pt de oxide vorming niet wordt beïnvloed door de aanwezigheid van methanol. De oxides op Sn of Ru, op gepromoteerd Pt blijken echter te verdwijnen in de aanwezigheid van methanol, wat erop duidt dat de promotor-metaaloxides verantwoordelijk zijn voor de oxidatie van het methanol. Daarom wordt een bifunctioneel mechanisme, waar het promotor metaal verantwoordelijk is voor de levering van het zuurstof-atoom, voorgesteld voor het effect van zowel Sn als Ru. Deze conclusie wordt verder ondersteund door de resultaten die zijn verkregen aan "codeposited" PtRu elektroden (Hoofdstuk 8). Er zijn geen oxides aanwezig op PtRu in het gebied waar kleine organische moleculen worden geoxideerd. Bovendien werd nog eens bevestigd dat Pt-oxides niet meedoen in de oxidatie van HCOOH, CO en CH₃OH. Hoewel de resultaten in deze twee hoofdstukken wijzen op een bifunctioneel effect, kan een ligand effect, waar de promotor de eigenschappen van het Pt verandert, niet worden uitgesloten. De resultaten in Hoofdstuk 9 lijken er bovendien op te duiden dat zo'n ligand effect

inderdaad aanwezig is; (i) een toename in de hoeveelheid promotor-metaal zorgt voor een afname in de begin-potentiaal van de methanol oxidatie, (ii) methanol adsorbeert makelijker op PtRu dan op Pt, en (iii) het effect van Ru is ook nog aanwezig op kool gedragen Pt met kleine deeltjes, die al bij lage potentiaal geoxideerd worden, zoals beschreven in Hoofdstuk 5. Deze resultaten zijn niet direct te verklaren vanuit het bifunctionele mechanisme, en suggereren dus dat er een ligand effect is. Dit wordt nog eens bevestigd door de in-situ IR metingen aan geadsorbeerd CO op PtRu, die aantonen dat de CO strek frequentie verschuift naar meer positieve potentialen in de aanwezigheid van Ru (Hoofdstuk 10). Bij het bestuderen van het gedrag van een katalysator is het nodig om de exacte samenstelling te kennen. Voor "codeposited" PtRu elektroden kan de samenstelling echter niet eenvoudig worden bepaald. Daarom hebben we een electrochemische methode ontwikkeld waarbij gebruik is gemaakt van de EQCMB. Deze methode wordt beschreven in Hoofdstuk 10. Aangetoond wordt dat de oxide reductie potentiaal gebruikt kan worden als een maat voor de hoeveelheid Ru aanwezig op het oppervlak. Door een calibratie-curve te gebruiken, die gemeten is met EQCMB, is het mogelijk om de Ru oppervlakte concentratie te bepalen van een PtRu electrode.

Hoewel Sn ook bekend staat als promotor voor de methanol electrooxidatie, is er minder consistentie in de literatuur dan voor het effect van Ru. Daarom hebben we het effect van Sn op Pt/C katalysatoren onderzocht als functie van de bereidingsmethode (Hoofdstuk 11). Het blijkt dat de bereidingsmethode inderdaad van invloed is, waarbij de effecten lopen van een kleine toename in de activiteit tot een afname. Net als voor Ru is het optimum Sn gehalte altijd laag, ca 10%.

De prestaties van de katalysatoren die tot nu toe zijn beschreven, zijn nog steeds te matig voor een praktische toepassing. Daarom was een deel van het onderzoek gericht op de ontwikkeling van alternatieve katalysatoren. De resultaten, die worden beschreven in Hoofdstuk 12, laten zien dat PtAu/C en Pt/WO₃ beide actiever zijn dan Pt, hoewel geen van beide de activiteit van een PtRu/C katalysator haalt. Daarnaast lijkt een katalysator zonder Pt, AuRuTiO₂/C ook in staat te zijn om methanol te oxideren. Het is echter nog niet duidelijk via welk mechanisme de methanol oxidatie aan dit systeem verloopt.

Dankwoord

Lewis Thomas schrijft in zijn boek "The Lives of a Cell" het volgende over het beoefenen van wetenschap:

"It sometimes looks like a lonely activity, but it is as much the opposite of lonely activity as human behavior can be. There is nothing so social, so communal, so interdependent."

Ik sluit me daar bij aan. Dit is niet het werk van één persoon, dat zou ook onmogelijk zijn. Ik wil daarom proberen om hier alle mensen te bedanken die een bijdrage hebben geleverd (hoe groot of klein dan ook) aan het ontstaan van dit proefschrift. Diegenen die hier niet persoonlijk genoemd worden moeten zich niet gepasseerd voelen, ik ben iedereen die in de afgelopen vier jaar in mijn directe omgeving heeft verkeerd dankbaar.

Allereerst wil ik mijn promotor Rob van Veen bedanken, niet alleen voor alle ideeën, de inspiratie, het enthousiasme en de begeleiding, maar ook voor alle aangename gesprekken die we hebben gehad over wetenschaps-geschiedenis en -filosofie en de boeken die daarover geschreven zijn. Mijn co-promotor Wil Visscher; jou wil ik bedanken voor de dagelijkse begeleiding, voor alle tijd en aandacht die je in het onderzoek gestopt hebt. De deur van je kamer was altijd open, en ik heb het als zeer prettig ervaren, dat ik te pas en te onpas binnen kon lopen.

Einige der in diese Arbeit vorgestellten Resultate wären ohne die Hilfe von Prof. Dr. Wolf Vielstich und seinem Mitarbeitern an der Universität Bonn nicht zustande gekommen. Ins besondere gilt mein Dank hier Dr. Michael Krausa für die Einführung in die "DEMS"-experimente, sowie Volkmar Schmidt, Andreas Kuver und Elena Pastor (Graças!) für die angenehme Zeit in Bonn. Herrn Prof. Dr. H. Bönemann und Mitarbeitern vom Max-Planck Institut für Kohleforschung, Mühlheim an der Ruhr, danke ich für die Synthese einige Pt/C katalysatoren.

Ad en Anton jullie kan ik natuurlijk niet vergeten. Jullie hebben allebei een enorme bijdrage geleverd aan de resultaten die in dit proefschrift beschreven zijn. Ad, jij hebt niet alleen "de DEMS" helemaal opgebouwd, je hebt ook een enorme hoeveelheid resultaten afgeleverd in de vorm van tabellen die soms astronomische afmetingen begonnen aan te nemen. Ik ben je zeer erkentelijk voor al het werk dat je voor me gedaan hebt. Anton, alle ellipsometrie metingen komen voor jou rekening. Ik ben je dankbaar voor het enthousiasme en de inzet waarmee je alles altijd gedaan hebt.

Bart Fokkink en Jeanette Sondag (Philips Research) wil ik graag bedanken voor alle hulp die ze geboden hebben bij het doen van de Quartz Microbalans metingen. Jeanette, vooral jou heeft het nogal eens wat tijd gekost, als ik weer een probleem had met een elektrode, hartelijk dank daarvoor. Ook de andere leden van de groep Grensvlakchemie wil ik bedanken voor alle aangename weken die ik daar heb doorgebracht. Rob van de Berg (Shell Research), dank je wel voor de hulp bij het interpreteren van de TEM foto's, en voor het doen van een (helaas vruchteloze) poging tot in-situ AFM metingen. Voor het doen van AFM (en XPS) metingen

wil ik ook Tiny Verhoeven, Pieter Gunther en Arthur de Jong bedanken, helaas hebben de soms verrassende resultaten mijn proefschrift niet gehaald, maar dat ligt zeker niet aan jullie (eerder aan de cel). Voor het maken van alle TEM en SEM foto's wil ik respectievelijk Dick Klepper en Martien Haanepen heel hartelijk danken.

Mijn enige afstudeerder, Erik Kemperman, de research stagiaires Ronald Gelten, Renee van Schijndel, Jelle Terpsma en Liane Schoonus, en Willy Zelen (2^e jaars praktikum) hebben alle in meer of mindere mate een bijdrage geleverd. Liane en Renee verdienen extra aandacht omdat ze samen verantwoordelijk zijn voor hoofdstuk 12. Erik, jou wil ik ook bedanken voor al het werk dat je verzet hebt, het was niet altijd even makkelijk door mijn frequente afwezigheid, maar je hebt je er goed doorheen geslagen. Mijn kamergenoot Albert Gootzen en mijn "halve" kamergenoot Frank de Bruin wil ik bedanken voor de prettige vier jaar die razendsnel voorbij zijn gegaan, en voor al jullie verbale en praktische hulp. Alle andere leden en ex-leden van TAK wil ik graag bedanken voor de goede sfeer in de groep.

Hoewel dit niet de plaats is om reclame te maken, wil ik toch de mensen achter het bedrijf dat onze elektrochemische apparatuur levert hier in het zonnetje zetten; Gert-Jan Brug en Cees van Velzen (en jullie medewerkers uiteraard!) van Eco Chemie, ik denk dat jullie service ongeëvenaard is in deze wereld. Een telefoontje over een fout in de software en vaak de volgende dag lag er dan al weer een diskette met een nieuwe versie op mijn bureau. Daarbuiten wil ik jullie bedanken voor alle lol die we gehad hebben op diverse congressen in het buitenland. Een hamburger scoren in Karlsruhe, sperziebonen eten in Ferrara, of naar Spencer Davis luisteren in Reno, het was altijd even gezellig.

Tot slot wil ik die mensen die me "niet wetenschappelijk" op de been hebben gehouden bedanken; mijn ouders, mijn broer Saul die altijd goed was voor de nodige relativering ("Wat heeft de wereld daar nou aan?"). Mijn "buren" Toon en Mieke, en al mijn andere vrienden wil ik bedanken voor alle mentale steun, en alle leden van voetbal vereniging Union, voor het "begrip"(?) dat ze hadden als ik me op het trainingsveld weer eens moest afreageren. Before turning to the last person I want to thank, I would like to express my thanks to my friends and colleagues abroad, all of whom I met during conferences and some of whom have made a considerable contribution to this thesis; Merci Yves et Abdou; Grazie Anna (Dank je wel); Obrigado Ana, Christina, Luis, e Joao; Thank you Miriam and Michael. I hope we will stay in touch for a long time, I will not easily forget the great time we had during the conferences, on beaches and in bars and restaurants.

Tot slot wil ik Anne bedanken, niet voor de koffie want die heb ik altijd zelf in moeten schenken, maar voor het geven van een aantal praktische tips en gewoon voor alle steun in de afgelopen jaren. Dank je wel.

List of publications.

Chapter 2: T. Frelink, W. Visscher, J.A.R. van Veen *To be published*.

Chapter 3 is partly based on: T. Frelink, W. Visscher, J.A.R. van Veen *Electrochim. Acta* 40, 545 (1995).

Chapter 4: T. Frelink, A.W. Wonders, W. Visscher, J.A.R. van Veen *Submitted for publication*.

Chapter 5: T. Frelink, W. Visscher, J.A.R. van Veen *J. Electroanal. Chem.* 382, 65 (1995).

Chapter 6: T. Frelink, A.W. Wonders, W. Visscher, J.A.R. van Veen *To be published*

Chapter 7: T. Frelink, W. Visscher, J.A.R. van Veen *Electrochim. Acta* 40, 1537 (1995).

Chapter 8: T. Frelink, A.P. Cox, W. Visscher, J.A.R. van Veen *Submitted for publication*.

Chapter 9: T. Frelink, W. Visscher, J.A.R. van Veen *Accepted for publication in Surf. Sci.*

Chapter 10: T. Frelink, W. Visscher, J.A.R. van Veen *Submitted for publication*.

Chapter 11: T. Frelink, W. Visscher, J.A.R. van Veen *Electrochim. Acta* 39, 1871 (1994).

Curriculum Vitae

- 1968: Geboren op 2 Februari te Amsterdam.
- 1985: Eindexamen Atheneum B aan de voormalige Rijkscholengemeenschap te 's-Hertogenbosch. Aanvang studie Scheikunde aan de Katholieke Universiteit Nijmegen.
- 1991: Doctoraal examen. Hoofdvak: Anorganische Chemie (Prof.Dr.Ir. J.J. Steggerda en Dr. J.G.M. van der Linden); Bijvak Molecuul-spectroscopie (Prof. Dr. W. Veeman).
Aanvang promotie-onderzoek aan de TU Eindhoven onder leiding van Prof. Dr. J.A.R. van Veen en Dr. W. Visscher.
- 1995: Met ingang van 17 Juli in dienst bij ECN in Petten.

Ik zink
tot aan mij schouders
in berusting

een kalme zee
van nauwelijks golving
houdt mij staande

en ik verroer geen vin

Ik fluister ingetogen woorden
over het water, denkend
aan wie er voorbijging, gisteren

En overal zeemeeuwen
luisterend
brokstukjes brood uit mijn mond

en ik glimlach
omdat het voorbij is

Nico Scheepmaker, uit "Poëtisch fietsen" (1955)